

Investigating the Role of Sphingolipids in Innate Immunity

Doctoral thesis at the Medical University of Vienna
for obtaining the academic degree

Doctor of Philosophy

Submitted by

Dipl.-Biol. Marielle S. Köberlin

Supervisor:

Prof. Giulio Superti-Furga

CeMM Research Center for Molecular Medicine
of the Austrian Academy of Sciences

Lazarettgasse 14, AKH BT 25.3, 1090 Vienna

Vienna, 09/2015

DECLARATION

The author of this cumulative thesis is a co-author on both manuscripts included in the thesis. The prologue and the epilogue preceding the manuscripts describe the individual contributions. The other parts were written by the author of this thesis, Marielle Köberlin. Giulio Superti-Furga, Berend Snijder, and Leonhard Heinz gave feedback for the writing of the thesis.

Most of the work performed here was done in the laboratory of Giulio Superti-Furga at CeMM Research Center for Molecular Medicine of the Austrian Academy of Sciences. Further work was carried out in collaboration with the laboratory of Sylvia Knapp at CeMM and the laboratory of Markus Wenk at the National University of Singapore, in the Department of Biochemistry and Department of Biological Sciences.

The publications arising from this thesis and included here are:

Manuscript #1 was published in **Cell**: Köberlin MS, Snijder B, Heinz LX, Baumann CL, Fauster A, Vladimer GI, Gavin AC, Superti-Furga G (2015) A Conserved Circular Network of Coregulated Lipids Modulates Innate Immune Responses. *Cell* 162: 170-83

(DOI: <http://dx.doi.org/10.1016/j.cell.2015.05.051>)

Manuscript #2 was published in **Cell Reports**: Heinz LX, Baumann CL, Köberlin MS, Snijder B, Gawish R, Shui G, Sharif O, Aspalter IM, Müller AC, Kandasamy RK, Breitwieser FP, Pichlmair A, Bruckner M, Rebsamen M, Blüml S, Karonitsch T, Fauster A, Colinge J, Bennett KL, Knapp S, Wenk MR, Superti-Furga G (2015) The Lipid-Modifying Enzyme SMPDL3B Negatively Regulates Innate Immunity. *Cell Reports* 11: 1919-28

(DOI: <http://dx.doi.org/10.1016/j.celrep.2015.05.006>)

The publications from chapters 2.2 and 2.4 were reprinted with permission of Elsevier under the terms of the Creative Commons Attribution-Non Commercial-No Derivatives License (CC BY NC ND).

Table of Contents

Declaration	3
List of Figures.....	6
Abbreviations	7
Acknowledgements	10
Abstract.....	11
Zusammenfassung	12
1. CHAPTER ONE: INTRODUCTION.....	13
1.1 Sphingolipids and Glycerophospholipids in Cellular Membranes	13
1.1.1 Sphingolipid Biosynthesis and the Regulation by ORM Proteins.....	14
1.1.2 Glycerophospholipid Biosynthesis.....	16
1.1.3 Sterol Biosynthesis.....	19
1.1.4 Biophysical Properties of Different Lipid Classes.....	20
1.1.5 Lipid Distribution and Trafficking in the Cell.....	21
1.1.6 Regulation of Membrane Lipid Metabolism	25
1.1.7 Crosstalk between Sterols, Sphingolipids, and Glycerophospholipids	26
1.1.8 Quantitative Lipidomics	29
1.1.9 Lipid Storage Disorders.....	30
1.2 Importance for Systematic Approaches to Study Lipid Metabolism	32
1.3 Innate Immunity	33
1.2.1 Toll-Like Receptors.....	34
1.2.2 Negative Regulators of TLR Signaling.....	39
1.2.3 Cytokine Secretion Mechanisms.....	39
1.2.4 Lipids and Inflammation	40
1.4 Aims of This Thesis	44
2. CHAPTER TWO: RESULTS	45
2.1 Prologue	45
2.2 A Conserved Circular Network of Coregulated Lipids Modulates Innate Immune Responses...	47
2.3 Epilogue	78
2.4 The Lipid-Modifying Enzyme SMPDL3B Negatively Regulates Innate Immunity	79
3. CHAPTER THREE: DISCUSSION	105
3.1 Summary.....	105
3.2 The Circular Network of Coregulated Lipids Advances Lipidomics Analysis	105
3.2.1 The Circular Network Reveals new Features of Lipid Coregulation.....	106
3.2.2 Why is Lipid Coregulation Important?	107
3.2.3 The Circular Network Facilitates the Identification of Lipid Function.....	107
3.3 Conservation of the Metabolic Network and Lipid Species	108

3.4 Redundancy of Pathways in Lipid Metabolism.....	108
3.5 Lipids and TLR Signaling – Mechanisms of Action	109
3.5.1 Lipids and TLR Signaling	109
3.5.2 Transmembrane Receptors: Internalization and Complex Formation	110
3.5.3 TLR Downstream Signaling	111
3.5.4 Cytokine Secretion.....	112
3.6 Future Perspectives.....	114
3.6.1 The Next Steps	114
3.6.2 Prediction of the Inflammatory Phenotype	114
3.6.3 Opportunities for Targeting Lipid Metabolism	115
3.7 Conclusions and Outlook.....	116
References.....	118
Curriculum Vitae	134

LIST OF FIGURES

Figure 1: The sphingolipid and glycerophospholipid metabolic networks

Figure 2: Lipid structures

Figure 3: Subcellular localization of sphingolipid metabolism

Figure 4: TLR signaling processes

Figure 5: TLR signaling over time

ABBREVIATIONS

ABC	ATP-binding cassette transporters
ABCA1	ABC transporter subfamily A
AC6	adenylyl cyclase 6
ACER1/2/3	alkaline ceramidases 1/2/3
AIM2	absent in melanoma 2
AP-1	activator protein 1
AP-2/4	adaptor protein 2/4
ARF6	ADP-ribosylation factor 6
ASAH1/2	acid ceramidases 1/2
ASM	acid sphingomyelinase
ATF3	cyclic AMP-dependent transcription factor
C1P	ceramide-1-phosphate
Ca ²⁺	calcium
CCL5	C-C motif chemokine 5
CD14	monocyte differentiation antigen CD14
CDP	cytidine diphosphate
CEPT	choline/ethanolamine phosphotransferase
CERS1 – 6	ceramide synthases 1- 6
CERT	ceramide transfer protein
clAP2	inhibitor of apoptosis protein 2
CoA	coenzyme A
COPI/II	coat protein complexes I/II
COX	cytochrome C oxidase
CpG-DNA	cytosine-phosphate-guanine DNA
cPLA2	cytosolic phospholipase 2
CR3/4	complement receptor 3/4
CRAC	cholesterol recognition amino acid consensus
CXCL10	C-X-C motif chemokine 10
DAG	diacylglycerol
EGFR	epidermal growth factor receptor
ER	endoplasmic reticulum
ERK1/2	extracellular signal-regulated kinase
FA	fatty acid
FAPP2	glucosylceramide transfer protein
Fpk1/2	flippase kinase 1/2
FRET	fluorescence resonance energy transfer
G3P	glycerol-3-phosphate
GALC	galactosylceramidase
GBA	glucocerebrosidase
GPCR	G-protein-coupled receptors
GPI	glycosylphosphatidylinositol
GTP	guanosine triphosphate
HDAC1	histone deacetylase 1
HMG	3-hydroxyl-3-methylglutaryl
IFN	type I interferon
IKK	I kappa B kinase
IL	Interleukin
IRAK	Interleukin-1 receptor-associated kinase

IRF3/4/5	interferon regulatory factor 3/4/5
I κ BNS	nuclear I κ B delta protein
JNK	c-Jun N-terminal kinase
K-Ras	Kirsten rat sarcoma
kb	kilo base
KSR	kinase suppressor of Ras
LBP	LPS-binding protein
LDL	low-density lipoprotein
LPA	lysophosphatidic acid
LPC	lysophosphatidylcholine
LPCAT	lysophospholipid acyltransferases
LPE	lysophosphatidylethanolamine
LPG	lysophosphatidylglycerol
LPS	lipopolysaccharide
LPSe	lysophosphatidylserine
LYST	lysosomal trafficking factor
MAPK	mitogen-activated protein kinases
MD2	myeloid differentiation factor 2
MIF	macrophage migration inhibitory factor
MyD88	myeloid differentiation primary response gene 88
NF κ B	nuclear factor kappa B
NOD	nucleotide-binding oligomerization domain
NPC1	Niemann-Pick C1 protein
NSMA/3	neutral sphingomyelinase /3
Orm1	orosomucoid-1
ORMDL1/2/3	orosomucoid-1 like protein 1/2/3
OSBP	oxysterol-binding protein
Osh4/6/7	oxysterol-binding protein homolog 4/6/7
PA	phosphatidic acid
PAF	platelet-activating factor
PAMP	pathogen-associated molecular pattern
PAP	phosphatidate phosphohydrolase
PBMCs	peripheral mononuclear cells
PC	phosphatidylcholine
PE	phosphatidylethanolamine
PG	phosphatidylglycerol
PGPS	PG phosphate synthase
PH	pleckstrin homology domain
PI	phosphatidylinositol
PI(4)P5	phosphatidylinositol 4-phosphate 5-kinase type-1 alpha
PI3K	phosphoinositide 3-kinase
PIS	PI Synthase
PKC	protein kinase C
PLA/C/D	phospholipase A/C/D
PM	plasma membrane
PMA	phorbol ester
PPA	serine/threonine protein phosphatases
PRAT4A	protein associated with TLR4
PS	phosphatidylserine
PSD	PS decarboxylase
PSS1	PS synthase 1
RAB10/11A	Ras-related protein

RIG-I	retinoic acid-inducible gene 1
RING	really interesting new gene domain
S1P	sphingosine-1-phosphate
Sac1	suppressor of actin mutations 1-like (phosphoinositide phosphatase)
SGMS1/2	sphingomyelin synthase 1/2
SGPL1	sphingosine-1-phosphate lyase
SGPP1	sphingosine-1-phosphate phosphatase
shRNA	short hairpin RNA
SM	sphingomyelin
SMPD1	acid sphingomyelinase gene
SMPDL3B	sphingomyelin phosphodiesterase, acid-like 3B
SNARE	soluble NSF attachment protein
SNP	single nucleotide polymorphism
SOCS	suppressor of cytokine signaling
SPHK1/2	sphingosine kinase 1/2
SPOT	serine palmitoyltransferase, ORM1/2, Tsc3, Sac1 complex
SPTLC1/2	Serine palmitoyltransferase 1/2
SREBP	sterol regulatory element-binding protein
STAR	steroidogenic acute regulatory domain
TAG	triacylglycerol
TBK1	TANK-binding kinase 1
TCR	T-cell receptor
TGN	trans-Golgi network
TIR	Toll/IL-1 receptor domain
TIRAP	TIR-domain containing adaptor protein
TLR 1 -13	Toll-like receptor 1 -13
TMED2/7	transmembrane emp24 domain-containing protein 2/7
TNFR	TNF receptor
TNF α	tumor necrosis factor α
Torc1/2	target of rapamycin 1/2
TRAF2/6	TNF receptor associated factor 2/6
TRAM	TRIF-related adaptor molecule
TRIF	TIR-domain-containing adapter-inducing interferon- β
VAMP-3	vesicle-associated membrane protein 3
Ypk1/2	serine/threonine-protein kinase 1/2

ACKNOWLEDGEMENTS

The time I have spent at CeMM was a wonderful and rewarding experience. This stimulating environment and the great crowd of unique people have shaped me professionally and personally and I will always look back to this time with joy and admiration.

First of all I would like to thank my PhD supervisor Giulio Superti-Furga for giving me the opportunity to independently work on this project, for providing me with this great work environment, and for supporting and mentoring me throughout this journey. His motivation, commitment, and 'Herzblut' have made CeMM to the unique and special place it has become and I am proud to have been a part of it. During my time in his laboratory I have learned a lot and I am grateful for this fantastic start of my scientific carrier.

Next, I would like to thank Berend Snijder, a postdoctoral fellow in the laboratory of Giulio Superti-Furga, who joined me on this project, when he started working at CeMM. During our great collaboration I learned a lot about what it takes to be an innovative scientist and systems biologist. Thank you for all the fun we had, your time, patience, support, and excellent mentorship during this journey.

My further gratitude goes to all the members of the Giulio Superti-Furga laboratory for their constant support, great scientific feedback, and input. The atmosphere in the lab made it a fun place to work and to discuss new, crazy ideas. I would also like to thank Leonhard Heinz for joining me on this, sometimes bumpy, ride; and for his patience, and honesty. And a special thanks goes to Maria Góna and Adriana Goncalves for being great friends and companions along the way, sharing dreams, hopes, and a lot of fun.

I would also like to thank my thesis committee members Anne-Claude Gavin and Christoph Binder for their helpful feedback and input during my PhD studies. I always enjoyed the inspiring scientific discussions and brain storming session.

I am grateful for the endless support from my husband, family, and friends. Thank you for encouraging me to continue whenever times got rough and for understanding my fears and hopes without questioning. You always make me feel happy and loved, and simply very special.

ABSTRACT

As key regulators of the innate immune system, Toll-like receptors (TLRs) are conserved transmembrane receptors that recognize molecular structures of pathogens and initiate the immediate immune response. Together with a large panel of other proteins and thousands of lipids they comprise the cellular membranes, whose physical properties strongly depend on their lipid composition. The majority of membrane lipids belong to the glycerophospholipids or sphingolipids and their abundance can be measured using mass spectrometry-based lipidomics. The combination of shRNA-mediated genetic perturbations of lipid-modifying enzymes important for the sphingolipid metabolism in mouse macrophages, with the lipidomics analysis of 245 different lipid species, revealed broad changes in sphingolipid and glycerophospholipid levels. Using this data, we could identify lipids, which were coregulated across all perturbed cell lines. Strikingly, visualization of the lipid-lipid coregulation across all lipid species revealed a circular network of lipid coregulation, reflecting lipid metabolism, adaptation mechanisms, and subcellular localization. To further dissect the consequences of perturbed membrane lipid composition on the innate immune response we functionally characterized the TLR-mediated responses of these cell lines. By combining the network of coregulated lipids with the detailed characterization of TLR biology, we could infer functions for single lipid species in TLR signaling. These inferred functions were validated using lipid supplementation approaches. Based on changes in the lipid composition upon genetic perturbation we could predict the pro-inflammatory response of the previously unknown gene *Smpd13b* (Sphingomyelin Phosphodiesterase, Acid-Like 3B) in a loss-of-function cell line. The gene product SMPDL3B was identified as a TLR4, TLR7, and TLR9 interactor, whose expression levels were induced upon diverse inflammatory stimuli. Further, in an *Smpd13b*-deficient mouse model the negative regulatory role of SMPDL3B was confirmed *in vivo* using a peritonitis model resulting in enhanced cytokine release after infection. Fibroblasts derived from a panel of patients suffering from lipid storage disorders were also analyzed using lipidomics and a comparison of the lipid coregulation revealed that the circular network was largely conserved between mouse and human cells. Using the functional lipid annotation of mouse macrophages we could correctly predict the inflammatory response of human fibroblasts solely based on their changes in lipid composition.

ZUSAMMENFASSUNG

Einer der Hauptakteure des angeborenen Immunsystems, ist die Gruppe der Toll-like Rezeptoren (TLRs). Diese konservierten Transmembranrezeptoren erkennen molekulare Strukturen von Pathogenen und initiieren daraufhin eine sofortige Immunantwort. Die große Gruppe der Membranproteine zusammen mit tausenden von Lipidmolekülen formen die zelluläre Membrane, deren physikalische Eigenschaften stark von der Zusammensetzung abhängen. Der Großteil der Membranlipide gehört zu den Glycerophospholipiden oder den Sphingolipiden, deren Mengen durch massenspektrometrische Analyse (Lipidomics) ermittelt werden können. Die Kombination von gezielten genetischen Störungen der Sphingolipid-modifizierenden Enzyme in murinen Macrophagen, zusammen mit der Lipidomics Analyse von 245 verschiedenen Lipidspezies in diesen Zelllinien, offenbarte umfassende Veränderungen der Lipidzusammensetzung. Mit Hilfe dieser Daten konnten wir die Koregulation der Lipide identifizieren. Bemerkenswerter Weise zeigte die Visualisierung dieser Lipid Koregulationen ein zirkuläres Netzwerk, welches den Metabolismus, Adaptierungsmechanismen und die subzelluläre Lokalisation der Lipide darstellte. Um die Konsequenzen einer gestörten Lipidzusammensetzung auf die angeborene Immunantwort zu identifizieren, charakterisierten wir funktionell die TLR-induzierte Signalweiterleitung dieser Zelllinien. Durch das Kombinieren des Netzwerkes der koregulierten Lipide mit der detaillierten Quantifizierung der TLR-abhängigen Prozesse, konnten wir Funktionen für einzelne Lipidspezies in der angeborenen Immunantwort ableiten und beschreiben. Basierend auf den Veränderungen der Lipidzusammensetzung in einer weiteren Zelllinie, in der das bisher nur dürftig beschriebene Gen *Smpd3b* genetisch dezimiert wurde, konnten wir mit Hilfe der vorher ermittelten Funktionen von verschiedenen Lipiden die pro-inflammatorische Immunantwort dieser Zelllinie vorhersagen. SMPDL3B wurde auch als Bindungspartner von TLR7, TLR9 und TLR4 identifiziert, und konnte durch diverse inflammatorische Stimuli induziert werden. Des Weiteren wurde die negative regulatorische Rolle dieses Proteins in einer *Smpd3b*-defizienten Maus mittels eines Peritonitismodells auch *in vivo* bestätigt, da erhöhte Zytokinausschüttung gemessen wurde. Zusätzlich wurden Fibroblasten von verschiedenen Patienten mit einer Lipidspeichererkrankung ebenfalls mittels Lipidomics analysiert und ein Vergleich der Lipid Koregulationen zeigte, dass das zirkuläre Netzwerk zwischen murinen und humanen Zellen konserviert ist. Mit Hilfe der funktionellen Lipidbeschreibung, basierend auf den Daten der murinen Macrophagen, konnten wir die Immunantwort der humanen Zellen genau vorhersagen. Diese Prognose beruhte einzig auf den Veränderungen ihrer Lipidzusammensetzung und konnte experimentell bestätigt werden.

1. CHAPTER ONE: INTRODUCTION

1.1 SPHINGOLIPIDS AND GLYCEROPHOSPHOLIPIDS IN CELLULAR MEMBRANES

“Cell membranes are complicated in composition but precise in purpose: to selectively compartmentalize the constituents of life away from environmental lifelessness.” (Lingwood & Simons, 2010)

The cellular membrane consists of thousands of different lipid molecules and a variety of transmembrane proteins important for cell-cell communication, motility, and monitoring of the cell's surrounding. This membrane fulfills a wide spectrum of functions ranging from large lipid reorganization important for cell division or vesicle fusion to fine adjustments in the immediate vicinity of membrane proteins, regulating their function. In order to execute these different roles the lipid component of cellular membranes consists of several different lipid classes providing the cell with a lipid repertoire to modulate its membrane properties such as fluidity, thickness, curvature, thermal stability, and protein content (van Meer et al., 2008). The majority of these membrane lipids belong to the classes of sterols, glycerophospholipids, or sphingolipids. While sterols consist of different steroid rings, glycerophospholipids and sphingolipids are comprised of two fatty acid (FA) chains varying in length and saturation level attached to a glycerol or sphingosine backbone, respectively. Other lipids found in the cell belong to the FAs, the sterol esters, which are made of FAs attached to a sterol and serve as lipid storage molecules and the triacylglycerols, which consist of a glycerol and FAs and are also important for lipid storage, forming lipid bodies. Thus a cell contains several thousand different lipid species that vary in form and function (Coskun & Simons, 2011). Interestingly, lipids and their metabolic processes show a high degree of conservation between yeast and human, so initially a lot of findings came from studies in yeast and could be confirmed in mammalian cells (Nielsen, 2009). However, it is becoming increasingly clear that lipids and their functions cannot be easily studied in an isolated system. Due to the complexity of the metabolic and structural connections, it is important to perform global analyses of the different pathways and lipids involved. Other findings have reported a metabolic 'ripple' effect when one lipid class is altered in the cell, further highlighting the interconnection of lipid metabolism. Over several decades scientist have thought of lipids primarily as energy storage and structural components and only recently is has been proposed

that deciphering the functional properties of lipids in signaling could open up an entire new field of research (Hannun & Obeid, 2008).

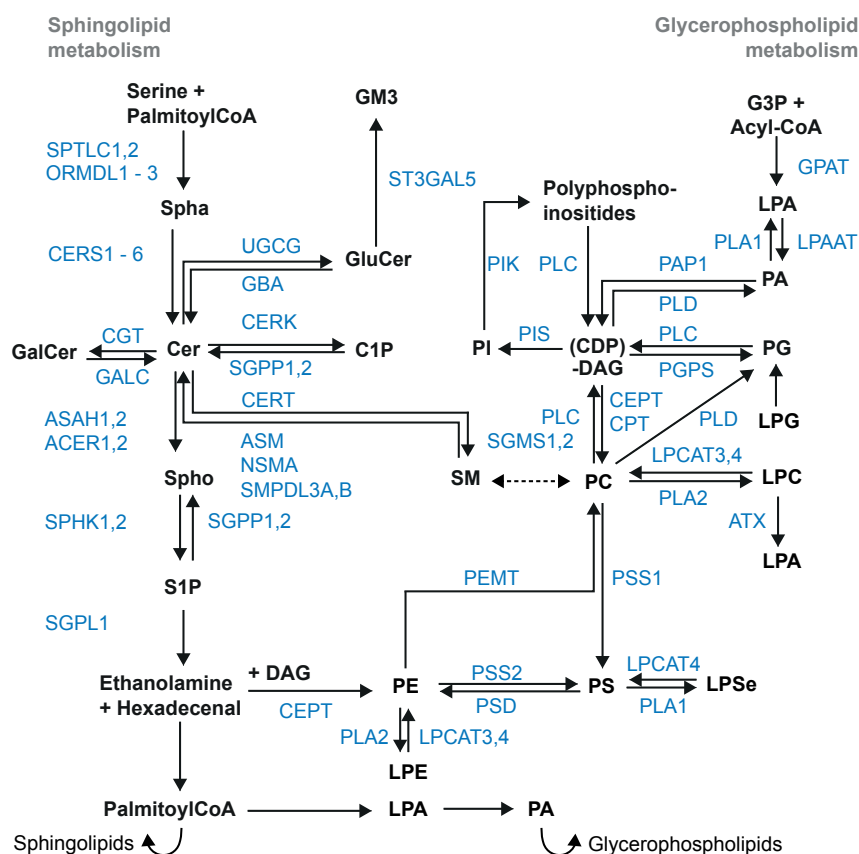


Figure 1: The sphingolipid and glycerophospholipid metabolic networks: The pathways show the different metabolic processes involved in sphingolipid (left) and glycerophospholipid (right) metabolism (lipids and other metabolites are in black, enzymes are in blue). Spha: Sphinganine, Cer: Ceramide, Spho: Sphingosine, GluCer: Glucosylceramide, GM3: Gangliosides, CGT: Galactosyltransferase, CERK: Ceramide kinase, UGCG: Ceramide glucosyltransferase, ST3GAL5: Ganglioside GM3 synthase, PIK: Phosphatidylinositol kinase, PEMT: Phosphatidylethanolamine N-methyltransferase, CPT: Carnitine palmitoyltransferase, ATX: Autotaxin, PAP1: Phosphatidic acid phosphohydrolase 1, LPAAT: Lysophosphatidic acid acyltransferase, GPAT: Glycerol-3-phosphate acyltransferase 1. Figure adapted from Köberlin, Snijder et al., 2015.

1.1.1 SPHINGOLIPID BIOSYNTHESIS AND THE REGULATION BY ORM PROTEINS

Most processes involved in the *de novo* synthesis of membrane lipids occur in the endoplasmic reticulum (ER), the cellular organelle which harbors the majority of enzymes

involved in lipid biosynthesis (Gault, Obeid et al., 2010). Importantly, the genes, proteins, and lipid molecules associated with lipid biosynthesis pathways are highly conserved (Guan, Riezman et al., 2010). The first step in sphingolipid metabolism is the synthesis of 3-keto-dihydrosphinganine resulting from the hydrolysis of serine and palmitoyl-CoA mediated by the SPOT complex, a multi-protein complex consisting of serine palmitoyltransferases (SPTLC1 and SPTLC2) as well as the proteins ORMDL1, ORMDL2, and ORMDL3 (Breslow & Weissman, 2010). After the reduction of this lipid to dihydrosphingosine, ceramide synthases (CERS 1 – 6) catalyze the reaction to different dihydroceramide molecules by attaching a second FA chain. Different ceramide synthases show selective specificity for various FA chain lengths (Pewzner-Jung, Ben-Dor et al., 2006). This specificity is further discussed in more detail below. Dihydroceramides are then desaturated to ceramides (Causeret, Geeraert et al., 2000). The ceramide transfer protein (CERT) shuttles ceramide molecules from the ER, their location of synthesis, to the trans-Golgi network (TGN) where they can further be trafficked to the plasma membrane (PM) and metabolized to sphingomyelin (SM) (Hanada, 2014) (Figure 1). This step is catalyzed by sphingomyelin synthases (SGMS1 and SGMS2), which attach a phosphocholine head group to ceramide molecules. This reaction can be reversed by neutral or acidic sphingomyelinases (NSMA and NSMA3 or ASM) residing at the PM or in endosomes, respectively (Milhas et al., 2010). Within the sphingolipid network ceramides represent the metabolic hub as these lipids can further be glycosylated, galactosylated, or phosphorylated by specific enzymes in the ER to form more complex sphingolipid molecules (Ichikawa & Hirabayashi, 1998) (Figure 1). Proteins such as glucocerebrosidases and galactosidases can degrade these complex sphingolipids to form ceramides again (Hakomori, 2000). The degradation of ceramides by ceramidases at the ER (ACER 1 and ACER3), at the Golgi (ACER2), or in lysosomal compartments (ASAH1 and ASAH2) leads to sphingosines, which can either be recycled to make ceramides or be phosphorylated by sphingosine kinases (SPHK1 and SPHK2) to form sphingosine-1-phosphates (S1P). This lipid class can be dephosphorylated by SGPP1 (sphingosine-1-phosphate phosphatase) to sphingosines, feeding back into the sphingosine pool of the cell, or be irreversibly degraded by sphingosine-1-phosphate lyase (SGPL) into the non-sphingolipid molecules phosphoethanolamine and hexadecenal (Johnson, Johnson et al., 2003, Nakahara et al., 2012). Enzymes that hydroxylate or desaturate the FA components further contribute to the diversity of sphingolipids (Degroote, Wolthoorn et al., 2004).

Although the main metabolic steps of sphingolipid biosynthesis have been known since several decades, the regulation principles of different enzymes involved in the pathways have begun to emerge only now. The most important protein-mediated regulation of the *de novo*

synthesis of sphingolipid metabolism is the SPOT complex. In mammalian cells, the ORMDL proteins have been found to interact with SPTLCs but not with the mammalian isoform of Sac1 as in yeast (Breslow & Weissman, 2010). The Orm proteins are a highly conserved family of transmembrane domain proteins without any known protein domains (Breslow, Collins et al., 2010). They have been reported to act as negative regulators of sphingolipid synthesis and recently also other lipid metabolic processes as well as protein quality control (Han, Lone et al., 2010, Shimobayashi, Oppliger et al., 2013). However, their exact function, especially if and how they are involved in the sensing of lipid composition, still remains to be elucidated. In yeast, different kinases and phosphatases controlled by the activity of target of rapamycin (Torc1 and Torc2) regulate the phosphorylation and the consecutive inhibition of Orm protein function (Sun, Miao et al., 2012). In mammals, there are three Orm1 homologues (ORMDL1, 2, and 3). Interestingly, single nucleotide polymorphisms (SNPs) influencing the expression levels of *Ormdl3* have been connected to the susceptibility of early-onset childhood asthma (Moffatt, Kabesch et al., 2007).

1.1.2 GLYCEROPHOSPHOLIPID BIOSYNTHESIS

Compared to sphingolipids, glycerophospholipids constitute the bulk of membrane lipids in a cell. The precursor of all glycerophospholipids is phosphatidic acid (PA), a product of the dual acylation of glycerol-3-phosphate (G3P) using acyl-CoA (Figure 1). Other lipids can be converted into PA by different mechanisms such as the phosphorylation of diacylglycerol (DAG) by DAG kinases (Sakane, Imai et al., 2007) or the degradation of phosphatidylcholines (PC) into PA regulated by phospholipase D (PLD) (Peng & Frohman, 2012). PA can also be dephosphorylated by the phosphatidate phosphohydrolase (PAP) into DAG, which in turn is used for the synthesis of the main glycerophospholipid classes PC, phosphatidylglycerols (PG), phosphatidylserines (PS), and phosphatidylethanolamines (PE) as well as triacylglycerols (TAG).

Phosphatidylcholine: The most abundant lipid class in eukaryotic cells representing up to 55% of all lipids is enriched at the outer leaflet of the PM as compared to the inner leaflet (Bohdanowicz & Grinstein, 2013). Because the head group and lipid backbone have the same molecular width this lipid has a cylindrical shape (Sprong et al., 2001). The choline/ethanolamine phosphotransferase (CEPT) uses CDP-choline and DAG to synthesize PC in the ER (Figure 1). PC can then be further metabolized into the important signaling molecules arachidonic acid,

important for the synthesis of prostaglandins and leukotrienes, and lysophosphatidylcholine (LPC) which can be further metabolized into platelet-activating factor (PAF) (Lagarde, Bernoud et al., 2001). PC is also involved in the synthesis of sphingomyelin, catalyzed by the sphingomyelin synthase (SGMS), which transfers the phosphocholine head group of PC to a ceramide molecule to form SM and DAG (Van Helvoort, Vant Hof et al., 1994). PC can additionally serve as a precursor for PS, a step that is catalyzed by the PS synthase 1 (PSS1) (Arikketh, Nelson et al., 2008).

Phosphatidylethanolamine: This glycerophospholipid is enriched at the inner mitochondrial membrane, at the inner leaflet of the PM and is, to a lesser extent, also present at the outer leaflet of the PM (Vance & Tasseva, 2013). The asymmetric distribution of PE at the PM is introduced by flippases, specific proteins, which will be discussed in more detail below (van Meer, 2011). PE belongs to the aminophospholipids because it harbors a primary amine attached to its head group. In comparison to PC, PE adopts a more conical molecular structure thereby introducing a curvature in the membrane it resides (Lonez, Lensink et al., 2010). The synthesis of PE can either be catalyzed by CEPT using CDP-ethanolamine and DAG or by the decarboxylation of PS mediated by PS decarboxylase (PSD), which occurs mostly in the mitochondria (Vance, 2008) (Figure 1).

Phosphatidylserine: In contrast to PC, anionic PS is mostly localized at the inner leaflet of the PM and in organelles involved in endocytosis. The synthesis of PS is catalyzed by the PS synthases PSS1 and PSS2, which attach an L-serine to PE or PC, respectively (Leventis & Grinstein, 2010) (Figure 1). The reaction of PSS2 is reversible and is necessary to counteract large amounts of PS building up in the membrane (Bohdanowicz & Grinstein, 2013). The major degradation pathway of PS into PE is mediated by the PSD. Importantly, flippases control the location of PS at the inner leaflet of the PM. During apoptosis, PS flips to the outer leaflet where it acts as a ligand for phagocytic receptors (Murakami, Tian et al., 2014). Other functional roles of PS were described in the context of blood clotting or mast cell degranulation (Martin, Pombo et al., 2000, Schoenwaelder, Yuan et al., 2009). Proteins harboring amphiphilic alpha helices such as K-Ras or Rho GTPases have been described to interact with membranes that are enriched for anionic PS because of electrostatic binding (Hancock, Paterson et al., 1990, Sun & Drubin, 2012).

Phosphatidylglycerol: As the first step of PG biosynthesis the phosphatidylglycerol phosphate synthase (PGPS) forms phosphorylated PG from glycerol-3-phosphate and CDP-DAG in the ER and in mitochondrial membranes before the product is further dephosphorylated

to make anionic PG (Ohtsuka, Nishijima et al., 1993). PGPS was found to be exclusively located at mitochondrial membranes (Kawasaki, Kuge et al., 2001).

Phosphatidylinositol: Phosphatidylinositol (PI) is synthesized by PI synthase (PIS) from inositol and CDP-DAG in the ER (Figure 1). PI is the only phospholipid that is phosphorylated directly at its head group. The inositol can be phosphorylated at three different positions by phosphatidylinositol kinases creating up to seven different polyphosphoinositides (PI(3)P, PI(4)P, PI(5)P, PI(3,4)P₂, PI(4,5)P₂, PI(3,5)P₂, PI(3,4,5)P₃) (Leventis & Grinstein, 2010). These phospholipids are very low abundant at the inner leaflet of cellular membranes and act as important signaling molecules for various cellular processes (Foster & Janmey, 2001), some of which are discussed further below.

Lysophospholipids: These lipids are generated by the phospholipase A (PLA)-mediated degradation of glycerophospholipids or the degradation of ceramide and are important signaling molecules (Hla, Lee et al., 2001). An interesting feature of lysolipids is that they are much less hydrophobic compared to lipid molecules with two FA chains, enabling them to move between different organelles through the cytosol (Bohdanowicz & Grinstein, 2013) (Figure 2). Similar to their glycerophospholipid counterparts, lysophosphatidylcholine (LPC) is the most abundant lysophospholipid (Makide, Kitamura et al., 2009). Lysophosphatidic acid (LPA) and S1P are lysolipids for which G-protein-coupled receptors (GPCRs) have been identified that can bind these lipids extracellularly and initiate downstream signaling processes including cell migration in lymphocytes and endothelial cells (Choi, Lee et al., 2008). Lysophosphatidylserine (LPSe) is involved in mast cell degranulation and triggers enhanced histamine release *in vivo* (Bruni, Bigon et al., 1984). The PS-specific PLA catalyzes the production of this lysolipid (Sato, Aoki et al., 1997). Lysophosphatidylethanolamine (LPE) has been recently implicated in increasing intracellular Ca²⁺ levels in breast cancer cells via an LPA GPCR indicating that these receptors can also bind other lysolipids (Park, Lee et al., 2013). And lysophosphatidylglycerol (LPG) was shown to stimulate chemotactic migration in human endothelial and natural killer cells (Jo, Kim et al., 2008, Lee, Lee et al., 2007). Lysophospholipids can also be reacylated by the activity of lysophospholipid acyltransferases (LPCAT) (Gijon, Riekhof et al., 2008).

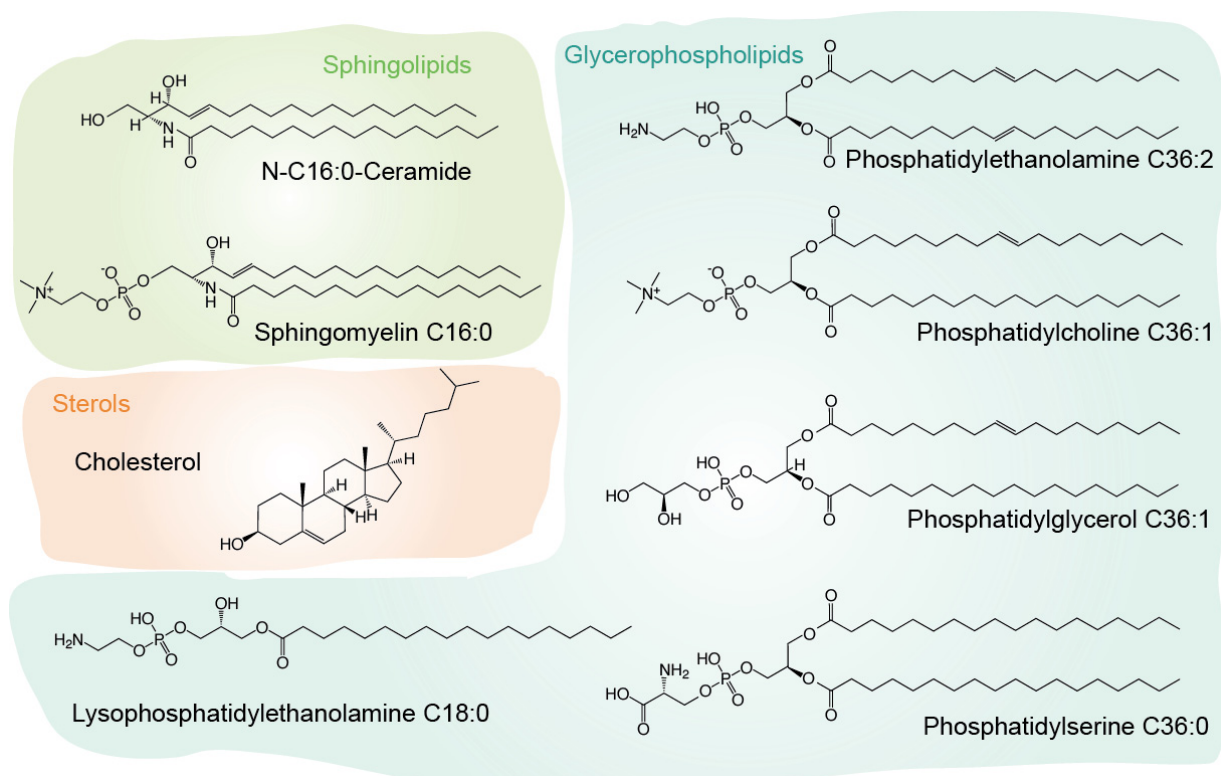


Figure 2: Lipid structures: Different lipid classes and examples of structures with specific FA chain lengths and saturation are shown

1.1.3 STEROL BIOSYNTHESIS

In contrast to glycerophospholipids and sphingolipids sterols are polycyclic consisting of several steroid rings and not FA chains (Figure 2). As other lipids, sterols are also amphipathic harboring a small polar head group, which is a single hydroxyl group and an apolar part, which is comprised of aliphatic groups attached to the steroid backbone (Fantini & Barrantes, 2009, Rose, Hanson et al., 1980). While cholesterol is the most abundant sterol in mammalian cells, yeast cells have high levels of ergosterol. The first steps in the biosynthesis of cholesterol and ergosterol are identical starting from acetyl-CoA used for the synthesis of mevalonate and catalyzed by HMG-CoA reductase (3-hydroxyl-3-methylglutaryl coenzyme A - HMGR) in the ER. Mevalonate is then further processed into squalene by a diverse set of kinases and synthases, which is subsequently used for the production of lanosterol. This sterol can then be further processed into ergosterol in yeast or into cholesterol in mammalian cells (Goldstein & Brown, 1990). When cellular cholesterol levels decrease, the sterol regulatory element-binding protein

(SREBP) is trafficked to the Golgi via COPII (coat protein complexes II) vesicles where SREBP is cleaved and can then enter the nucleus to drive the transcription of *Hmgcr* creating a feedback response to outbalance low levels of cholesterol in the cell (Espenshade & Hughes, 2007). Cholesterol is present in both leaflets of the membrane, but is more abundant in the inner leaflet (Mondal, Mesmin et al., 2009).

1.1.4 BIOPHYSICAL PROPERTIES OF DIFFERENT LIPID CLASSES

The variety of lipids translates into diverse biophysical properties of the different lipid classes. All glycerophospholipids are comprised of FA chains and a phosphate head group, which differs between the glycerophospholipid classes and is linked to the glycerol backbone. These different head groups further determine the overall charge of the membrane. While PC and PE molecules are zwitterionic, PS and PI molecules are anionic. Both, head group and FA chains can influence the biophysical properties of lipids. A variety of FAs are found in glycerophospholipid molecules differing in chain length and/or saturation level, especially influencing the packing properties of the membranes they constitute (Litman & Mitchell, 1996). PC, for instance, usually harbors one unsaturated acyl chain, which lowers the packing density and increases membrane fluidity (Koynova & Caffrey, 1998). The other zwitterionic glycerophospholipid PE has a comparatively small head group which leads to an overall more conical shape of the entire molecule, similar to PA. This property allows the molecule to induce a negative curvature in the membrane, which increases with the level of unsaturation of its FA chains (Hui, Stewart et al., 1981). Lysophospholipids can induce negative and positive curvatures because their head group is larger than the tail (Sprong et al., 2001). As anionic lipids PS and PI also serve to modulate the charge of the membrane and are mostly found in the inner leaflet mediating interactions with polycationic proteins (Magalhaes & Glogauer, 2010, Yeung & Grinstein, 2007). Additionally, different transmembrane domain proteins harbor cytoplasmic tails that can detect membrane charge and thus induce conformational changes in the protein in response to a change of the membrane surface charge (Alexander, Jaumouille et al., 2011).

Sphingolipids are usually comprised of saturated or monounsaturated FAs, thus compared to PC, they increase the packing density of the membranes (Slotte, 2013). This packing density is relieved by the addition of sterols, which interfere with the acyl chain binding of two lipid molecules directly, making the membrane more fluid. On the other hand, sterols can also rigidify a membrane, which consists mostly of loosely packed lipid with unsaturated FA

chains (Simons & Ikonen, 2000). This means that the addition of sterols provides the cell with a mechanism to fine-tune its membrane fluidity in response to changes in lipid composition. Together with sphingolipids and membrane-associated proteins sterols form dynamic segregations at the outer leaflet of the PM membrane, called rafts or microdomains. These sphingolipid-rich regions are characterized to be more ordered than other regions of the membrane and can be detected using fluorescent probes (Harder, Rentero et al., 2007, Lingwood & Simons, 2010). Especially glycosylphosphatidylinositol (GPI)-anchored proteins are associated with these membrane microdomains (Friedrichson & Kurzchalia, 1998).

1.1.5 LIPID DISTRIBUTION AND TRAFFICKING IN THE CELL

Although the majority of lipids are synthesized in the ER or the Golgi, their distribution varies between the different cellular organelles as well as the two leaflets of cellular membranes. These differences in lipid distribution regulate the biophysical properties of membranes and translate into functional consequences, tailored to the requirements of the cell. To achieve this selective distribution, lipid molecules translocate through the cytosol or are actively trafficked between organelles and across the leaflets of the membranes by specialized proteins or vesicle transfer (Pomorski, Hrafnisdottir et al., 2001).

Lipid Trafficking in the Cytoplasm: Following the synthesis of lipids in the ER, different lipid classes are shuttled through the cell using vesicles from the TGN. Specific lipid compositions have been identified in these vesicles and are thought to contribute to the formation of lipid microdomains found at the PM (Lingwood & Simons, 2010). More specifically, analysis of the lipid composition revealed that retrograde vesicles transported from the TGN to the ER contained lipids that were predominately found in the ER while anterograde vesicles transported from the TGN to the PM contained high levels of SM and cholesterol, lipids that are enriched at the PM compared to the donor membrane of the TGN (Brügger, Sandhoff et al., 2000). These findings hint towards lipid sorting mechanisms involved in vesicles formation. In fact, this sorting could be necessary for the initiation of the budding and vesicle formation. Lateral separation of lipids with different biophysical properties in the membrane can cause tension between the ordered and the less ordered phases. This tension is relieved when a part of the membrane curves and is budded outward (Jülicher & Lipowsky, 1993). And this budding process could be further implicated in a feed-forward mechanism recruiting more lipids favoring

curved membranes as well as proteins with domains recognizing the membrane curvature (Itoh & De Camilli, 2006, Sorre, Callan-Jones et al., 2009). Interestingly, depletion of PC levels only altered protein transport within the TGN and not from the ER to the TGN. However, strong morphological changes were observed in the ER and not in the Golgi or the PM. These findings indicate that the protein transport function of vesicles and the morphology of organelles depend on different lipids and their composition (Testerink, van der Sanden et al., 2009). Analysis of the vesicle shuttling from the ER to the PM also shows that lipids and proteins use the same routes and their functions could possibly depend on this coupled transport (Surma, Klose et al., 2011) (Figure 3).

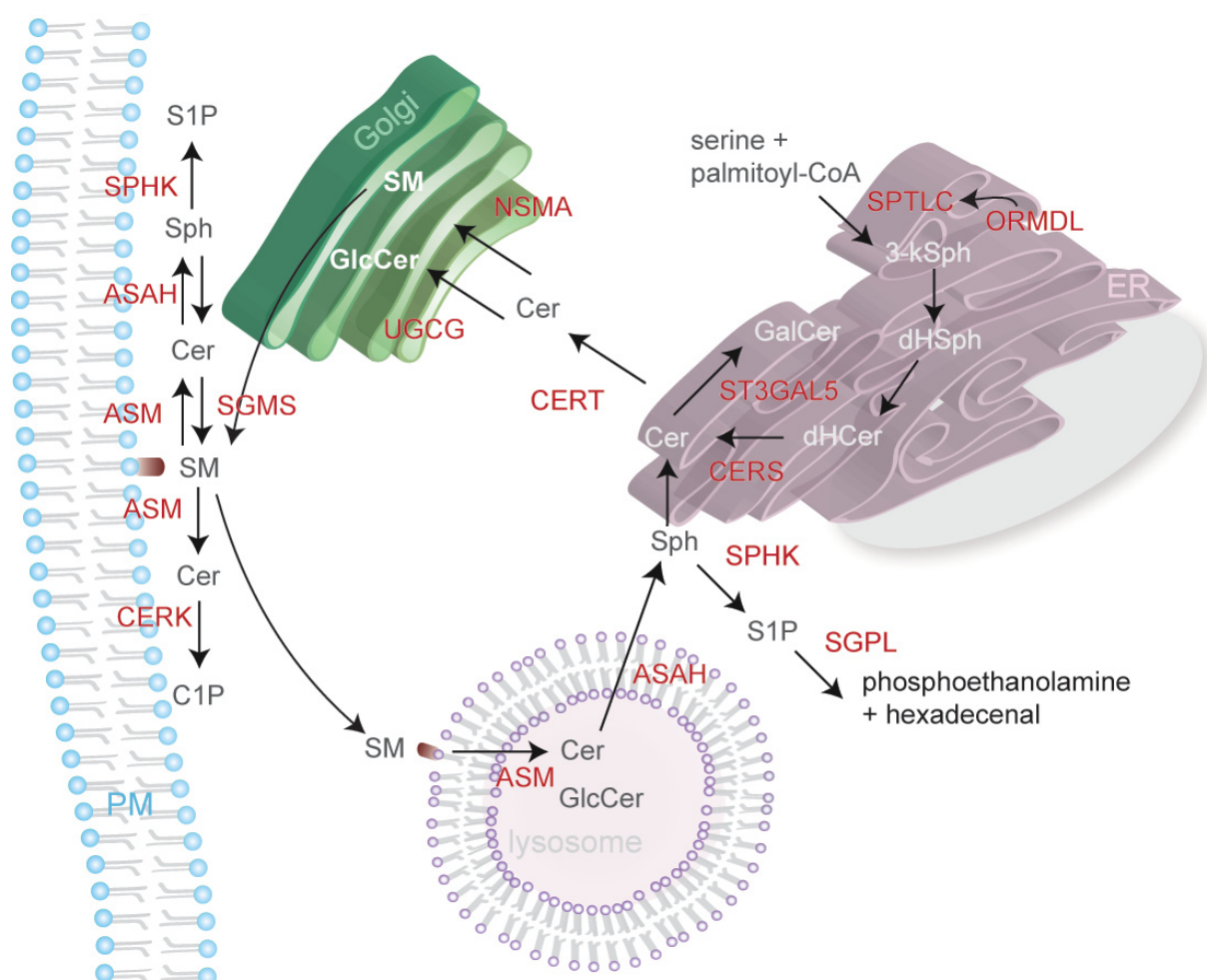


Figure 3: Subcellular localization of sphingolipid metabolism: Different metabolic steps are illustrated in the sphingolipid metabolism. CERK: Ceramide kinase, UGCG: Ceramide glucosyltransferase, ST3GAL5: Ganglioside GM3 synthase, Cer: Ceramide, 3-kSph: 3-ketosphingosine, Sph: Sphingosine, dhSph: Dihydrosphingosine, dhCer: Dihydroceramide, GalCer: Galactosylceramide, GluCer: Glucosylceramide. PM is represented in blue, lysosome is represented in pink, Golgi is represented in green, and ER is represented in purple.

Lipid Transfer Proteins: Since lipids are strongly hydrophobic molecules the spontaneous translocation between separated membranes occurs very slowly but still contributes to the differences in lipid distribution. It has been shown, for instance, that unsaturated glycerophospholipids are able to translocate faster between membranes compared to their saturated forms *in vitro* (Silvius & Leventis, 1993). Especially, lysolipids can move rather rapidly between different membranes and it is intriguing to speculate that these lipids could mediate glycerophospholipid transfer between organelles by being reacylated at the target membrane. Apart from vesicle transfer, lipids can also be transported as single molecules from one membrane to the other. This is especially important to fine-tune the lipid composition of organelles, which are not connected to the ER by vesicular trafficking such as the mitochondria or peroxisomes (Tatsuta, Scharwey et al., 2014). To mediate the quick bidirectional lipid transfer between different organelles within the cell, proteins with specific hydrophobic lipid-binding domains have evolved. These lipid transfer proteins harbor binding motifs making them selective for certain membranes in the cell. The pleckstrin homology (PH) domains, for instance, bind PI(4)P and are required for the protein recruitment to the TGN (Godi, Di Campli et al., 2004). The oxysterol binding proteins (OSBPs) can bind and carry glycerophospholipids such as PS, transported by Osh6 and Osh7, from the ER to the PM in yeast (Maeda, Anand et al., 2013). Osh4, a different lipid binding protein in yeast can bind sterols or PI(4)P in a mutually exclusive way, thus shuttling sterols from the ER to the TGN and PI(4)P back to the ER (Mesmin, Bigay et al., 2013). And the steroidogenic acute regulatory (STAR) proteins have been shown to mediate cholesterol transport from the outer to the inner mitochondrial membranes in mammalian cells (Miller, 2007). Some lipid carriers such as CERT or the glucosylceramide transfer protein (FAPP2) can bind two membranes simultaneously as they contain two specific binding motifs (Hanada, Kumagai et al., 2003, Yamaji, Kumagai et al., 2008). This feature enables CERT to function at the ER and the TGN and perhaps to even mediate the formation of membrane contact sites between the two organelles (Levine, 2004) (Figure 3).

Lipid Transport in the Membrane Bilayer: Lipid composition not only varies between the different organelles of a cell, it also varies between the inner and the outer leaflet of the lipid bilayer. Glycerophospholipids are asymmetrically arranged between the leaflets of cellular membranes, with the aminophospholipids PS, PE, and PI mainly located at the inner leaflet of the PM, while PC and PG are evenly distributed across both leaflets (van Meer, 2011). Within a cellular membrane only a few lipid classes such as DAGs can flip spontaneously across the lipid bilayer. Other lipids contain large head groups that hinder the translocation across the

hydrophobic membrane (Beyers, Comfurius et al., 1999). To aid their translocation there are specialized proteins namely scramblases, flippases, and floppases. Scramblases are energy-independent proteins that move lipids across the leaflets in both directions. During apoptosis, for example, these proteins are important for exposing PS on the outer leaflet of the PM (Leventis & Grinstein, 2010). While scramblases work against the asymmetric distribution of different lipid classes between the two leaflets, flippases and floppases create this distribution. These enzymes are energy-dependent and transport lipids actively from the outer leaflet (flippases) to the inner leaflet and back (floppases) (Hankins, Baldrige et al., 2015). Flippases belong to the family of P4 ATPases and are important for maintaining mainly PS and PE at the inner leaflet (Perez, Gerber et al., 2015) while floppases belong to the ATP-binding cassette (ABC) transporters which are transmembrane domain proteins transporting a variety of different molecules across the cellular membranes. These floppases also transfer lipids onto acceptors outside of the cell membrane, for instance onto lipoprotein particles (van Meer, Halter et al., 2006). So far specific flippases or floppases have only been identified for glycerophospholipids and sterols, not for sphingolipids. However, ceramide molecules were shown to flip between the two leaflets and this movement was inhibited as soon as ceramides were located within microdomains (Hannun & Obeid, 2008, Lopez-Montero, Rodriguez et al., 2005). Further, glycosylated ceramides are usually detected at the outer leaflet of the PM or the Golgi even though the glycosylation events occur at the inner leaflet of the Golgi indicating that glycosylated ceramides are also able to flip across the bilayer (van Meer & Hoetzel, 2010).

Distribution and Function of Lipids in Cellular Membranes: As the main site of lipid synthesis, the ER produces the majority of glycerophospholipids, ceramides, and sterols. Interestingly, the ER only has low amounts of detectable sterols, because upon synthesis, sterols are rapidly distributed to other cellular membranes via vesicle-mediated lipid trafficking pathways or lipid transfer proteins described earlier (Bretscher & Munro, 1993, van Meer et al., 2008). Another important organelle of lipid biosynthesis is the Golgi, specialized for the synthesis of sphingomyelin and more complex ceramides such as glucosylceramides and galactosylceramides (Henneberry, Wright et al., 2002) (Figure 3). These glycosphingolipids are trafficked to the PM and flipped to the outer leaflet by a yet unknown mechanism (Devaux, 1991). In contrast to the ER and the Golgi, the PM contains high levels of sphingolipids and sterols, which introduce a higher packing density and increase the rigidity of the membrane (Klemm, Ejlsing et al., 2009). Several proteins important for the synthesis or degradation of specific lipids are found at the PM, including the sphingomyelin synthases, the neutral sphingomyelinases, or the sphingosine kinases (Milhas et al., 2010) (Figure 3). The lipid composition of the early

endocytic vesicles is similar to that of the PM, rich in cholesterol and PS, and during endosomal maturation PS and cholesterol levels are strongly decreased. Polyphosphoinositide species at the vesicle membrane are used as markers to distinguish between the different steps of endosomal maturation. More specifically, PI(4,5)P₂ is present at the PM, PI(3)P is found in early endosomal membranes, PI(3,5)P₂ is located in late endosomal membranes, and PI(4)P is detected in the TGN. These different polyphosphoinositide species are recognized by proteins of the vesicle transport machinery, positioning lipid-protein interactions as an important regulatory mechanism of endosome maturation (Di Paolo & De Camilli, 2006). FA chain length of a lipid molecule as well as the saturation level also determines the localization inside the cell. Sphingolipids and glycerophospholipids with longer FA chains are found at the PM, where they interact with sterols, increasing the membrane thickness compared to the ER membrane. Shorter and more saturated FA chains are found in lipids of the ER or Golgi membranes (Schneider, Brügger et al., 1999). In the sphingolipid metabolic pathway specific CERS regulate the FA chain length of ceramides. While CERS6 catalyzes the reaction to shorter ceramide species with a FA chain length of C14 to C16, CERS1 and CERS4/5 synthesize species of chain lengths C16 to C20, and CERS2 forms the longest ceramide species ranging from C22 to C26 (Mullen, Hannun et al., 2012). The biological function of different ceramide species is mostly unknown which is why this topic is currently subject to extensive investigations.

1.1.6 REGULATION OF MEMBRANE LIPID METABOLISM

Regulation of Glycerophospholipid Homeostasis: Apart from the spatial regulation of lipid synthesis and lipid trafficking, the expression of the different enzymes is strictly regulated to maintain membrane lipid homeostasis or to adapt to different cell stresses. One mechanism of protein-mediated regulation is product inhibition, which has been mostly studied using PS-containing vesicles. Treatment of mammalian cells with these vesicles and not any other lipid vesicles inhibited the synthesis of PS by PSS1 and PSS2 (Kuge, Saito et al., 1999). Similarly, the PIS could be inhibited with vesicles containing high levels of PI (Imai & Gershengorn, 1987). These feedback mechanisms do not necessarily have to be product specific but could be initiated by changes in the biophysical properties of the membrane properties. Differences in the absolute levels of certain lipid classes also alter the lipid composition of the membrane as well as its biophysical properties. Several studies simulated membrane properties and proposed, for instance, that stored elastic energy could be a potential regulator of membrane homeostasis by

feeding back to modulate the biosynthesis of PC and other lipids (Alley, Ces et al., 2008, Beard, Attard et al., 2008). Another regulatory mechanism is the metabolic crosstalk between the different lipids important for directing the metabolic fluxes across the network in case of a perturbation. For example, cells with decreased PC biosynthesis were shown to increase their PE and PI content, thereby adapting to the low levels of PC by enhancing its synthesis from PE (Boumann et al., 2006). Protein and lipid synthesis are also tightly linked as increased protein load of the ER leads to an expansion of its membranes to buffer high protein concentration. This membrane expansion was shown to be mediated by an increase in PC synthesis leading to an excess production of PC, which was then counteracted by upregulation of PLA2 (Lykidis, Baburina et al., 1999).

Regulation of Sphingolipid Homeostasis: The most important regulators of sphingolipid homeostasis are proteins mediating the underlying metabolic processes. Several enzymatic steps in the sphingolipid metabolism are reversible and can be shifted in one or the other direction; however, the initial step of *de novo* synthesis catalyzed by the SPT complex and the terminal step catalyzed by the S1P lyase are considered to be unidirectional (Breslow & Weissman, 2010). Interestingly, the initial step involving serine and palmitoyl-CoA is strongly dependent on the intracellular serine levels of a cell linking sphingolipid metabolism and amino acid levels (Dickson, Lester et al., 2000). In yeast, one important signaling pathway for the regulation of sphingolipid metabolism is Torc2, which is required for optimal ceramide synthase activity. This regulation is mediated by the kinase Ypk2 and is inhibited by the phosphatase calcineurin (Aronova, Wedaman et al., 2008). This pathway has not been studied in mammalian cells and the exact mechanism of how Torc2 senses and increases ceramide levels is yet unknown.

1.1.7 CROSSTALK BETWEEN STEROLS, SPHINGOLIPIDS, AND GLYCEROPHOSPHOLIPIDS

The lipid composition of different organellar membranes described earlier is strongly dependent on each of the membrane components and changes when lipid classes increase or decrease. Sphingolipids, for example, are associated with sterols in microdomains. Therefore, a change in sphingolipid levels also greatly alters the absolute levels of sterols in the membrane (Guan, Souza et al., 2009). Studies have shown that upon decreased sphingolipid levels more sterols shuttle from the PM to the ER where they are detected by the specific sterol sensor

SREBP, leading to the initiation of downstream signaling and activating the uptake and biosynthesis of cholesterol (Brown & Goldstein, 2009, Chang, Chang et al., 2006). Additionally, non-vesicular transport of ceramides from the ER to the Golgi via CERT is increased, hence, forming a sterol-mediated feedback loop to enhance the production of sphingomyelin at the PM (Olkonen & Li, 2013). This sterol-dependent regulation of CERT is mediated by OSBP whose sterol trafficking function is also increased upon SM depletion at the PM (Perry & Ridgway, 2006). Sphingolipids have been further implicated in the post-translational control of SREB and sphingolipid synthesis was shown to induce SREBP-mediated transcription (Worgall, 2008). Sterols and sphingolipids also share the same extracellular transport mechanisms within lipoprotein particles (Nilsson & Duan, 2006). In human macrophages, free cholesterol loading led to the degradation of ORMDL1 following its relocation from the ER to autophagosomes. This enhanced the activity of *de novo* ceramide synthesis in the ER (Wang, Robinet et al., 2015). In *Drosophila melanogaster*, evidence for regulatory crosstalk between sphingolipids and other lipid classes has also been found. The only ceramide synthase *schlank* has been identified to not only regulate sphingolipid metabolism but also FA synthesis by increasing the expression of SREBP and decreasing the expression of triacylglycerol lipase (Bauer, Voelzmann et al., 2009). The inhibition of cholesterol synthesis inhibits PC synthesis and, conversely, cholesterol loading of macrophages induces the synthesis of PC (Cornell & Goldfine, 1983, Shiratori, Okwu et al., 1994). This metabolic relationship is described to buffer increasing ER cholesterol levels to avoid ER stress. It also facilitates the induction of the unfolded protein response and apoptosis if the PC synthesis is blocked (Feng, Yao et al., 2003).

Metabolic Crosstalk between Sphingolipids and Glycerophospholipids: Even though the general structure of FA chains attached to a head group is quite similar between sphingolipids and glycerophospholipids, surprisingly little is known about the metabolic crosstalk between these two lipid classes. So far the best-described points of metabolic overlap have been identified between (1) SM and PC, and between (2) S1P and PE. (1) SM and PC both have a phosphocholine group attached to their functional head group which, when cleaved off, results in the formation of ceramide or DAG, respectively. This way, the sphingomyelin synthases and phospholipases C can, depending on the requirements of the cell either limit the amounts of SM or PC (Huitema, van den Dikkenberg et al., 2004). (2) S1P is another metabolic link between sphingolipids and glycerophospholipids. It can be irreversibly degraded by the enzyme SGPL1 generating phosphoethanolamine and hexadecenal. Both products are important in the synthesis of glycerophospholipids. Phosphoethanolamine can enter the pathway of PE synthesis via the CDP-ethanolamine pathway (Kihara, 2014). And hexadecenal is used in

the FA metabolic pathway and the generation of palmitoyl-CoA, which contributes to the synthesis of LPA (Hannun & Obeid, 2008) (Figure 1).

The FA molecules that are present in sphingolipids and glycerophospholipids also link the lipid classes metabolically. For instance, during lipid degradation the FA chains derived from PC can be used for the biosynthesis of ceramide, and the degradation of sphingolipids yields FAs used for the synthesis of glycerophospholipids (Meyer, Karow et al., 2005). The conversion of sphingolipids into glycerophospholipids has been shown by a study supplementing different human cell lines with radioactively labeled sphingosine. In the course of four hours glycerophospholipids had incorporated up to 35% of total radioactivity (Nakahara et al., 2012).

Regulatory Crosstalk between Sphingolipids and Glycerophospholipids: In yeast, a regulatory mechanism between sphingolipids and glycerophospholipids has been identified during which the kinase Ypk1 downregulates the aminophospholipid flippase activator Fpk2. This downregulation could be counteracted by a complex ceramide species, thus, regulating the overall distribution of glycerophospholipid between the lipid bilayer. Conversely, inhibition of the synthesis of this ceramide species restored the downregulation of another flippase activator kinase Fpk1 (Roelants, Baltz et al., 2010). These findings show that there are regulatory feedback mechanisms between sphingolipids and glycerophospholipids, modulating the distribution of different lipids across the membrane.

Important links between the polyphosphoinositide species PI(4)P and sphingolipid metabolism has been recently reported in yeast. A member of the SPOT complex that regulates the *de novo* synthesis of sphingolipids is the PI(4)P phosphatase Sac1 (Breslow & Weissman, 2010). However, the mechanism of how this protein and its lipid-binding properties regulate sphingolipid metabolism is so far unknown. PI(4)P is also important for the function of the proteins CERT and FAPP2, regulating non-vesicular ceramide and glucosylceramide transfer, respectively. Both proteins harbor PH domains that bind to PI(4)P, which are thought to mediate the recognition of the acceptor membrane of the Golgi (D'Angelo, Polishchuk et al., 2007). Furthermore, ceramide-1-phosphate (C1P) has been implicated in the direct regulation of cPLA2 and its translocation from the cytosol to the Golgi (Pettus, Bielawska et al., 2004). This finding describes another interesting regulatory mechanism how sphingolipids can regulate enzymes important for glycerophospholipid metabolism.

Interestingly, the ABCA1-mediated efflux (floppase activity) of cholesterol and PS is influenced by sphingomyelin levels. The pharmacological depletion of sphingomyelin levels

leads to higher PS exposure and higher cholesterol efflux (Gulshan, Brubaker et al., 2013). Furthermore, SPTLC1 has been shown to bind directly to ABCA1 in the ER, thus limiting the protein expression of ABCA1 at the PM. Myriocin, an inhibitor of SPT can disrupt this binding and ABCA1 is then trafficked to the PM (Tamehiro, Zhou et al., 2008). Sphingomyelin reduction also inhibits the protein turnover of ABCA1 at the PM (Yamauchi, Hayashi et al., 2003).

Functional Crosstalk between Sphingolipids and Glycerophospholipids: Although there is a lot known about the general metabolism and cellular distribution of sphingolipids and glycerophospholipids throughout the different membranes, there are surprisingly few studies on the functional relationships between these two lipids classes. It is apparent that lipids from both classes are required for proper membrane function and cellular integrity as genetic perturbations of important enzymes of both metabolic networks lead to lethality in mice (Schiffmann, 2015, Vance & Vance, 2009). Electron microscopy of human epithelial cell membranes could show that PS is not evenly distributed at the inner leaflet of the PM. Instead, it is connected to clusters of sphingomyelin and cholesterol, which are at the outer leaflet of the membrane (Fairn, Schieber et al., 2011). Studies on membrane composition have further revealed that sphingomyelin can directly bind to PC (Massey, 2001). Both of these lipid molecules have a cylindrical shape inside the membrane, important for densely packed FA chains. And only recently, studies could show that loss of lipids from one lipid class can be counteracted by increasing lipids from the other lipid class. In yeast, for example, genetic targeting of a phosphoinositide phosphatase in combination with an inhibitor of sphingolipid metabolism led to synthetic lethality, showing that the genetic impairment of glycerophospholipid metabolism could be counteracted by the cell as long as the sphingolipid metabolism was intact (Tani & Kuge, 2010). Other studies in yeast could demonstrate that a loss of complex and long-chained sphingolipids induced the synthesis of glycerophospholipids containing very long chained FA chains, possibly functionally compensating for the missing sphingolipid species (dos Santosa, Riezman et al., 2014, Vionnet, Roubaty et al., 2011).

1.1.8 QUANTITATIVE LIPIDOMICS

An important step in lipid research has been the development of lipidomics. This is a mass spectrometry-based method used for the identification and quantification of individual lipid species (Wenk, 2005). It has become clear that even though lipids are seemingly simple

molecules compared to proteins, for instance, a cell can have up to 100 000 different lipid species in their membranes (Shevchenko & Simons, 2010, van Meer, 2005). These lipid species differ in saturation and hydroxylation levels, in FA chain lengths or ester/ether linkage of the moieties to the backbone. All of these features can be detected and quantified using lipidomics. The detection and the identification of individual FA chains of one lipid molecule require tandem mass spectrometry (Han & Gross, 2005). In general, the field of lipidomics depends on the availability of synthetic standards to be able to quantify the absolute levels of individual lipids in a sample. Additionally, the unification of lipid extraction protocols and lipid nomenclature is still ongoing in the field. Other drawbacks are the exact localization of double bonds within the molecules and the discovery of new unknown lipid molecules, which is still dependent on the comparison with known lipid species (Wenk, 2010).

1.1.9 LIPID STORAGE DISORDERS

The degradation of most sphingolipids occurs in the lysosomal compartments, which provide the responsible enzymes with the acidic environment they require for optimal efficiency. Mutations in genes involved in lipid degradation or transport cause lipid storage disorders in humans, of which around 40 have been identified until now (Sillence & Platt, 2003). Selected examples are described here.

Gaucher Disease: This autosomal recessive disorder is caused by mutations in the glucocerebrosidase gene *GBA*. The gene product, glucosylceramidase, catalyzes the reaction of glucosylceramide to ceramide. A large neonatal screening campaign of newborns revealed that the prevalence for Gaucher disease is one in around 17 000 births (Mechtler, Stary et al., 2012). Around 300 unique mutations have been identified of which most are missense mutations leading to the misfolding of the protein and further to its degradation (Hruska, LaMarca et al., 2008). Patients harboring these mutations show a severely reduced enzymatic activity of glucosylceramidase and suffer from hepatosplenomegaly, thrombocytopenia, and bone malformations. According to the severity of the symptoms and whether or not they also involve neuropathological symptoms, patients are classified in three different types of Gaucher disease. While type 2 manifests early after birth, type 1 or type 3 patients either develop symptoms in early adolescence or in early childhood, respectively (Grabowski, 2008).

Krabbe Disease: This autosomal recessive disorder is caused by mutations in the gene *GALC*, which severely reduce the enzymatic activity of the gene product galactosylceramidase. Similar to the mutated *GBA* causing Gaucher disease, the mutated *GALC* shows impaired activity to degrade a complex sphingolipid and form ceramide. Over 110 different mutations have been identified; however, the most common mutation is a 30kb deletion reducing the residual enzyme activity to 5% or less. One child in 100 000 births is diagnosed with this disorder and around 90% of the patients develop severe neurological symptoms early after birth leading to death before the age of two (Wenger, Rafi et al., 1997).

Farber Disease: This extremely rare disorder is also called Farber lipogranulomatosis and only occurs once in one million births (Fensom, Neville et al., 1979). Patients harbor mutations in the acid ceramidase gene *ASAH1* leading to greatly reduced enzymatic ceramidase activity. Currently, 17 different mutations have been identified of which most are point mutations (Bar et al., 2001). Similar to Krabbe disease the onset of Farber disease is shortly after birth leading to deformed joints and neurological phenotypes causing death before the age of two (Bar et al., 2001).

Chediak-Higashi Syndrome: In contrast to the other diseases, this lysosomal storage disorder is not caused by mutations in metabolic enzymes but rather by mutations in the gene *LYST*, which encodes for a lysosomal trafficking factor important for lysosome morphology (Ward, Griffiths et al., 2000). Patients diagnosed for Chediak-Higashi syndrome show symptoms such as progressive neurologic defects, lymphoproliferative phenotypes, and hypopigmentation (Introne, Boissy et al., 1999). There is also a high incidence of deaths caused by bacterial infections of the skin or the respiratory tract (Padgett, Reiquam et al., 1967) suggesting that this lysosomal regulator is important for an efficient immune response.

Other well-described lysosomal storage disorders include Niemann-Pick disease A, B, and C, caused by mutations in the acid sphingomyelinase gene *SMPD1*, or the cholesterol transporter *NPC1*, respectively (Schuchman & Wasserstein, 2015). Also, Fabry disease, Sandhoff, and Tay-Sachs diseases manifest in patients with mutations in lipid metabolizing enzymes (Kolter & Sandhoff, 2006). Since almost all of these diseases show progressive neurological symptoms, early diagnosis is the first critical step of treatment. After diagnosis, therapeutic strategies used for these patients are hematopoietic stem cell transplantations or enzyme replacement therapy (Malatack, Consolini et al., 2003). Currently, other treatment options are being developed such as substrate reduction therapy. This approach is based on metabolically limiting the levels of the lipid substrate and thereby also reducing the enhanced

product levels in these diseases. This strategy is already used in the treatment of Gaucher disease by pharmacologically inhibiting the enzyme glucosyltransferase CGT and was recently proposed to work in Fabry disease as well, a disease that also leads to the accumulation of glycosphingolipids (Ashe, Budman et al., 2015, Platt & Jeyakumar, 2008). For Niemann-Pick Type C patients, who accumulate cholesterol in the lysosome, clinical trials with statins or low-cholesterol diet failed, however, to improve the clinical outcome (Patterson & Platt, 2004). Another approach that has been developed is the pharmacological chaperone therapy, a strategy that uses molecules, which have been found to chaperone the misfolded proteins and stabilize them, thereby inhibiting their degradation and increasing the transport into the lysosome. Clinical trials for this chaperone therapy are currently ongoing for Gaucher and Fabry disease patients (Parenti, 2009).

1.2 IMPORTANCE FOR SYSTEMATIC APPROACHES TO STUDY LIPID METABOLISM

The enzymatic machinery of lipid metabolism has been discovered and characterized extensively over the past decades and especially genetic screens in yeast have contributed tremendously to the advances in dissecting lipid metabolism (Beeler, Bacikova et al., 1998, Desfarges, Durrens et al., 1993). Only in the last years, studies in lipid biology have focused more on the functional properties of lipids in a cell. These studies have suggested that cellular lipids act in concert with a variety of other lipids, proteins, and metabolites (Dickson, Sumanasekera et al., 2006). Apart from providing the cell with structural boundaries and the environment for transmembrane proteins, lipids are also important signaling molecules that can bind directly to proteins and act as regulators of protein activity. While this has been, so far, only shown for single lipid molecules, the notion that a group of lipids can functionally regulate proteins inside the membrane is becoming increasingly clear. A cell does not only regulate the function of single proteins with the help of its membrane lipids but it can also regulate entire cellular processes such as polarization, cell growth, or cell movement (Zanghellini, Natter et al., 2008). The coordination of these processes requires a finely tuned regulation of lipid metabolism and trafficking in order to maintain the ratio of different lipids and, with that, membrane function and integrity (Walker, Jacobs et al., 2011). Regulatory processes, which are used to guarantee that lipid rearrangement does not alter the overall lipid ratio, have been described already (van Meer et al., 2008). However, the exact consequence of altered lipid ratios is still unknown. The study of the function and regulation of lipid metabolism requires a systematic approach

dissecting various parts of the different membrane lipid pathways, characterizing their function, and integrating the results to obtain a global picture of how a cell regulates their lipid metabolism in biological processes (Ejsing, Sampaio et al., 2009). It is essential to study the functional roles of lipids in the context of the entire cell and not in isolated systems. Given this high order of complexity, systems biology approaches have shown to be successful in integrating high-throughput transcriptional, proteomic, and metabolomics data (Herrgard, Lee et al., 2006, Kell & Oliver, 2004). Using these approaches, lipid fluxes in the network could be detected and mapped. Predictive simulations have also been performed, identifying new regulators of lipid metabolism (Gombert, Moreira dos Santos et al., 2001). Especially the intersection of experimental data and mathematical modeling has been shown to synergize in retrieving new insights into the metabolic regulation (Famili, Forster et al., 2003). With this quantitative description of biological processes new regulators, lipid transfer mechanisms, and novel metabolic connections have been revealed (dos Santos et al., 2014, Maeda et al., 2013). The advances in lipidomics have now enabled the data-driven approach to not only reveal novel insights into lipid regulation but to also to begin the systematic annotation of lipid function in various biological processes (Dennis, 2006). Especially the macrophage biology has been in focus recently, as inflammatory stimuli have been shown to greatly and rapidly change the lipidome of these cells (Dennis, Deems et al., 2010).

1.3 INNATE IMMUNITY

The innate immune system is the first line of defense against various pathogens. Upon encounter of a virus or a bacterium, cells of the immune system such as macrophages or dendritic cells recognize the pathogen-associated molecular patterns (PAMPs) using specific receptors and activate signaling pathways that lead to the expression of inflammatory genes including cytokines and chemokines. These are important molecules mediating cell-cell communication throughout the entire organism to coordinate innate and adaptive immune responses (Janeway & Medzhitov, 2002).

1.2.1 TOLL-LIKE RECEPTORS

There are several classes of pathogen recognition receptors in mammalian cells, including NOD-like receptors, AIM2-like receptors, RIG-I-like receptors, and intracellular DNA sensors (Fritz, Ferrero et al., 2006, Pichlmair, Schulz et al., 2006, Schroder, Muruve et al., 2009). One of the well-characterized receptor families of the innate immune system are the Toll-like receptors (TLRs), which are highly conserved transmembrane proteins that recognize a variety of PAMPs. Ten different members of the TLR family have been identified in human and 12 in mouse (Akira & Hemmi, 2003). These receptors are either localized at the PM (TLR1, 2, 4 – 6 and 10) or in endosomal compartments (TLR3, 7 – 9, 11 – 13). They are expressed in immune cells such as macrophages or dendritic cells, as well as in cells that are not directly associated with the immune system such as fibroblasts or adipocytes (Batra, Pietsch et al., 2007). Recognition of PAMPs by TLRs is mediated by homo- or heterodimers in combination with different cofactors assisting ligand binding and regulating complex assembly (Takeda & Akira, 2004).

PAMP Recognition: In order to cover a variety of pathogens the TLRs have evolved and specialized to recognize different pathogen-specific molecules. This recognition also depends on their location within the cell (Figure 4). More specifically, TLRs that reside at the PM recognize bacteria-specific components such as diacylated and triacylated lipopeptides or lipoteichoic acids and peptidoglycan bound by TLR1, TLR2, or TLR6, respectively. TLR4 recognizes lipopolysaccharide (LPS) and TLR5 is activated by flagellin. All of these PAMPs are highly abundant in either gram-positive or gram-negative bacteria (Takeda & Akira, 2015). In contrast, the intracellular TLRs recognize PAMPs that are derived from bacterial or viral nucleic acids. For instance, TLR3 binds double-stranded RNA, while TLR7 binds single-stranded RNA and TLR9 recognizes unmethylated bacterial or viral CpG-DNA motifs (Kawai & Akira, 2010).

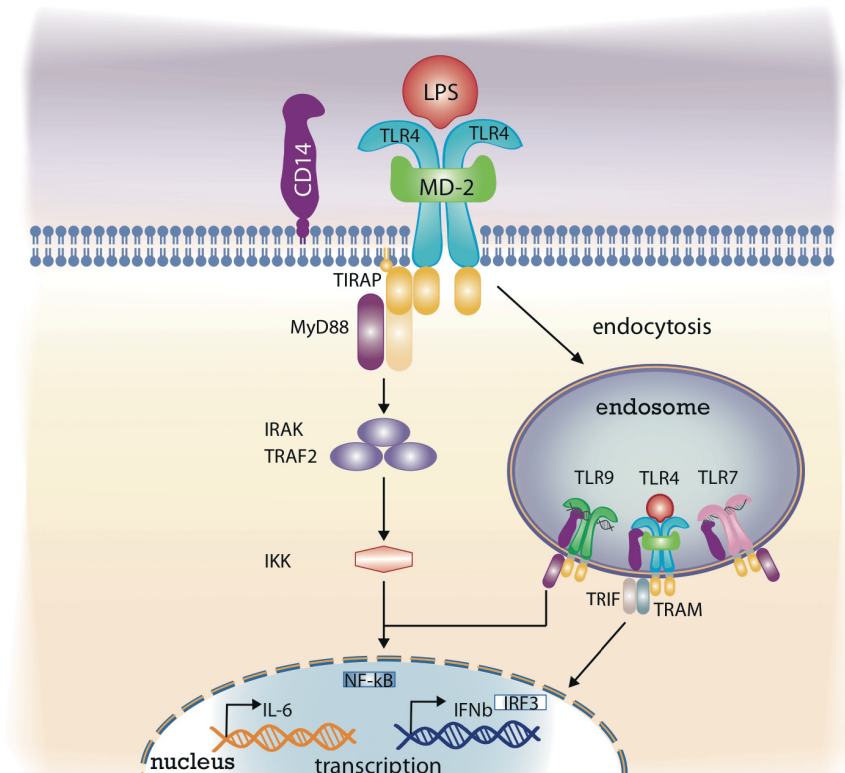


Figure 4: TLR signaling processes: TLRs are located at the PM or the endosomal membrane. Different TLRs and their ligands are depicted (TLR9, green; TLR4, blue; TLR7, pink). TRIF domain-containing adaptor proteins (yellow) and downstream signaling proteins are shown (MyD88, purple; IRAK, TRAF2, blue; IKK, orange). Transcription of representative cytokines (IL-6 and IFN β) is shown.

TLR Adaptors and Signaling: Different signaling pathways downstream of TLRs are activated upon PAMP recognition. While the extracellular domain of the receptor mediates the recognition of PAMPs, the intracellular Toll/IL-1 receptor (TIR) domain at the inner leaflet of the membrane binds to the TIR domain of different adaptor proteins to initiate the signaling events (Botos, Segal et al., 2011). All TLRs, except TLR3, can recruit the adaptor protein MyD88 (myeloid differentiation primary response gene 88), which forms a complex with the IRAK (Interleukin-1 receptor-associated kinase) and then leads, via the E3 ubiquitin ligase TRAF6 (TNF receptor-associated factor 6), to the activation of the mitogen-activated protein kinases (MAPK) such as ERK1/2 (extracellular signal-regulated kinase), p38, and JNK (c-Jun N-terminal kinase) inducing AP-1 (activator protein 1)-mediated transcription of inflammatory genes (Kawasaki & Kawai, 2014). A second pathway that is activated upon MyD88 binding leads to the recruitment of the IKK (I kappa B kinase) complex and consequently to the nuclear translocation of the transcription factor NF κ B (nuclear factor kappa B) initiating the transcription of pro-inflammatory genes (Akira & Takeda, 2004) (Figure 4). Important for the membrane recruitment of MyD88 is the sorting adaptor TIRAP (TIR-domain containing adaptor protein), which was shown to bind specifically to PI(4,5)P₂ at the PM and PI(3)P at the endosome, thereby inducing

receptor signaling downstream of TLR2, and TLR4, or TLR9, respectively (Bonham, Orzalli et al., 2014). Other adaptor proteins important for downstream signaling of activated endosomal TLRs are TRIF (TIR-domain-containing adapter-inducing interferon- β) binding to TLR3 and TRAM (TRIF-related adaptor molecule), a molecule that bridges the interaction between TRIF and TLR4 at the endosome (Sheedy & O'Neill, 2007). TRIF interacts with TRAF6 and TRAF3 leading to the recruitment of downstream kinases TBK1 and IKK ϵ , and to the activation of NF κ B or IRF3 (Interferon Regulatory Factor 3), respectively. IRF3 induces the transcription of type I interferon (IFN) genes (Tatematsu, Ishii et al., 2010).

TLRs and the Membrane: As transmembrane domain proteins, TLRs are embedded in different membranes and their adaptor proteins are associated with these membranes, thus TLR signaling depends on the membrane lipid composition. In the last years studies have suggested the potential involvement of membrane lipids in TLR function (Chang, Lee et al., 2011, Parker, Prestwich et al., 2008, Zhu, Owen et al., 2010b). Important regulatory mechanisms of TLR signaling are conformational changes upon ligand binding which induce the intracellular TIR domain dimerization. For TLRs these conformational changes have not been studied in such detail, as there are only a few crystal structures available. However, a comparison with another ligand-activated transmembrane receptor, epidermal growth factor receptor (EGFR), whose structure is very similar to those of the TLRs can be used as a model to understand this functional mechanism (Gay, Symmons et al., 2014). Ligand-mediated activation of EGFR leads to a rearrangement of the transmembrane helices causing the formation of a new dimerization interface and pulling the juxtamembrane sequences off the PM. In an inactive state, these domains, containing mostly basic amino acid residues, are directly associated with the anionic head groups of PS or PI at the inner leaflet of the membrane. Repositioning of these domains facilitates the dimerization of the intracellular kinase domains and their cross-phosphorylation (Endres, Das et al., 2013, Sengupta, Bosis et al., 2009). A similar mechanism could be important for TIR dimerization and subsequent signaling. The TIR-domain containing adaptor proteins TIRAP and TRAM are also associated with the membrane by binding of the lipid species PI(4,5)P₂ or by harboring a myristoyl group at a glycine residue, respectively (Kagan & Medzhitov, 2006, Rowe, McGettrick et al., 2006). The membrane association of TRAM is disrupted by its phosphorylation, an event that is essential for further progression of TLR4 signaling (McGettrick, Brint et al., 2006). Interestingly, purified TIR-domains do not form complexes *in vitro*, indicating that they require an additional factor to dimerize. Indeed, the computational modeling of a TLR4-TIR homodimer revealed that the cytoplasmic juxtamembrane sequences were oriented on the same membrane-proximal surface, similar to

the lipid-binding domain of amphiphysin, indicating a direct involvement of the membrane during TLR dimerization (Casal, Federici et al., 2006, Gay et al., 2014, Miguel, Wong et al., 2007).

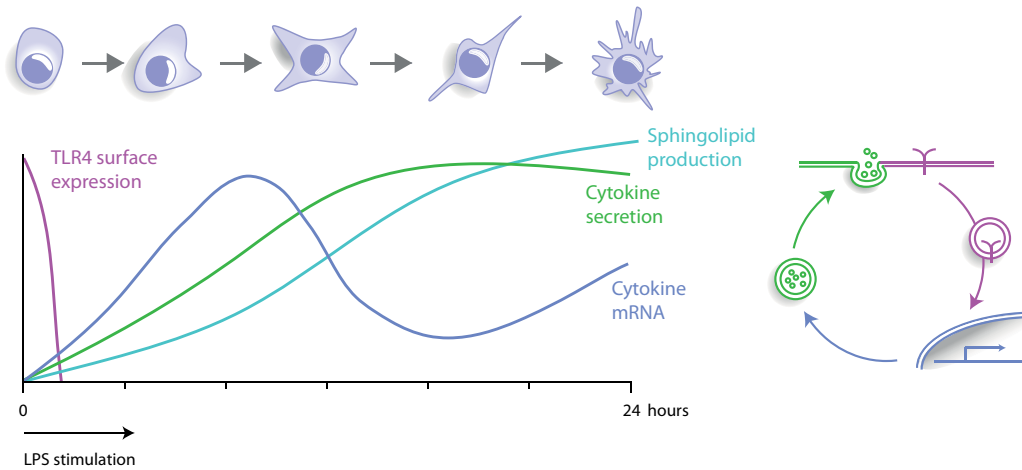


Figure 5: TLR signaling over time: Schema shows the dynamic processes induced by TLR4 stimulation and their localization. Macrophage differentiation (purple cell), TLR4 endocytosis (pink), sphingolipid production (turquoise), cytokine secretion (green), cytokine transcription (purple) are shown.

TLR Trafficking: TLRs are translated in the ER and are trafficked via the Golgi to their destination membranes. Specific adaptor proteins such as UNC93B1, PRAT4A, and gp96 facilitate this trafficking by acting as chaperones for different TLRs (Kim, Brinkmann et al., 2008, Takahashi, Shibata et al., 2007, Yang, Liu et al., 2007), while the function of other TLR cofactors such as the binding of MD2 (myeloid differentiation factor 2) to TLR4 in the ER is important for the glycosylation pattern and responsiveness of the receptor (Nagai, Akashi et al., 2002). The trafficking mechanisms of TLR4 has been further characterized and TMED7 (transmembrane emp24 domain-containing protein 7), a protein that sorts correctly folded proteins for packaging into COPII vesicles was identified to be specifically required for the regulation of the anterograde trafficking of TLR4 (Liaunardy-Jopeace, Bryant et al., 2014). At the PM, TLR4 is rapidly endocytosed upon LPS stimulation and then signals from endosomal compartments via TRIF (Figure 4 and 5). This clathrin-dependent endocytosis requires the cofactors CD14 and RAB11A (Husebye, Aune et al., 2010, Zanoni, Ostuni et al., 2011). After LPS stimulation, replenishing of TLR4 from the Golgi or endosome to the PM is mediated by the small G protein RAB10 (Wang, Lou et al., 2010).

Similar to TMED7, UNC93B1 regulates the anterograde trafficking of TLR7 and TLR9 from the Golgi to the endosome in COPII-coated vesicles (Lee, Moon et al., 2013). One study

also showed that the trafficking of TLR9 additionally requires the clathrin adaptor protein AP-2 (Lee et al., 2013). Intriguingly, this adaptor is important for trafficking of cargo to the PM suggesting that TLR9 is first shuttled to the PM before it is endocytosed. In contrast, this mechanism was not observed for TLR7; instead, TLR7 binds to AP-4, a protein that mediates the trafficking of cargo directly from the TGN to the endosome (Lee et al., 2013). TLR9 signals from different intracellular compartments to induce either an IRF7-dependent IFN response or an NF κ B-dependent response. After binding CpG-DNA, TLR9 traffics to early endosomes, which is facilitated by UNC93B1. The pre-form of TLR9 is cleaved by cathepsins and to trigger NF κ B activation. Subsequently, TLR9 is trafficked to lysosomes facilitated by AP3, where it induces IRF7 activation (Sasai, Linehan et al., 2010).

Cofactors of TLRs: Apart from the proteins that regulate the intracellular trafficking of TLRs to their destination membrane, cofactors are important for local TLR activation as well as for the downstream signaling. One example is the GPI-anchored CD14, which mediates the recognition of LPS and promotes the endocytosis of TLR4 upon LPS stimulation, together with the LPS-binding protein (LBP) and MD2 (Zanoni et al., 2011). CD14 was also shown to be required for the activation of TLR7 and TLR9 in the endosome (Baumann, Aspalter et al., 2010). Another TLR cofactor is the scavenger receptor CD36, important for binding of long-chained FAs from oxidized LDL (low-density lipoprotein). CD36 was shown to induce the heterodimer formation of TLR4 and TLR6 leading to an inflammatory response (Stewart, Stuart et al., 2010, Triantafilou, Triantafilou et al., 2007). Importantly, upon stimulation TLRs as well as their cofactors migrate into sphingolipid- and cholesterol-rich lipid rafts (Plociennikowska, Hromada-Judycka et al., 2015).

The β_2 -integrins and complement receptors CR3 and CR4 are another important class of proteins involved in the LPS-dependent TLR4 response. Studies in neutrophils demonstrated that CD14 clustering induced by LPS also increased the CR3 levels and consequently the adhesive properties of the cells (Zarewych, Kindzelskii et al., 1996). The downstream signaling of TLR4 requires the recruitment of TIRAP, which binds to PI(4,5)P₂-rich regions of the membrane and β_2 -integrins have been implicated in the induction of PI(4,5)P₂ synthesis by activating PI(4)P5 kinase via ARF6. And macrophages deficient for CD11b, which is part of CR3, showed reduced levels of IL-6 (Interleukin 6) production due to an impaired recruitment of TIRAP (Hynes, 2002). This increase of PI(4,5)P₂ in response to TLR4 could act as a feed-forward loop to enhance the TLR response by recruiting more downstream adaptors to the membrane as well as the cytoskeletal components important for endocytosis (Botelho, Teruel et

al., 2000). A dynamic control of the lipid levels is, however, required for these endocytic processes because hydrolysis of PI(4,5)P₂ is also involved in promoting the actin remodeling during endocytosis (Scott, Dobson et al., 2005).

1.2.2 *NEGATIVE REGULATORS OF TLR SIGNALING*

In order to prevent harmful hyperinflammatory processes induced by TLR signaling such as sepsis, leading to fatal tissue damage, there are multiple negative regulators of TLR signaling acting at different steps of the signaling pathway. These negative regulators are also implicated in the context of resolution of inflammation. While some interfere with the TLR adaptor complexes, others mediate the degradation of proteins involved in signaling, or modulate the transcriptional response. Since the recruitment of TIR domain-containing proteins is one of the first steps after TLR activation its negative regulation is very efficient. Additionally, there are proteins that only interfere with specific TIR domain-containing adaptors. TAG, a variant of TRAM, for instance, can compete for the binding to TRIF and thus block signaling via TLR4-TRAM. This process could also be important to initiate the degradation of the TLR4 signaling complex after LPS binding (Palsson-McDermott, Doyle et al., 2009). Similarly, IRF4 can compete with IRF5 for MyD88-binding, thereby inhibiting its transcriptional response, acting as a negative feedback loop, because *Irf4* transcription is induced by TLR signaling (Negishi, Ohba et al., 2005). SOCS (suppressor of cytokine signaling) proteins harbor an SH2-domain and function as E3 ubiquitin ligases, mediating the ubiquitylation and degradation of TIRAP and TRAF (Yoshimura, Naka et al., 2007). A mechanism of transcriptional regulation is mediated by ATF3 (cyclic AMP-dependent transcription factor), which recruits the histone deacetylase 1 (HDAC1), thus inhibiting transcription factor binding (Whitmore, Iparraguirre et al., 2007). Furthermore, a TLR-inducible nuclear IκB protein (IκBNS) can negatively regulate a subset of TLR-induced genes such as IL-6 by regulating NFκB activation (Kuwata, Matsumoto et al., 2006).

1.2.3 *CYTOKINE SECRETION MECHANISMS*

A rapid and efficient communication is essential for the function of the immune system, and cells use cytokines to enhance or dampen an inflammatory response within the organism. Upon receptor activation, cytokines are secreted into the extracellular space and can bind to

receptors to initiate downstream signaling in a paracrine or autocrine way. Different cytokines are secreted via different mechanisms; however, most cytokines are translated and packaged in the ER before they are trafficked to the Golgi in vesicles (Lacy & Stow, 2011). Cytokines such as IL-2, IL-3, and IL-7 harbor a signal sequence that is important for proper intracellular targeting to the ER (Goodwin, Lupton et al., 1989, Yang, Ciarletta et al., 1986). In macrophages, these cytokine-containing vesicles are trafficked from the ER to the Golgi and the PM. IL-6 and TNF α (tumor necrosis factor alpha) both also localize to recycling endosomes; however, intracellular staining has shown that they localize to different subcompartments of recycling endosomes, indicating an additional sorting step for these cytokines (Manderson, Kay et al., 2007). The membrane fusion events involved in cytokine secretion are regulated by the SNARE (Soluble NSF attachment protein) complex (Mollinedo, Calafat et al., 2006). Other cytokines do not have any signal sequences such as IL-18, which, after maturation, is trafficked from the cytosol into secretory lysosomes and is then released (Blott & Griffiths, 2002). This cytosolic localization is important for tubulin-mediated, restricted secretion of IL-18 at the synaptic cleft of dendritic cells, for instance, interacting with natural killer cells without spreading of the cytokine (Semino, Angelini et al., 2005). Other cytokines such as IL-1 β (Interleukin 1 beta) or MIF (Macrophage migration inhibitory factor) are described to be released via non-classical secretion pathways because they never enter the ER/Golgi pathways and could possibly even be released via specific ABC transporters (Eder, 2009, Flieger, Engling et al., 2003).

1.2.4 LIPIDS AND INFLAMMATION

Several links have been identified between inflammatory processes and lipid biosynthesis. The best-studied lipids in inflammation are the eicosanoids prostaglandin, lipoxin, as well as the newly discovered lipid mediators resolvins, maresins, and protectins, synthesized from arachidonic acid, which have been identified to resolve inflammatory processes (Serhan & Savill, 2005). The most important proteins in eicosanoid generation are PLA2 and COX, mediating the degradation of glycerophospholipids and the generation of arachidonic acid from PC, for example (Brash, 2001).

Phorbol ester (PMA) mimics the structure of DAG and is used to activate PKC, inducing an inflammatory response leading to the activation of p38 and the production of IL-6, and it also enhances ceramide levels. One study showed that silencing of *Gba*, also mutated in Gaucher

disease, led to enhanced levels of IL-6 upon PMA activation in human breast cancer cells. Ceramide treatment of the cells could reverse the hyperinflammatory response as well as silencing of an isoform of p38, indicating that the hyperproduction of IL-6 was regulated by the ceramide levels produced by GBA and the isoform of p38 mediated this response downstream of PKC (Kitatani, Sheldon et al., 2009). Similarly, also acid sphingomyelinase was found to regulate TNF α - or PMA-induced IL-6 production via p38 (Perry, Newcomb et al., 2014). Acid sphingomyelinase has been further implicated in the outcome of sepsis-induced organ failure as patients that had suffered from sepsis showed elevated plasma levels of ASMase (Claus, Bunck et al., 2005). Free cholesterol loading of macrophages enhanced the TLR4-mediated response also via p38 (Sun, Ishibashi et al., 2009). Conversely, high-density lipoproteins, important for reversed cholesterol transport, have been shown to act anti-inflammatory via the transcription factor ATF3, which downregulates the expression of TLR-induced cytokines (De Nardo, Labzin et al., 2014).

TLR Signaling and Sphingolipids: Specifically in the context of TLR function, several observations have been made connecting sphingolipids and the TLR-mediated inflammatory response. TLR4 stimulation induces the *de novo* sphingolipid synthesis and also increased levels of other lipids (Dennis et al., 2010, Sims, Haynes et al., 2010) (Figure 5). Conversely, exogenously added ceramides could reduce the production of IL-5, IL-10, and IL-13 in mast cells upon stimulation with LPS (Chiba, Masuda et al., 2007). Pathogens and cytokines have also been described to specifically activate sphingomyelinases to generate ceramide directly at the PM or to increase the *de novo* synthesis of sphingolipids (Milhas et al., 2010). In dendritic cells, sphingomyelinase activation upon host pathogen interaction is important for the generation of ceramide accumulation at the outer leaflet of the PM (Avota, Gulbins et al., 2011). Mouse embryonic fibroblasts, deficient in sphingomyelinase showed decreased levels of the chemokine CCL5 release upon TNF α stimulation (Jenkins, Clarke et al., 2011). S1P was also shown to be generated upon TNF α stimulation in a TRAF-dependent mechanism (Xia, Gamble et al., 1998, Xia, Wang et al., 2002). And IL-1 β treatment can induce the protein complex formation of SPHK1, cIAP2 and IRF1 inducing the expression of chemokines important for sterile inflammation (Harikumar, Yester et al., 2014).

TLRs and Membrane Lipids *in vivo*: Several studies have described the role of membrane lipids and TLR signaling *in vivo*. Cholesterol levels, for instance, were identified to be modulators of the TLR response, since TLR re-localization into lipid rafts and complex formation is essential for downstream signaling. Cholesterol loading of macrophages or a deficiency of the

cholesterol exporter ABCA1 (ATP-binding cassette subfamily A1) enhanced the TLR4-induced inflammatory signaling while depletion of free cholesterol reduced the inflammatory response (Fessler & Parks, 2011, Sun et al., 2009, Zhu, Owen et al., 2010a). Enhanced inflammatory gene expression was also measured in *Abca1* and *Abcg1* double knockout mice when TLR2, 3, or 4 were stimulated but not TLR7 or 9. This hyperresponse could be rescued when cholesterol was depleted from the membrane (Yvan-Charvet, Welch et al., 2008).

The role of sphingomyelin was also studied in this context. Macrophages derived from *Sgms1*- or *Sgms2*-deficient mice showed impaired TLR4 responses due to decreased abundance of TLR4-MD2 complexes at the cell surface (Gowda, Yeang et al., 2011, Li, Fan et al., 2012). And impaired downstream signaling was measured in macrophages from haploinsufficient *Sptlc2* mice upon TLR4 stimulation due to reduced receptor surface levels (Chakraborty, Lou et al., 2013).

Mechanisms of TLR Signaling and Lipids: Potential mechanisms of TLR signaling and membrane lipids have been suggested in several studies. An exogenously added cationic lipid, for instance, was shown to disrupt the TLR4-CD14 interaction and thus inhibit LPS-induced signaling (Leon-Ponte, Kirchhof et al., 2005). This disruption of TLR4 signaling has also been suggested as mechanism for oxidized phospholipids in inflammatory signaling (Erridge, Webb et al., 2007). An oxidized PE species has been shown to inhibit LPS-mediated TLR4 signaling by inducing the activation of neutral sphingomyelinase thus increasing the levels of long-chained ceramides (Walton, Gugiu et al., 2006). Another study could identify endogenous globotetraosylceramide binding directly to the TLR4-MD2 complex at the PM thereby counteracting the TLR4-induced response (Kondo, Ikeda et al., 2013). One important prerequisite for TLR4 signaling, recently identified, is the incorporation of LPS into the membrane, preferentially into sphingomyelin- and cholesterol-rich domains suggesting that depletion of these lipids in the PM could also lead to altered binding of LPS (Ciesielski, Griffin et al., 2013). A PI(3)K isoform has been identified which regulates the internalization of TLR4 by inducing the dissociation of TIRAP from the membrane potentially by inhibiting the binding to PI(4,5)P₂. Blocking of this kinase induced a prolonged and enhanced TLR4 signaling in response to stimulation and knockout mice were more susceptible to endotoxin-mediated death (Aksoy, Taboubi et al., 2012).

The sequence analysis of TLRs revealed that several harbor cholesterol recognition amino acid consensus (CRAC) domains close to their transmembrane domain (Ruysschaert & Loney, 2015). These motifs are located next to the TIR domain in the cytoplasmic part indicating

that this region is essential for binding cholesterol at the inner leaflet of the PM. Previously, this part of the protein was implicated in the activation and dimerization of TLR4 (Nishiya, Kajita et al., 2006). Since lipids located in rafts increase the membrane thickness, the cholesterol binding of the TLR molecule could only be enabled when the TLR is localized in rafts, consecutively leading to the conformational changes important for dimerization and activation. This way the interaction between the TIR domain of the TLR and the TIR domain of the adaptor protein, which binds to the inner leaflet of the membrane, is initiated and stabilized when the receptor is located in a cholesterol- and sphingolipid-rich environment. A sphingolipid-binding domain has also recently been identified and this sequence was found in the transmembrane regions of TLR3 and TLR5 (Contreras, Ernst et al., 2012, Ruysschaert & Loney, 2015).

Lipid Storage Disorders and Inflammation: Abnormal inflammatory responses have been characterized in patients suffering from different storage disorders. In Gaucher disease, for instance, elevated IL-6 and IL-10 levels have been measured in the serum of patients (Allen, Myer et al., 1997). These findings were further confirmed in a mouse model of Gaucher disease, where enhanced inflammation was measured, especially in the brain, with elevated levels of IL-1 β , TNF α , and several chemokines, whose levels also increased with disease progression (Vitner, Farfel-Becker et al., 2012). These findings suggest elevated neuroinflammation to be involved in the neurodegenerative symptoms of the disease. Peripheral mononuclear cells (PBMCs) of a Fabry disease patient were found to have elevated basal pro-inflammatory cytokine production, which further increased with LPS stimulation and was abolished with the treatment of a TLR4 blocking antibody (De Francesco, Mucci et al., 2013). These findings highlight an interesting connection between lipid storage disorders and potential inflammatory deregulation.

1.4 AIMS OF THIS THESIS

By combining lipid biology, characterization of innate immune responses, and systems biology approaches we aimed to characterize the functional role of membrane lipid metabolism in TLR-mediated signaling.

More specifically, the following main aims were addressed. (1) Dissection of the transcriptional regulation of lipid metabolism upon TLR stimulation. By monitoring gene regulation of 25 genes located in the sphingolipid metabolic pathway over time, the general patterns of induced and repressed genes could be assessed. (2) Analysis of the lipid composition after genetic perturbation of genes important for sphingolipid metabolism. Using quantitative mass spectrometry-based lipidomics we could monitor the changes in abundance of 245 different glycerophospho- and sphingolipids. (3) Monitoring of how changes in lipid composition affect TLR-mediated signaling. Several quantitative read-outs were used to measure changes in TLR function, such as receptor surface expression, cytokine release, and cytokine transcription. For the novel sphingomyelinase –like gene *Smpd13b* we also tested the *in vivo* role in a peritonitis model. (4) Uncovering of general roles of lipid coregulation in a panel of perturbed cell lines. Calculation of lipid-lipid correlations between all possible combinations identified different clusters of coregulated lipid species. The visualization of these coregulated lipids revealed a circular network. (5) Annotation of lipid function using the circular network of lipid coregulation. By combining the quantitative characterization of TLR signaling with the changes in lipid composition we could infer a function of each measured lipid in the different TLR-induced processes. The circular network could be used to visualize the function of the coregulated lipids. (6) Comparison of lipid coregulation between mouse and human cells and testing of a predictive model of lipid function in diseased fibroblasts. We performed quantitative lipidomics on a panel of different fibroblasts derived from patients suffering from lipid storage disorders. Analysis of lipid coregulation showed that the circular architecture of the network was conserved. Using the functional annotation of lipid function we could further predict the different inflammatory responses of the human fibroblasts solely based on the changes in lipid composition.

2. CHAPTER TWO: RESULTS

2.1 PROLOGUE

A Conserved Circular Network of Coregulated Lipids Modulates Innate Immune Responses.

Köberlin MS*, Snijder B*, Heinz LX, Baumann CL, Fauster A, Vladimer GI, Gavin AC, Superti-Furga G (2015) CELL 162: 170-83

*: contributed equally

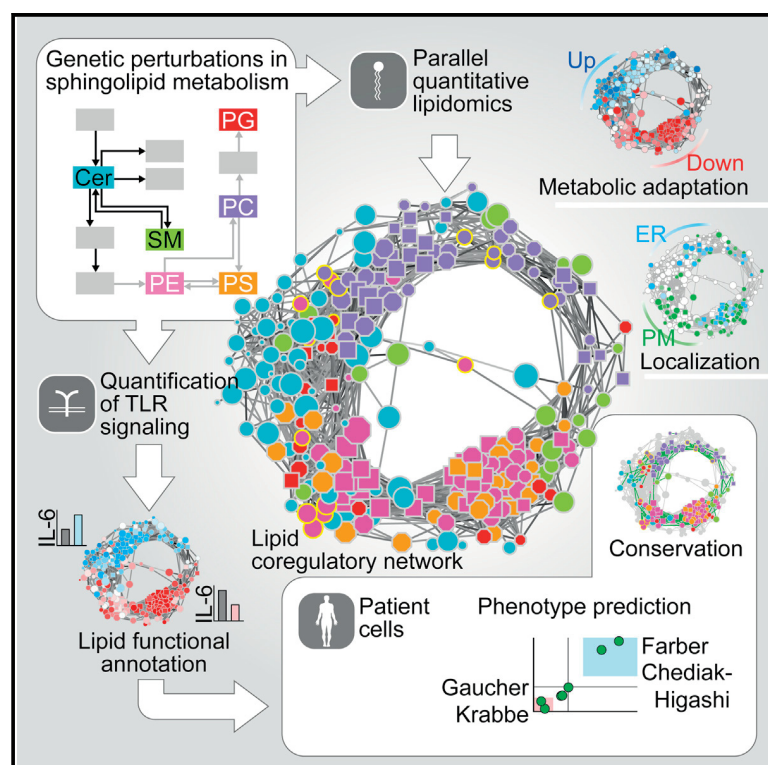
Here, we used a genetic loss-of-function approach in mouse macrophages characterizing TLR-dependent signaling processes, coupled to a mass spectrometry-based analysis of 245 different lipid species to dissect the contribution of lipid composition in the innate immune response. A novel lipid-modifying enzyme was further characterized in a second study, published in parallel, and its role as negative regulator could be shown *in vivo* (Heinz, Baumann et al., 2015).

The author of this thesis contributed as follows:

In this work, the author of the thesis designed and performed most experiments. I performed the transcriptional measurements and the loss-of-function approach generating 129 genetically perturbed mouse macrophage cell lines. Further, I functionally characterized these cell lines performing several rounds of stimulation and cytokine measurements. A subset of cell lines was then screened by me for TLR4 surface expression and cytokine transcription after stimulation over time. I further prepared 10 mouse macrophage cell lines and human fibroblast cells for lipidomics analysis. I performed lipid supplementation assays and corresponding control experiments, as well as the TLR stimulation of human fibroblasts. Berend Snijder analyzed the data characterizing the TLR-mediated responses and the lipidomics data resulting in the circular network of lipid coregulation. Further functional annotation of the lipid species in TLR responses were calculated by him. All data and interpretation were discussed with the last author and with the other authors on the manuscript. Figure preparation and writing of the manuscript was done by the first two authors at equal contribution together with the last author Giulio Superti-Furga.

A Conserved Circular Network of Coregulated Lipids Modulates Innate Immune Responses

Graphical Abstract



Authors

Marielle S. Köberlin, Berend Snijder, Leonhard X. Heinz, ..., Gregory I. Vladimer, Anne-Claude Gavin, Giulio Superti-Furga

Correspondence

gsuperti@cemm.oeaw.ac.at

In Brief

Combining lipidomics with genetic perturbations in immune cells reveals the logic of inter-lipid regulatory structure and enables the functional assignment of lipids to different steps of Toll-like receptor signaling. Moreover, quantitative lipidomics alone can predict the inflammatory response of patient-derived cells.

Highlights

- Coregulation between membrane lipid species is organized in a circular network
- The lipid network is conserved and reflects metabolism, localization, and adaptation
- Sphingolipid metabolism regulates TLR trafficking, signaling, and cytokine release
- Network-wide functional lipid annotations predict TLR responses in patient cells



Köberlin et al., 2015, Cell 162, 170–183
July 2, 2015 ©2015 The Authors
<http://dx.doi.org/10.1016/j.cell.2015.05.051>

A Conserved Circular Network of Coregulated Lipids Modulates Innate Immune Responses

Marielle S. Köberlin,^{1,5} Berend Snijder,^{1,5} Leonhard X. Heinz,¹ Christoph L. Baumann,^{1,4} Astrid Fauster,¹ Gregory I. Vladimer,¹ Anne-Claude Gavin,² and Giulio Superti-Furga^{1,3,*}

¹CeMM Research Center for Molecular Medicine of the Austrian Academy of Sciences, 1090 Vienna, Austria

²European Molecular Biology Laboratory, EMBL, 69117 Heidelberg, Germany

³Center for Physiology and Pharmacology, Medical University of Vienna, 1090 Vienna, Austria

⁴Present address: Austrianni GmbH, 1030 Vienna, Austria

⁵Co-first author

*Correspondence: gsuperti@cemm.oeaw.ac.at

<http://dx.doi.org/10.1016/j.cell.2015.05.051>

This is an open access article under the CC BY-NC-ND license (<http://creativecommons.org/licenses/by-nc-nd/4.0/>).

SUMMARY

Lipid composition affects the biophysical properties of membranes that provide a platform for receptor-mediated cellular signaling. To study the regulatory role of membrane lipid composition, we combined genetic perturbations of sphingolipid metabolism with the quantification of diverse steps in Toll-like receptor (TLR) signaling and mass spectrometry-based lipidomics. Membrane lipid composition was broadly affected by these perturbations, revealing a circular network of coregulated sphingolipids and glycerophospholipids. This evolutionarily conserved network architecture simultaneously reflected membrane lipid metabolism, subcellular localization, and adaptation mechanisms. Integration of the diverse TLR-induced inflammatory phenotypes with changes in lipid abundance assigned distinct functional roles to individual lipid species organized across the network. This functional annotation accurately predicted the inflammatory response of cells derived from patients suffering from lipid storage disorders, based solely on their altered membrane lipid composition. The analytical strategy described here empowers the understanding of higher-level organization of membrane lipid function in diverse biological systems.

INTRODUCTION

The cellular membrane defines the minimal unit of life and creates the compartmentalization that orchestrates the transport of molecules, intracellular signaling, cell-cell communication, pathogen recognition, and many other processes (van Meer et al., 2008). Membrane function is an emergent property of the intricate interactions of its protein and lipid constituents, with glycerophospholipids, sphingolipids, and sterols as most abundant membrane lipids. Glycerophospholipids and sphingolipids are categorized into distinct lipid classes defined by the

chemical structure of their head group. Each lipid class contains hundreds of different lipid species, further varying in fatty acid chain length, linkage, and saturation, among others (Coskun and Simons, 2011), the exact measurement of which has been empowered by the advent of lipidomics (Shevchenko and Simons, 2010; Wenk, 2005). Distinct lipid species are asymmetrically distributed across the plasma membrane (PM) and the various intracellular membranes (van Meer et al., 2008), in part due to locally confined synthesis and active transport of lipids (Maeda et al., 2013), providing a functionally distinct spatial organization to the lipid landscape of a cell (Holthuis and Menon, 2014).

The plasma membrane and endosomal membranes mediate the first line of defense in cellular innate immunity by establishing a physical barrier against microbial pathogens and constitute the main site of pathogen recognition by accommodating specialized cell surface receptors such as Toll-like receptors (TLRs). TLRs are a conserved family of transmembrane proteins that recognize distinct pathogen-associated molecular patterns and activate key signaling pathways in innate immunity (Kawai and Akira, 2010). The plasma membrane and endosomal resident TLR4, for instance, mainly recognizes gram-negative bacterial lipopolysaccharides (LPS), while the endosomal TLR7 and TLR9 recognize nucleic acids derived from a wide range of microbes. TLR ligand-binding leads to receptor dimerization and the activation of subsequent signaling cascades, which, for most TLRs, involves a partially overlapping set of accessory molecules (Bonham et al., 2014; Lee et al., 2012). This in turn leads to transcriptional and metabolic changes, including the induction and secretion of cytokines (Kawai and Akira, 2010), as well as the upregulation of sphingolipid synthesis (Memon et al., 1998). TLR signaling eventually triggers pathogen-specific responses by the adaptive immune system, thus linking cellular innate immunity to the adaptive immune system of the host (Kawai and Akira, 2010). In macrophages, TLR activation induces changes in the lipid composition and properties of cellular membranes (Andreyev et al., 2010; Dennis et al., 2010), adapting the cellular morphology for polarization and pathogen phagocytosis. TLR signaling is meticulously regulated to clear pathogens yet avoid host damage through hyperinflammation (Serhan et al., 2008). Mechanisms of regulation act, among others, at the level of transmembrane domains of TLRs, mediating dimerization and

activation (Kawai and Akira, 2010) and at the level of receptor trafficking, altering the adaptor protein complexes and signaling (Bonham et al., 2014; Lee et al., 2012). While selected species of sphingolipids have been characterized in the context of inflammation (Alvarez et al., 2010; Józefowski et al., 2010; Vandanmagsar et al., 2011), the chemical complexity of biological membranes requires more global approaches to deconvolute the function of the lipid landscape (Atilla-Gokcumen et al., 2014; da Silveira Dos Santos et al., 2014).

RESULTS

Sphingolipid Metabolism Is Regulated by TLR Stimulation and Modulates TLR-Induced IL-6 Release

Previously, quantitative lipidomics and genome-wide transcriptional changes upon TLR4 stimulation were measured in bone marrow-derived macrophages (BMDMs) and in the murine macrophage RAW264.7 (RAW) cell line (Dennis et al., 2010; Ramsey et al., 2008) (Figures S1A–S1C), which revealed sphingolipid metabolism to be strongly differentially regulated upon TLR stimulation (Figure S1B). We therefore selected 24 genes based on the sphingolipid metabolic network (Kanehisa and Goto, 2000) focusing on ceramide metabolism, including several poorly studied genes, all expressed in RAW cells (Figure S1D; Table S1) (Hannun and Obeid, 2011). Their TLR4- and TLR9-driven transcriptional regulation was measured by stimulating RAW macrophages with LPS and unmethylated CpG DNA (CpG), respectively (Figures 1A, S1D, and S1E).

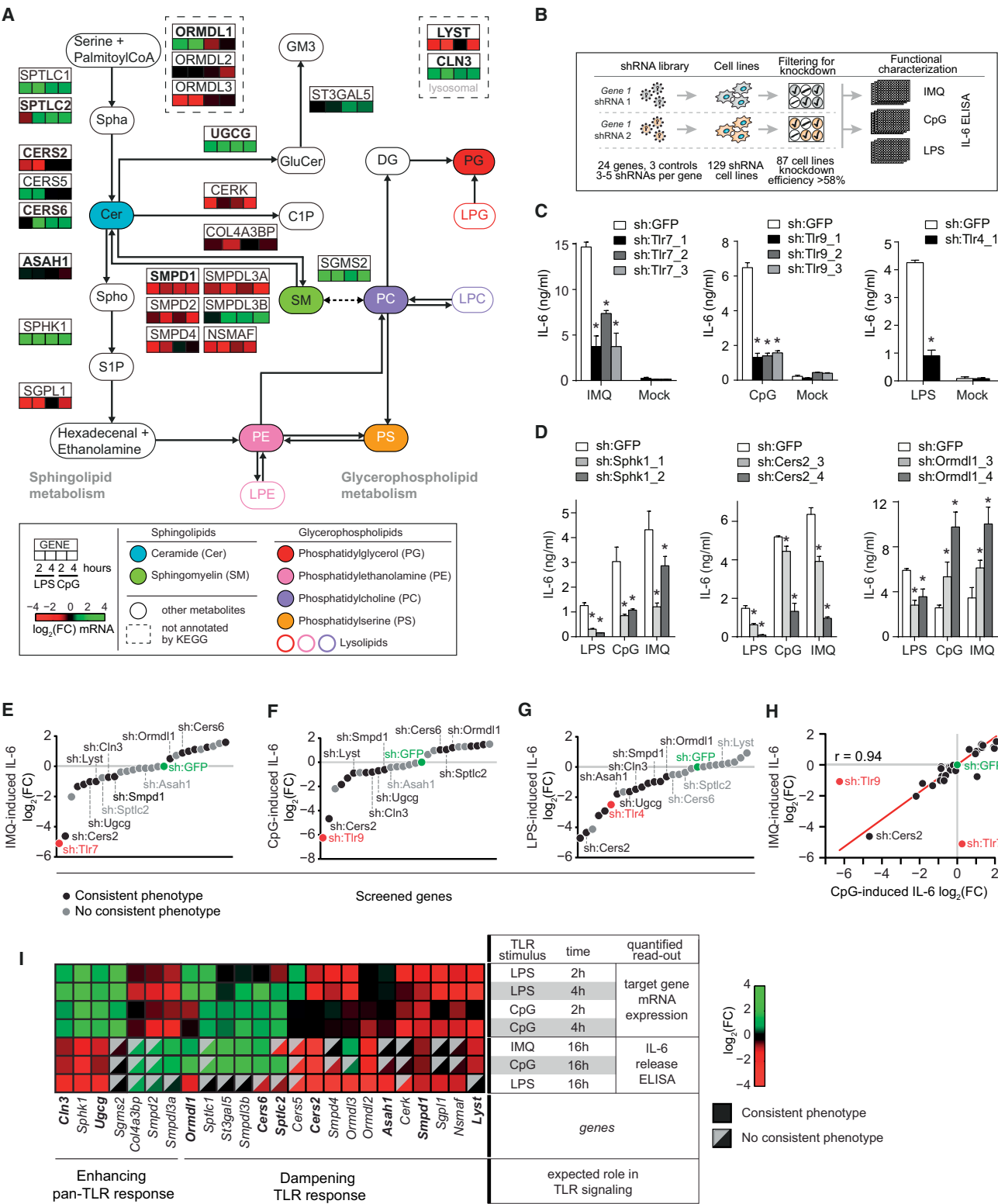
Mapping our expression results onto the known sphingolipid metabolic pathway showed that 18 of the 24 genes were similarly regulated by both TLRs (Figures 1A and S1E), consistent with the fact that TLR4 and TLR9 activate a partially overlapping set of downstream transcription factors (Kawai and Akira, 2010). Genes induced by at least one TLR ligand were associated with the de novo synthesis of ceramides (*Sptlc1* and *Sptlc2*, *Cers5* and *Cers6*, and *Ormdl1*) and their downstream processing into other key sphingolipids including sphingomyelins (SMs) by *Sgms2*, sphingosine-1-phosphate (S1P) by *Sphk1*, and glucosylceramides (GluCers) by *Ugcg* (Figure 1A). In contrast, genes involved in the degradation of sphingomyelins (*Smpd1* and related genes) and S1P (*Sgpl1*) were predominantly downregulated (Figure 1A). This significant and consistent transcriptional pattern across the network ($p < 1.7 \times 10^{-8}$; Figure S1F) suggested increased levels of ceramides, sphingomyelins, S1P, and glucosylceramides upon TLR stimulation, as indeed observed in the publicly available lipidomics data (Figure S1A).

To study the roles of sphingolipids in TLR biology, we genetically perturbed these 24 genes to identify reproducible and diverse effects on TLR signaling and quantify the corresponding changes in membrane lipid abundance, allowing an integrated analysis of these two cellular properties. Each of the 24 genes and three TLR controls were targeted by three to five short hairpin RNAs (shRNAs) in RAW macrophages resulting in 129 stable shRNA cell lines (Figure 1B; Table S1). Filtering for a knockdown efficiency of at least 58% resulted in 87 cell lines with a median knockdown efficiency of 88% (Figure S1G). These 87 cell lines covered the 24 genes with on average three shRNA cell lines per gene (Table S1).

In a focused screening campaign, these 87 cell lines were monitored for differences in TLR signaling as measured by the release of the cytokine interleukin 6 (IL-6) into the supernatant after stimulation, a late quantitative read-out of TLR activation (Kawai and Akira, 2010). To measure the activity of diverse TLRs, cells were stimulated with Imiquimod (IMQ) or CpG, which are recognized by the endosomal TLRs 7 or 9, respectively, or with LPS, recognized by TLR4. As expected, silencing of the TLR controls (sh:TLR4, sh:TLR7, sh:TLR9) strongly attenuated their respective ligand-induced IL-6 release compared to sh:GFP control (Figure 1C). Silencing of genes involved in sphingolipid metabolism led to various TLR-induced IL-6 release phenotypes (Figure 1D). For instance, knockdown of *Sphk1* or *Cers2* led to significantly reduced IL-6 release after stimulation with all three TLR ligands, while knockdown of *Ormdl1* led to enhanced IL-6 release upon endosomal TLR stimulation and decreased IL-6 release upon TLR4 stimulation (Figure 1D). Cytoplasmic recognition of pathogen-associated molecular patterns (Stetson and Medzhitov, 2006) was not affected by silencing of *Sphk1*, as stimulation with interferon stimulatory DNA or poly(dA:dT) resulted in equal levels of interferon β release for sh:SPHK1 and sh:GFP (Figure S1H). To summarize the TLR-induced IL-6 release measurements over all shRNA cell lines per gene and per stimulus, the log₂ fold-change relative to the corresponding sh:GFP control value was calculated and averaged over technical and biological replicates. We next either averaged the values of consistent and strong (absolute log₂ fold-change >0.7) shRNA phenotypes per gene (Figures 1E–1G, black dots), or, in case these criteria were not met, the values of all shRNAs per gene (Figures 1E–1G, gray dots). Knockdown of 18 genes affected IL-6 release after stimulation with at least one TLR ligand consistently for two or more shRNA cell lines (Figures 1E–1G), while cell viability was unaffected in all cases. In unstimulated conditions, the 87 shRNA cell lines showed only background IL-6 levels in the supernatant.

In both the IMQ and CpG screens, the associated sh:TLR7 and sh:TLR9 controls led to the strongest reduction in IL-6 release, respectively (Figures 1E and 1F). In contrast, the LPS screen revealed five genes whose knockdown led to an even stronger reduction than the sh:TLR4 control (Figure 1G). The CpG and IMQ screens not only manifested decreased IL-6 release but also revealed several genes which, upon knockdown, led to increased IL-6 release after stimulation (Figures 1E and 1F). Comparing the results of the three IL-6 release screens showed that the CpG and IMQ screens were strongly correlated ($r = 0.94$) (Figure 1H), while the LPS screen correlated considerably less with the other two screens (mean $r = 0.71$). This suggested that the sphingolipid metabolic pathway affected the endosomal TLRs 7 and 9 to an equal extent, while TLR4 at the plasma membrane was differentially affected.

Integrating the TLR-induced transcriptional regulation of sphingolipid metabolism with the corresponding gene perturbation phenotypes could reveal mechanisms by which a cell either boosts or resolves inflammation through modulation of its membrane lipid composition. To reveal the presence of such mechanisms, the IL-6 screening results for all three TLR stimuli were combined with the relative expression of target genes in wild-type RAW cells after stimulation of TLR4 and



(legend on next page)

TLR9 (Figure 1I). This integration revealed a group of genes acting to enhance pan-TLR signaling. Among those were *Ugcg* and *Sphk1*, associated with the synthesis of the ceramide-derived metabolites glucosylceramides and S1P, respectively, which were required for and induced by pan-TLR signaling. However, the majority of the genes appeared to dampen TLR signaling. For instance, six genes were identified as negative regulators of CpG- and IMQ-driven signaling and transcriptionally upregulated upon TLR stimulation. Four of these six genes encoded proteins that are associated with de novo ceramide synthesis (*Ormdl1*, *Sptlc1*, *Cers6*, and *Sptlc2*) (Figure 1I) and could be involved in preventing hyperinflammation and promoting the resolution of inflammation in response to endosomal TLR activation (Serhan et al., 2008). Further, a different set of genes associated with ceramide synthesis was specifically regulated by and functionally involved in TLR4 signaling (*Cers5*, *Cers2*, *Smpd4*, and *Ormdl3*) (Figure 1I). Taken together, the integration of TLR-induced transcriptional regulation of sphingolipid metabolic genes with their corresponding perturbation phenotypes revealed both positive and negative modulators of TLR function across various branches of sphingolipid metabolism.

To resolve these different phenotypes at the level of individual membrane lipids, nine gene perturbations (sh:Sptlc2_1, sh:Cers2_4, sh:Cers6_2, sh:Smpd1_4, sh:Ormdl1_3, sh:Ugcg_1, sh:Asah1_2, sh:Lyst_1, and sh:Cln3_1) were selected for further characterization by quantitative lipidomics (Table S1). The IL-6 release phenotypes upon knockdown of these genes were consistent across multiple independent shRNAs (Figures 1D and S1I). To maximize the statistical power by which lipid-phenotype relationships could be inferred, this subset of genes was chosen to represent diverse IL-6 release phenotypes across the different regulatory mechanisms and across sphingolipid metabolic branches (indicated in Figures 1A, 1E–1G, and 1I).

Genetic Perturbations of Sphingolipid Metabolism Lead to Diverse Membrane Lipid States

Mass spectrometry-based lipidomics was used to measure the abundance of 245 membrane lipids at steady state in the nine

selected cell lines and the sh:GFP control (Figure 2A). Specifically, glycerophospholipids (phosphatidylcholines [PC], phosphatidylethanolamines [PE], phosphatidylglycerols [PG], and phosphatidylserines [PS]) and sphingolipids (ceramides [Cer] and sphingomyelins [SM]) were quantified. The developing field of lipidomics still lacks standardized methods for data normalization, analysis, and visualization, as well as for lipid annotation (Snijder et al., 2014). Here, lipid levels were normalized to total lipid content and transformed as log₂ fold-change relative to the sh:GFP control (Figure S2A). Both raw and transformed formats are available as supplementary results, annotating all lipids with two complementary nomenclatures (Table S2). The three biological replicates displayed high reproducibility (average $r = 0.89$). Throughout this data set, significant increases and decreases were observed for the majority of lipid classes in each of the nine perturbations, defining the unique lipid states in which their cellular phenotypes manifested (Figure 2B).

Analysis of the changes in lipid composition caused by the nine perturbations revealed both expected and unexpected results. As expected, in most cases silencing of an enzyme led to increased substrate levels and/or decreased product levels. For instance, knockdown of the serine palmitoyltransferase *Sptlc2*, a key enzyme for de novo synthesis of ceramides (Hanada, 2003), led to a strong reduction in ceramide levels (Figure 2B). Knockdown of ceramide synthases 2 or 6 also reduced ceramide levels, including individual species with specific fatty acid chain lengths that have previously been associated with each enzyme (Figures 2A, 2B, and S2B) (Levy and Futerman, 2010). Total ceramide levels were decreased, and sphingomyelin levels were increased, upon knockdown of the sphingomyelinase *Smpd1* (Figure 2B). Following this consistent pattern, ceramide levels were significantly increased upon knockdown of *Ormdl1*, a negative regulator of ceramide synthesis (Breslow et al., 2010), and upon knockdown of *Ugcg*, the ceramide glucosyltransferase (Figure 2B). An unexpected reduction in total ceramide levels was however measured upon the depletion of the acid ceramidase ASAH1. This observation supports the notion that ASAH1 may function bimodally, mediating not just degradation but also synthesis of ceramides, consistent

Figure 1. TLR-Driven Transcription of the Sphingolipid Metabolic Network and Characterization of Cytokine Release upon shRNA-Mediated Silencing of This Network

(A) Selected sphingolipid and glycerophospholipid metabolic reactions (KEGG), shown together with main metabolites (rounded rectangles) and 24 selected proteins (rectangles). Protein location based on KEGG where possible. Heatmaps show relative expression of 24 selected genes after stimulation of RAW cells with LPS (100 ng/ml) or CpG (5 μ M) for indicated time points measured by qRT-PCR. Bold protein names indicate selection for lipidomics analysis. Metabolites are colored consistently throughout the study. Data are combined of at least two independent experiments with technical triplicates. FC, fold-change; Spha, sphinganine; Spho, sphingosine; C1P, ceramide-1-phosphate. For other abbreviations, see text or legend and Table S1.

(B) Schematic representation of the generation and characterization of stable shRNA RAW cell lines, filtered based on knockdown efficiency.

(C) IL-6 release as measured by ELISA in sh:TLR and sh:GFP control cell lines stimulated with IMQ (5 μ M), or LPS (100 ng/ml) or CpG (5 μ M) for 16 hr. Data are representative of at least five independent experiments and shown as mean \pm SD of four technical replicates. * $p < 0.0001$.

(D) As in (C), but for sh:Sphk1, sh:Cers2, and sh:Ormdl1 cell lines. Data are representative of at least five independent experiments and shown as mean \pm SD of four technical replicates. * $p < 0.005$.

(E–G) Screening results of three IL-6 release screens in 87 loss-of-function cell lines stimulated for 16 hr with IMQ, CpG, and LPS as measured by ELISA. Values are plotted as log₂ fold-change relative to the respective sh:GFP control cell line and averaged over multiple shRNA cell lines. Black dots represent the averages of two or more shRNA cell lines with consistent phenotypes, while gray dots represent averages of all shRNA cell lines per gene. Indicated genes are selected for lipidomics analysis. Data are combined of at least five independent experiments.

(H) Scatter plot of IMQ and CpG screening results. Red line indicates linear fit. Data are combined of at least five independent experiments.

(I) Heatmap shows integration of target gene expression in wild-type RAW cells after stimulation with LPS and CpG and IL-6 release screening results of shRNA cell lines. Gray triangles indicate absence of consistent phenotypes for multiple shRNAs per gene. Data are combined of at least five independent experiments. See also Figure S1 and Table S1.

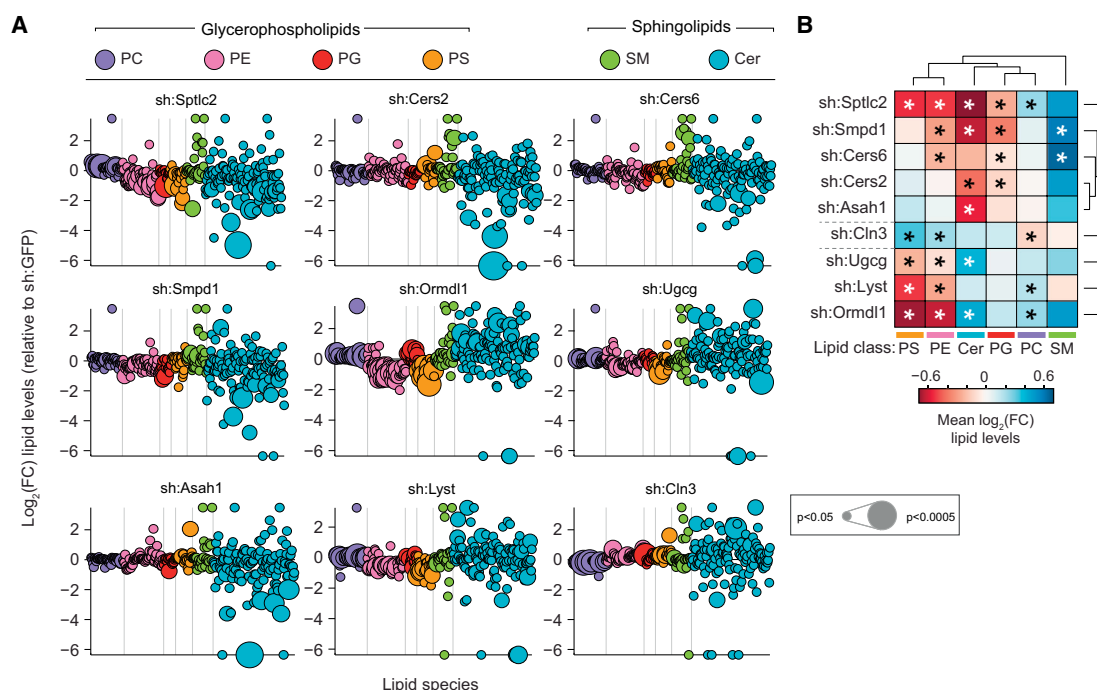


Figure 2. Quantitative Lipidomics of Nine Stable shRNA Cell Lines Targeting Sphingolipid Metabolism Reveals Strongly Altered Lipid States

(A) Lipidomics analysis of nine loss-of-function cell lines. Values are shown as \log_2 fold-change relative to sh:GFP. Each dot represents a lipid species, color coded per lipid class. Dot size indicates significance. Lipidomics data are combined of three independent experiments and represented as mean.

(B) Hierarchical clustering of average \log_2 fold-change lipid levels per lipid class and cell line. Lipidomics data are combined of three independent experiments and represented as mean. * $p < 0.05$.

See also Figure S2 and Table S2.

with previous in vitro data (Okino et al., 2003) (Figure 2B). Given that most of these perturbed genes are members of larger conserved gene families, based on either sequence similarity or enzymatic function, the strongly altered lipid states revealed an absence of redundancy between these family members. This goes against previous findings suggesting functional redundancy within the ORM1-like gene family (Siow and Wattenberg, 2012).

Perturbing sphingolipid metabolism unexpectedly led to changes in glycerophospholipid levels, with strongest changes observed upon knockdown of *Sptlc2* and *Ormdl1* (Figure 2B). Knockdown of *Lyst* and *Cln3*, both involved in lysosomal trafficking, only led to significantly altered glycerophospholipid levels (Figure 2B). In summary, the selected set of genetic perturbations targeting sphingolipid metabolism translated to a remarkable heterogeneity in lipid states, revealing considerable tolerance of cells to such perturbations and establishing these as an effective method to alter cellular lipid composition and study the functional consequences. Additionally, this membrane lipidomics analysis underscored a strong link between the sphingolipid and glycerophospholipid metabolic networks.

Hierarchical clustering of the average fold-changes per lipid class and per cell line separated genes associated with ceramide synthesis from those associated with other processes (Figure 2B). We therefore applied the hierarchical interaction score (HIS) for network reconstruction between perturbed genes

(Snijder et al., 2013), analyzing hierarchical patterns among the measured lipid species of each perturbation (Figure S2C). The HIS correctly inferred the known metabolic hierarchy of the different enzymes starting with SPTLC2, over CERS2 and CERS6, to ASAH1 and SMPD1 (Figure S2C). This intriguingly suggested that diverse membrane lipid states resulting from genetic perturbations may be instrumental for the unbiased reconstruction of gene-centered metabolic networks, as also shown in yeast (da Silveira Dos Santos et al., 2014).

A Logical Circular Network of Coregulated Lipids

Given the broad changes in lipid composition over the diverse genetic perturbations, we next analyzed the coregulation of lipid abundance at the level of individual lipid species to expose the larger organizational principles that orchestrate membrane lipid composition. Comparing the lipid abundance of individual lipid species across all nine perturbations revealed pairs of positively and negatively correlated lipids (Figure 3A). Such positive correlations, indicative of lipid coregulation, occurred both within and between lipid classes (Figure 3B). Hierarchical clustering of the complete lipid-lipid correlation matrix describing 29,890 unique pairs of lipids revealed ten distinct lipid clusters of positively correlated lipids, organized along the diagonal of the matrix (Figure 3C). Neighboring clusters showed positive correlations, whereas distant clusters were negatively correlated with each other (Figure 3C). Intriguingly, analysis of the lipid composition

per cluster revealed sphingolipids to be distributed over all clusters, whereas significant separation of glycerophospholipid classes was observed between different clusters (Figure 3D). Positively correlated glycerophospholipid classes reflected their proximity in the metabolic pathway, as clusters 8 and 9, the two largest clusters, contained most PS and PE species, and clusters 1 to 5 grouped most PC and PG species. Interestingly, the strong negative correlation between these two sets of clusters identified that a loss in PS and PE was associated with increased levels of PC, as observed for *sh:Sptlc2* and *sh:Ormdl1* and inversely for *sh:Cln3* (Figure 2B). This general trend has also been reported in yeast and may be indicative of conserved metabolic adaptation (Boumann et al., 2006). Positive correlations therefore indicated coregulation between lipids driven by proximity in metabolic pathways and structural dependencies. Negative correlations, in turn, reflected compensation or adaptation between lipids within the cell. Analysis of fatty acid chain length properties per cluster and lipid class further revealed that separation of lipid species from the same class into different clusters was associated with significant changes in chain length, following a trend over neighboring clusters ($p < 0.01$ – $p < 0.001$, Figure 3E).

Interestingly, the most distant lipid clusters 1 and 10 were positively correlated, which suggested that this hierarchical view on cluster organization was a suboptimal representation of lipid coregulation (Figure 3C). We therefore transformed the lipid-lipid correlation matrix into a network where nodes represented individual lipid species and edges represented positive correlations of 0.7 or higher (Figure 3F). Strikingly, this correlation network displayed near-perfect circularity. Continuity across the different lipid clusters was revealed by mapping different lipid features, including lipid class, and fatty acid linkage and chain length, onto the network (Figures 3F, S3A, and S3B). This network view furthermore emphasized the distribution of sphingomyelins and, to a lesser extent, ceramides across the network, indicative of a general strong coregulation of individual sphingolipids with glycerophospholipids (Figure 3F).

Color-coding each node in this network according to the \log_2 fold-change in lipid abundance revealed significant ($p < 3.6 \times 10^{-28}$) bimodal separation of increased and decreased lipids for each of the nine perturbations (Figure 3G). These bimodalities reflected an imbalance in the lipid state of each perturbation, supporting the notion that opposite segments of the circular network were also defined by metabolic adaptation. Validating the relevance of this circular network beyond this dataset, the results of an independently performed lipidomics analysis in RAW cells stably silencing *Smpd3b* were projected on this network, which also led to the significant separation of increased and decreased lipids ($p < 1.2 \times 10^{-5}$), revealing yet another unique lipid state (Figure S3C) (Heinz et al., 2015).

Cellular membranes are known to be comprised of lipids with similar fatty acid chain lengths (Holthuis and Menon, 2014; van Meer et al., 2008). Indeed, the majority (58%) of lipid coregulation was found between lipid species with fatty acid chain length differences of two or less, with only ceramides not following this trend (Figure 3H). To assess if the circular network reflected the spatial organization of lipids, we used publicly available lipidomics measurements of subcellular membrane fractions of

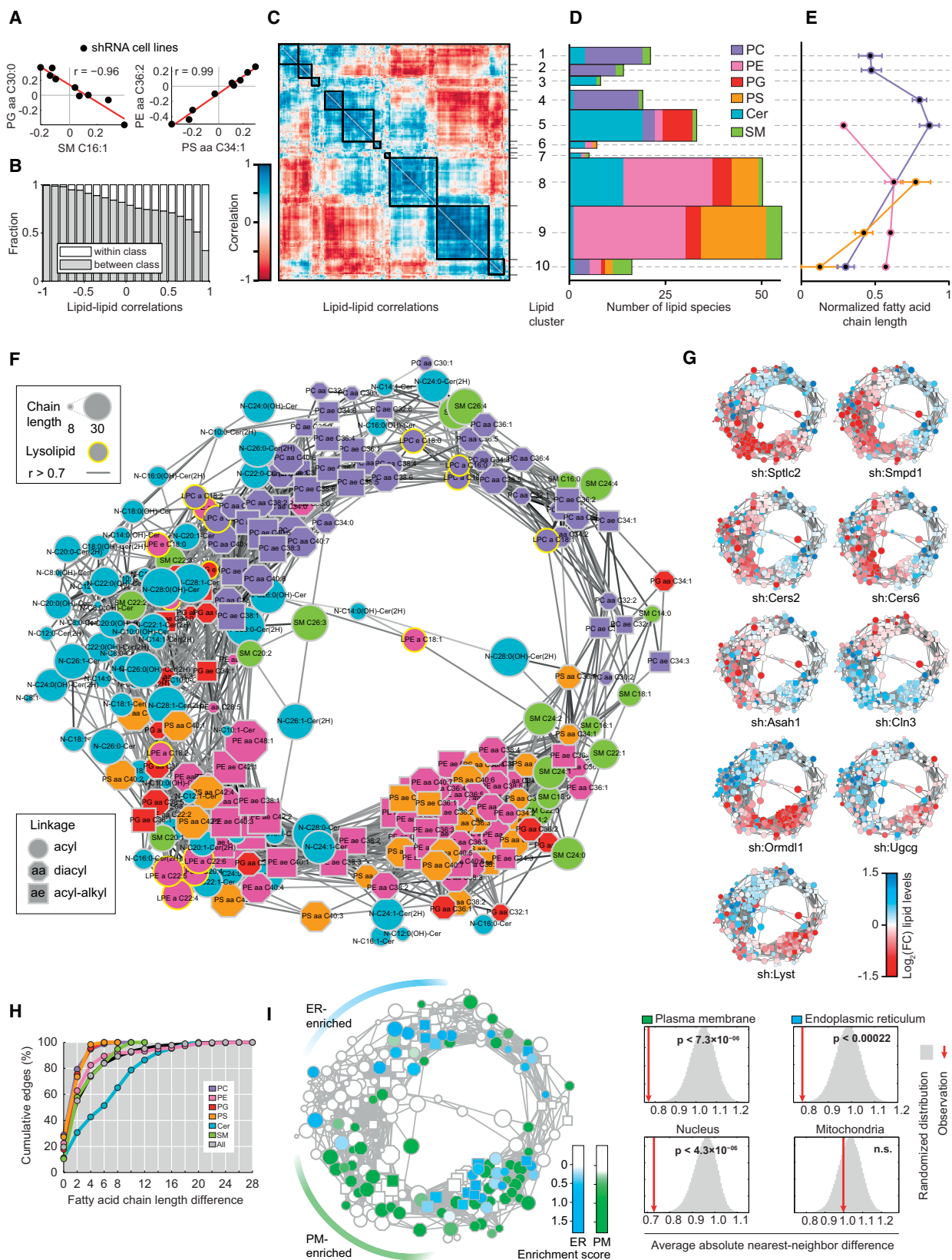
RAW cells (Andreyev et al., 2010). Mapping of lipids enriched in the different fractions identified distinct segments of the circular network predominantly connecting lipids enriched in either plasma membrane (PM; $p < 7.3 \times 10^{-6}$) or ER ($p < 0.00022$) fractions (Figure 3I). Consistent with previous reports, the coregulated long-chained PS and PE species were mostly enriched in the plasma membrane fraction, while the PC species were mostly ER-enriched (Figure 3I) (van Meer et al., 2008). Calculating the significance of the clustering of enriched lipids on the circular network further revealed significant clustering of nuclear-enriched lipids ($p < 4.3 \times 10^{-6}$), but not of mitochondrial-enriched lipids (Figure 3I).

As an alternative to a protein-centered view on metabolic networks, this analysis of lipid coregulation offered a unique view of the mammalian lipid landscape, revealing a potentially universal logic in lipid organization. Intriguingly, circularity is not typically observed in biological coregulation networks (Costanzo et al., 2010) and may therefore be a unique property of metabolic networks.

Functional Annotation of the Lipid Landscape in TLR Signaling

We next sought to resolve the diverse TLR-phenotypes at the level of earlier TLR signaling and integrate the phenotypes with the abundance of individual lipid species. IL-6 release into the supernatant is a late read-out of TLR activation, as it depends on TLR expression, trafficking, signaling, and cytokine transcription. Therefore, TLR4 plasma membrane levels at steady state as well as LPS-induced internalization dynamics over time (Figure S4A) were monitored for all 24 genetic perturbations and controls using representative cell lines (Figure 4A; Table S1). Silencing of eight genes showed significant reductions of TLR4 surface levels at steady state (>40% reduction at $p < 0.01$) although none of the genetic perturbations led to a reduction stronger than *sh:Tlr4* (87.5%) (Figures S4B–S4D). LPS-dependent activation of TLR4 led to partial receptor internalization at 5 min and a near complete internalization after 30 min for all monitored perturbations (Figures 4A, S4C, and S4D). Normal TLR4 surface levels at steady state were observed for most of the genetic perturbations that led to the strongest reductions in LPS-induced IL-6 release (Figure S4E). However, increased internalization of the receptor 5 min post-stimulation was observed for several perturbations including the three that led to the strongest reductions in IL-6 release (*Cers2*, *Cers5*, *Ormdl2*). Sphingolipid metabolism therefore mostly modulated LPS-induced IL-6 release by altering the trafficking and likely subsequent signaling of TLR4 after stimulation rather than by altering the steady-state TLR4 surface levels.

To monitor changes in early TLR signaling we performed time course measurements of TLR-induced *Il6* transcription for a subset of genetic perturbations including the nine cell lines analyzed by lipidomics (Table S1). Strong changes in *Il6* transcript levels were observed, while peak *Il6* transcript levels were maintained at 10 hr post-stimulation for all tested cell lines (Figures 4B and S4F), indicating that sphingolipid metabolism affected early TLR signaling, modulating the amplitude not the dynamics of TLR-induced *Il6* transcription. Integration with the corresponding IL-6 release phenotypes could separate changes in TLR



(legend on next page)

signaling from defects in cytokine secretion. As expected, most of the cell lines tested displayed altered *Il6* transcription coherent with the measured changes in IL-6 release (Figure S4G). Surprisingly though, knockdown of *Cers2* showed increased *Il6* transcription but decreased IL-6 release, suggestive of enhanced TLR signaling being followed by a post-transcriptional block, potentially at the level of secretion (Figures S4F and S4G). Indeed, intracellular staining of IL-6 after stimulation revealed a strong perinuclear accumulation in a subset of *Cers2* silenced cells, while no intracellular accumulation was observed in the controls (sh:GFP or sh:TLR4) (Figure S4H). Knockdown of *Cers2* did however not affect the regulated exocytosis of chemokine CCL5 (Lacy and Stow, 2011), as its TLR-induced release was not reduced (Figure S4I).

Integration of TLR-dependent read-outs with the changes in lipid abundance could allow functional annotation of individual lipids across the lipid landscape. To identify the changes of lipid abundance associated with, for instance, TLR4 surface levels, we analyzed consistent trends over all nine perturbations. This correlation analysis revealed potential functional relationships, as exemplified by the negative correlation ($r = -0.84$) between the relative abundance of ceramide C20:0 and TLR4 PM levels (Figure 4C). An increase of this lipid species, strongest in sh:Ormdl1 and sh:Ugcg, was associated with reduced TLR4 levels at the plasma membrane (Figure 4D). However, the strong coregulation in the abundance of lipid species identified in this study necessitated a more global analysis of potential lipid function. Therefore, correlations between each TLR-related process and the relative abundance of each lipid were calculated ($n = 2,205$; Table S2) and mapped onto the lipid coregulatory network (Figures 4E–4H). This resulted in highly significant ($p < 3.1 \times 10^{-63}$) separations of positive and negative correlations between functional readouts and lipid abundance (Figures 4E–4H and S4J). Comparing the functional annotations for TLR4 PM levels with *Il6* transcription and IL-6 release revealed different yet overlapping segments of the circular network to be positively and negatively correlated (Figure 4E–4H). This suggested that

distinct sets of lipids were functionally related to each step in TLR signaling. The distribution of the functional annotations on the network did not considerably change depending on the different ligands for TLR-induced IL-6 release or time points for LPS-induced TLR4 surface levels, despite changes at the individual lipid level (Figures 4E–4H and S4J).

The similarity in predicted lipid function of neighboring and coregulated lipids in the lipid landscape is consistent with the view that the majority of membrane lipids function in concert with other lipids. Mapping the different correlations onto the circular lipid network revealed short-chained glycerophospholipids and sphingomyelins as positively associated with TLR4 surface expression (Figures 4E and 3F). The majority of ceramides were predicted to negatively modulate TLR4 surface expression, similar to studies reporting that accumulation of ceramides at the plasma membrane led to altered surface expression of the nicotinic acetylcholine receptor (Gallegos et al., 2008). Among the other lipids negatively correlated with TLR4 PM levels were the glycerophospholipids with the longest fatty acid chains associated with the plasma membrane, as well as their lysolipids (Figure 4E). Lysolipids facilitate membrane curvature required for vesicle trafficking (Holthuis and Menon, 2014). The subset of lipids negatively correlated with both IL-6 release and TLR4 PM levels contained most PS species (Figures 4E, 4G, and 4H), for which individual species have been described to negatively influence TLR-induced responses by disrupting membrane microdomains (Parker et al., 2008). Intriguingly, sphingomyelins and ceramides were predicted to both positively and negatively regulate IL-6 release: unsaturated sphingomyelins and short-chained ceramides resided within the positively correlated region of the network, while saturated or nearly saturated sphingomyelins and long-chained ceramides resided within the negatively correlated region at the opposite segment of the network (Figures 4G, 4H, and S4K).

To validate the different predicted functions of sphingolipids in TLR-induced IL-6 release, candidate lipids were selected from the coregulated lipid clusters most enriched for either positive

Figure 3. Analysis of Lipid Abundance Reveals the Circular Organization of the Lipid Coregulatory Network

(A) Scatter plots show example pairs of lipids whose relative abundance over the nine perturbations is negatively (left panel) or positively (right panel) correlated. Red lines indicate linear fit. Data are combined of three independent experiments and shown as mean.

(B) Analysis of the fraction of correlations that link lipids of the same lipid class (white) or different lipid classes (gray), as function of correlation strength. Data are combined of three independent experiments and shown as mean.

(C) Hierarchical clustering of the lipid-lipid correlation matrix. Rows and columns correspond to the 245 measured lipid species. Black boxes indicate clusters of strongly positively correlated lipids. Lipid cluster numbers indicated on the right. Data are combined of three independent experiments and shown as mean.

(D) Analysis of the number of lipids in each cluster per lipid class. Width of the bars is scaled to match (C). Data are combined of three independent experiments and shown as mean.

(E) Normalized fatty acid chain lengths for selected clusters and lipid classes. Lipid classes are colored as in (D). Chain length is normalized from the shortest to the longest fatty acid side chain per class. Data are combined of three independent experiments and shown as mean. Values are mean \pm SEM.

(F) Network visualization of the positive lipid-lipid correlations. Edges are correlations of $r \geq 0.7$. Nodes are lipids. Node shape, size, and outline represent fatty acid bonds, chain length, and lysolipids, respectively (see legends). Data are combined of three independent experiments and shown as mean.

(G) Nodes of the network are color-coded based on the fold-change of relative lipid abundance for each of the nine shRNA cell lines as indicated in legend. Data are combined of three independent experiments and shown as mean.

(H) Cumulative percentage of lipid coregulation as a function of the maximum fatty acid chain length difference per lipid class and for all (see legend). Data are combined of three independent experiments and shown as mean.

(I) Left: network visualization of lipid enrichment in either ER (blue) or plasma membrane (PM, green) subcellular fractions. White nodes depict not enriched or not measured lipids. Right: significance of the clustering on the circular network for the enrichment in four subcellular fractions. Red lines indicate the average absolute difference between enrichment scores of direct neighbors in the network, gray areas indicate the distribution of randomized repeats. NS, not significant. Subcellular fraction data are from <http://lipidmaps.org> combined of three independent experiments and shown as mean.

See also Figure S3.

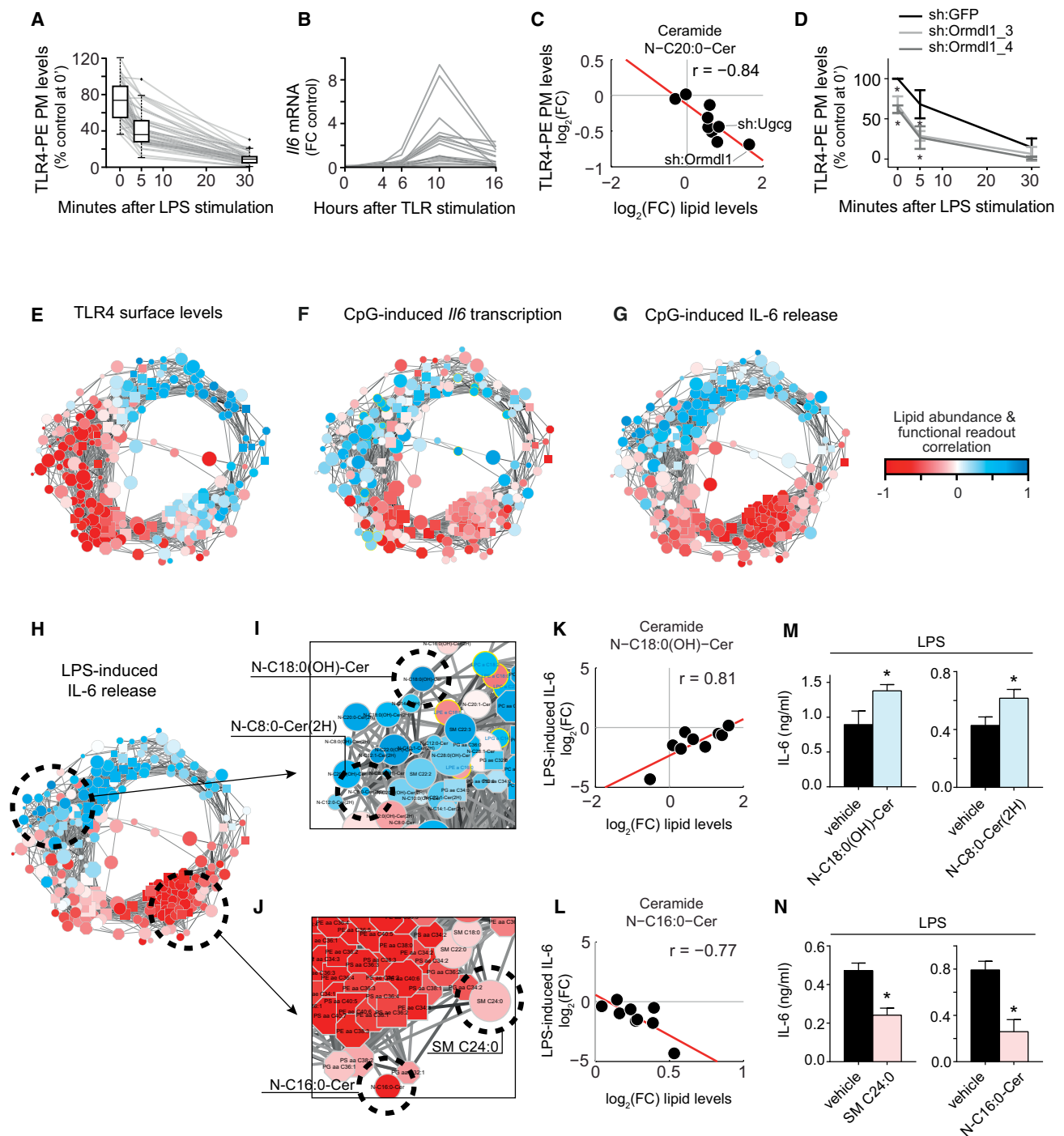


Figure 4. Inference and Validation of Lipid Function in TLR-Related Processes

(A) TLR4 PM levels after stimulation with LPS for indicated time points normalized to unstained and steady-state control levels for 41 cell lines silencing 24 genes. Both box-and-whisker plots and individual line plots are shown. Lines represent mean values of two independent experiments.

(B) *Il6* expression after TLR stimulation measured at indicated time points and normalized to unstimulated and 10h sh:GFP control for 14 cell lines. Lines represent mean values of two independent experiments.

(C) Scatter plot shows example correlation between relative lipid abundance and TLR4 PM levels over the nine perturbations. Red line indicates linear fit.

(D) As in (A), TLR4 PM levels for sh:Ormdl1_3, sh:Ormdl1_4 and sh:GFP control. Data are shown as mean \pm SD of two technical replicates * $p < 0.05$.

(E–H) Correlations between relative lipid abundance and measurements of selected TLR-related processes plotted on the circular network.

(I and J) Network close-up of lipids positively (I) and negatively (J) correlated with LPS-induced IL-6 release.

(legend continued on next page)

or negative correlations (Figures 4I–4L). A determining factor in candidate selection was the availability of synthetic lipids in a chemically pure form. Compared to vehicle treatment, RAW macrophages showed enhanced LPS-stimulated IL-6 release when pre-treated with the ceramides N-C18:0(OH)-Cer or N-C8:0(2H)-Cer (Figure 4M), validating the inferred function of these two ceramides. Treatment with these lipids alone did not induce IL-6 release. Conversely, LPS-induced IL-6 release after pre-treatment with the sphingomyelin SM C24:0 or the ceramide N-C16:0-Cer was dampened compared to vehicle treatment (Figure 4N), validating the inferred inhibitory function of these lipids on IL-6 release. Lipid supplementation did not affect viability in any of the experiments (Figure S4L).

As sh:Smpd13b was not included in the set of perturbations that led to the identification of the lipid coregulatory network and to the lipid functional annotations, the lipidomics analysis of sh:Smpd13b, performed with different infrastructure, was used to test the predictive power of the complete functional annotation of the lipid landscape (Figure S4M). The lipid state of sh:Smpd13b displayed a highly significant increase of lipids positively associated with, and a decrease of lipids negatively associated with LPS-induced IL-6 release ($p < 2.4 \times 10^{-8}$). This, therefore, correctly predicted a TLR-induced hyperinflammatory phenotype upon knockdown of *Smpd13b* in the same cellular system, based solely on the changes in lipid abundance. Validation experiments confirmed increased pan-TLR signaling in *Smpd13b* knockdown cells, and *Smpd13b* knockout mice displayed enhanced inflammation in LPS- and *Escherichia coli*-induced peritonitis models (Heinz et al., 2015). Further, pre-treatment of the hyperinflammatory sh:Smpd13b cells with a set of ceramide lipid species here predicted to act anti-inflammatory lowered LPS-induced IL-6 release to the levels observed in sh:GFP control (Heinz et al., 2015).

In conclusion, organization of the lipid coregulatory network strongly reflected lipid function across the diverse steps of TLR signaling, revealing a higher-level functional organization for membrane lipids with predictive power at the level of single lipids and the global lipid landscape.

The Lipid Coregulatory Network Is Conserved between Human and Mouse

Mutations in genes associated with sphingolipid metabolism lead to sphingolipid storage disorders associated with severe neurodegeneration and premature death (Futerman and van Meer, 2004). In both patients and mouse models of these diseases, altered cytokine levels have been reported previously (Barak et al., 1999; Wang et al., 2014). To test the validity of the functional annotation of the lipid landscape in a human setting, and independent of shRNA-mediated gene silencing, we performed quantitative lipidomics on patient-derived fibro-

blasts and their age-matched healthy controls at steady state (Table S3). The patient fibroblasts harbored mutations associated with Gaucher disease, Krabbe disease, Farber disease, and Chediak-Higashi syndrome (Figure 5A). Calculation of the fold-changes of membrane lipid abundance by normalizing against the corresponding healthy controls showed that the fibroblasts also displayed broadly altered lipid states, affecting both glycerophospholipids and sphingolipids (Figure S5A). Measuring lipid-lipid coregulation in this smaller dataset derived from human fibroblasts significantly confirmed the circular lipid coregulatory network derived from mouse RAW macrophages ($p < 10^{-222}$, Figure 5B). This striking overlap showed conservation of the circular organization of lipid coregulation across species, cell types, and genetic perturbations. Plotting the fold-change lipid abundance for each disease onto the circular network further confirmed the bimodal separation of increased and decreased lipids, indicating that the adaptation mechanisms revealed by the circular organization also occurred in human cells (Figure 5C).

Lipid Functional Annotation Predicts the TLR-Induced Response of Patient-Derived Fibroblasts

To globally test the validity of the functional lipid annotations, we next used the changes in lipid abundance to predict the inflammatory states of the patient fibroblasts. The lipid states of Krabbe and Gaucher patient-derived fibroblasts displayed strong positive correlations with the functional lipid annotations for IL-6 release, predictive of a hyperinflammatory response (Figure 5D). Inversely, the lipid states of Farber and Chediak-Higashi patient-derived fibroblasts were predictive of a dampened cytokine release in response to LPS and CpG (Figure 5D). Strikingly, TLR stimulation of the four patient fibroblast samples and corresponding healthy control samples confirmed the predicted inflammatory states; with increased IL-6 release measured for Krabbe and Gaucher and decreased IL-6 release measured for Farber and Chediak-Higashi fibroblasts (Figure 5E). In unstimulated conditions, all of the human samples showed only background IL-6 levels in the supernatant (Figure 5E). When calculating the log₂ fold-changes in lipid abundance between pairs of healthy controls, the resulting lipid states were not predictive of either a hyperinflammatory or dampened inflammatory response (Figures 5F and S5B). Indeed, when stimulated under equal conditions, no significant differences in TLR-induced IL-6 release were measured between the healthy control fibroblasts (Figure S5C). In total, the functional lipid annotation derived from RAW cells correctly predicted the inflammatory state of seven of the eight different human fibroblast samples (Figure 5F). The lipid state of the second Gaucher patient fibroblast sample was significantly clustered on the circular network of lipid coregulation (Figure S5D), but was not predictive of an altered IL-6

(K) Example correlation of the relative abundance of N-C18:0(OH)-Cer with LPS-induced IL-6 release over all nine cell lines. Red line indicates linear fit.

(L) As in (K), but for the negatively correlated N-C16:0-Cer.

(M) IL-6 release as measured by ELISA after pre-treatment with N-C18:0(OH)-Cer (15 μ M) or N-C8:0-Cer(2H) (15 μ M) or respective vehicle controls. Data are representative of three independent experiments and presented as mean \pm SD of four technical replicates. * $p < 0.005$.

(N) As in (M), pre-treatment with N-C16:0-Cer (15 μ M) or SM C24:0 (15 μ M) or respective vehicle controls. Data are representative of three independent experiments and presented as mean \pm SD of four technical replicates. * $p < 0.005$.

See also Figure S4 and Table S1.

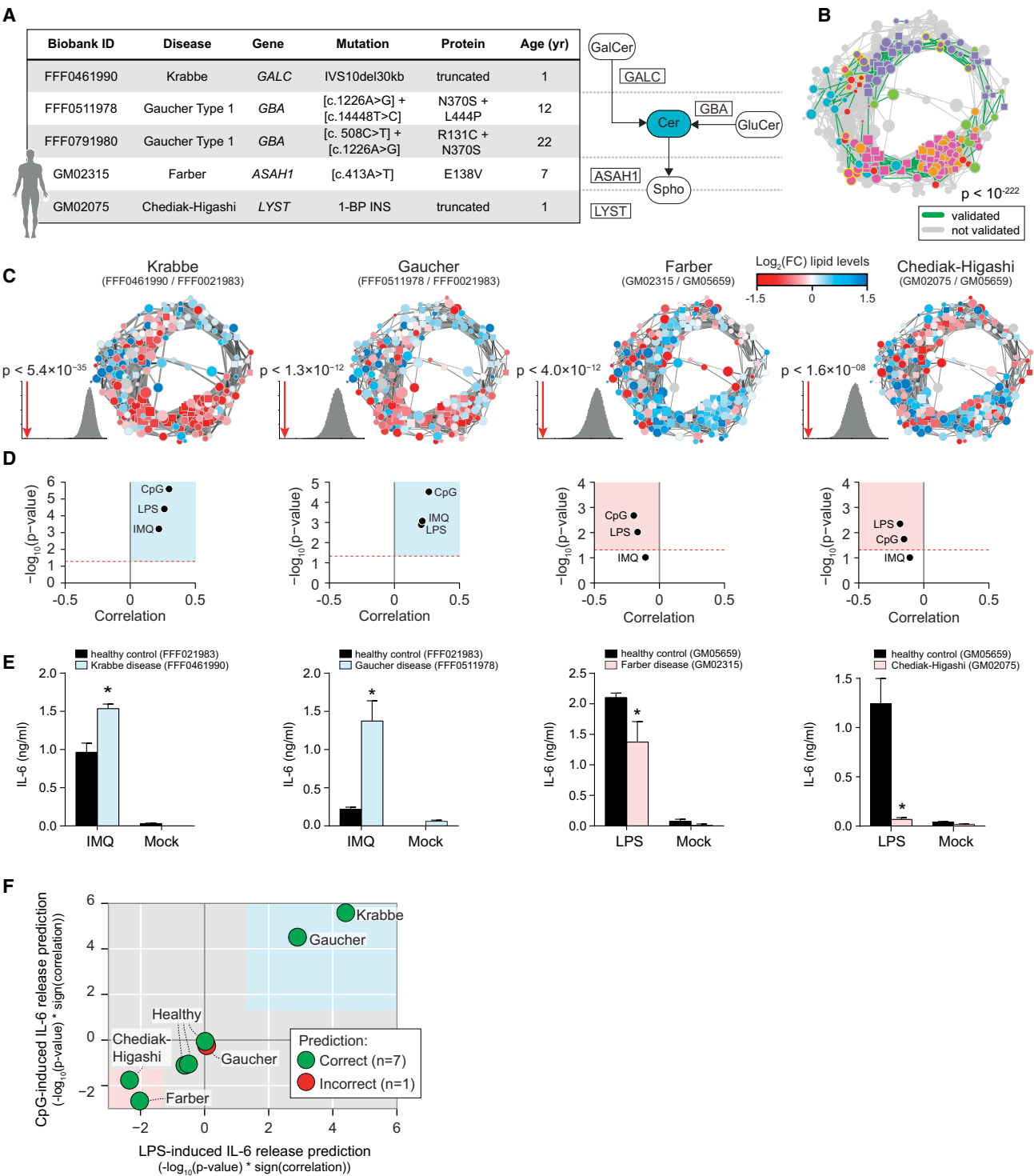


Figure 5. Lipidomics Analysis of Patient-Derived Fibroblasts Confirms the Circular Lipid Coregulatory Network and Functional Lipid Annotations

(A) Overview of different patient-derived fibroblast samples. Mutated genes are indicated in a close-up of the ceramide metabolic network. (B) Coregulated lipids observed in both datasets (see legend). Significance ($p < 10^{-222}$) calculated by the hypergeometric distribution. Data are combined of three independent experiments.

(legend continued on next page)

release phenotype (Figure S5E), even though this was experimentally shown (Figure S5F). Taken together, quantitative lipidomics of patient-derived fibroblasts confirmed both the lipid coregulatory network and the functional annotation of lipids in TLR-induced IL-6 release.

DISCUSSION

Building on the previous success of network-informed perturbation strategies (Bouwmeester et al., 2004) and the ability to quantitatively measure lipid abundance of hundreds of lipid species (Shevchenko and Simons, 2010; Wenk, 2005), we have developed an integrative framework that combined quantitative lipidomics with genetic perturbations and their phenotypic assessment across various TLR-related parameters. In analogy to the early advances in transcriptomics (Eisen et al., 1998), our approach led to the discovery of the conserved circular organization of lipid coregulation and the unbiased inference of lipid function in innate immunity across the lipid landscape.

As the circular lipid network reflects the intersection of different lipid metabolic pathways, metabolic adaptability, and the spatial organization of lipids, it offers a global view of the mammalian lipid landscape. Metabolic pathways commonly display circular motifs, with the citric acid cycle and the urea cycle as well-known examples. Circularity in metabolite coregulation at the order of magnitude discovered here may therefore be a fundamental property of lipid and potentially other metabolic networks. The tight coregulation between lipid species of different classes, most notably between sphingolipids and glycerophospholipids, suggested that part of the robustness of cells to loss of certain membrane lipids may stem from the fact that they are able to functionally compensate this by increasing other lipids (Boumann et al., 2006). It is conceivable that the identified coregulatory interactions are context-dependent, as observed for genetic interactions and signaling networks (Bandyopadhyay et al., 2010). Future comparisons with lipid coregulatory networks measured in different physiological contexts and with measurements of additional lipid classes such as sterols will allow to distinguish general properties from context-dependent variation.

Since membrane lipids predominantly act in concert, and given the strong coregulation of lipids observed, annotation of functions for single lipid species in mammalian cells is challenging and may be uniquely amenable to systematic approaches such as the one developed here. The inference of lipid function, validated at the individual and global lipid level, revealed strikingly opposite functions for individual ceramide species in TLR-driven inflammation

(Hannun and Obeid, 2011), consistent with previous contradictory reports on the role of ceramide in inflammation (Józefowski et al., 2010; Vandanmagsar et al., 2011). The functional annotations of membrane lipids in the different TLR-related processes were organized in a continuum on the circular lipid coregulatory network, the implication of which requires further investigation.

The finding that the inflammatory state of perturbed cells could be predicted based solely on this global functional annotation of lipids indicates that the protein state of a cell mediating the inflammatory phenotype is strongly dependent on and intertwined with the cellular lipid state. The concept of predicting functional phenotypes based on different lipid states as outlined in this work should be applicable to more membrane-dependent processes such as cell division (Atilla-Gokcumen et al., 2014), proliferation, apoptosis (Pettus et al., 2002), and autophagy (Singh et al., 2009). Since many of the lipids measured here are present in identical chemical form in different organisms (Guan et al., 2010), the conservation of the identified lipid coregulation and function is an exciting avenue for further research. The unbiased functional annotation of lipids therefore advances lipidomics to complement the genomic and proteomic characterization of cells, expanding our toolset for the investigation and diagnosis of complex diseases. Intriguingly, it may aid the informed design of therapeutic interventions that modulate the cellular lipid state. The framework developed here can identify the function of the lipid landscape in additional biological settings, is scalable to more and diverse perturbations and likely applicable to other metabolites, invaluable for a systems-level understanding of cellular physiology across organisms.

EXPERIMENTAL PROCEDURES

Human Fibroblasts

The following fibroblast samples were obtained from the NIGMS Human Genetic Cell Repository at the Coriell Institute for Medical Research: (GM02075, GM02315, GM05659). The “Cell line and DNA biobank from patients affected by genetic diseases” (Istituto G. Gaslini), member of the Telethon Network of Genetic Biobanks (project no. GTB12001) funded by Telethon Italy, provided us with specimens of human fibroblasts.

Lipid Supplementation

All lipids were solubilized as previously described using ethanol/dodecane (Wijesinghe et al., 2009). RAW264.7 cells were incubated for 30 min with indicated lipid concentrations prior to LPS stimulation.

Lipidomics

Targeted lipidomics analysis was performed on an AB SCIEX triple-quadrupole mass spectrometer operating in positive and negative MRM mode (BIOCRATES Life Sciences AG, Innsbruck, Austria). Forty-three Calibrators in seven levels and

(C) Lipid abundance plotted on the circular network for four patient fibroblast samples. Significance of the clustering on the circular network for the lipid abundance measurements is calculated and shown as in Figure 3I. Data are combined of three independent experiments.

(D) IL-6 release phenotype predictions for each of the patient fibroblast samples are based on the correlation between lipid functional annotation and lipid abundance. Red dashed line indicates $p < 0.05$. Colored areas indicate significant phenotype predictions (blue, increased IL-6 release; red, reduced IL-6 release).

(E) IL-6 release after stimulation with IMQ (25 μ M) and LPS (1 μ g/ml) as measured by ELISA for patient fibroblasts and age-matched healthy controls. Mock: unstimulated. Patient fibroblast bars are colored according to the predictions. Data are representative of three independent experiments and presented as mean \pm SD of four technical replicates. * $p < 0.001$.

(F) Summary of the LPS- and CpG-induced phenotype predictions for all fibroblast samples, colored according to the agreement between predictions and experiments. Blue and red areas indicate significant ($p < 0.05$) phenotype predictions as in (D).

See also Figure S5 and Table S3.

five internal standards (three of them were deuterated) were used to measure a panel of glycerophospholipids and sphingolipids.

Lipidomics Data Normalization

The lipidomics results were normalized based on the sum of concentrations for all lipid species measured in a single biological replicate. Values were next averaged over the three biological replicates and \log_2 transformed against the corresponding average concentrations measured in sh:GFP.

Network Clustering Significance

The significance of clustering of various features was calculated by comparing the absolute difference of the given feature between a node and its nearest neighbor as defined by the network, averaged over all nodes, with the distribution of over 10,000 repeats of the same calculation using randomly shuffled feature values.

Membrane Fraction Enrichment Score

The lipid subcellular membrane fraction enrichment scores were calculated as the Z score over the lipid concentrations measured for any one lipid species over all the analyzed fractions (Andreyev et al., 2010).

Lipid Function Prediction

Functional predictions or associations for lipids were performed based on Pearson's linear correlation coefficients between the \log_2 (FC) readouts of the TLR-related functional assays and the \log_2 (FC) in lipid levels, over the nine shRNA cell lines.

General Statistics

P values were calculated with two-tailed t tests, unless otherwise indicated. Correlation values given are Pearson's linear correlation coefficients, unless otherwise indicated.

See also the [Supplemental Experimental Procedures](#).

SUPPLEMENTAL INFORMATION

Supplemental Information includes Supplemental Experimental Procedures, five figures, and three tables and can be found with this article online at <http://dx.doi.org/10.1016/j.cell.2015.05.051>.

AUTHOR CONTRIBUTIONS

M.S.K., B.S., L.X.H., C.L.B., A.F., and G.I.V. designed and performed experiments. M.S.K., B.S., L.X.H., C.L.B., A.F., G.I.V., A.-C.G., and G.S.-F. analyzed and interpreted data. M.S.K., B.S., and G.S.-F. wrote the manuscript.

ACKNOWLEDGMENTS

We thank Manuela Bruckner for technical assistance and Omar Sharif, Rüdiger Klein, and the entire G.S.-F. lab for feedback. We gratefully acknowledge funding from the Swiss National Science Foundation (P300P3_147897, to B.S.), EMBO (1543-2012, to G.I.V.), the Austrian Academy of Sciences (to Research Center for Molecular Medicine of the Austrian Academy of Sciences), and the ERC i-FIVE advanced investigator grant (to G.S.-F.). "Cell Line and DNA Biobank from Patients Affected by Genetic Diseases," member of the Telethon Network of Genetic Biobanks (project GTB12001), funded by Telethon Italy, provided us with specimens. We thank Mirella Filocamo from the Instituto G. Gaslini for assistance and feedback.

Received: December 22, 2014

Revised: April 25, 2015

Accepted: May 15, 2015

Published: June 18, 2015

REFERENCES

Alvarez, S.E., Harikumar, K.B., Hait, N.C., Allegood, J., Strub, G.M., Kim, E.Y., Maceyka, M., Jiang, H., Luo, C., Kordula, T., et al. (2010). Sphingosine-1-phos-

phate is a missing cofactor for the E3 ubiquitin ligase TRAF2. *Nature* 465, 1084–1088.

Andreyev, A.Y., Fahy, E., Guan, Z., Kelly, S., Li, X., McDonald, J.G., Milne, S., Myers, D., Park, H., Ryan, A., et al. (2010). Subcellular organelle lipidomics in TLR-4-activated macrophages. *J. Lipid Res.* 51, 2785–2797.

Atilla-Gokcumen, G.E., Muro, E., Relat-Goberna, J., Sasse, S., Bedigian, A., Coughlin, M.L., Garcia-Manyes, S., and Eggert, U.S. (2014). Dividing cells regulate their lipid composition and localization. *Cell* 156, 428–439.

Bandyopadhyay, S., Mehta, M., Kuo, D., Sung, M.K., Chuang, R., Jaehnig, E.J., Bodenmiller, B., Licon, K., Copeland, W., Shales, M., et al. (2010). Rewiring of genetic networks in response to DNA damage. *Science* 330, 1385–1389.

Barak, V., Acker, M., Nisman, B., Kalickman, I., Abrahamov, A., Zimran, A., and Yatziv, S. (1999). Cytokines in Gaucher's disease. *Eur. Cytokine Netw.* 10, 205–210.

Bonham, K.S., Orzalli, M.H., Hayashi, K., Wolf, A.I., Glanemann, C., Weninger, W., Iwasaki, A., Knipe, D.M., and Kagan, J.C. (2014). A promiscuous lipid-binding protein diversifies the subcellular sites of toll-like receptor signal transduction. *Cell* 156, 705–716.

Boumann, H.A., Gubbens, J., Koorengevel, M.C., Oh, C.S., Martin, C.E., Heck, A.J., Patton-Vogt, J., Henry, S.A., de Kruijff, B., and de Kroon, A.I. (2006). Depletion of phosphatidylcholine in yeast induces shortening and increased saturation of the lipid acyl chains: evidence for regulation of intrinsic membrane curvature in a eukaryote. *Mol. Biol. Cell* 17, 1006–1017.

Bouwmeester, T., Bauch, A., Ruffner, H., Angrand, P.O., Bergamini, G., Croughton, K., Cruciat, C., Eberhard, D., Gagneur, J., Ghidelli, S., et al. (2004). A physical and functional map of the human TNF- α /NF- κ B signal transduction pathway. *Nat. Cell Biol.* 6, 97–105.

Breslow, D.K., Collins, S.R., Bodenmiller, B., Aebersold, R., Simons, K., Shevchenko, A., Ejsing, C.S., and Weissman, J.S. (2010). Orm family proteins mediate sphingolipid homeostasis. *Nature* 463, 1048–1053.

Coskun, U., and Simons, K. (2011). Cell membranes: the lipid perspective. *Structure* 19, 1543–1548.

Costanzo, M., Baryshnikova, A., Bellay, J., Kim, Y., Spear, E.D., Sevier, C.S., Ding, H., Koh, J.L., Toufighi, K., Mostafavi, S., et al. (2010). The genetic landscape of a cell. *Science* 327, 425–431.

da Silveira Dos Santos, A.X., Riezman, I., Aguilera-Romero, M.A., David, F., Piccolis, M., Loewith, R., Schaad, O., and Riezman, H. (2014). Systematic lipidomic analysis of yeast protein kinase and phosphatase mutants reveals novel insights into regulation of lipid homeostasis. *Mol. Biol. Cell* 25, 3234–3246.

Dennis, E.A., Deems, R.A., Harkewicz, R., Quehenberger, O., Brown, H.A., Milne, S.B., Myers, D.S., Glass, C.K., Hardiman, G., Reichart, D., et al. (2010). A mouse macrophage lipidome. *J. Biol. Chem.* 285, 39976–39985.

Eisen, M.B., Spellman, P.T., Brown, P.O., and Botstein, D. (1998). Cluster analysis and display of genome-wide expression patterns. *Proc. Natl. Acad. Sci. USA* 95, 14863–14868.

Futerman, A.H., and van Meer, G. (2004). The cell biology of lysosomal storage disorders. *Nat. Rev. Mol. Cell Biol.* 5, 554–565.

Gallegos, C.E., Pediconi, M.F., and Barrantes, F.J. (2008). Ceramides modulate cell-surface acetylcholine receptor levels. *Biochim. Biophys. Acta* 1778, 917–930.

Guan, X.L., Riezman, I., Wenk, M.R., and Riezman, H. (2010). Yeast lipid analysis and quantification by mass spectrometry. *Methods Enzymol.* 470, 369–391.

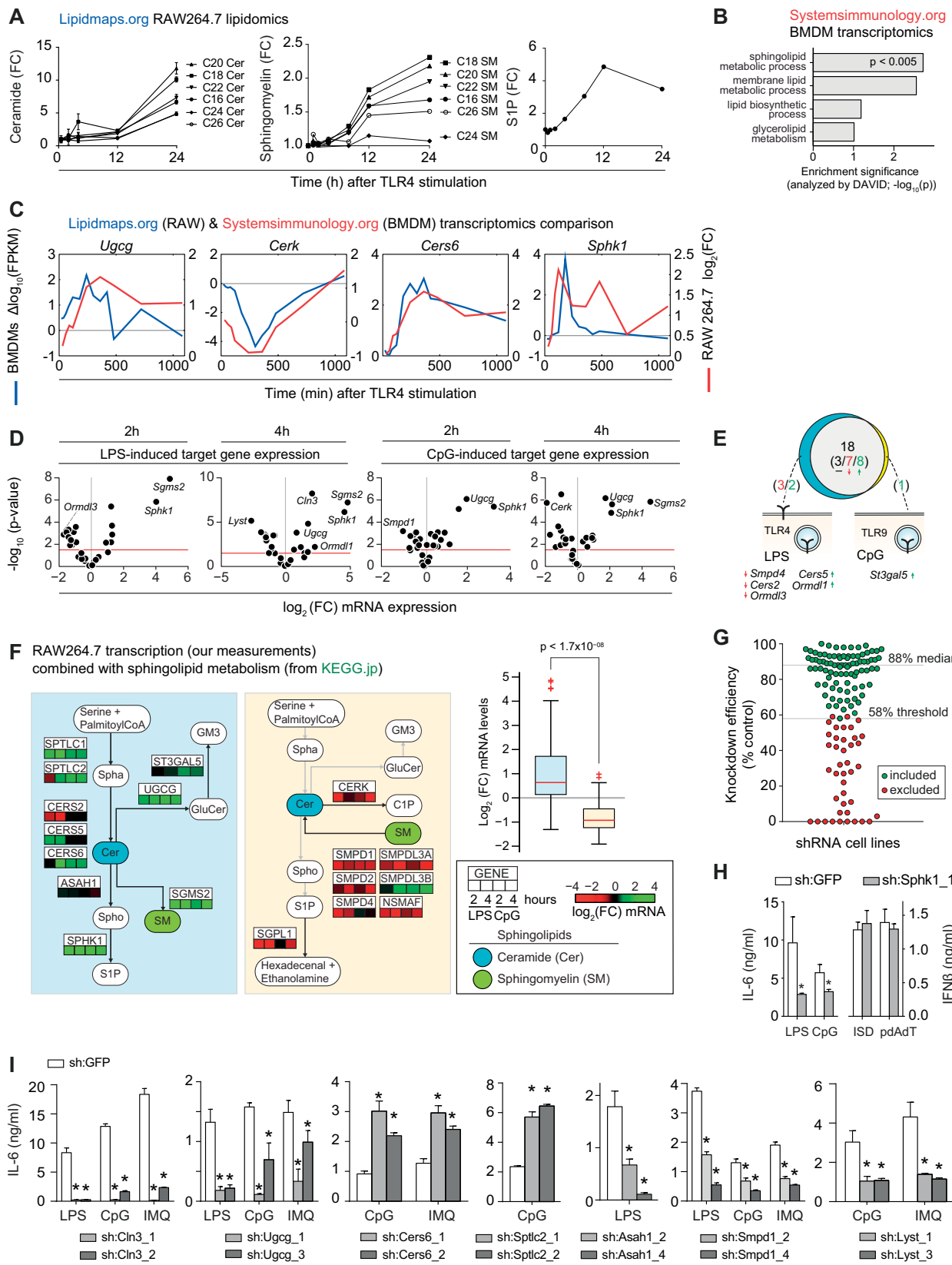
Hanada, K. (2003). Serine palmitoyltransferase, a key enzyme of sphingolipid metabolism. *Biochim. Biophys. Acta* 1632, 16–30.

Hannun, Y.A., and Obeid, L.M. (2011). Many ceramides. *J. Biol. Chem.* 286, 27855–27862.

Heinz, L.X., Baumann, C.L., Köberlin, M.S., Snijder, B., Gawish, R., Shui, G., Sharif, O., Aspalter, I.M., Müller, A.C., Kandasamy, R.K., et al. (2015). The lipid-modifying enzyme SMPDL3B negatively regulates innate immunity. *Cell Rep.* Published online June 18, 2015. <http://dx.doi.org/10.1016/j.celrep.2015.05.006>.

- Holthuis, J.C., and Menon, A.K. (2014). Lipid landscapes and pipelines in membrane homeostasis. *Nature* 510, 48–57.
- Józefowski, S., Czerkies, M., Łukasik, A., Bielawska, A., Bielawski, J., Kwiatkowska, K., and Sobota, A. (2010). Ceramide and ceramide 1-phosphate are negative regulators of TNF- α production induced by lipopolysaccharide. *J. Immunol.* 185, 6960–6973.
- Kanehisa, M., and Goto, S. (2000). KEGG: Kyoto encyclopedia of genes and genomes. *Nucleic Acids Res.* 28, 27–30.
- Kawai, T., and Akira, S. (2010). The role of pattern-recognition receptors in innate immunity: update on Toll-like receptors. *Nat. Immunol.* 11, 373–384.
- Lacy, P., and Stow, J.L. (2011). Cytokine release from innate immune cells: association with diverse membrane trafficking pathways. *Blood* 118, 9–18.
- Lee, C.C., Avalos, A.M., and Ploegh, H.L. (2012). Accessory molecules for Toll-like receptors and their function. *Nat. Rev. Immunol.* 12, 168–179.
- Levy, M., and Futerman, A.H. (2010). Mammalian ceramide synthases. *IUBMB Life* 62, 347–356.
- Maeda, K., Anand, K., Chiapparino, A., Kumar, A., Poletto, M., Kaksonen, M., and Gavin, A.C. (2013). Interactome map uncovers phosphatidylserine transport by oxysterol-binding proteins. *Nature* 501, 257–261.
- Memon, R.A., Holleran, W.M., Moser, A.H., Seki, T., Uchida, Y., Fuller, J., Shigenaga, J.K., Grunfeld, C., and Feingold, K.R. (1998). Endotoxin and cytokines increase hepatic sphingolipid biosynthesis and produce lipoproteins enriched in ceramides and sphingomyelin. *Arterioscler. Thromb. Vasc. Biol.* 18, 1257–1265.
- Okino, N., He, X., Gatt, S., Sandhoff, K., Ito, M., and Schuchman, E.H. (2003). The reverse activity of human acid ceramidase. *J. Biol. Chem.* 278, 29948–29953.
- Parker, L.C., Prestwich, E.C., Ward, J.R., Smythe, E., Berry, A., Triantafyllou, M., Triantafyllou, K., and Sabroe, I. (2008). A phosphatidylserine species inhibits a range of TLR- but not IL-1 β -induced inflammatory responses by disruption of membrane microdomains. *J. Immunol.* 181, 5606–5617.
- Pettus, B.J., Chalfant, C.E., and Hannun, Y.A. (2002). Ceramide in apoptosis: an overview and current perspectives. *Biochim. Biophys. Acta* 1585, 114–125.
- Ramsey, S.A., Klemm, S.L., Zak, D.E., Kennedy, K.A., Thorsson, V., Li, B., Gilchrist, M., Gold, E.S., Johnson, C.D., Litvak, V., et al. (2008). Uncovering a macrophage transcriptional program by integrating evidence from motif scanning and expression dynamics. *PLoS Comput. Biol.* 4, e1000021.
- Serhan, C.N., Chiang, N., and Van Dyke, T.E. (2008). Resolving inflammation: dual anti-inflammatory and pro-resolution lipid mediators. *Nat. Rev. Immunol.* 8, 349–361.
- Shevchenko, A., and Simons, K. (2010). Lipidomics: coming to grips with lipid diversity. *Nat. Rev. Mol. Cell Biol.* 11, 593–598.
- Singh, R., Kaushik, S., Wang, Y., Xiang, Y., Novak, I., Komatsu, M., Tanaka, K., Cuervo, A.M., and Czaja, M.J. (2009). Autophagy regulates lipid metabolism. *Nature* 458, 1131–1135.
- Siow, D.L., and Wattenberg, B.W. (2012). Mammalian ORMDL proteins mediate the feedback response in ceramide biosynthesis. *J. Biol. Chem.* 287, 40198–40204.
- Snijder, B., Liberali, P., Frechin, M., Stoeger, T., and Pelkmans, L. (2013). Predicting functional gene interactions with the hierarchical interaction score. *Nat. Methods* 10, 1089–1092.
- Snijder, B., Kandasamy, R.K., and Superti-Furga, G. (2014). Toward effective sharing of high-dimensional immunology data. *Nat. Biotechnol.* 32, 755–759.
- Stetson, D.B., and Medzhitov, R. (2006). Recognition of cytosolic DNA activates an IRF3-dependent innate immune response. *Immunity* 24, 93–103.
- van Meer, G., Voelker, D.R., and Feigenson, G.W. (2008). Membrane lipids: where they are and how they behave. *Nat. Rev. Mol. Cell Biol.* 9, 112–124.
- Vandanmagsar, B., Youm, Y.H., Ravussin, A., Galgani, J.E., Stadler, K., Myntt, R.L., Ravussin, E., Stephens, J.M., and Dixit, V.D. (2011). The NLRP3 inflammasome instigates obesity-induced inflammation and insulin resistance. *Nat. Med.* 17, 179–188.
- Wang, L., Kantovitz, K.R., Cullinane, A.R., Nociti, F.H., Jr., Foster, B.L., Roney, J.C., Tran, A.B., Introne, W.J., and Somerman, M.J. (2014). Skin fibroblasts from individuals with Chediak-Higashi Syndrome (CHS) exhibit hyposensitive immunogenic response. *Orphanet J. Rare Dis.* 9, 212.
- Wenk, M.R. (2005). The emerging field of lipidomics. *Nat. Rev. Drug Discov.* 4, 594–610.
- Wijesinghe, D.S., Subramanian, P., Lamour, N.F., Gentile, L.B., Granado, M.H., Bielawska, A., Szulc, Z., Gomez-Munoz, A., and Chalfant, C.E. (2009). Chain length specificity for activation of cPLA2 α by C1P: use of the dodecane delivery system to determine lipid-specific effects. *J. Lipid Res.* 50, 1986–1995.

Supplemental Figures



(legend on next page)

Figure S1. TLR-Driven Transcription of the Sphingolipid Metabolic Network and Characterization of Cytokine Release upon shRNA-Mediated Silencing of This Network, Related to Figure 1

- (A) TLR4-induced changes in the abundance of selected sphingolipids in RAW macrophages. Data from <http://lipidmaps.org> (Dennis et al., 2010).
- (B) Pathway enrichment analysis of all differentially regulated genes in a genome-wide analysis of TLR4-stimulated bone marrow-derived macrophages (BMDMs). Shown are the highest enriched lipid-related annotations. Data from <http://systemsimmunology.org> (Ramsey et al., 2008). Enrichment analyzed by DAVID.
- (C) Relative expression of key regulators of sphingolipid metabolism upon TLR4 stimulation over indicated time points in BMDMs and RAW cells. Relative expression calculated as $\Delta \log_{10}$ of the FPKM, or as \log_2 fold-change.
- (D) Scatter plot of \log_2 fold-change expression (x axis) versus significance (y axis; t test) of RAW macrophages stimulated with LPS or CpG for 2 and 4 hr. Red lines indicate $p < 0.05$. Strongest regulated genes are indicated. Data are combined of two independent experiments with two technical replicates each.
- (E) Venn diagram shows the number of regulated genes upon TLR4 stimulation by LPS and/or TLR9 stimulation by CpG. Predominant TLR localizations indicated in schemas. Red and green numbers in brackets indicate down- and upregulated genes respectively.
- (F) LPS- and CpG-induced relative expression of selected genes separated by different branches of the sphingolipid metabolic pathway (KEGG). Boxplots group all expression values per subnetworks, with colors corresponding to subnetwork background colors. Abbreviations are as in Figure 1. Data are combined of two independent experiments with two technical replicates each.
- (G) Knockdown efficiency measured by qRT-PCR of all 129 shRNA cell lines, normalized to sh:GFP. Each dot represents one cell line. Green dots were included in the screen, red dots were excluded due to insufficient knockdown efficiency. Threshold and median knockdown efficiency are indicated. Data are mean of technical triplicates.
- (H) IL-6 release after stimulation with LPS or CpG, and IFN β release after stimulation with Interferon-stimulatory DNA (ISD) or pdAdt in sh:Sphk1_1 and sh:GFP. Data are representative of three independent experiments.
- (I) IL-6 release after stimulation with LPS, CpG or IMQ after 16 hr measured in selected shRNA cell lines and sh:GFP. * indicates $p < 0.005$. Data are representative of five independent experiments and shown as mean \pm SD of four technical replicates.
- See also Table S1.

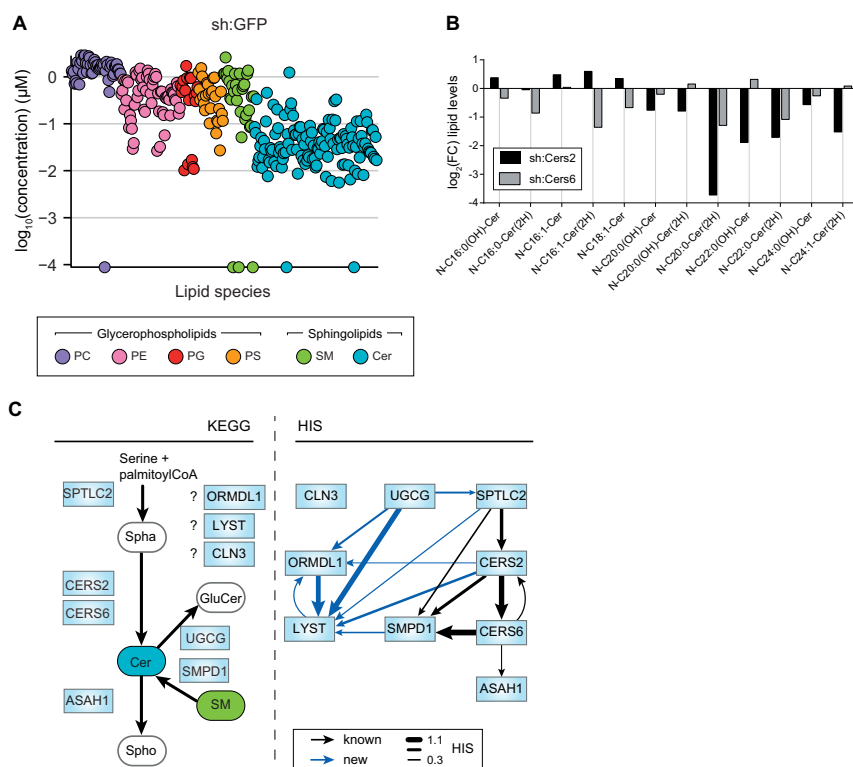


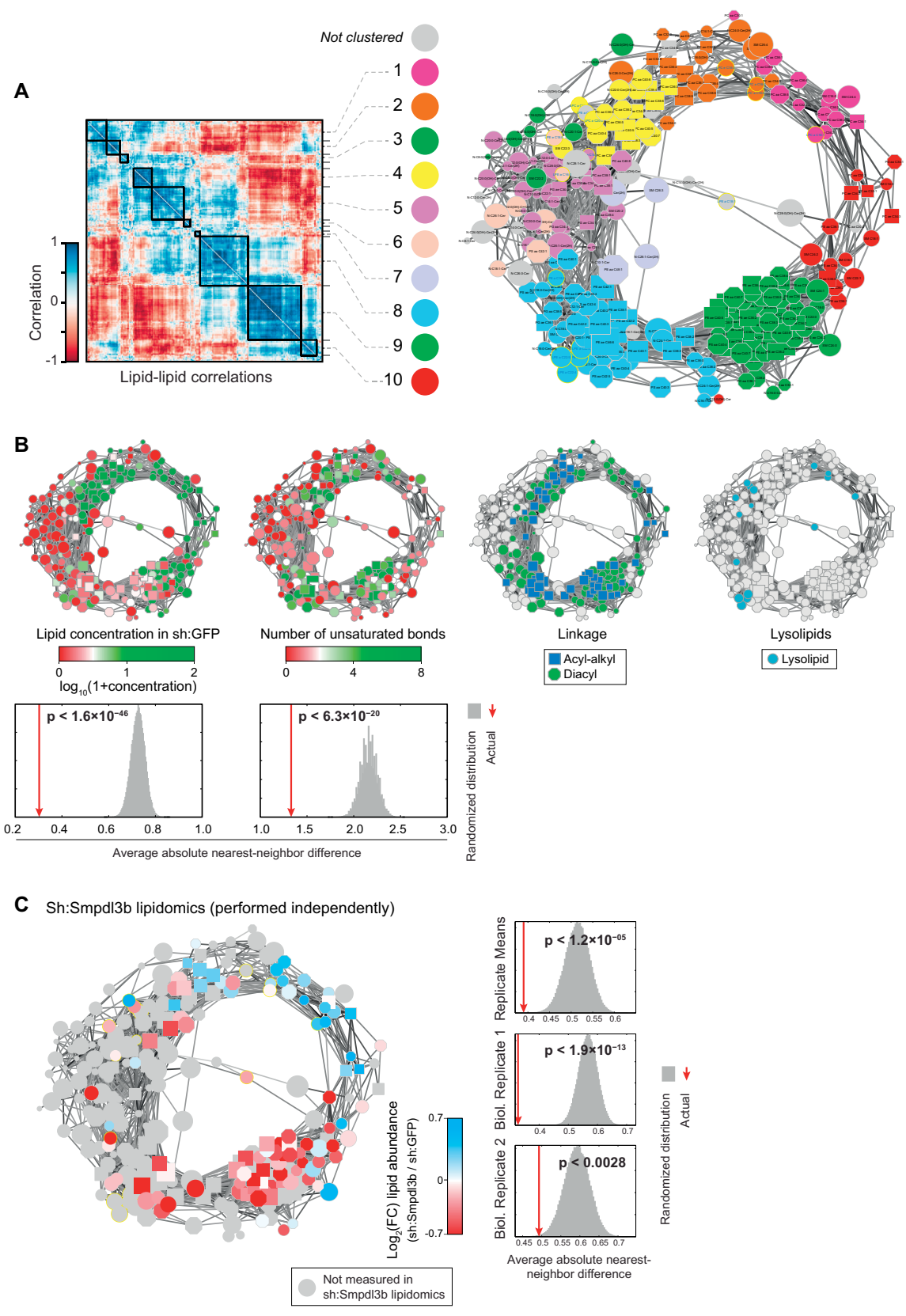
Figure S2. Quantitative Lipidomics of Nine Stable shRNA Cell Lines Targeting Sphingolipid Metabolism Reveals Strongly Altered Lipid States, Related to Figure 2

(A) Lipidomics measurements of sh:GFP control cell line shown as log₁₀-transformed lipid concentrations (μM).

(B) Values are log₂ fold-change relative abundance of selected ceramide species in sh:Cers2 (black bars) and sh:Cers6 (gray bars) relative to sh:GFP.

(C) Part of the sphingolipid metabolic pathway as defined by KEGG (left) compared to the hierarchical interactions (Snijder et al., 2013) between proteins inferred from changes in lipid abundance (right). Arrows indicate inferred hierarchy; known metabolic connections are indicated in black, unknown inferred interactions indicated in dark blue. Line thickness represents strength of hierarchical interaction. Spha: Sphinganine; Spho: Sphingosine; GluCer: Glucosylceramide. (A–C) Lipidomics data are combined of three independent experiments and represented as mean.

See also Table S2.



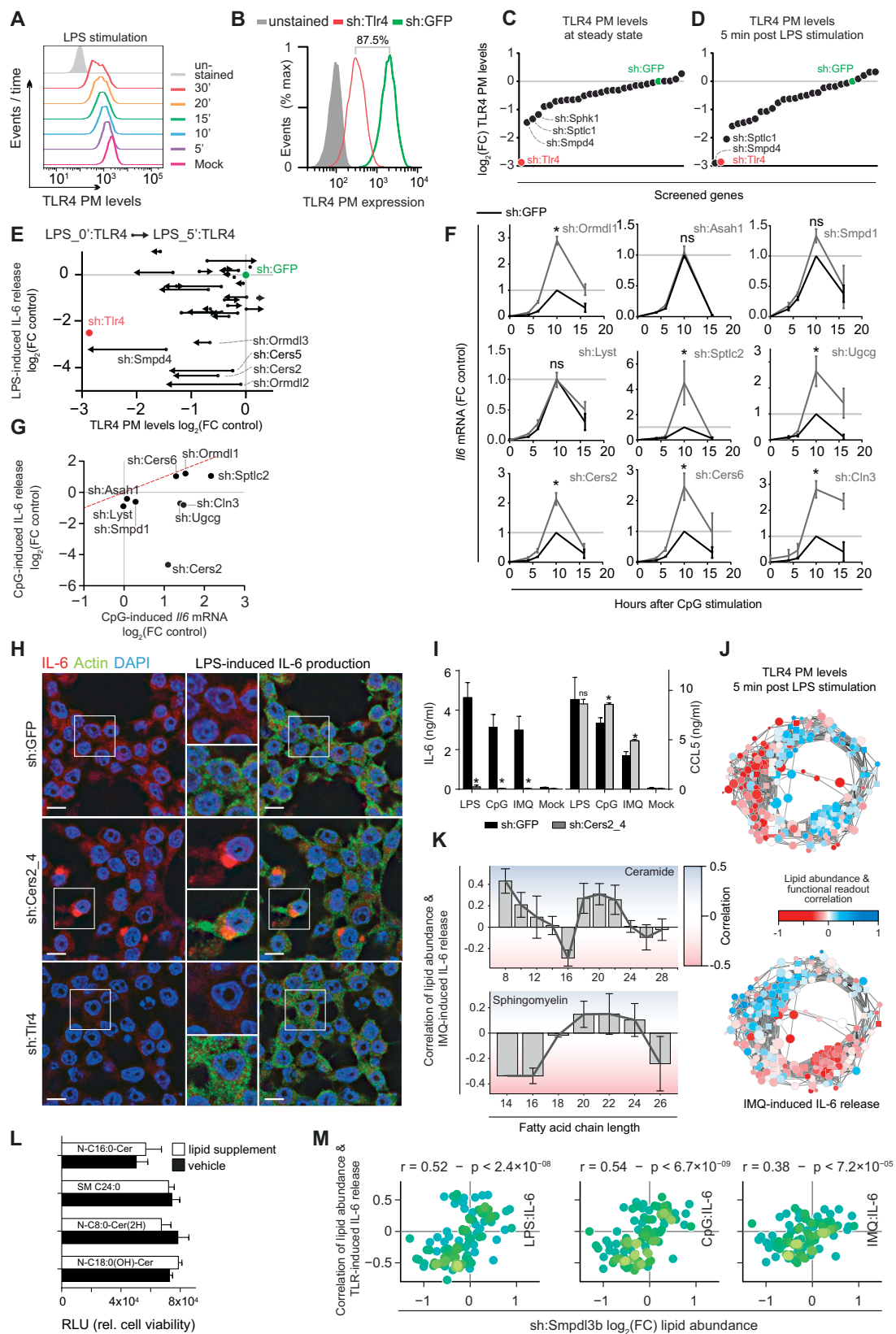
(legend on next page)

Figure S3. Further Characterization and Validation of the Circular Lipid Coregulatory Network, Related to Figure 3

(A) Lipid clusters as identified in Figure 3C indicated in different colors on the lipid coregulatory network. Lipids that could not be assigned to any single cluster are indicated in gray.

(B) Visualization of diverse measurements on the network: lipid abundance in sh:GFP (far left), the number of unsaturated bonds (left), the type of linkage (right), or lysolipids (far right). For lipid abundance and the number of unsaturated bonds the significance of clustering of these properties are displayed below the respective networks. Color-coded as indicated in corresponding legends.

(C) Left: Relative lipid abundance in sh:Smpd13b (Heinz et al., 2015) mapped onto the lipid network. Color-coded as indicated in legend. Significances of clustering of these features on the network are displayed.



(legend on next page)

Figure S4. Inference and Validation of Lipid Function in TLR-Related Processes, Related to Figure 4

(A) Histograms of TLR4-PE PM levels measured by FACS at steady state or after LPS (100ng/ml) stimulation at indicated time points in wild-type RAW cells.

(B) Histogram of steady-state TLR4-PE PM levels measured in sh:TLR4 and sh:GFP cell lines analyzed by FACS.

(C and D) Screening results of TLR4 PM levels unstimulated (C) and after 5 min (D) of LPS (100 ng/ml) stimulation in loss-of-function cell lines stained with TLR4-PE and measured by FACS. Values are \log_2 fold-change of mean fluorescence intensity relative to sh:GFP. Indicated are genes with strongest knockdown phenotypes.

(E) Vector plot of \log_2 fold-change TLR4 PM levels from 0 to 5 min (x axis) versus \log_2 fold-change in LPS-induced IL-6 release (y axis). Vector origin (dot) indicates 0 min and end (arrow) indicates 5 min.

(F) Time course measurements of CpG-induced *IL6* transcription in the nine knockdown cell lines used for lipidomics (gray line) normalized to unstimulated and 10h sh:GFP control (black line).

(G) Scatter plot of \log_2 fold-change CpG-induced *IL6* mRNA levels (x axis) versus \log_2 fold-change in CpG-induced IL-6 release (y axis). Indicated are the nine genes selected for lipidomics analysis.

(H) Immunofluorescence microscopy of IL-6 protein levels in sh:Cers2_4, sh:GFP and sh:TLR4 reveals perinuclear accumulation after 8h stimulation with LPS in sh:Cers2_4. IL-6 (red), actin (green), DAPI (blue). Scale bars indicate 10 μ m. Inserts show close-ups of indicated areas.

(I) IL-6 and CCL5 release after stimulation with LPS, CpG, or IMQ, in sh:GFP and sh:Cers2_4.

(J) Correlations between relative lipid abundance and measurements of LPS-induced TLR4 PM levels (top) and IMQ-induced IL-6 release (bottom) plotted on the circular network. Nodes of the network are color coded based on the strength of the correlation as indicated in legend.

(K) Average (gray bars) and SEM of the correlations between lipid abundance and IMQ-stimulated IL-6 release, per lipid fatty acid chain length, for ceramides (top) and sphingomyelins (bottom). Dark gray lines indicate chain length trends. Background colors vary with strength of correlation (red for negative, blue for positive correlations).

(L) Cell viability as measured by CellTiter-Glo luminescence, expressed in relative luminescence units (RLU) after supplementation with selected lipids (gray) or respective vehicle control (black).

(M) Scatter plots between relative lipid abundance independently measured for sh:Smpd13b (x axis) against functional lipid correlations (y axis) for all measured TLR-induced IL-6 release. Dots represent individual lipids, colored based on the local data density. Strong and significant positive correlations of IL-6 release predict a pro-inflammatory phenotype, as confirmed (Heinz et al., 2015).

P-values are indicated above panels. (A) and (B) Data are representative of at least two independent experiments. (C) and (D) Data are combined of two independent experiments with two technical replicates each. (F) Transcriptional data are combined of two independent experiments and shown as mean \pm SEM (H) Microscopy results are representative of two independent experiments. (I) Data are representative of at least two independent experiments. * indicate $p < 0.05$. ns: not significant. (L) Data are representative of at least three independent experiments.

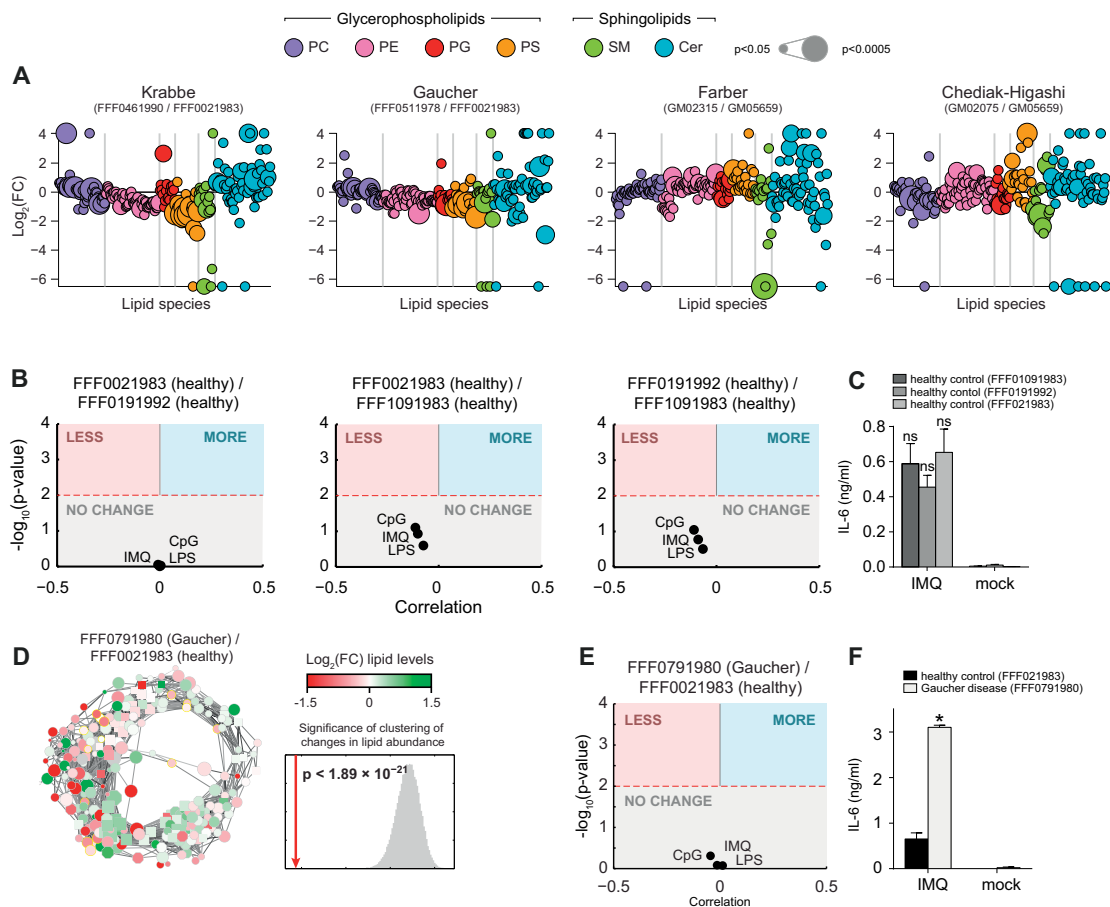


Figure S5. Lipidomics Analysis of Patient-Derived Fibroblasts Confirms Functional Lipid Annotations, Related to Figure 5

(A) Lipidomics analysis of 245 lipid species in four human fibroblast samples. Values are shown as \log_2 fold-change relative to the respective healthy controls. Each dot represents a lipid species, color coded per lipid class; dot size indicates significance. Vertical gray bars separate lipid classes.

(B) IL-6 release phenotype prediction for the \log_2 fold-change normalized lipid states of pairs of healthy controls derived from the same biobank, based on the correlation between lipid functional annotation and lipid abundance. Red dashed line indicates $p < 0.05$. Colored areas indicate significant phenotype predictions (blue, increased IL-6 release; red, reduced IL-6 release).

(C) IL-6 release after stimulation with IMQ as measured by ELISA for different healthy fibroblast samples (see legend).

(D) Lipid abundance plotted on the circular network for the second Gaucher patient fibroblast sample relative to the respective healthy control. Significance of the clustering on the circular network for the lipid abundance measurements is shown. Red line indicates the average absolute difference between abundance of direct neighbors in the network; gray area indicates the distribution of randomized repeats.

(E) As in (B), for the second Gaucher patient fibroblast sample.

(F) IL-6 release after stimulation with IMQ as measured by ELISA for the second Gaucher patient fibroblast sample and age matched healthy control (see legend). Mock: Unstimulated. (A) and (D) Data are combined of three independent experiments. (C) and (F) Data are representative of three independent experiments and presented as mean \pm SEM of three technical replicates. * indicated $p < 0.005$; ns: not significant.

See also Table S3.

Cell

Supplemental Information

A Conserved Circular Network of Coregulated Lipids Modulates Innate Immune Responses

Marielle S. Köberlin, Berend Snijder, Leonhard X. Heinz, Christoph L. Baumann, Astrid Fauster, Gregory I. Vladimer, Anne-Claude Gavin, and Giulio Superti-Furga

Supplemental Experimental Procedures

Cell culture

RAW264.7 macrophages and human embryonic kidney (HEK293T) cells were cultured in DMEM (Sigma Aldrich) and 10% FCS (Gibco) containing 1% Penicillin-Streptomycin (GE Healthcare) at 37°C and 5% CO₂. The “Cell line and DNA biobank from patients affected by genetic diseases” (Istituto G. Gaslini), member of the Telethon Network of Genetic Biobanks (project no. GTB12001) funded by Telethon Italy, provided us with specimens of human fibroblasts. The following fibroblast samples were obtained from the NIGMS Human Genetic Cell Repository at the Coriell Institute for Medical Research: (GM02075, GM02315, GM05659). Fibroblasts were cultured in DMEM (Sigma Aldrich) and 20% FCS (Gibco) containing 1% Penicillin-Streptomycin (GE Healthcare) at 37°C and 5% CO₂.

Reagents

TLR ligands such as ultrapure lipopolysaccharide (LPS) *E.coli* 0111:B4, Imiquimod (IMQ) – R837, and CpG DNA ODN 1826 were obtained from Invivogen. Interferon-stimulatory DNA (ISD) oligonucleotides (Stetson and Medzhitov, 2006) were synthesized by Microsynth. Poly(dA:dT) was obtained from Sigma Aldrich and Lipofectamine 2000 was obtained from Invitrogen. Cell viability was determined by CellTiter-Glo (Promega) according to the manufacturer’s instructions.

TLR stimulation

5×10⁵ RAW264.7 cells/ml or human fibroblasts were seeded in 96-well microtiter plates and incubated in serum-free medium for 2 hours prior stimulation. RAW cells were stimulated with the following TLR ligands for indicated time points: LPS (100ng/ml), CpG DNA (5μM), Imiquimod (5μM). For stimulation with ISD (1μg/ml) or poly(dA:dT) (500ng/ml) cells were transfected using Lipofectamine 2000 according to manufacturer’s instructions. Human fibroblasts were stimulated with LPS (1μg/ml) or IMQ (25μM). Each stimulation condition was performed in quadruplicates.

shRNA transduction

Briefly, shRNA constructs were obtained as glycerol stocks from Sigma Aldrich and Open Biosystems Thermo Scientific. Lentiviral particles were produced by transfecting helper plasmids together with the pLKO.1 vector containing the shRNA template into 5×10^5 HEK293T. The supernatant was collected for three consecutive days before it was ultracentrifuged at 30,000 rpm for 90 min to concentrate lentiviral particles. Prior to infection, 60-80% confluent 10^6 RAW264.7 cells were treated with polybrene (8 μ g/ml; Santa Cruz Biotechnology). Then, the produced virus was added in 400 μ l Optimem (Gibco). After 12 hours the medium was changed and after another 12 hours the culturing medium was replaced by DMEM 10% FCS 1% Penicillin-Streptomycin and 7,5 μ g/ml puromycin (Sigma Aldrich) to select for shRNA positive cells. Cells were kept under puromycin selection for passaging throughout the study.

RNA isolation and qRT-PCR

RNA was isolated using Qiashredder and RNeasy Kit (Qiagen) and was reverse transcribed using oligo dT primers and RevertAid Reverse Transcriptase (both Fermentas). qRT-PCR was performed using SensiMix SYBR Green (Bioline) in technical triplicates analyzed on Rotor-Gene Q from Qiagen. Results were normalized to the housekeeping gene cyclophilin B (Ppib) (Table S1).

Cytokine measurement

Stimulated cell supernatants were analyzed by enzyme-linked immunosorbent assay (ELISA) using mouse or human IL-6 ELISA Ready-SET-Go (eBioscience) and mouse CCL5/RANTES (R&D Systems) according to the manufacturer's instructions.

Il6 transcription measurements

5×10^5 RAW cells were seeded, incubated in serum-free media for 2 hours and stimulated with LPS (100ng/ml) or CpG (5 μ M) for indicated time points. *Il6* mRNA expression was measured by qRT-PCR (see above).

Confocal microscopy

Stable shRNA expressing RAW cells were seeded on glass coverslips overnight. Cells were washed and incubated with serum free media for 2 hours prior to 16 hours stimulation with LPS (100ng/ml). Coverslips were washed, then fixed, and permeabilized with 4% formalin/0.1% TritonX-114 in PBS. IL-6 was visualized with directly conjugated APC anti-Mouse-IL-6 (MP5-20F3, BD Biosciences), and actin with anti-pan actin (Cytoskeleton, Inc); secondary anti-rabbit AlexFlour594 (Invitrogen). Slides were visualized using an LSM700 (Carl Zeiss) utilizing sequential laser line interrogation into two MPTs. Images were taken at 63 \times and analyzed with ImageJ (NIH, open source).

Lipid supplementation

All lipids were purchased from Avanti Polar Lipids and solubilized as previously described using Ethanol/Dodecane (Wijesinghe et al., 2009). Briefly, long-chained lipids (starting from a fatty acid chain length of C16) were sonicated for 25 minutes at 40°C and vortexed every 5 minutes. For the lipid supplementation assay lipids (15 μ M) were added to a 96-well microtiter plate in 50 μ l serum-free media. Each condition was performed in technical quadruplicates per experiment. 5×10^5 RAW264.7 cells/ml were seeded and incubated for 30 minutes in indicated lipid concentrations prior to stimulation. Cells were stimulated with LPS (100ng/ml) for 8 hours.

Lipidomics

RAW264.7 cells and human fibroblasts were grown to 80% confluence and after washing first with PBS then with serum free medium and then were incubated in serum free medium for 2 hours. The cells were harvested, washed with PBS and counted. Sample preparation was done using a methanol/chloroform extraction protocol with 20µl sample volume of frozen cell pellets according to the manufacturer's instructions (BIOCRATES Life Sciences AG, Innsbruck, Austria). The non-diluted extracts were measured with two acquisition methods, and the diluted extracts were measured with a third acquisition method. Targeted metabolomics analysis was performed using the validated in-house method LIPIDS analyzed on an AB SCIEX triple-quadrupole mass spectrometer operating in positive and negative MRM mode (BIOCRATES Life Sciences AG, Innsbruck, Austria). 43 calibrators in 7 levels and 5 internal standards (3 of them were deuterated) were used to measure a panel of glycerophospholipids and sphingolipids. 5 quality controls were measured after 20 samples to improve the quality of the measurement. Data analysis was performed using the MetIDQ software (BIOCRATES Life Sciences AG, Innsbruck, Austria). An isotope-correction tool was included to correct and recalculate the measured signals, to avoid any influence of neighbored MRMs and to ensure the quality of the measurement.

Flow cytometry

For analysis of TLR4 PM levels RAW264.7 cells were stimulated with LPS (100ng/ml) for indicated time points in a 96-well microtiter plate at 37°C. After washing with cold PBS, nonpermeabilized cells were incubated with anti-TLR4-PE antibody (clone MTS510 from BioLegend) for 20 minutes on ice. Cells were then analyzed on FACS Fortessa measuring 10,000 cells per sample.

Statistics and computational analysis

Annotation enrichment analysis

Annotation enrichment analysis was performed on the differentially expressed genes (at $p < 0.05$ and an absolute $\log_2(\text{fold-change})$ in expression ≥ 1.5) upon TLR4 stimulation of BMDMs as published on systemsimmunology.org, for any of the differentially expressed genes found between 2 and 6 hours post-stimulation. Annotation enrichment analysis was calculated using the webservice DAVID (<http://david.abcc.ncifcrf.gov/home.jsp>) with default settings. Reported are the top-enriched annotations containing the word “lipid” and selected non-enriched annotations.

ShRNA phenotype calculation per gene

Experiments were filtered based on viability and on the induction of IL-6 release upon TLR stimulation for sh:GFP. ShRNA phenotypes per gene were calculated by either averaging out the ELISA results from all technical replicates from the most recent biological replicate, or from the two or more shRNAs per gene that displayed absolute \log_2 fold-changes of above 0.7 over the corresponding sh:GFP with a consistent sign (i.e. consistently increasing or decreasing IL-6 release) within a single experimental repeat and consistent between repeated experiments.

Lipidomics data normalization

The lipidomics results were normalized based on the sum of concentrations for all lipid species measured in a single biological replicate. Values were next averaged over the three biological replicates, and \log_2 transformed against the corresponding average concentrations measured in sh:GFP.

Hierarchical clustering and Hierarchical Interaction Score

Hierarchical clustering was performed using Matlab on non-normalized data using correlation as distance measure and average linkage. Hierarchical interaction scores (HIS) were calculated as described in (Liberali et al., 2014; Snijder et al., 2013). Specifically, interaction scores were calculated between genes from z-score normalized $\log_2(\text{FC})$ transformed lipidomics results, thresholding between

z-scores from 1 to 3 on both the positive and negative end of the data distribution (i.e. default settings), Edges scored with $HIS < 0.3$ were discarded, and all remaining edges are shown.

Lipid coregulation network analysis

Lipid coregulation (as visualized in the circular correlation network) was defined as correlation values of 0.7 or higher. Various natural network layout algorithms (as implemented in Cytoscape) were tested to confirm that the circularity shown was not an artefact from the selected network layout optimization algorithm. The threshold of 0.7 was tested to be high enough to be sufficiently robust to leaving out the single assay that most contributed to any one correlation value, and therefore likely not solely determined by the phenotype of any single cell line.

Network clustering significance

The significance of clustering of various features per node (i.e. lipid) was calculated by comparing the absolute difference of the given feature between a node and its nearest neighbor as defined by the network, averaged over all nodes, with the distribution of over 10,000 repeats of the same calculation using randomly shuffled feature values. If the actual nearest neighbor distance was lower than the lowest value observed in the 10,000 randomized repeats, the significance of this difference was calculated by two-tailed t-test between the actual observation and the >10,000 repeats. This was confirmed to approximate true values, and a reasonable approximation as all randomized distributions were highly normally distributed.

Lipid subcellular membrane fraction enrichment score

The lipid subcellular membrane fraction enrichment scores were calculated as the z-score over the lipid concentrations measured for any one lipid species over all the different fractions analyzed by the lipidmaps.org consortium.

Lipid function prediction

Functional predictions or associations for lipids were performed based on Pearson's linear correlation coefficients between the $\log_2(\text{FC})$ readouts of the TLR4-related functional assays (i.e. IL-6 release, *Il6* transcription, TLR4 surface levels) and the $\log_2(\text{FC})$ in lipid levels, over the 9 shRNA cell lines.

General statistics

P-values were calculated with two-tailed t-tests, unless otherwise indicated. Correlation values given are Pearson's linear correlation coefficients, unless otherwise indicated. The significance of the overlap in lipid-lipid coregulation between the RAW264.7 dataset and the fibroblast dataset were calculated by the hypergeometric distribution.

Supplemental References

- Liberali, P., Snijder, B., and Pelkmans, L. (2014). A hierarchical map of regulatory genetic interactions in membrane trafficking. *Cell* *157*, 1473-1487.
- Snijder, B., Liberali, P., Frechin, M., Stoeger, T., and Pelkmans, L. (2013). Predicting functional gene interactions with the hierarchical interaction score. *Nat Methods* *10*, 1089-1092.
- Stetson, D.B., and Medzhitov, R. (2006). Recognition of cytosolic DNA activates an IRF3-dependent innate immune response. *Immunity* *24*, 93-103.
- Wijesinghe, D.S., Subramanian, P., Lamour, N.F., Gentile, L.B., Granado, M.H., Bielawska, A., Szulc, Z., Gomez-Munoz, A., and Chalfant, C.E. (2009). Chain length specificity for activation of cPLA2alpha by C1P: use of the dodecane delivery system to determine lipid-specific effects. *J Lipid Res* *50*, 1986-1995.

2.3 EPILOGUE

The Lipid-Modifying Enzyme SMPDL3B Negatively Regulates Innate Immunity.

Heinz LX,* Baumann CL*, Köberlin MS, Snijder B, Gawish R, Shui G, Sharif O, Aspalter IM, Müller AC, Kandasamy RK, Breitwieser FP, Pichlmair A, Bruckner M, Rebsamen M, Blüml S, Karonitsch T, Fauster A, Colinge J, Bennett KL, Knapp S, Wenk MR, Superti-Furga G (2015) Cell Reports 11: 1919-28

*: contributed equally

This study describes the identification, detailed characterization, and *in vivo* validation of a novel lipid-modifying enzyme SMPDL3B in the TLR-mediated immune response. As described in the previous publication, this enzyme was found to be transcriptionally regulated by TLR stimulation and the genetic loss-of-function in mouse macrophages led to a hyperinflammatory TLR-mediated response (Köberlin, Snijder et al., 2015).

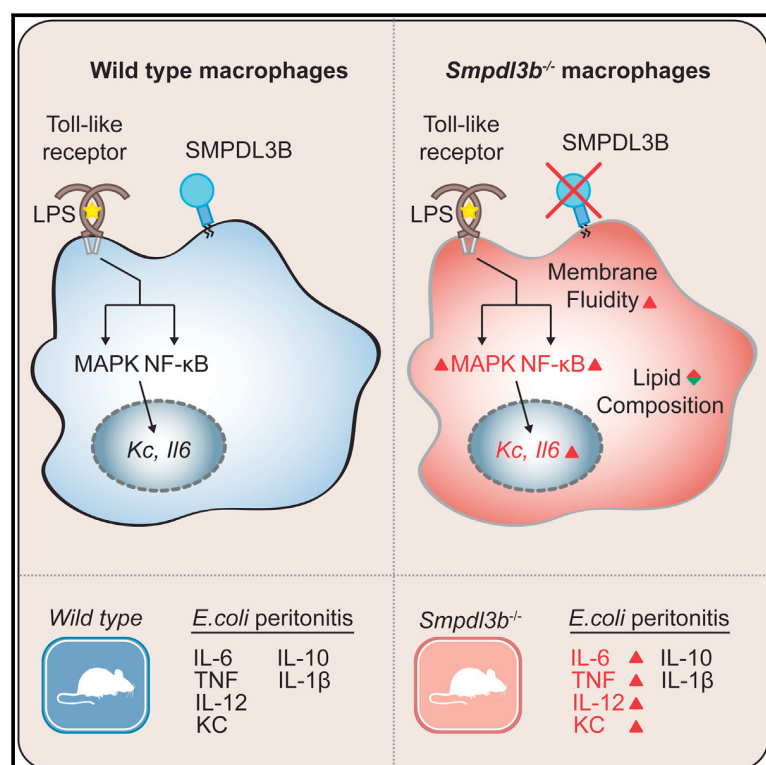
The author of this thesis contributed as follows:

Several experiments in this manuscript were designed and performed by the author. The transcriptional regulation measurements in murine macrophages, the generation of genetically perturbed macrophage cell lines, the TLR stimulation, and cytokine measurements of these cell lines were done by me. I prepared the cell samples for lipidomics analysis done by the laboratory of Markus Wenk at the National University of Singapore. I also performed all lipid supplementation experiments. The other experiments were performed and designed by Leonhard Heinz, Christoph Baumann, and the co-authors. The *in vivo* work was done by the laboratory of Sylvia Knapp at CeMM and the Medical University of Vienna. The data was discussed and interpreted with the co-authors regularly. I also contributed to making the figures and writing the manuscript.

Cell Reports

The Lipid-Modifying Enzyme SMPDL3B Negatively Regulates Innate Immunity

Graphical Abstract



Authors

Leonhard X. Heinz,
Christoph L. Baumann,
Marielle S. Köberlin, ..., Sylvia Knapp,
Markus R. Wenk, Giulio Superti-Furga

Correspondence

gsuperti@cemm.oeaw.ac.at

In Brief

Heinz et al. identify the lipid-modulating phosphodiesterase SMPDL3B as negative regulator of Toll-like receptor function. *Smpdl3b*-deficiency strongly affected macrophage lipid composition and fluidity and led to higher responsiveness to TLR stimulation. Peritonitis models in *Smpdl3b*-deficient mice confirmed the negative regulatory role in vivo.

Highlights

- Identification of SMPDL3B as lipid-modulating phosphodiesterase on macrophages
- Negative regulatory role for SMPDL3B in Toll-like receptor function
- Strong influence of SMPDL3B on membrane lipid composition and fluidity
- *Smpdl3b*-deficient mice show enhanced responsiveness in TLR-dependent peritonitis



Heinz et al., 2015, Cell Reports 11, 1919–1928
June 30, 2015 ©2015 The Authors
<http://dx.doi.org/10.1016/j.celrep.2015.05.006>

CellPress

The Lipid-Modifying Enzyme SMPDL3B Negatively Regulates Innate Immunity

Leonhard X. Heinz,^{1,8} Christoph L. Baumann,^{1,8,9} Marielle S. Köberlin,¹ Berend Snijder,¹ Riem Gawish,^{1,2} Guanghou Shui,⁵ Omar Sharif,^{1,2} Irene M. Aspalter,^{1,10} André C. Müller,¹ Richard K. Kandasamy,¹ Florian P. Breitwieser,¹ Andreas Pichlmair,^{1,11} Manuela Bruckner,¹ Manuele Rebsamen,¹ Stephan Blüml,^{1,3} Thomas Karonitsch,^{1,12} Astrid Fauster,¹ Jacques Colinge,¹ Keiryn L. Bennett,¹ Sylvia Knapp,^{1,2} Markus R. Wenk,^{4,6} and Giulio Superti-Furga^{1,7,*}

¹CeMM Research Center for Molecular Medicine of the Austrian Academy of Sciences, 1090 Vienna, Austria

²Department of Medicine I, Laboratory of Infection Biology, Medical University of Vienna, 1090 Vienna, Austria

³Division of Rheumatology, Department of Medicine III, Medical University of Vienna, 1090 Vienna, Austria

⁴Department of Biochemistry and Department of Biological Sciences, National University of Singapore, Singapore 117456, Singapore

⁵State Key Laboratory of Molecular Developmental Biology, Institute of Genetics and Developmental Biology, Chinese Academy of Sciences, Beijing 100101, China

⁶Swiss Tropical and Public Health Institute, University of Basel, 4003 Basel, Switzerland

⁷Center for Physiology and Pharmacology, Medical University of Vienna, 1090 Vienna, Austria

⁸Co-first author

⁹Present address: Austrianni, GmbH, 1030 Vienna, Austria

¹⁰Present address: MRC Laboratory for Molecular Cell Biology, University College London, Gower Street, London WC1E 6BT, UK

¹¹Present address: Max-Planck Institute of Biochemistry, 82152 Martinsried, Germany

¹²Present address: Division of Rheumatology, Department of Medicine III, Medical University of Vienna, 1090 Vienna, Austria

*Correspondence: gsuperti@cemm.oeaw.ac.at

<http://dx.doi.org/10.1016/j.celrep.2015.05.006>

This is an open access article under the CC BY-NC-ND license (<http://creativecommons.org/licenses/by-nc-nd/4.0/>).

SUMMARY

Lipid metabolism and receptor-mediated signaling are highly intertwined processes that cooperate to fulfill cellular functions and safeguard cellular homeostasis. Activation of Toll-like receptors (TLRs) leads to a complex cellular response, orchestrating a diverse range of inflammatory events that need to be tightly controlled. Here, we identified the GPI-anchored Sphingomyelin Phosphodiesterase, Acid-Like 3B (SMPDL3B) in a mass spectrometry screening campaign for membrane proteins co-purifying with TLRs. Deficiency of *Smpdl3b* in macrophages enhanced responsiveness to TLR stimulation and profoundly changed the cellular lipid composition and membrane fluidity. Increased cellular responses could be reverted by re-introducing affected ceramides, functionally linking membrane lipid composition and innate immune signaling. Finally, *Smpdl3b*-deficient mice displayed an intensified inflammatory response in TLR-dependent peritonitis models, establishing its negative regulatory role in vivo. Taken together, our results identify the membrane-modulating enzyme SMPDL3B as a negative regulator of TLR signaling that functions at the interface of membrane biology and innate immunity.

INTRODUCTION

Toll-like receptors (TLRs) are important sensors of pathogens as well as cellular and environmental stress (Kawai and Akira, 2010;

Moresco et al., 2011; O'Neill, 2008). Stimulation of these receptors leads to a complex inflammatory response, orchestrating a diverse range of cellular functions such as cytokine secretion, cell migration, and antigen presentation (Kawai and Akira, 2007). To avoid unnecessary tissue damage or manifestation of chronic inflammation, these events are tightly controlled (Kawai and Akira, 2010; Liew et al., 2005; Medzhitov, 2008). Many proteins have been identified previously as regulators of TLRs acting via different mechanisms (Kondo et al., 2012; Lee et al., 2012; Liew et al., 2005). These include accessory proteins involved in folding and vesicular transport, facilitators of receptor-ligand interactions, transcriptional regulators as well as intracellular proteins involved in activation of receptor-proximal signaling.

Lipids are involved in most cellular processes by serving at the same time as structural components of membranes, energy storage molecules, and second messengers in signaling events (Hannun and Obeid, 2008; van Meer et al., 2008). While the function of membrane-bound or associated proteins is strongly influenced by the lipid composition and state of the accommodating membrane, the molecular connections responsible for these relationships are only beginning to be elucidated (Ernst et al., 2010). Stimulation of macrophages with TLR ligands strongly impacts on cellular gene expression and morphology. This also involves regulation of the cellular lipid repertoire, further highlighting the high degree of interdependence of these processes (Andreyev et al., 2010; Dennis et al., 2010; Maurya et al., 2013). In addition to the TLRs themselves, several components of the receptor sorting and signaling machinery are associated with different cellular membranes (Gay et al., 2014). This extensive interconnection with membrane biology suggests that the receptor function is sensitive to changes in cellular lipid composition. Therefore, it is not surprising that perturbations influencing

cellular lipid flux or membrane microdomain composition have been shown to affect TLR-dependent signaling events (Fessler and Parks, 2011; Triantafyllou et al., 2002, 2004; Zhu et al., 2010).

Here, we report on the identification of SMPDL3B as a lipid-modifying enzyme and demonstrate its involvement in the regulation of TLR-induced signaling processes. We could show that this GPI-anchored glycoprotein is prominently expressed on macrophages and dendritic cells (DCs) and further strongly upregulated by TLR stimuli and interferon gamma (IFN- γ). Functionally, *Smpdl3b*-deficient macrophages and DCs showed hyper-responsiveness to TLR stimulation, suggesting a negative regulatory role for SMPDL3B in TLR-induced signaling. Enzymatic measurements revealed that SMPDL3B is a potent phosphodiesterase active on the surface of these cells. Identifying a role in lipid metabolism, *Smpdl3b* knockdown or knockout macrophages showed a strong reduction in membrane order. This was further highlighted by changes associated with SMPDL3B depletion on the global cellular lipid composition as assessed by lipidomics analysis. In particular, specific ceramide species appeared to be depleted. Supplementation of these lipids in *Smpdl3b* knockdown cells reverted their hyper-inflammatory phenotype, thus confirming an implication of these molecules in the regulation of TLR signaling. Finally, *Smpdl3b*-deficient mice manifested higher inflammatory responses in models of TLR-dependent peritonitis, establishing the importance of this enzyme in vivo. Taken together, our results identify SMPDL3B as lipid-modifying enzyme that acts as a negative regulator of TLR signaling at the interface of lipid metabolism and inflammatory signaling.

RESULTS

Identification of SMPDL3B as GPI-Anchored TLR Interactor

The discovery of proteins modulating the activity of TLRs is crucial for the understanding of TLR-dependent immune responses. The characterization of TLR-associated protein complexes by affinity purification followed by mass spectrometry has previously led to the identification of CD14 as co-receptor for nucleic acid recognition by the endosomal TLRs 7 and 9 (Baumann et al., 2010). In the same screening campaign, SMPDL3B (UniProt: P58242, entry name: ASM3B_MOUSE) was consistently identified as membrane protein co-purifying with endosomal TLRs 3, 7, 8, and 9 with robust sequence coverage from RAW264.7 macrophages suggesting association with the same membrane compartments harboring TLRs (Figure 1A).

SMPDL3B contains an N-terminal signal peptide (amino acid [aa] 1–18), a central metallo-phosphodiesterase domain (MPP_ASMase, aa 23–323) as well as a C-terminal GPI-membrane anchor signal and belongs to a small family of three evolutionarily related enzymes (Figure 1B) (Masuishi et al., 2013). Of these, Sphingomyelin Phosphodiesterase 1/Acid Sphingomyelinase (SMPD1/ASM) is a well-characterized lysosomal protein involved in the degradation of sphingomyelin to ceramide and phosphorylcholine (Hannun and Obeid, 2011; Milhas et al., 2010; Seto et al., 2004). In contrast, less is known

about the precise functions of the related proteins SMPDL3A and SMPDL3B. SMPDL3A was shown to be regulated by the oxysterol-inducible transcription factor LXR α , linking it to lipid metabolism, and recently confirmed to harbor phosphodiesterase activity (Noto et al., 2012; Pehkonen et al., 2012; Traini et al., 2014). SMPDL3B was shown to be a membrane-associated protein proposed to play a role in podocytes in human kidney diseases including focal segmental glomerulosclerosis as well as diabetic kidney disease (Fornoni et al., 2011; Yoo et al., 2015).

To study the topology of SMPDL3B and related proteins in overexpression experiments, HEK293T cells were transiently transfected or stably transduced with the corresponding expression constructs (Figure S1A). SMPDL3B could be detected on the surface of HEK293T cells stably expressing the protein while mutants lacking the C-terminal GPI-membrane anchor signal (SMPDL3B Δ GPI) accumulated in cell supernatants (Figures 1C, S1A, and S1B). While overexpressed SMPDL3A was also detected in cell supernatants, confirming a previous report that it is a secreted protein (Traini et al., 2014), SMPD1/ASM, a well-established lysosomal protein, was not found at this location (Figure S1B). Confocal microscopy of overexpressed SMPDL3B in HEK293T cells confirmed the predominantly surface-associated localization (Figure S1C). As the co-purification of SMPDL3B with several TLRs was initially observed in RAW264.7 macrophages, we used these cells to study the properties of the endogenous protein. In line with the human variant (Masuishi et al., 2013), endogenous murine SMPDL3B was enriched in the membrane fraction of these cells and showed sensitivity to phosphatidylinositol-specific phospholipase C (PI-PLC) treatment, an enzyme known to cleave GPI anchors (Figures 1D, 1E, and S1D). Additionally, we assessed the presence of N-linked glycosylation sites on murine or human SMPDL3B or murine SMPDL3A and found that all proteins were highly glycosylated as evidenced by sensitivity of proteins to PNGase F (Figure S1E).

GPI-anchored proteins such as the TLR co-receptor CD14 are known to localize to sphingomyelin- and cholesterol-enriched membrane subdomains that can be purified based on their insolubility in certain detergents (Mayor and Riezman, 2004). We found SMPDL3B and CD14 both enriched in these detergent resistant membranes isolated from RAW264.7 macrophages (Figure S1F). In this light, we also evaluated whether the association of SMPDL3B with TLRs could be confirmed by co-immunoprecipitation (Figure 1F). SMPDL3B co-purified with the TLRs 4, 7, 8, and 9 and only weakly with TLR3 (Figure 1F), thus indeed resembling the behavior of CD14 (Baumann et al., 2010; Lee et al., 2012). Although these data are compatible with physical proximity of SMPDL3B and TLRs, it is also possible that the observations made reflect the presence of these proteins in membrane and/or detergent complexes obtained under the experimental solubilization conditions used, without the involvement of direct protein-protein interactions.

Taken together, we found that SMPDL3B is a GPI-anchored glycoprotein with putative enzymatic function that efficiently co-purified with several TLRs from macrophages and was therefore chosen for further functional evaluation as potential modulator of TLR activity.

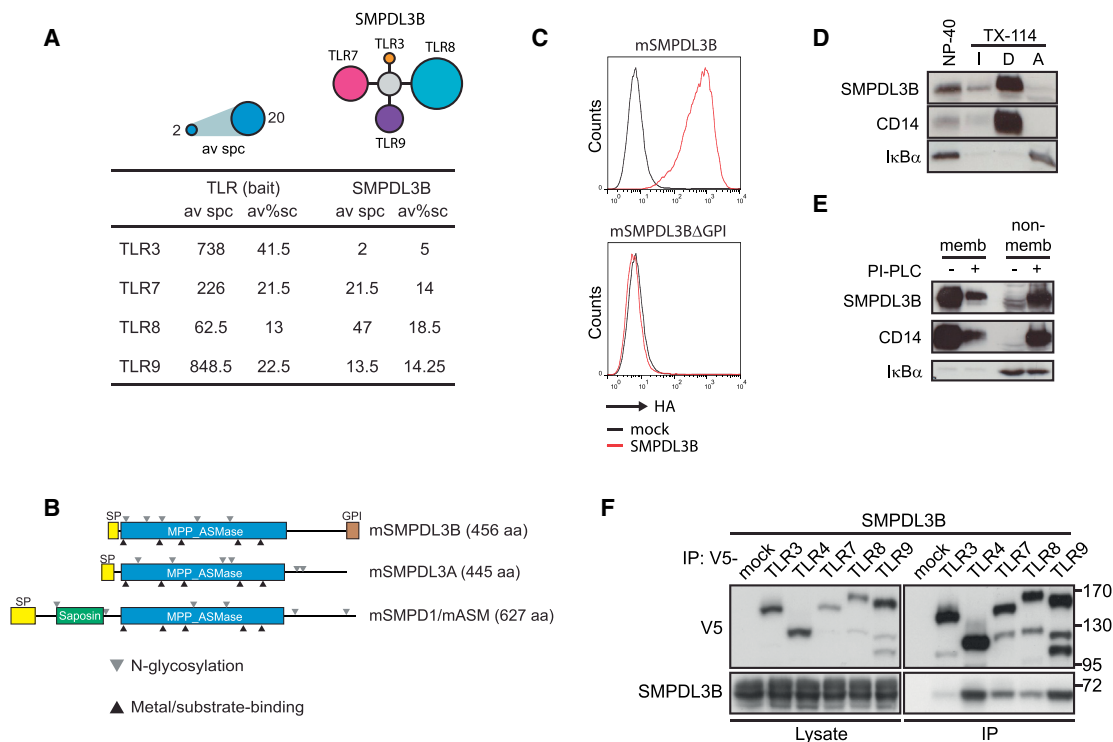


Figure 1. Identification of SMPDL3B as GPI-Anchored TLR Interactor

(A) Average spectral counts (av spc) and average % sequence coverage (av%sc) of SMPDL3B detected by mass spectrometry in endosomal TLR tandem affinity purifications.

(B) Domain organization of SMPDL3B, SMPDL3A, and SMPDL1/ASM. Gray triangles indicate predicted or validated N-linked glycosylation sites; black triangles indicate conserved motifs in metal coordination/substrate binding.

(C) HA-specific FACS analysis of HEK293T cells stably expressing murine SMPDL3B or a deletion mutant lacking the C-terminal GPI signal.

(D) Cells were lysed using 1% NP-40 or subjected to TX-114 phase separation. Proteins were analyzed by western blot for SMPDL3B, CD14, and IκBα. I, detergent-insoluble proteins; D, detergent phase, amphiphilic integral membrane proteins; A, aqueous phase, hydrophilic proteins.

(E) Cells were lysed with TX-114; lysates were divided in two and treated or not with PI-PLC. Proteins were subjected to phase separation, and fractions were analyzed by western blot for SMPDL3B, CD14, and IκBα.

(F) HEK293T cells were transfected with SMPDL3B and V5-tagged TLRs as indicated. Immunoprecipitates and extracts were analyzed by western blot using SMPDL3B- and V5-specific antibodies.

(C–F) Data are representative of at least two independent experiments. See also Figure S1.

SMPDL3B Is a Negative Regulator of TLR Signaling

SMPDL3B expression was prominently observed in macrophages and DCs (Figure S1G). Consistent with a possible role for this enzyme in the course of inflammatory processes, *Smpdl3b* transcription in bone marrow-derived macrophages (BMDMs) and DCs (BMDCs) was robustly induced upon TLR stimulation (Figure 2A). To further study the role of this protein in primary cells, we decided to generate *Smpdl3b*-deficient mice. The knockout mice were viable and did not have any overt developmental phenotype. Interestingly, BMDMs and BMDCs from *Smpdl3b*-deficient mice showed higher expression and release of the chemokine KC/CXCL1 upon stimulation with TLR agonists in comparison to wild-type cells (Figures 2B–2F and S2A). In line with this, knockdown of *Smpdl3b* in RAW264.7 macrophages increased the release of interleukin 6 (IL-6) upon treatment with lipopolysaccharide (LPS), CpG-DNA (CpG), and imiquimod (IMQ) (Figures S2B and S2C). To evaluate whether other important membrane-dependent events that

occur early upon TLR activation were affected by SMPDL3B depletion, we measured the internalization rates of TLR4 and the phagocytic uptake of CpG (Figures S2D–S2F). Endocytosis of TLR4 upon LPS stimulation was unchanged in RAW264.7 macrophages or primary BMDMs depleted or deficient in *Smpdl3b*, suggesting that the enhanced release of cytokines in SMPDL3B-depleted cells was not caused by retaining TLR4 at the plasma membrane or malfunctioning of receptor endocytosis (Figures S2D and S2E). Also, uptake of fluorescently labeled Cy3-CpG was unaltered in knockdown cells further indicating that endocytic functions were intact (Figure S2F). Taken together, these data show that *Smpdl3b* expression is induced upon TLR stimulation and reveal that SMPDL3B negatively affects TLR-dependent responses.

SMPDL3B Affects TLR-Dependent Signaling Processes

TLR signaling proceeds through the activation of mitogen-activated protein kinases (MAPKs) and the transcription factor

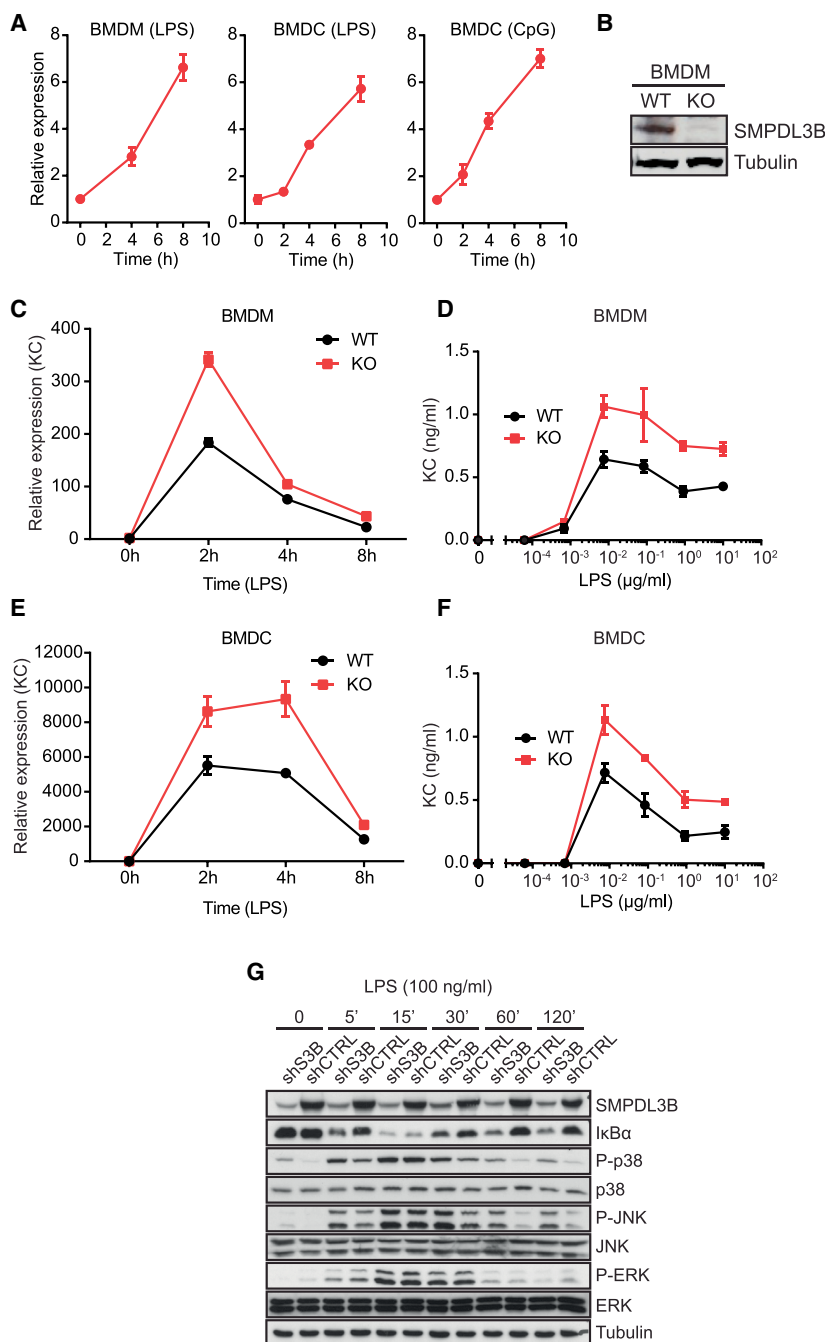


Figure 2. SMPDL3B Is a Negative Regulator of TLR Signaling

(A) BMDMs or BMDCs were stimulated with 100 ng/ml LPS or 1 μ M CpG-DNA for the indicated time and relative expression of *Smpdl3b* was measured by RT-PCR.

(B) Expression of SMPDL3B and tubulin in wild-type and *Smpdl3b*-deficient BMDMs was analyzed by western blot.

(C and E) BMDMs or BMDCs from wild-type (WT) or *Smpdl3b*-deficient (KO) mice were stimulated with 100 ng/ml LPS for the indicated time, and relative expression of KC was measured by RT-PCR.

(D and F) BMDMs or BMDCs from wild-type (WT) or *Smpdl3b*-deficient (KO) mice were stimulated with LPS for 8 hr, and supernatants were analyzed for KC by ELISA.

(G) The phosphorylation status of p38, JNK, and ERK and protein levels of I κ B α in the lysates of control (shCTRL) and SMPDL3B-depleted RAW264.7 cells (shS3B) upon stimulation with LPS were analyzed by western blot.

(A and C–F) Data show mean \pm SD of technical triplicates and are representative of at least two independent experiments. (G) Data are representative of two independent experiments. See also Figure S2.

tion of I κ B α , which is indicative of enhanced NF- κ B activity (Figure 2G). Together, these results revealed that signaling processes occurring relatively early after TLR engagement are affected by the absence of SMPDL3B.

Identification of SMPDL3B as TLR-Inducible Neutral Phosphodiesterase

The similarity to other phosphodiesterases prompted us to assess SMPDL3B activity by monitoring phosphodiesterase-dependent hydrolysis of chromogenic bis(4-nitrophenyl)phosphate (bis-pNPP) (Figure S3A). Recombinant SMPDL3B lacking the C-terminal GPI signal, purified from supernatants of Sf9 insect cells or HEK293T cells, efficiently hydrolyzed the substrate, exerting highest activity at neutral pH (Figures 3A, 3B, and S3B). This indicated that the enzyme is fully active at the pH found at the plasma membrane location. Confirming specificity, a mutant (H135A) replacing a conserved histidine residue of SMPDL3B predicted to be involved in substrate hydrolysis (Seto et al., 2004), showed reduced enzymatic activity (Figure 3C). In line with the abundant expression on the plasma membrane, substrate hydrolysis could also be detected on HEK293T cells stably expressing murine or human SMPDL3B, indicating that this assay was well suited for measuring activity on the surface of intact cells (Figures 3D, S3C, and S3D). Indeed, RAW264.7 cells showed robustly detectable enzymatic activity, which was strongly reduced in the *Smpdl3b* knockdown cells,

NF- κ B (Arthur and Ley, 2013; Kawai and Akira, 2007). To determine the effect of *Smpdl3b* knockdown on these signaling events, we monitored phosphorylation of the MAPKs p38 α , c-Jun N-terminal kinase (JNK) or extracellular signal-regulated kinase (ERK) (Figure 2G). SMPDL3B-depleted cells showed higher levels of phosphorylated p38 α and JNK, whereas phosphorylation of ERK appeared rather reduced. In addition to the differences in these important phosphorylation events, SMPDL3B-depleted macrophages showed sustained degrada-

tion of I κ B α , which is indicative of enhanced NF- κ B activity (Figure 2G). Together, these results revealed that signaling processes occurring relatively early after TLR engagement are affected by the absence of SMPDL3B.

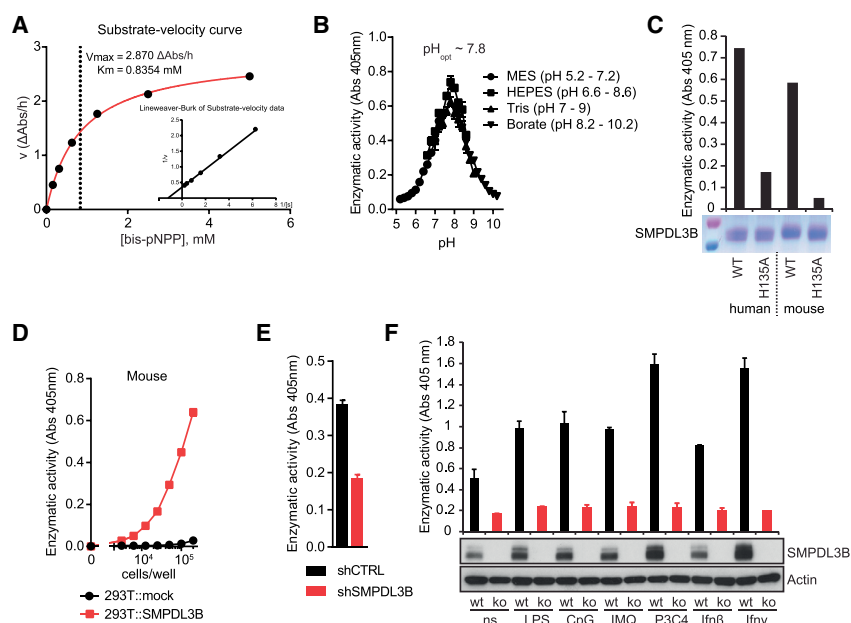


Figure 3. Enzymatic Activity and Inducibility of SMPDL3B

(A) Substrate velocity curve and Lineweaver-Burk diagram for murine SMPDL3B produced in Sf9 insect cells.

(B) Influence of pH on the enzymatic activity of murine SMPDL3B produced in Sf9 insect cells.

(C) Coomassie staining of SDS-PAGE gel containing equal amounts of human or mouse SMPDL3B and H135A point mutants. Bar graphs show phosphodiesterase activity of the indicated proteins.

(D) Measurement of phosphodiesterase activity on HEK293T cells stably expressing an empty vector (mock) or murine SMPDL3B.

(E) Phosphodiesterase activity on control (shCTRL) and *Smpdl3b*-depleted (shSMPDL3B) RAW264.7 cells.

(F) Wild-type (wt) or *Smpdl3b*-deficient (ko) BMDMs were stimulated or not with 100 ng/ml LPS, 1 μM CpG, 2.5 μM IMQ, 200 ng/ml Pam3Csk4 (P3C4), and 1,000 U/ml IFN- β or 1,000 U/ml IFN- γ for 16 hr, and SMPDL3B or Actin protein levels were analyzed by western blotting. Bar graphs represent phosphodiesterase activity measured after stimulation. (A and C) Data are representative of at least two independent experiments. (B and D–F) Data show mean \pm SD of technical triplicates and are representative of at least two independent experiments. See also Figure S3.

highlighting SMPDL3B as an important phosphodiesterase enzyme significantly contributing to substrate hydrolysis on macrophages (Figures 3E and S3E).

Given that *Smpdl3b* transcription was upregulated upon TLR activation in macrophages and DCs (Figure 2A), we next determined the effect of inflammatory stimuli on protein levels and enzymatic activity. In line with enhanced transcription, SMPDL3B protein levels were upregulated in BMDMs upon stimulation with different TLR ligands, including LPS, CpG, IMQ, and Pam3CSK4, and also the pro-inflammatory cytokine interferon γ (Figure 3F). Consistent results were also obtained for RAW264.7 macrophages (Figure S3F). The cellular enzymatic activity correlated well with the protein levels and was strongly reduced in BMDMs from knockout mice, further highlighting SMPDL3B as the dominant phosphodiesterase on the surface of these immune cells (Figure 3F).

Deficiency in SMPDL3B Leads to a Global Increase in Membrane Fluidity

To evaluate the impact of SMPDL3B, a lipid-associated enzyme, on the cellular membrane environment, we measured membrane fluidity of macrophages. The lipid phase of membranes in intact cells can be studied using fluorescent probes that alter their spectral emission properties dependent on lipid packing and can thus reflect membrane order (Owen et al., 2012). The generalized polarization (GP) function can be used to calculate a normalized ratio between the measured intensities of ordered and unordered fractions in fluorescence microscopy images and therefore allows the quantification of changes in membrane order. In line with a role for SMPDL3B in membrane biology, microscopy-based measurements of membrane fluidity using the

fluorescent probe di-4-ANEPPDHQ revealed a strong decrease of membrane order (i.e., increase of membrane fluidity) in SMPDL3B-depleted RAW264.7 macrophages (Figures 4A–4C). Treatment with the cholesterol-extracting agent methyl- β -cyclodextrin (M β CD) also led to reduced measurable membrane order and served as a positive control for this assay system. As an increase in membrane fluidity associated with SMPDL3B knockdown might affect the integrity of lipid rafts found on the cell surface, we measured the concentration of the raft marker GM1 ganglioside by flow cytometry. Interestingly, the concentration of GM1 was not affected by knockdown of *Smpdl3b*, suggesting no general modulatory effect on lipid raft abundance (Figure S4A). Highly consistent with the data obtained in RAW264.7 cells, also *Smpdl3b*-deficient BMDMs showed a decrease in membrane order, indeed assigning a role to SMPDL3B in membrane biology (Figure 4D).

Lipidomics Analysis

The clear changes of membrane fluidity in SMPDL3B knockdown or knockout cells strongly suggested that the TLR-modulating activity of SMPDL3B is associated with a change in macrophage lipid composition. To test this, we assessed the global impact of SMPDL3B on the cellular lipid repertoire by mass spectrometry-based lipidomics. RAW264.7 cells were incubated for 2 hr in serum-free medium and lipids from control (shCTRL) and SMPDL3B-depleted cells (shSMPDL3B) were extracted and analyzed for sphingo- and glycerophospholipid as well as cholesterol levels (Table S1). In line with the strong reduction in membrane order, knockdown of SMPDL3B led to a profound global change in the cellular lipid composition, with significant alterations observed for components of most analyzed lipid

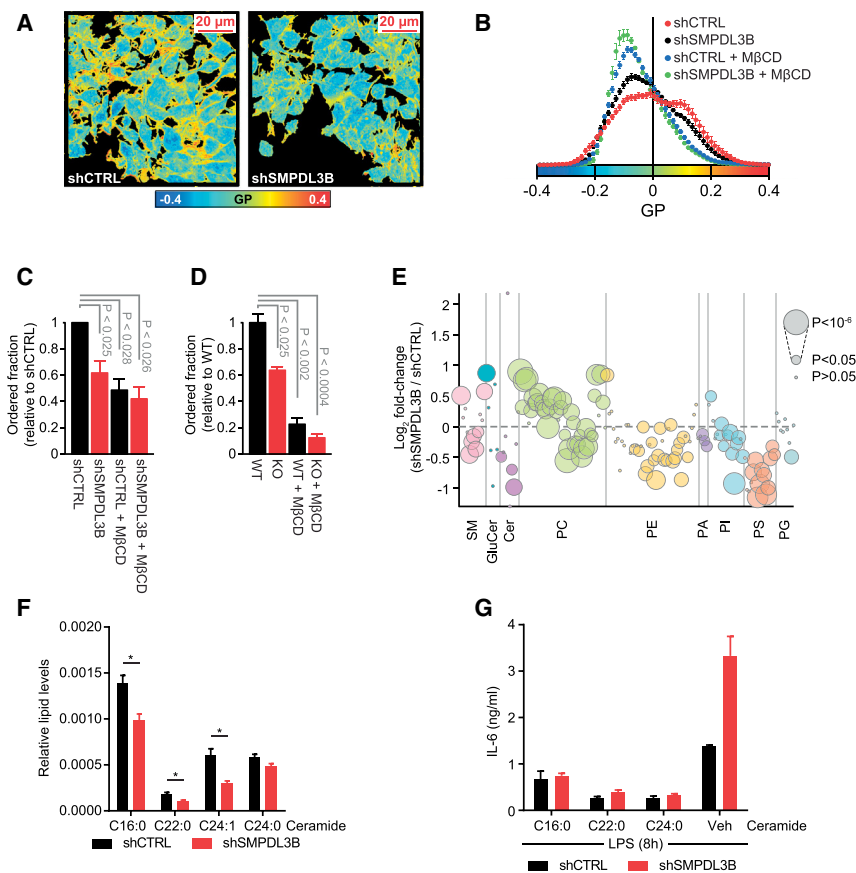


Figure 4. SMPDL3B Alters the Biophysical Properties and Composition of Cellular Membranes

(A–D) Membrane fluidity measurements. (A) Confocal images pseudocolored based on GP values (see color bar). Left: shCTRL; right: shSMPDL3B. Scale bar, 20 μ m. (B) GP value distribution from representative experiment. Mean \pm SEM, n = 7. (C) Fraction of ordered membrane of RAW264.7 relative to shCTRL. Mean \pm SD of at least three biological replicates is shown. (D) Fraction of ordered membrane of BMDMs relative to WT. Mean \pm SD, n = 5. Figure is representative of two biological replicates.

(E) Lipids were extracted from control (shCTRL) or SMPDL3B-depleted (shSMPDL3B) RAW264.7 macrophages and analyzed by MS for glycerophospho- and sphingolipids. Bubble plots represent mean log₂-transformed fold-change differences between cell lines. SM, sphingomyelin; GluCer, glucosylceramide; Cer, ceramide; PC, (lyso-) phosphatidylcholine; PE, (lyso-) phosphatidylethanolamine; PA, phosphatidic acid; PI, (lyso-) phosphatidylinositol; PS, (lyso-) phosphatidylserine; PG, phosphatidylglycerol. Data are representative of two biological replicates each consisting of five technical replicates.

(F) Relative lipid levels for ceramide in control (shCTRL) and SMPDL3B-depleted RAW264.7 macrophages (shSMPDL3B). Cer d18:1/16:0 is abbreviated as C16:0, Cer d18:1/22:0 as C22:0, Cer d18:1/24:0 as C24:0, and Cer d18:1/24:1 as C24:1. Data represent mean \pm SEM of two biological replicates each consisting of five technical replicates. *p \leq 0.05.

(G) Control (shCTRL) and SMPDL3B-depleted RAW264.7 macrophages (shSMPDL3B) were

pretreated for 30 min with vehicle (VEH) or the indicated synthetic ceramide species (15 μ M) and then stimulated with 100 ng/ml LPS for 8 hr. IL-6 release was measured by ELISA.

Data show mean \pm SD of technical triplicates and is representative of at least two independent experiments. See Figure S4.

classes (Figures 4E, S4B, and S4C). Among sphingolipid species, significant decreases were observed for ceramide species upon knockdown of SMPDL3B, and two sphingomyelin species were significantly increased while five were decreased (Figures 4E and S4B). Also, glycerophospholipids were strongly affected by SMPDL3B depletion. Phosphatidylcholine species were rather increased, whereas most phosphatidylethanolamine, -inositol and -serine, were decreased (Figures 4E and S4B). Finally, cellular cholesterol levels were also significantly decreased in SMPDL3B-depleted cells (Figure S4D). Taken together, our membrane fluidity and lipidomics measurements identified SMPDL3B as regulator of macrophage membrane composition and order.

Silencing of *Smpdl3b* Leads to a Pro-inflammatory Lipid State

Given that the depletion of SMPDL3B in RAW264.7 cells did not only affect a subset of measured lipid species, but led to a global change in the cellular lipid repertoire, the interpretation of these data required further analysis. Based on a systematic perturbation screen targeting genes involved in sphingolipid metabolism combined with lipidomics analysis and measure-

ment of TLR-related processes the function of 245 diverse lipid species could be inferred (see Köberlin et al., 2015). Utilizing this resource, we compared the changes in lipid abundance upon SMPDL3B knockdown with their predicted function in IL-6 release for those lipid species that were detected in both lipidomics data sets. Consistent with the increased inflammatory response observed in SMPDL3B-depleted cells, we found lipids associated with increased IL-6 release upon LPS or CpG stimulation to be increased in abundance while lipids associated with reduced IL-6 release were decreased in abundance (Figure S4E). Interestingly, several ceramide species predicted to dampen TLR-dependent IL-6 release (Cer d18:1/16:0, d18:1/22:0, and d18:1/24:1) were significantly reduced upon SMPDL3B knockdown (Figures 4F and S4E). To validate their potential involvement in regulating LPS-induced IL-6 release, we performed lipid supplementation experiments. Indeed, when control and SMPDL3B-depleted macrophages were pre-treated with the synthetic ceramide species Cer d18:1/16:0, Cer d18:1/22:0, and Cer d18:1/24:0, the SMPDL3B-dependent increase in IL-6 release upon LPS stimulation could be reverted (Figures 4G and S4F). Similarly, the IL-6 release induced upon stimulation with CpG and IMQ was reduced by

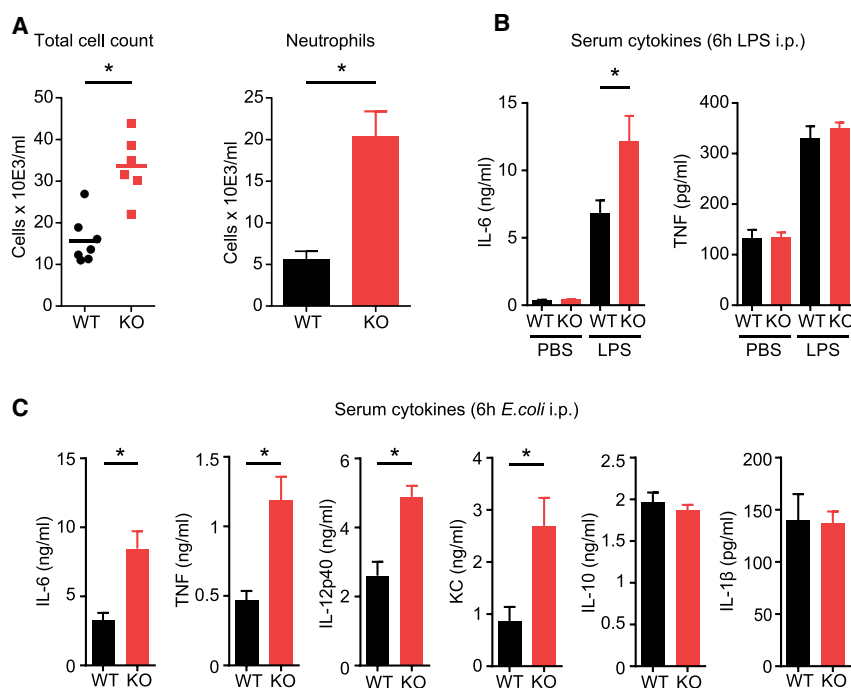


Figure 5. SMPDL3B Is a Negative Regulator of Inflammation In Vivo

(A and B) Wild-type (WT) and *Smpdl3b*-deficient (KO) mice were injected with 50 μ g LPS i.p. After 6 hr, mice were sacrificed, and (A) peritoneal lavage was taken and total cells and neutrophils were counted, and (B) serum IL-6 and TNF were measured by ELISA.

(C) Wild-type (WT) and *Smpdl3b*-deficient (KO) mice were injected i.p. with 1×10^4 cfu of *E. coli*. After 6 hr, mice were sacrificed, and the serum cytokine levels of IL-6, TNF, IL-12p40, KC, IL-10, and IL-1 β were analyzed by ELISA. Bars are means of each group \pm SEM (* $p \leq 0.05$) and are representative of two independent experiments, each performed with eight mice/group.

supplementation of ceramide Cer d18:1/24:0 further experimentally confirming the predicted roles on other TLRs (Figure S4G).

Taken together, changes in cellular lipid species abundance associated with SMPDL3B depletion were highly indicative of pro-inflammatory responses. Furthermore, our lipidomics analysis combined with lipid supplementation experiments allowed us to highlight several long-chained ceramide species as putative modulators of the enhanced inflammatory response upon SMPDL3B depletion.

SMPDL3B Negatively Regulates TLR Activity In Vivo

If, as all evidence so far would show, SMPDL3B is involved in homeostasis of membrane lipid composition and TLR signaling, then it should have a role in TLR-mediated inflammatory processes in vivo. To assess this, we used an LPS-dependent mouse inflammation model. Wild-type or *Smpdl3b*-deficient mice were injected intraperitoneally with LPS and peritoneal cell influx as well as serum cytokine levels were determined 6 hr later (Figures 5A and 5B). *Smpdl3b*-deficient mice contained higher numbers of immune cells in the peritoneal lavage fluid (PLF), due to a significantly enhanced influx of neutrophils, in line with an aberrantly strong inflammatory response (Figure 5A). Concomitantly, *Smpdl3b*-deficient mice showed increased IL-6 levels in the serum as compared to control mice (Figure 5B). Serum levels of TNF were not significantly affected under these conditions (Figure 5B). To test whether SMPDL3B also affects the host-response against viable pathogens, we used an *E. coli*-induced peritonitis model. Hence, wild-type and *Smpdl3b*-deficient mice were injected with bacteria in the peritoneum and serum cytokine levels were quantified 6 hr later. Serum levels of IL-6, TNF, IL-12p40, and KC

were significantly elevated in *Smpdl3b*-deficient mice as compared to wild-type (Figure 5C). Interestingly, we did not detect significant alterations in the serum levels of the cytokines IL-10 and IL-1 β , indicating that not all inflammatory mediators were equally affected by *Smpdl3b* deficiency (Figure 5C). Taken together,

our experiments indeed establish SMPDL3B as negative regulator of TLR-dependent inflammatory responses in vivo.

DISCUSSION

In the present study, we have identified the GPI-anchored lipid-modifying enzyme SMPDL3B as negative regulator of TLR signaling. We found that this sphingomyelinase-related protein is abundantly expressed on macrophages and DCs and can be further upregulated by inflammatory stimuli. Furthermore, enzymatic assays on intact cells revealed that SMPDL3B is responsible for a large fraction of measurable phosphodiesterase activity on these important immune cells. Loss-of-function of this enzyme led to increased cellular responses upon TLR stimulation while *Smpdl3b*-deficient mice showed enhanced inflammation in models of TLR-dependent peritonitis. Confirming the involvement of this protein in lipid metabolism, we found that lack of the cellular activity of this enzyme was associated with a significant change in membrane fluidity and the global cellular lipid composition. Supplementation of specific ceramide species that were reduced in SMPDL3B-depleted cells was able to revert the SMPDL3B-dependent hyper-inflammatory phenotype.

Bioactive lipids such as ceramides, sphingosine-1-phosphate and phosphatidylinositol derivatives as well as changes in structural components of cellular membranes have all been implicated in modulation of TLR signaling (Fessler and Parks, 2011; Liew et al., 2005). The inducibility upon TLR stimulation and impact of SMPDL3B on cellular lipid composition and consequently membrane fluidity is suggestive of a not yet described regulatory mode of macrophage function acting at the interface of membrane biology and inflammatory signaling.

The lipid environment of TLRs, including membrane microdomains rich in sphingolipids and cholesterol, has been shown to play a role in receptor function (Fessler and Parks, 2011; Lingwood and Simons, 2010; Triantafyllou et al., 2002, 2004; Zhu et al., 2010). Perturbations affecting the receptor-accommodating membranes, as observed in macrophages defective for the cholesterol efflux transporters ABCA1 and ABCG1 that display an increase in free cholesterol, lead to enhanced responsiveness of TLRs, presumably as a consequence of altered plasma membrane composition (Draper et al., 2010; Yvan-Charvet et al., 2008; Zhu et al., 2008, 2010). In cells deficient for SMPDL3B, we could not detect changes in the amount of GM1, a marker for sphingolipid- and cholesterol-enriched microdomains, indicating that these structures are intact. Instead, we observed a global decrease in membrane order and change in the cellular lipid repertoire that was associated with upregulation of TLR-triggered signaling, suggesting that SMPDL3B activity may affect innate immunity signaling by an alternative, possibly composite mechanism.

Interestingly, whereas TLR receptor-proximal signaling and cytokine production were clearly changed by SMPDL3B depletion, other processes, including TLR4 surface expression and endocytosis or CpG uptake, appeared normal. This indicates that membrane-dependent functions are differently sensitive to SMPDL3B depletion, which might also affect other TLR-associated processes including receptor-lipid interactions, adaptor recruitment dynamics, receptor diffusion and trafficking, or ligand dissociation (Ernst et al., 2010; Gay et al., 2014). While in the context of TLR signaling SMPDL3B-depleted or deficient macrophages manifested a stronger inflammatory response, the global changes in the cellular lipid repertoire are likely to have more pleiotropic functional effects and affect other cellular signaling pathways and processes that were not covered in our study. Therefore, future experiments will aim at the identification and elucidation of additional roles of SMPDL3B in macrophages and other cellular systems in which SMPDL3B is expressed.

Generation of ceramide has been observed in response to various stimuli, leading to the formation of ceramide-rich membrane platforms, thought to be involved in the regulation of transmembrane signaling processes (Hannun and Obeid, 2008; Milhas et al., 2010; Stancevic and Kolesnick, 2010). Based on observations in experimental lipid bilayers, an increase in ceramide species causes higher membrane order, highlighting a regulatory effect of these lipids on membrane biophysical properties (Stancevic and Kolesnick, 2010). Interestingly, several ceramide species (Cer d18:1/16:0, Cer d18:1/22:0, and Cer d18:1/24:1), which were found to be negatively correlated with TLR-induced IL-6 release, were also significantly reduced upon SMPDL3B depletion, potentially explaining the effect on membrane order observed in these cells.

Despite the complexity of the mechanism at play, the specific and high expression of SMPDL3B in immune cells, the inducibility of its expression and activity by immune stimuli, combined with the unequivocal phenotype observed in *Smpdl3b*-deficient mice, demonstrate an intimate link between a major cell surface lipid-modulating enzyme and the regulation of pro-inflammatory processes. Undoubtedly, more connections between metabolism, tissue homeostasis, and the resolution of inflammation

are likely to emerge in the future and further elucidate these interdependent regulatory networks.

EXPERIMENTAL PROCEDURES

Information on reagents, plasmids, cell culture, and protein purification can be found in the [Supplemental Experimental Procedures](#).

FACS

All samples were analyzed on a BD Biosciences FACSCalibur or LSR Fortessa flow cytometer. See the [Supplemental Experimental Procedures](#) for further information.

RT-PCR

RNA was isolated with the QIAGEN RNeasy Mini Kit. 100 ng RNA/sample was reversely transcribed using RevertAid reverse transcriptase (Fermentas). cDNA was diluted 1:20, and relative transcript levels were analyzed using SYBR green (GeneXpress) using the following primers: Cyclophilin B 5'-CAG CAA GTT CCA TCG TGT CAT CAA GG-3' and 5'-GGA AGC GCT CAC CAT AGA TGC TC-3'; *Smpdl3b* 5'-AAG TCT ATG CTG CTC TGG GAA-3' and 5'-TGC CAC CTG GTT ATA GAT GC-3'; mKC 5'-CAATGAGCTGCGCTG TCAGTG-3' and 5'-CTTGGGGACACCTTTTAGCATC-3'. Real-time PCR analysis was performed on a Rotor Gene 6000 (QIAGEN) in technical duplicates or triplicates. Expression of target genes was normalized to that of the housekeeping gene Cyclophilin B.

ELISA

All ELISA experiments were performed according to the manufacturers' instructions. The kit for detection of KC was from R&D Systems, TNF was from BioLegend, and all others were from BD Biosciences.

Triton X-114 Phase Separation and PI-PLC Sensitivity Assays

Triton X-114 (TX114) phase separation experiments were performed according to Bordier (1981) and as described previously (Heinz et al., 2012). PI-PLC experiments were carried out by incubation of samples with 0.5 U/ml PI-PLC (Invitrogen) for 30 min on ice. See the [Supplemental Experimental Procedures](#) for further information.

Phosphodiesterase Enzymatic Activity

Generation of *p*-nitrophenol from bis-*p*-nitrophenolphosphate by phosphodiesterase activity was measured as absorbance at 405 nm in 96-well plates with 100 μ l reaction volume. Kinetic measurements were carried out using 325 ng/ml enzyme purified from Sf9 insect cells in HEPES buffer (20 mM [pH 7.8]) with a substrate concentration as indicated. pH optima were determined by incubation of enzymes purified from Sf9 insect cells or HEK293T cells in the presence of different buffers adjusted to the indicated pH in the presence of 1 mM substrate. For determination of the impact of point mutations, enzymes were incubated with HEPES buffer (20 mM [pH 7.8]) in the presence of 1 mM substrate. For measurement of cell-associated enzymatic activity, cells were incubated in 96-well plates with isotonic Tris-buffered saline (TBS) in the presence of 1 mM substrate at 37°C and 5% CO₂.

Membrane Fluidity Measurements

Membrane fluidity measurements were carried out using the fluorescent probe di-4-ANEPPDHQ following a modified protocol from Owen et al. (2012). See the [Supplemental Experimental Procedures](#) for additional information.

Lipidomics

1.5 $\times 10^7$ RAW264.7 cells stably expressing SMPDL3B-specific or control small hairpin RNA (shRNAs) were seeded in 10-cm dishes in serum-free DMEM medium as five technical replicates and incubated for 2 hr at 37°C, 5% CO₂. Cells were harvested into ice-cold PBS and centrifuged for 5 min at 300 $\times g$, 4°C, and pellets were resuspended in 50 μ l PBS, transferred to Eppendorf tubes, and frozen in liquid nitrogen for further processing. Samples were hydrated by adding 200 μ l H₂O and extracted by addition of 600 μ l

methanol/chloroform (1:2 v/v) by vigorously vortexing the samples three times for 1 min with 5-min intervals. After addition of 300 μ l chloroform and 2 μ l of 100 mM KCl samples were vortexed three times for 30 s with 1-min intervals. Samples were centrifuged at 9,000 rpm for 2 min at 4°C; the lower, organic phase was transferred to new tubes and dried in a SpeedVac centrifuge. Lipids were quantified by HPLC/MS as described previously with corresponding internal standards including C17-Cer, C12-SM, C8-GluCer, C20-LPC, and PC-14:0/14:0 (Avanti Polar Lipids) (Shui et al., 2011). Individual lipids were normalized to phosphatidylcholine and sphingomyelin levels.

In Vivo Experimental Procedures

Heterozygous *Smpd13b*^{+/-} mice (B6N;B6N-Smpd13b < tm1a(EUCOMM)Wtsi > /H) were purchased from the EMMA consortium (EUCOMM) and shipped from the MRC. *Smpd13b* homozygous knockout was confirmed by genotyping using the following primers: SMPDL3B WT 5' -GTG TAA GCC TTC TCC CCC AG-3'; SMPDL3B WT 5' -CAG AAA AAG TTC TAC GGA CCA GC-3'; SMPDL3B MUT 5' -TTG GTG ATA TCG TGG TAT CGT T-5'. Wild-type C57BL/6J mice were obtained from Charles River Laboratories and bred at the same location as *Smpd13b*-deficient mice. Pathogen-free 9- to 11-week-old female C57BL/6J and homozygous B6N;B6N-Smpd13b^{tm1a(EUCOMM)Wtsi}/H *Smpd13b*^{-/-} mice were used in all in vivo experiments, which were approved by the Animal Care and Use Committee of the Medical University of Vienna. Mice were injected intraperitoneally with 50 μ g LPS in 200 μ l of saline per mouse. After 6 hr, mice were sacrificed, peritoneal lavage was performed, and blood was taken. Cell counts were determined on each peritoneal lavage sample stained with Tuerks solution, and differential cell counts were performed on cytospin samples stained with Giemsa. *E. coli*-dependent peritonitis was induced as described previously (Knapp et al., 2007). In brief, *E. coli* O18:K1 was cultured in Luria-Bertani medium (Difco) at 37°C, harvested at mid-log phase, and washed twice before inoculation. Mice were injected i.p. with 1–2 \times 10⁴ cfu *E. coli* in 200 μ l saline per mouse. The inoculum was plated on blood agar plates to determine viable counts. Mice were sacrificed, and blood was isolated after 6 hr.

Bioinformatic Analysis and General Statistics

Protein sequences and information were retrieved from UniProtKB database (2012). Additional information on domain organization was obtained through the NCBI conserved domain database (CDD) (Marchler-Bauer et al., 2011). Protein homology searches were carried out using NCBI Blast (Altschul et al., 1990). Expression data for murine SMPDL3B were extracted from the BioGPS gene annotation portal (Lattin et al., 2008; Wu et al., 2009). p values were calculated with two-tailed t tests, unless otherwise indicated.

SUPPLEMENTAL INFORMATION

Supplemental Information includes Supplemental Experimental Procedures, four figures, and one table and can be found with this article online at <http://dx.doi.org/10.1016/j.celrep.2015.05.006>.

AUTHOR CONTRIBUTIONS

L.X.H., C.L.B., and G.S.-F. conceived the study. C.L.B., R.G., O.S., and S.K. designed and performed in vivo experiments. A.C.M., K.L.B., F.P.B., J.C., R.K.K., C.L.B., L.X.H., and G.S.-F. designed and performed proteomics experiments and data analysis. G.S. and M.R.W. performed lipidomics analysis. B.S. performed image and lipidomics data analysis. L.X.H., C.L.B., M.S.K., and M.B. performed other experiments. L.X.H., C.L.B., and G.S.-F. designed other experiments. I.A., A.F., T.K., S.B., M.R., and A.P. generated reagents and contributed scientific insights. L.X.H., C.L.B., and G.-S.F. wrote the manuscript. All authors contributed to the discussion of results and participated in manuscript preparation.

ACKNOWLEDGMENTS

We thank Gregory Vladimer for critically reading of the manuscript, Ruth Fuchs and Denise Barlow for help with mouse genotyping, and Sabine Jungwirth and

Sarah Niggemeyer for breeding of mice. The work was funded by the Austrian Academy of Sciences (G.S.-F., M.K., I.A., A.C.M., S.B., T.K., and A.F.), the Medical University of Vienna (S.K. and O.S.), the European Research Council under the European Union's Seventh Framework Programme (FP7/2007–2013)/ERC Grant agreement no. 250179 (G.S.-F., L.X.H., R.K.K., and A.P.), and Marie Curie Fellowship agreement no. 220596 (C.L.B.) and no. 301663 (M.R.), the EMBO Fellowships ATLF 2008-463 (C.L.B.), ALTF 1346-2011 (M.R.) and ATLF 314-2012 (R.K.K.), the Austrian Science Fund FWF1291B09 (M.B.) and FWF1205B09 (R.G.), and the Austrian Federal Ministry for Science and Research GEN-AU/BIN (J.C.) and GEN-AU/APP (K.L.B.). B.S. is supported by a fellowship from the Swiss National Science Foundation (Project no. P300P3_147897). M.R.W. is supported by grants from the National University of Singapore via the Life Sciences Institute (LSI), the Singapore National Research Foundation under CRP Award No. 2007-04, and the SystemsX.ch RTD project LipidX.

Received: December 22, 2014

Revised: March 23, 2015

Accepted: May 1, 2015

Published: June 18, 2015

REFERENCES

- Altschul, S.F., Gish, W., Miller, W., Myers, E.W., and Lipman, D.J. (1990). Basic local alignment search tool. *J. Mol. Biol.* 215, 403–410.
- Andreyev, A.Y., Fahy, E., Guan, Z., Kelly, S., Li, X., McDonald, J.G., Milne, S., Myers, D., Park, H., Ryan, A., et al. (2010). Subcellular organelle lipidomics in TLR-4-activated macrophages. *J. Lipid Res.* 51, 2785–2797.
- Arthur, J.S., and Ley, S.C. (2013). Mitogen-activated protein kinases in innate immunity. *Nat. Rev. Immunol.* 13, 679–692.
- Baumann, C.L., Aspalter, I.M., Sharif, O., Pichlmair, A., Blüml, S., Grebien, F., Bruckner, M., Pasierbek, P., Aumayr, K., Planavsky, M., et al. (2010). CD14 is a coreceptor of Toll-like receptors 7 and 9. *J. Exp. Med.* 207, 2689–2701.
- Bordier, C. (1981). Phase separation of integral membrane proteins in Triton X-114 solution. *J. Biol. Chem.* 256, 1604–1607.
- Dennis, E.A., Deems, R.A., Harkewicz, R., Quehenberger, O., Brown, H.A., Milne, S.B., Myers, D.S., Glass, C.K., Hardiman, G., Reichart, D., et al. (2010). A mouse macrophage lipidome. *J. Biol. Chem.* 285, 39976–39985.
- Draper, D.W., Madenspacher, J.H., Dixon, D., King, D.H., Remaley, A.T., and Fessler, M.B. (2010). ATP-binding cassette transporter G1 deficiency dysregulates host defense in the lung. *Am. J. Respir. Crit. Care Med.* 182, 404–412.
- Ernst, A.M., Contreras, F.X., Brügger, B., and Wieland, F. (2010). Determinants of specificity at the protein-lipid interface in membranes. *FEBS Lett.* 584, 1713–1720.
- Fessler, M.B., and Parks, J.S. (2011). Intracellular lipid flux and membrane microdomains as organizing principles in inflammatory cell signaling. *J. Immunol.* 187, 1529–1535.
- Fornoni, A., Sageshima, J., Wei, C., Merscher-Gomez, S., Aguilon-Prada, R., Jauregui, A.N., Li, J., Mattiazzi, A., Ciancio, G., Chen, L., et al. (2011). Rituximab targets podocytes in recurrent focal segmental glomerulosclerosis. *Sci. Transl. Med.* 3, 85ra46.
- Gay, N.J., Symmons, M.F., Gangloff, M., and Bryant, C.E. (2014). Assembly and localization of Toll-like receptor signalling complexes. *Nat. Rev. Immunol.* 14, 546–558.
- Hannun, Y.A., and Obeid, L.M. (2008). Principles of bioactive lipid signalling: lessons from sphingolipids. *Nat. Rev. Mol. Cell Biol.* 9, 139–150.
- Hannun, Y.A., and Obeid, L.M. (2011). Many ceramides. *J. Biol. Chem.* 286, 27855–27862.
- Heinz, L.X., Rebsamen, M., Rossi, D.C., Staehli, F., Schroder, K., Quadroni, M., Gross, O., Schneider, P., and Tschopp, J. (2012). The death domain-containing protein Unc5CL is a novel MyD88-independent activator of the pro-inflammatory IRAK signaling cascade. *Cell Death Differ.* 19, 722–731.
- Kawai, T., and Akira, S. (2007). TLR signaling. *Semin. Immunol.* 19, 24–32.

- Kawai, T., and Akira, S. (2010). The role of pattern-recognition receptors in innate immunity: update on Toll-like receptors. *Nat. Immunol.* **11**, 373–384.
- Knapp, S., Matt, U., Leitinger, N., and van der Poll, T. (2007). Oxidized phospholipids inhibit phagocytosis and impair outcome in gram-negative sepsis in vivo. *J. Immunol.* **178**, 993–1001.
- Köberlin, M.S., Snijder, B., Heinz, L.X., Baumann, C.L., Fauster, A., Vladimer, G.I., Gavin, A.-C., and Superti-Furga, G. (2015). A conserved circular network of coregulated lipids modulates innate immune responses. *Cell*, Published online June 18, 2015. <http://dx.doi.org/10.1016/j.cell.2015.05.051>.
- Kondo, T., Kawai, T., and Akira, S. (2012). Dissecting negative regulation of Toll-like receptor signaling. *Trends Immunol.* **33**, 449–458.
- Lattin, J.E., Schroder, K., Su, A.I., Walker, J.R., Zhang, J., Wiltshire, T., Saijo, K., Glass, C.K., Hume, D.A., Kellie, S., and Sweet, M.J. (2008). Expression analysis of G Protein-Coupled Receptors in mouse macrophages. *Immunome Res.* **4**, 5.
- Lee, C.C., Avalos, A.M., and Ploegh, H.L. (2012). Accessory molecules for Toll-like receptors and their function. *Nat. Rev. Immunol.* **12**, 168–179.
- Liew, F.Y., Xu, D., Brint, E.K., and O'Neill, L.A. (2005). Negative regulation of toll-like receptor-mediated immune responses. *Nat. Rev. Immunol.* **5**, 446–458.
- Lingwood, D., and Simons, K. (2010). Lipid rafts as a membrane-organizing principle. *Science* **327**, 46–50.
- Marchler-Bauer, A., Lu, S., Anderson, J.B., Chitsaz, F., Derbyshire, M.K., DeWeese-Scott, C., Fong, J.H., Geer, L.Y., Geer, R.C., Gonzales, N.R., et al. (2011). CDD: a Conserved Domain Database for the functional annotation of proteins. *Nucleic Acids Res.* **39**, D225–D229.
- Masuishi, Y., Nomura, A., Okayama, A., Kimura, Y., Arakawa, N., and Hirano, H. (2013). Mass spectrometric identification of glycosylphosphatidylinositol-anchored peptides. *J. Proteome Res.* **12**, 4617–4626.
- Maurya, M.R., Gupta, S., Li, X., Fahy, E., Dinasarapu, A.R., Sud, M., Brown, H.A., Glass, C.K., Murphy, R.C., Russell, D.W., et al. (2013). Analysis of inflammatory and lipid metabolic networks across RAW264.7 and thioglycolate-elicited macrophages. *J. Lipid Res.* **54**, 2525–2542.
- Mayor, S., and Riezman, H. (2004). Sorting GPI-anchored proteins. *Nat. Rev. Mol. Cell Biol.* **5**, 110–120.
- Medzhitov, R. (2008). Origin and physiological roles of inflammation. *Nature* **454**, 428–435.
- Milhas, D., Clarke, C.J., and Hannun, Y.A. (2010). Sphingomyelin metabolism at the plasma membrane: implications for bioactive sphingolipids. *FEBS Lett.* **584**, 1887–1894.
- Moresco, E.M., LaVine, D., and Beutler, B. (2011). Toll-like receptors. *Curr. Biol.* **21**, R488–R493.
- Noto, P.B., Bukhtiyarov, Y., Shi, M., McKeever, B.M., McGeehan, G.M., and Lala, D.S. (2012). Regulation of sphingomyelin phosphodiesterase acid-like 3A gene (SMPDL3A) by liver X receptors. *Mol. Pharmacol.* **82**, 719–727.
- O'Neill, L.A. (2008). The interleukin-1 receptor/Toll-like receptor superfamily: 10 years of progress. *Immunol. Rev.* **226**, 10–18.
- Owen, D.M., Rentero, C., Magenau, A., Abu-Siniyeh, A., and Gaus, K. (2012). Quantitative imaging of membrane lipid order in cells and organisms. *Nat. Protoc.* **7**, 24–35.
- Pehkonen, P., Welter-Stahl, L., Diwo, J., Ryyänen, J., Wienecke-Baldacchino, A., Heikkinen, S., Treuter, E., Steffensen, K.R., and Carlberg, C. (2012). Genome-wide landscape of liver X receptor chromatin binding and gene regulation in human macrophages. *BMC Genomics* **13**, 50.
- Seto, M., Whitlow, M., McCarrick, M.A., Srinivasan, S., Zhu, Y., Pagila, R., Mintzer, R., Light, D., Johns, A., and Meurer-Ogden, J.A. (2004). A model of the acid sphingomyelinase phosphoesterase domain based on its remote structural homolog purple acid phosphatase. *Protein Sci.* **13**, 3172–3186.
- Shui, G., Stebbins, J.W., Lam, B.D., Cheong, W.F., Lam, S.M., Gregoire, F., Kusunoki, J., and Wenk, M.R. (2011). Comparative plasma lipidome between human and cynomolgus monkey: are plasma polar lipids good biomarkers for diabetic monkeys? *PLoS ONE* **6**, e19731.
- Stancevic, B., and Kolesnick, R. (2010). Ceramide-rich platforms in transmembrane signaling. *FEBS Lett.* **584**, 1728–1740.
- Traini, M., Quinn, C.M., Sandoval, C., Johansson, E., Schroder, K., Kockx, M., Meikle, P.J., Jessup, W., and Kritharides, L. (2014). Sphingomyelin phosphodiesterase-like 3A (SMPDL3A) is a novel nucleotide phosphodiesterase regulated by cholesterol in human macrophages. *J. Biol. Chem.* **289**, 32895–32913.
- Triantafyllou, M., Miyake, K., Golenbock, D.T., and Triantafyllou, K. (2002). Mediators of innate immune recognition of bacteria concentrate in lipid rafts and facilitate lipopolysaccharide-induced cell activation. *J. Cell Sci.* **115**, 2603–2611.
- Triantafyllou, M., Morath, S., Mackie, A., Hartung, T., and Triantafyllou, K. (2004). Lateral diffusion of Toll-like receptors reveals that they are transiently confined within lipid rafts on the plasma membrane. *J. Cell Sci.* **117**, 4007–4014.
- van Meer, G., Voelker, D.R., and Feigenson, G.W. (2008). Membrane lipids: where they are and how they behave. *Nat. Rev. Mol. Cell Biol.* **9**, 112–124.
- Wu, C., Orozco, C., Boyer, J., Leglise, M., Goodale, J., Batalov, S., Hodge, C.L., Haase, J., Janes, J., Huss, J.W., 3rd, and Su, A.I. (2009). BioGPS: an extensible and customizable portal for querying and organizing gene annotation resources. *Genome Biol.* **10**, R130.
- Yoo, T.H., Pedigo, C.E., Guzman, J., Correa-Medina, M., Wei, C., Villarreal, R., Mitrofanova, A., Leclercq, F., Faul, C., Li, J., et al. (2015). Sphingomyelinase-like phosphodiesterase 3b expression levels determine podocyte injury phenotypes in glomerular disease. *J. Am. Soc. Nephrol.* **26**, 133–147.
- Yvan-Charvet, L., Welch, C., Pagler, T.A., Ranalletta, M., Lamkanfi, M., Han, S., Ishibashi, M., Li, R., Wang, N., and Tall, A.R. (2008). Increased inflammatory gene expression in ABC transporter-deficient macrophages: free cholesterol accumulation, increased signaling via toll-like receptors, and neutrophil infiltration of atherosclerotic lesions. *Circulation* **118**, 1837–1847.
- Zhu, X., Lee, J.Y., Timmins, J.M., Brown, J.M., Boudyguina, E., Mulya, A., Gebre, A.K., Willingham, M.C., Hiltbold, E.M., Mishra, N., et al. (2008). Increased cellular free cholesterol in macrophage-specific Abca1 knock-out mice enhances pro-inflammatory response of macrophages. *J. Biol. Chem.* **283**, 22930–22941.
- Zhu, X., Owen, J.S., Wilson, M.D., Li, H., Griffiths, G.L., Thomas, M.J., Hiltbold, E.M., Fessler, M.B., and Parks, J.S. (2010). Macrophage ABCA1 reduces MyD88-dependent Toll-like receptor trafficking to lipid rafts by reduction of lipid raft cholesterol. *J. Lipid Res.* **51**, 3196–3206.

Cell Reports

Supplemental Information

The Lipid-Modifying Enzyme SMPDL3B

Negatively Regulates Innate Immunity

Leonhard X. Heinz, Christoph L. Baumann, Marielle S. Köberlin, Berend Snijder, Riem Gawish, Guanghou Shui, Omar Sharif, Irene M. Aspalter, André C. Müller, Richard K. Kandasamy, Florian P. Breitwieser, Andreas Pichlmair, Manuela Bruckner, Manuele Rebsamen, Stephan Blüml, Thomas Karonitsch, Astrid Fauster, Jacques Colinge, Keiryn L. Bennett, Sylvia Knapp, Markus R. Wenk, and Giulio Superti-Furga

Supplemental Experimental Procedures

Reagents and antibodies. All synthetic TLR ligands, imiquimod, CpG-DNA-ODN1826 and LPS (*E. coli* K12) were obtained from InvivoGen. Alexa488-conjugated anti-mouse antibodies and cholera toxin beta (CTx β -Alexa488) were from Life Technologies. Mouse anti-HA was from Covance, V5 from Invitrogen and Tubulin from Abcam. Rabbit anti-p38, JNK and phosphorylated forms of p38 (Thr180, Tyr182), ERK (Thr202/Tyr204) and JNK (Thr183, Tyr185) were from Cell Signaling, I κ B α and ERK from Santa Cruz. Rat anti-CD14 was from Pharmingen, rabbit anti-actin from Cytoskeleton Inc. PE-conjugated rat anti-TLR4 antibodies (clone MTS510) were from BioLegend. HRP-conjugated secondary antibodies were from Jackson ImmunResearch, fluorescence-conjugated antibodies were from Invitrogen. Custom rabbit anti-SMPDL3B antibodies raised against recombinant murine SMPDL3B (aa1-281) produced in *E. coli* were obtained from Charles River. Ceramides Cer d18:1/24 (C24), Cer d18:1/22 (C22) and Cer d18:1/16 (C16) were obtained from Avanti Polar Lipids and dissolved in ethanol/dodecan (98:2 v/v) vehicle by sonication for 25 minutes with vortexing steps every 5 min in 40°C warm water as previously described (Wijesinghe et al., 2009).

Plasmids. Murine TLR constructs (available from GenBank/EMBL/DDBJ under the following accession nos.: mTLR3, NM_126166; mTLR4, NM_021297; mTLR7, NM_133211; mTLR8, NM_133212; mTLR9, NM_031178) were cloned from InvivoGen vectors (pUno-HA vectors) into pTracer-V5 (Invitrogen) and pCeMM CTAP(SG) using the Gateway LR Clonase (Invitrogen) system. All gateway entry clones for C-terminal tagging of full-length cDNAs were created using 20–25 bp of flanking regions and the following gateway primer sequences: sense attB1 primer, 5'-GGG GAC AAG TTT GTA CAA AAA AGC AGG CTA GAC TGC CAT G(NNN) 5–10-3'; and antisense attB1 primer, 5'-GGG GAC CAC TTT GTA CAA GAA AGC TGG GTT NOSTOP(NNN)10–15-3'. For N-terminal HA-tagged expression, cDNAs were cloned in the entry vector pEntry1A-SP-HA, a derivative of pEntry1A (Invitrogen) containing the signal peptide of influenza hemagglutinin followed by an HA tag and a short multiple cloning site by ligation of two annealed oligos corresponding to the sequence 5'-GTC GAC GCC ACC ATG GCT ATC ATC TAC CTC ATC CTC CTG TTC ACC GCT GTG CGG GGC TAT CCA TAT GAC GTC CCA GAC TAC GCA GGA CCC GGA AAG CTT

GGA TCC GAA TTC-3' in the Sall and EcoRI sites of the plasmid. cDNAs were amplified by PCR from plasmid templates or cDNA libraries (Takara Bio Inc.) using the primers: mSMPDL3B (19-456) 5'-GCG AAG CTT CAA CTA GGG AGG TTC TGG CAC-3' and 5'-GCG GCG GCC GCT CAT AAC ACC TCC AGT ACG TG-3'; hSMPDL3B (19-455) 5'-GCG AAG CTT GAA CCA GGG AAG TTC TGG CAC-3' and 5'-GCG GCG GCC GCT CAC AGC ACG AGC GTG CAC AG-3'; mSMPDL3BΔGPI (19-435) 5'-GCG AAG CTT CAA CTA GGG AGG TTC TGG CAC-3' and 5'-GCG GCG GCC GCT CAC TTG GCA CCA AGA CCA TGC AA-3'; hSMPDL3BΔGPI (19-435) 5'-GCG AAG CTT GAA CCA GGG AAG TTC TGG CAC-3' and 5'-GCG GCG GCC GCT CAC GTG GTG CCA GAG GCA TAC AG-3'; mSMPDL1/mASM (45-627) 5'-GCG AAG CTT CTG TTT GAC TCC ACG GTT CTT-3' and 5'-GCG GCG GCC GCC TAG GAC AAC AGG GGG CGT GA-3'; mSMPDL3A (23-445) 5'-GCG AAG CTT GTG CCC CTG GCG CCG GCG GAT-3' and 5'-GCG GCG GCC GCT TAT AAA TGC TGT TTA AGG CA-3' and were ligated in the plasmid using HindIII and NotI. Site-directed mutagenesis for murine and human SMPDL3B H135A was carried out using the Quikchange II kit (Stratagene). cDNAs containing the N-terminal signal peptide and HA tag were transferred from pEntry1A-SP-HA in pTO or pMSCV-GW expression vectors using LR Clonase. For expression and secretion from insect cells, the mSMPDL3BΔGPI (19-435) cDNA was cloned into a derivative of pFastbac1 containing the mellitin signal peptide followed by a HIS-tag and an MCS using HindIII and NotI. pLKO.1 lentiviral shRNA vectors for SMPDL3B-1, clone Id TRCN0000099681 and shSMPDL3B-2, clone Id TRCN0000099683) and GFP as control were from Sigma. If not otherwise stated, shSMPDL3B-1 was used in experiments.

Cell culture. RAW264.7, HEK293T and primary bone marrow cells were cultured in DMEM (PAA) supplemented with 10% FCS (Invitrogen) and antibiotics (100 U/ml penicillin and 100 µg/ml streptomycin) at 37°C, 5% CO₂. In all types of direct stimulation experiments involving RAW264.7 macrophages, cells have been washed twice and shifted to serum-free medium 1h prior stimulation to avoid lipid rescue by FCS-derived lipids. For stimulation experiments involving synthetic ceramide pretreatment, cells were incubated for 30 min in serum free medium containing 15 µM ceramide or the corresponding ethanol/dodecan vehicle control and were stimulated with LPS (100 ng/ml), CpG (5 µM) or imiquimod (5 µM) for 8h. Cell viability was assessed using CellTiter-Glo (Promega)

according to the manufacturer's instructions. Primary cells were stimulated in full medium. BMDMs and BMDCs were generated by differentiation of bone marrow cells with 10 ng/ml rmM-CSF (Peprotech) or 20 ng/ml rmGM-CSF (R&D Systems) at a concentration of 1×10^6 cells/ml in non-tissue culture treated dishes for 7-8 days. For stimulation experiments, cells were transferred to 96-well cell culture-treated dishes and stimulated for 8h as indicated. Sf9 cells were cultured in Sf-900TM III SFM medium (Life Technologies) containing 2% FCS and antibiotics (100 U/ml penicillin and 100 µg/ml streptomycin) at 27°C.

Transfection, co-immunoprecipitation and western blot. For co-immunoprecipitation experiments, HEK293T cells were transfected using Lipofectamine 2000 (Invitrogen) according to the manufacturer's instructions. 24 h later, cells were lysed in E1A lysis buffer containing 1% NP-40, 50 mM Tris pH 8.0, 250 mM NaCl, 5 mM EDTA, Complete protease inhibitor cocktail (Roche) for 15 min, 4°C; lysates were cleared by centrifugation in a microcentrifuge (13 000 r.p.m., 10 min, 4°C) and incubated overnight on the wheel with anti-V5 beads (Sigma-Aldrich). Beads were washed with E1A buffer and eluted with Laemmli sample buffer. Lysates and immunoprecipitated proteins were resolved by SDS-PAGE, transferred to nitrocellulose membranes (Whatman) and analyzed by western blot. For other applications, cells were lysed in RIPA buffer containing 10 mM Tris-HCl pH 7.5, 150 mM NaCl, 1% NP-40, 1% sodium deoxycholate, 0.1% SDS, 1 mM EDTA, Halt phosphatase inhibitor cocktail (Thermo Scientific), Complete protease inhibitor cocktail and 250 u/ml Benzonase (Novagen). Protein concentration was measured using Bradford protein assay (Bio-Rad) and normalized using RIPA buffer. Samples were mixed with Laemmli sample buffer, resolved by SDS-page and analyzed by western blot. For purification of recombinant SMPDL3B lacking the C-terminal GPI anchor from HEK293T cells, proteins were immunoprecipitated from cellular supernatants using HA beads (Sigma-Aldrich) and competitively eluted using HA peptide (Sigma-Aldrich). For glycosylation assays, eluted proteins were incubated with PNGaseF (New England BioLabs) according to the manufacturers' instructions and analyzed by western blot.

FACS. HEK293T cells stably expressing murine or human SMPDL3B were stained with mouse monoclonal anti-HA antibodies (Covance) diluted 1:1000 in PBS for 30 minutes at 4°C. Cells were

washed once with PBS and stained with AlexaFluor488 goat anti-mouse secondary antibodies (Invitrogen) diluted 1:1000 in PBS for 30 minutes at 4°C. For TLR4 endocytosis assays RAW264.7 cells or BMDMs were stimulated for the indicated time points with 100 ng/ml LPS. Cells were harvested and stained with anti-TLR4 antibodies for 20 minutes at 4°C. For GM1 staining, RAW264.7 cells were harvested and stained for 15 minutes using 100 ng/ml CTx β -Alexa488. Cy3-CpG-DNA uptake was determined as previously described (Baumann et al., 2010)

Triton X-114 phase separation and PI-PLC sensitivity assays.

3x10⁶ RAW264.7 cells were resuspended in 500 μ l PBS and 100 μ l 6% pre-condensed TX114, mixed by pipetting and lysed for 15 min on ice. Samples were centrifuged for 1 min at 13 000 r.p.m., the supernatants were transferred to new tubes, the pellets, correspond to the insoluble fractions, were resuspended in 200 μ l Laemmli sample buffer. Supernatants were incubated for 5 min at 37°C to induce phase separation and centrifuged for 1 min at 13 000 r.p.m. at room temperature. The upper aqueous phases were transferred to new tubes. To wash, the lower, detergent phase was mixed with 500 μ l PBS, the upper phase with 100 μ l 6% TX114 and incubated for 5 min on ice and for 5 min at 37°C. Samples were centrifuged and the initial phases were kept for further processing. Proteins were precipitated by adding 500 μ l methanol and 125 μ l chloroform to the aqueous and 450 μ l PBS, 500 μ l methanol and 125 μ l chloroform to the detergent phases. Samples were centrifuged for 4 min at 13 000 r.p.m., 750 μ l of the upper phases were removed, 400 μ l methanol was added and mixed by pipetting. Samples were centrifuged again for 1 min at 13 000 r.p.m. and the protein pellets were dried under the chemical hood. Precipitated proteins from the aqueous phase were resuspended in 200 μ l, those from the detergent phase in 50 μ l Laemmli sample buffer. Samples were analyzed by western blot.

To assess sensitivity to PI-PLC, after initial lysis using PBS/TX114 and before phase separation, samples were incubated or not for 30 min on ice with 0.5 u/ml PI-PLC (Invitrogen). Samples were processed as described above and analyzed by western blot. In parallel, 3x10⁶ RAW264.7 cells in 500 μ l PBS were incubated on ice with or without 0.5 u/ml PI-PLC to release GPI-anchored proteins from the cell surface. Cells were centrifuged, the pellet was resuspended directly in 300 μ l sample buffer,

supernatants were precipitated using methanol/chloroform and suspended in 50 µl sample buffer. All samples were analyzed by western blot.

Purification of recombinant murine SMPDL3B from Sf9 insect cells. Recombinant murine SMPDL3B lacking the C-terminal GPI anchor (SMPDL3BΔGPI) was produced using the BAC-TO-BAC baculovirus expression system (Invitrogen) according to the manufacturer's instructions and purified from supernatants of baculovirus-infected Sf9 insect cells. Briefly, 1l serum-free Sf9 insect cell culture at a concentration of 2×10^6 cells/ml were infected by addition of 20 ml p3 virus stock and incubated for 72h at 27°C on the shaker. The serum-free supernatant was cleared by centrifugation and recombinant protein was purified using Ni-NTA-Agarose (Qiagen) according to the manufacturer's instructions. Beads were washed with Buffer A (50 mM Tris/HCl, pH 7.5, 500 mM NaCl, 1mM MgCl₂) and eluted with Buffer A containing 250 mM imidazole. Protein was dialyzed against PBS in a Slide-A-Lyzer Dialysis Cassettes, MWCO 10 kDA (Pierce) and kept at -80°C for further use.

Isolation of detergent resistant membranes (DRMs)

DRMs were isolated using an adapted protocol as described by Brown et al. (Brown, 2002). Briefly, RAW264.7 macrophages were lysed for 20 minutes on ice in 1 ml TNE buffer (25 mM Tris-HCl, 150 mM NaCl, 5 mM EDTA, pH 7.4) containing 1% Triton X-100 and Complete protease inhibitor cocktail (Roche). The lysate was mixed with 1.25 ml TNE buffer containing 80% sucrose and layered on the bottom of a 14 ml ultracentrifugation tube (Beckman Coulter). The sample was carefully overlaid with 7 ml TNE buffer containing 35% sucrose followed by 3.5 ml TNE buffer containing 5% sucrose. The sample was centrifuged overnight at 100.000g at 4°C in an SW40Ti swinging bucket rotor (Beckman Coulter) and 1 ml fractions were collected from the top. Fractions were mixed with Laemmli sample buffer, resolved by SDS-page and analyzed by western blot.

Confocal microscopy and membrane fluidity measurements.

For confocal microscopy of overexpressed, HA-tagged SMPDL3B, HEK293T cells were seeded on fibronectin-coated glass cover slips. 16h later, cells were washed with PBS and either fixed (4% formaldehyde in PBS, 10 min., RT) and permeabilized (0.3% saponin, 10% FCS in PBS, 30 min., RT)

or left untreated. Slides were incubated with anti-HA antibodies (1h, RT), washed and incubated with anti-mouse AlexaFluor488 antibodies (1h, RT). Non-permeabilized samples were washed and fixed with formaldehyde (4% formaldehyde in PBS, 10 min., RT). All samples were incubated with DAPI stain, washed and mounted on cover slips with ProLong Gold (Life Technologies). Images were acquired on a Zeiss LSM700 confocal microscope.

For membrane fluidity measurements 2.5⁵ RAW264.7 cells or primary macrophages were seeded on glass cover slips in 24-well plates and adhered in DMEM (PAA) supplemented with 10% FCS (Invitrogen) and antibiotics (100 U/ml penicillin and 100 µg/ml streptomycin) at 37°C, 5% CO₂. Medium was exchanged with serum-free DMEM and cells were stained with 5 µM di-4-ANEPPDHQ for at least 30 minutes. In case of MβCD extraction, cells were preincubated for 1 hour with 2.5 mM MβCD (Sigma) in serum-free medium and then stained as described above. Coverslips were mounted using ProLong®Gold (Invitrogen), images were acquired on a Zeiss LSM700 confocal microscope. The fluorescent dye was excited at 488 nm and images corresponding to ordered and disordered phase were acquired sequentially. These images were used to calculate generalized polarization (GP) values as previously described (Owen et al., 2012).

Supplemental Figure legends

Figure S1, Related to Figure 1 – SMPDL3B GPI-anchor, glycosylation and expression. (A) Schematic representation of SP-HA expression constructs of SMPDL3B, SMPDL3A and SMPDL1/ASM. (B) HEK293T cells were transfected with the indicated SP-HA-tagged constructs. 48h later, cell lysates and supernatants were analyzed using HA-specific antibodies. (C) Confocal microscopy of non-permeabilized or permeabilized HEK293T cells stably expressing mock or HA-tagged murine SMPDL3B (mSMPDL3B). Blue: DAPI, green: HA. (D) RAW264.7 cells were treated or not with PI-PLC. Cells were lysed in sample buffer; supernatants were precipitated with methanol/chloroform and resuspended in sample buffer. Samples were analyzed by western blot using SMPDL3B, CD14 and $\text{I}\kappa\text{B}\alpha$ -specific antibodies. (E) HEK293T cells were transfected with expression constructs for murine (m) and human (h) SMPDL3B lacking the C-terminal GPI signal (ΔGPI) or murine SMPDL3A. 48 h later, proteins were immunoprecipitated from cell supernatants, eluted using HA peptides and treated or not with PNGase F. Samples were analyzed by western blot using HA-specific antibodies. (F) Western blot of SMPDL3B, CD14 and Tubulin in detergent resistant membrane (DRM) and soluble fractions from RAW264.7 macrophages. (G) BioGPS data for GeneAtlas MOE430 murine dataset, probeset 1417300_at for SMPDL3B. Only tissues with normalized expression > 20 are shown. Red bars highlight expression in macrophages or DCs. (B,D-F) Data are representative of two independent experiments.

Figure S2, Related to Figure 2 - Enhanced secretion of cytokines in the absence of SMPDL3B. (A) BMDMs or BMDCs from wildtype (WT) or *Smpdl3b*-deficient (KO) mice were stimulated with the indicated TLR ligands for 8h and supernatants were analyzed for KC by ELISA. (B) Control (shCTRL) and SMPDL3B-depleted RAW264.7 macrophages were stimulated for the indicated time points with 100 ng/ml LPS. The effect of SMPDL3B depletion on pro-inflammatory cytokine secretion was analyzed by ELISA for IL-6. (C) Control (shCTRL) and SMPDL3B-depleted RAW264.7 macrophages were stimulated for 8h with 5 μM CpG or 5 μM IMQ. The effect of SMPDL3B depletion on pro-inflammatory cytokine secretion was analyzed by ELISA for IL-6. (A-C) Data show mean \pm SD of (A) technical triplicates and (B,C) technical quadruplicates and are representative of at

least two independent experiments. (D,E) TLR4 endocytosis upon stimulation with 100 ng/ml LPS for the indicated time in (D) RAW264.7 cells expressing the indicated shRNAs and (E) wild-type (wt) and *Smpdl3b*-deficient (ko) BMDMs. Diagrams show average mean fluorescence intensity \pm SD of (D) two and (E) three technical replicates. (F) Phagocytosis rates of Cy3-CpG-DNA in RAW264.7 expressing the indicated shRNAs. Data shows mean \pm SD of technical triplicates.

Figure S3, Related to Figure 3 – SMPDL3B enzymatic activity and inducibility. (A) Schematic representation of SMPDL3B-dependent enzymatic cleavage of bis(p-nitrophenyl)phosphate (bis-pNPP) to (p-nitrophenyl)phosphate (pNPP) and p-nitrophenol (pNP). (B) pH dependence of murine and human SMPDL3B produced in HEK293T cells. (C) Measurement of phosphodiesterase activity on HEK293T cells stably expressing an empty vector (mock) or human SMPDL3B. Data shows mean \pm SD of technical triplicates and are representative of two independent experiments. (D) Western blot for HA and Tubulin of HEK293T cells used in (Figure 3D, S3C). (E) RAW264.7 cells were lentivirally transduced with shRNAs for SMPDL3B (sh3B) or control (shCTRL). Knockdown efficiency was analyzed by western blotting for endogenous SMPDL3B and Tubulin. (F) RAW264.7 cells were stimulated with 100 ng/ml LPS, 200 ng/ml Pam3Csk4 (P3C4), 1000 u/ml Ifn γ or the indicated combinations for 16h and SMPDL3B or Actin protein levels were analyzed by western blotting. Data are representative of two independent experiments.

Figure S4, Related to Figure 4 - Lipidomics analysis. (A) CTx β -staining of RAW264.7 cells expressing control (shCTRL) or SMPDL3B-specific (shSMPDL3B) shRNAs. (B) Lipids were extracted from control (shCTRL) or SMPDL3B-depleted (shSMPDL3B) RAW264.7 macrophages and analyzed by MS for glycerophospho- and sphingolipids. Bubble plots represent mean difference between cell lines. SM, sphingomyelin; GluCer, glucosylceramide; Cer, ceramide; PC, (lyso-) phosphatidylcholine; PE, (lyso-) phosphatidylethanolamine; PA, phosphatidic acid; PI, (lyso-) phosphatidylinositol; PS, (lyso-) phosphatidylserine; PG, phosphatidylglycerol. (C) Correlation of difference in normalized lipid concentration between two biological replicates. Only data points significant in both replicates are shown. (D) Relative cellular cholesterol levels in control shRNA-expressing RAW264.7 macrophages (shCTRL) and SMPDL3B-depleted cells (shSMPDL3B). Data

represents mean \pm SEM. (E) Correlation of mean log₂-transformed fold-change differences of lipids (shSMPDL3B/CTRL) mapped with predicted lipid function for LPS- (left) and CpG-induced (right) IL-6 release. (F) Control (shCTRL) and SMPDL3B-depleted (shSMPDL3B) RAW264.7 macrophages were pre-incubated with the indicated ceramides or a vehicle control and then stimulated for 8 hours with LPS (100 ng/ml). Cell viability was assessed by CellTiter-Glo. (G) SMPDL3B-depleted RAW264.7 macrophages were pre-incubated with Cer d18:1/24 ceramide (C24) or a vehicle control (VEH) and then stimulated for 8 hours with CpG (5 μ M) or imiquimod (5 μ M). Supernatants were analyzed for IL-6 by ELISA. (B,C,E) Data is representative of two biological replicates each consisting of 5 technical replicates. (F,G) Data shows mean \pm SD of technical quadruplicates and is representative of at least two independent experiments.

Figure S1, Related to Figure 1 - SMPDL3B GPI-anchor, glycosylation and expression

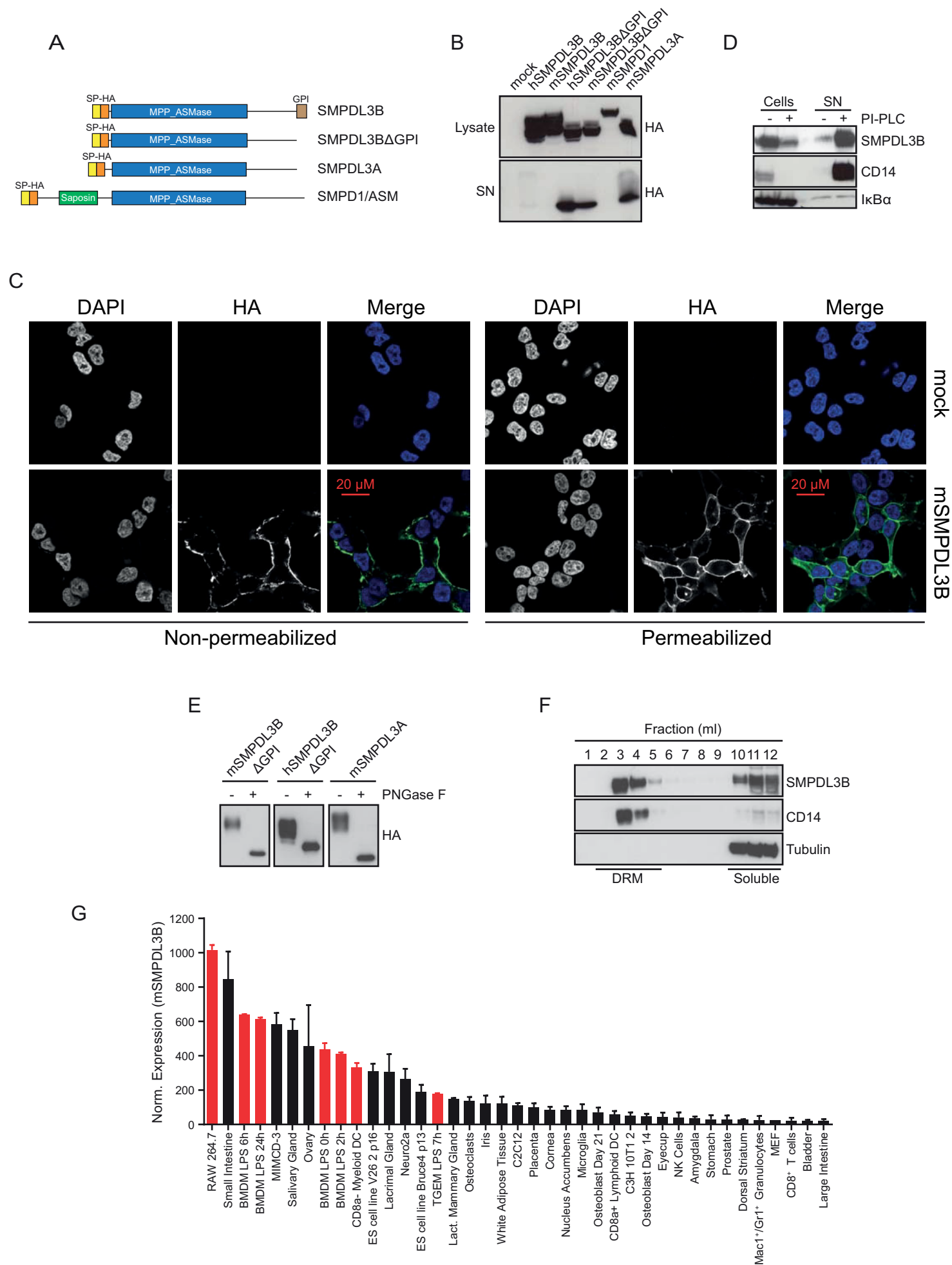


Figure S2, Related to Figure 2 - Enhanced secretion of cytokines in the absence of SMPDL3B

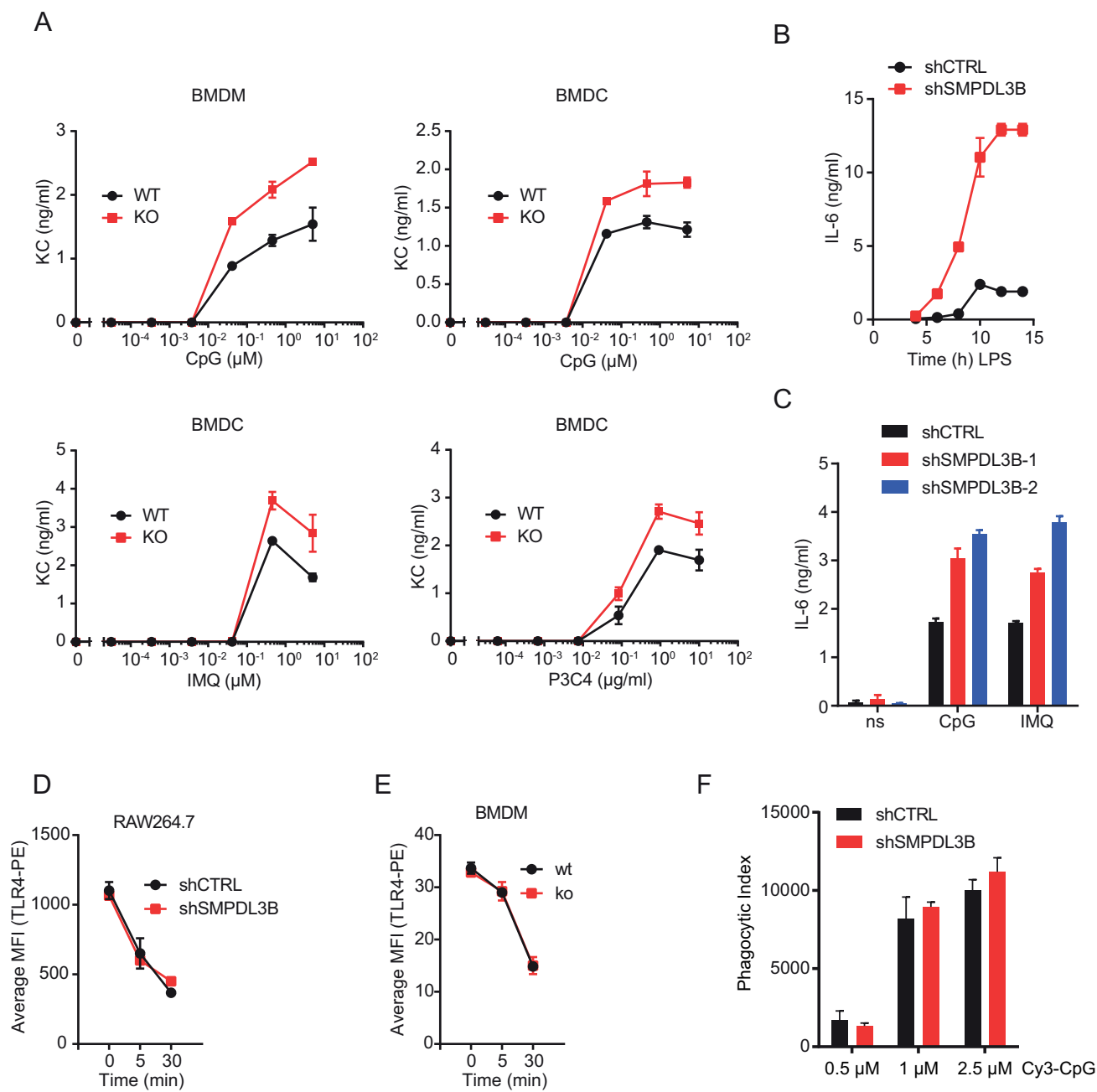


Figure S3, Related to Figure 3 - SMPDL3B enzymatic activity and inducibility

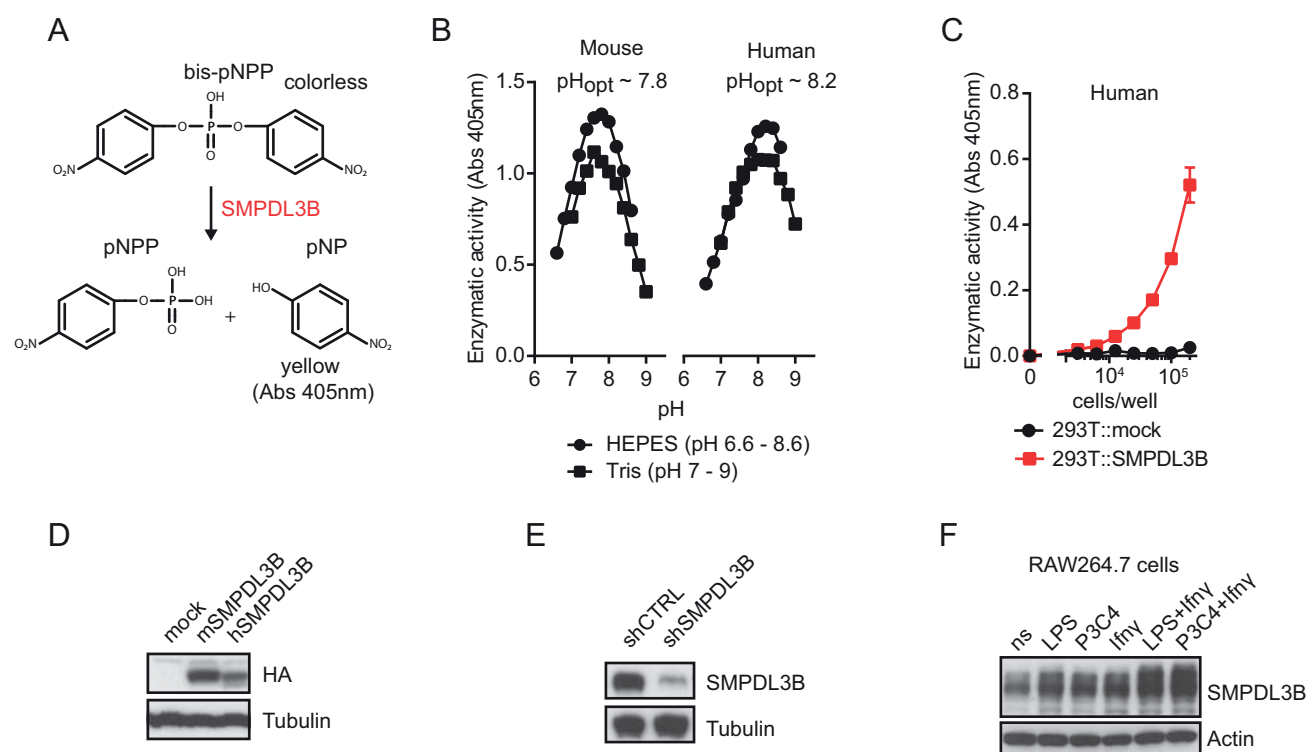
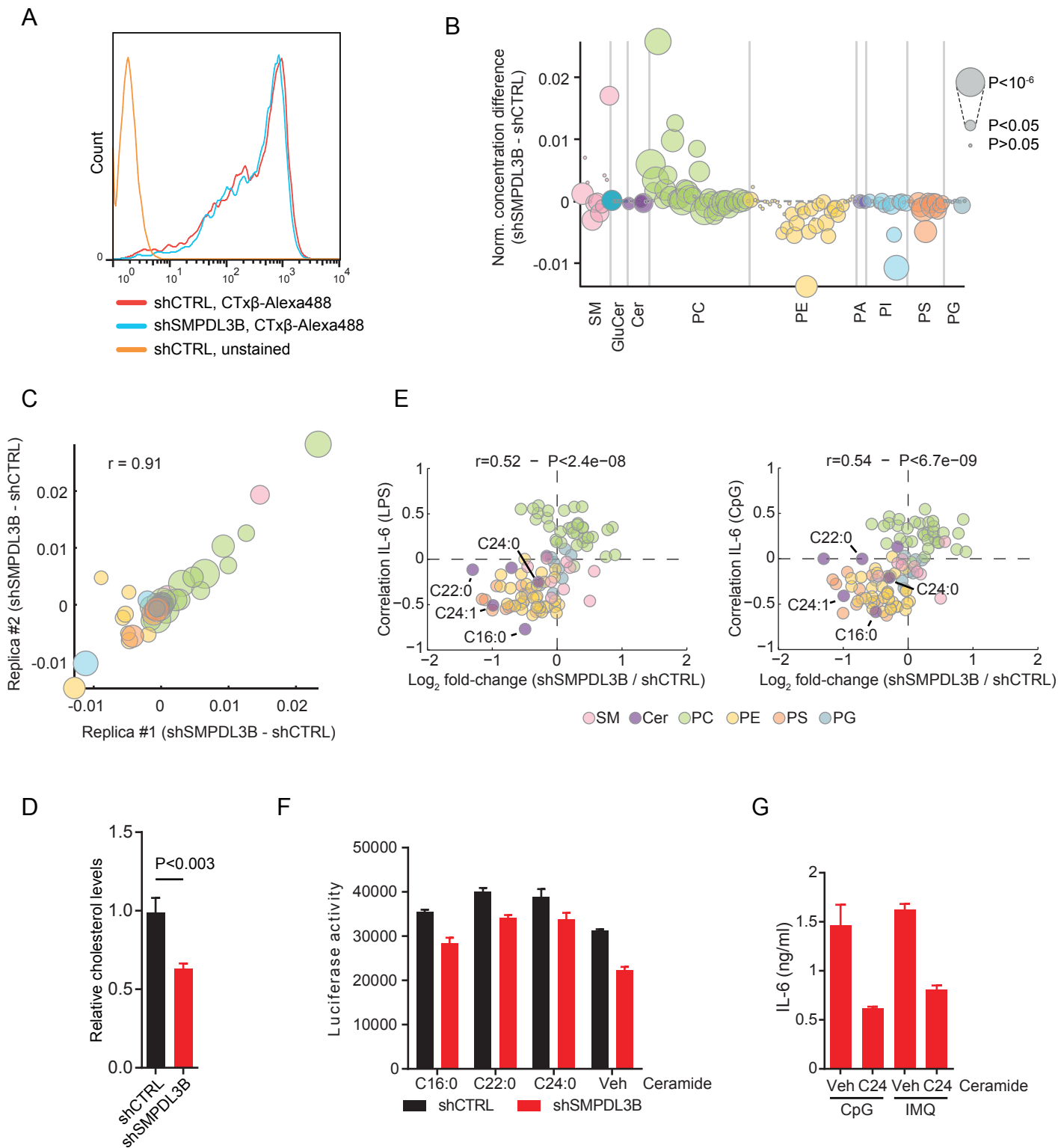


Figure S4, Related to Figure 4 - Lipidomics analysis



Supplemental Tables

Table S1 - Lipidomics analysis of sphingo- and glycerophospholipid species in control and SMPDL3B-depleted RAW264.7 cells, related to Figure 4.

Supplemental References

Baumann, C.L., Aspalter, I.M., Sharif, O., Pichlmair, A., Bluml, S., Grebien, F., Bruckner, M., Pasierbek, P., Aumayr, K., Planyavsky, M., *et al.* (2010). CD14 is a coreceptor of Toll-like receptors 7 and 9. *J Exp Med* 207, 2689-2701.

Brown, D.A. (2002). Isolation and use of rafts. *Curr Protoc Immunol Chapter 11*, Unit 11 10.

Owen, D.M., Rentero, C., Magenau, A., Abu-Siniyeh, A., and Gaus, K. (2012). Quantitative imaging of membrane lipid order in cells and organisms. *Nat Protoc* 7, 24-35.

Wijesinghe, D.S., Subramanian, P., Lamour, N.F., Gentile, L.B., Granado, M.H., Bielawska, A., Szulc, Z., Gomez-Munoz, A., and Chalfant, C.E. (2009). Chain length specificity for activation of cPLA2alpha by C1P: use of the dodecane delivery system to determine lipid-specific effects. *J Lipid Res* 50, 1986-1995.

3. CHAPTER THREE: DISCUSSION

3.1 SUMMARY

This work constitutes a global assessment of the intersection between membrane lipids and TLR-mediated innate immunity signaling. The activity of 20 out of 25 proteins representing important nodes within the sphingolipid network affects TLR function. Characterization of loss-of-function cell lines connected genetic perturbation to TLR4 levels at the PM, receptor endocytosis, and differences in IL-6 transcription and secretion after TLR stimulation. Further, quantitative lipidomics and lipid clustering after systematic perturbation revealed a circular network of coregulated lipids, conserved in mouse and human cells. For the first time, this analysis allowed to decouple the mammalian lipidome from single proteins and to observe lipid dynamics influenced by an entire protein network. Based on this network, lipids predicted to act pro- or anti-inflammatory on TLR signaling could be identified. Further, the inflammatory state of human fibroblasts derived from patients suffering from lipid storage disorders was accurately predicted solely based on their membrane lipid composition, revealing an altered inflammatory response in these cells upon TLR stimulation. In a second, related study, a novel sphingomyelinase-like protein, SMPDL3B, could be identified as a negative regulator of TLR signaling using interaction proteomics and *in vivo* infection models.

3.2 THE CIRCULAR NETWORK OF COREGULATED LIPIDS ADVANCES LIPIDOMICS ANALYSIS

Deciphering thousands of different lipid species inside a cell, their relationships between each other, and functions in different processes, has only become imaginable with the development of mass spectrometry-based lipidomics (Shevchenko & Simons, 2010, Wenk, 2005). However, this developing field is facing several problems that require a clear structure and representation of the data obtained (Snijder, Kandasamy et al., 2014). The main points to address are (1) a unified lipid nomenclature, (2) standardized data processing, and (3) integrated representation of the results. This study provides a unified framework of how to analyze, compare, and represent lipidomics data as a network of lipid coregulation. Another problem arising when comparing lipidomics results is that the general abundance of different

membrane lipids within the cell varies between lipid classes. This prevents the direct comparison of the absolute abundance of lipid species. To enable this comparison, we normalized the abundance of one lipid species to the overall lipid levels per cell line. This way, the fold change of one species could be monitored compared to a control cell line to obtain the relative changes in lipid abundance over all measured lipids. Lipid coregulation was then calculated by comparing the lipid composition across all perturbed cell lines.

3.2.1 *THE CIRCULAR NETWORK REVEALS NEW FEATURES OF LIPID COREGULATION*

Based on our results, the coregulation of lipid species could be plotted as a network in which nodes and edges represent lipids and their coregulation, respectively. In our analysis, the circular network architecture revealed several interesting findings. (1) Lipid coregulation is not limited to lipid classes. Instead, different lipid classes were distributed across the network and closely linked with other lipids classes, indicating that coregulation is an important feature between lipid classes and not only within one class. This finding also supports observations connecting reduction of one lipid class to an increase in another lipid class (Boumann et al., 2006). (2) Sphingolipids and glycerophospholipids are coregulated. Especially sphingomyelin and ceramide species were rather coregulated with glycerophospholipid classes than with each other. Intriguingly, sphingolipids were broadly spread across the circular network and located at those regions of the network that represented connections between glycerophospholipid classes, for example, between PC and PE/PS. This observation illustrates the impact of perturbing sphingolipid metabolism on glycerophospholipids and highlights the close link and metabolic crosstalk between these networks. (3) Lipids with similar chain length properties are coregulated within and between classes. Independent of the lipid class, the circular network of lipid coregulation illustrates that and how lipid species with similar FA chain lengths are coregulated (i.e. PCs; PE and PS). Since the difference in FA chain length is especially important for subcellular localization, this finding shows how lipids comprising different membranes (i.e. PM or ER) are strongly coregulated (van Meer et al., 2008).

3.2.2 *WHY IS LIPID COREGULATION IMPORTANT?*

It is intriguing to speculate that a cell integrates different regulatory feedback mechanisms to coordinate metabolic processes leading to the concerted and efficient synthesis or degradation of lipids required for certain functions. The basis for many biological processes is the fast rearrangement of a large number of lipid molecules; even more than compared to the number of proteins. Hence, lipid coregulation plays an important role in quick adaptations of the cellular lipid landscape. More specifically, there are around 2 – 4 million proteins per cubic micron in a cell (Milo, 2013) and there are approximately 5 million lipid molecules in the same sized area of the PM (Lamond, 2002). The regulation of these large amounts of lipid molecules is controlled by sensing of the lipid composition, trafficking of lipid molecules, and regulation of their biosynthesis. In order to not have to regulate the level of each lipid molecule independently at the expense of energy and time, lipids are coregulated. This way there is a so-called “domino” or ripple effect allowing for an efficient automated lipid rearrangement. Hence, lipid coregulation assures a constant ratio between the thousands of different lipids within a cell. This means, for instance, during cell growth all required lipids are adjusted correctly without creating an imbalanced composition, leading to altered biophysical membrane properties, and thus to malfunctions (Deguil, Pineau et al., 2011). Upon perturbation this coregulatory mechanism also enables a cell to stabilize the ratios between different lipids with similar biophysical and chemical properties, at the expense of fluctuations at the absolute level of different lipids. It is further important that lipid coregulation is the organizing principle also at the subcellular level, as the function of lipids is clearly different depending if they reside in the ER or at the PM (van Meer et al., 2008).

3.2.3 *THE CIRCULAR NETWORK FACILITATES THE IDENTIFICATION OF LIPID FUNCTION*

The discovery of the circular network of lipid coregulation could also facilitate the identification of lipid function in other biological processes. While there are numerous studies on single lipid species and their function in cytokinesis (Atilla-Gokcumen, Muro et al., 2014), autophagy (Singh, Kaushik et al., 2009), apoptosis (Pettus, Chalfant et al., 2002), or receptor regulation the network allows to depict these functions in the context of the lipid landscape. This way different lipid functions are represented, identifying the connected coregulated lipids that potentially have similar functions in these processes. Ideally, each quantifiable read-out should

be coupled to mass spectrometry-based lipidomics to study the relationship between a biological process and the abundance of a lipid species.

3.3 CONSERVATION OF THE METABOLIC NETWORK AND LIPID SPECIES

Lipid metabolism and especially the different building blocks of lipids are highly conserved between yeast and human cells, and large studies in yeast have contributed extensively to our understanding of the lipid metabolic pathways (Guan et al., 2010). Especially the main lipid classes and their structures are identical in most organisms. While yeast and mammalian cells produce their essential FAs using the FA synthase, mammalian cells can also use FAs from the diet and convert them into polyunsaturated FAs, which are further used for the synthesis of arachidonic acid (James, Gibson et al., 2000). Thus mammalian cells have a larger variety of FAs compared to yeast. However, all lipid biosynthesis pathways in yeast and mammalian cells use acetyl-CoA as the universal carbon precursor of lipids. Furthermore, PA, the lipid precursor for all glycerophospholipids is synthesized by attaching two FAs to G3P in both yeast and human (Nielsen, 2009). Other lipid classes are different between yeast and mammalian cells. Sphingomyelin, for example, is not produced in yeast cells, which synthesize other types of sphingolipids (Steiner, Smith et al., 1969). And the most important sterol in yeast is ergosterol while mammalian cells harbor large amounts of cholesterol. The synthesis pathways of these sterol species are nevertheless very similar and also start from the common precursor lanosterol (Goldstein & Brown, 1990).

3.4 REDUNDANCY OF PATHWAYS IN LIPID METABOLISM

In our study, stable knockdown of genes in the sphingolipid metabolic network led to strongly altered and diverse cellular lipid compositions in both sphingolipids and glycerophospholipids, revealing a lack of compensation of these genetic perturbations at the individual lipid level. This lack of compensation is further illustrated by two observations: (1) The severe symptoms associated with lysosomal storage disorders, many of which stem from somatic mutations in genes associated with sphingolipid metabolism (Futerman & van Meer, 2004); and (2), the considerable number of genes in sphingolipid metabolism that are embryonically lethal in mice, including acid ceramidase, the *Sptlc* family, and

glucosylceramidase (Hojjati, Li et al., 2005, Li, Park et al., 2002, Yamashita, Wada et al., 1999). This low capacity to outbalance missing key enzymes of the sphingolipid network can be partially explained by the absence of redundancy within conserved gene families associated with sphingolipid metabolism. Members of the CERS family, for instance, each synthesize a distinct subset of ceramide species (Levy & Futerman, 2010). Along these lines, we observed differential regulation of the function of the three *Ormdl* genes upon TLR signaling, strongly different perturbation phenotypes for the individual family members, and sh:Ormdl1 displaying the overall second strongest perturbed lipid state. All these findings argue against redundancy between the three ORMDL proteins, as suggested elsewhere (Siow & Wattenberg, 2012). This means that, rather than having the same function, these proteins display specialized or opposite roles within the network, which cannot easily be adopted by closely related proteins. Systematic perturbation of the network also showed that the entire sphingolipid system is not easily buffered and cannot compensate these genetic impacts as depletion of a specific gene translated into massive changes in the glycerophospholipid and sphingolipid levels.

3.5 LIPIDS AND TLR SIGNALING – MECHANISMS OF ACTION

As described earlier, several studies identified a role of single lipid species or lipid classes in TLR biology. However, the mechanisms and the global picture of lipid function in these immune processes are still unknown.

3.5.1 LIPIDS AND TLR SIGNALING

A recent report showed that macrophages reduce their TLR response by modulating free cholesterol levels in lipid rafts (Zhu et al., 2010b). This observation provides evidence that a cell can selectively regulate their metabolic processes to change the lipid content of their microdomains and modulate TLR signaling. Sphingomyelin, as one of the most abundant lipids in the PM, but also ceramide, both could act in a similar way and change the membrane composition or fluidity locally to affect signaling of TLRs. We found that TLR activation differentially regulates gene transcription across the sphingolipid metabolic network, with opposite regulation observed for different members of the same gene families (i.e. *Ormdl*, *Cers*, *Smpd*), indicative of a precise level of control. This regulatory system based on lipid metabolism

could provide the cell with a fine-tuning mechanism that mediates the spatio-temporal activation of TLR signaling. Further, the membrane lipid composition could act as a cellular memory device integrating and adapting to signaling events in response to a pathogen over time.

3.5.2 TRANSMEMBRANE RECEPTORS: INTERNALIZATION AND COMPLEX FORMATION

Among the TLRs, most studies have focused on TLR4, its interacting proteins, and the underlying signaling mechanisms. However, the function of the membrane in these processes, or the recruitment mechanisms involving membrane lipids has not been elucidated yet. Recently, the TLR4 dimers together with ceramides have been shown to mobilize into membrane rafts in response to *Helicobacter pylori* infection (Lu, Chen et al., 2012). And a new mechanism of negative regulation of TLR4 involving the recruitment into lipid rafts has also been found. It is mediated by adenylyl cyclase 6 (AC6), whose activation shifts TLR4 endocytosis from a clathrin-mediated to a lipid raft-mediated and caveolin-independent process, accelerating endocytosis and inhibiting downstream signaling (Cai, Du et al., 2013). This means that changes of the lipid composition in the membrane could shift the clathrin-mediated to a lipid raft-mediated endocytosis thereby regulating TLR4 signaling. Recently, TMED7 has been identified as a protein that specifically mediates the sorting of TLR4 into COPII vesicles for the shuttling to the PM (Liaunardy-Jopeace et al., 2014). Interestingly, TMED2, another member of the p24 protein family has been identified to specifically bind to the SM C18:0 species. This binding induces the dimerization of TMED2 and is necessary for the transport function of COPI and COPII vesicles (Contreras et al., 2012). In our data, SM C18:0 is strongly positively correlated with TLR4 surface expression at steady state as well as five minutes after stimulation. These findings suggest that SM C18:0 is important for TLR4 surface expression possibly mediated by the protein-lipid interaction regulating protein transport to the PM.

Several other potential regulatory mechanisms have been found in the context of different transmembrane receptors and are likely to be applicable, to some extent, to TLR signaling as well. The transferrin receptor, for instance, was shown to induce ceramide production upon activation via acid sphingomyelinase. Blocking of the generation of cell surface ceramide resulted in a faster clathrin-independent internalization of the receptor and its recycling was inhibited (Shakor, Atia et al., 2012). This finding identifies a feedback mechanism for the production of ceramides upon receptor activation, which is important for prolonged receptor signaling and recycling. A misbalance between endocytosis and replenishing of the receptor

could thereby result in an increased or diminished signaling. Another mechanism involving ceramides has been identified in a *Cers2* null mouse. These mice, lacking long-chained ceramides, do not internalize the TNFR (TNF α receptor) after stimulation, indicating that the length of the ceramide species in the membrane influences their function in receptor internalization processes (Ali, Fritsch et al., 2013). And in resting T-cells, the T-cell receptor (TCR) interacts with anionic glycerophospholipids at the inner leaflet of the membrane. Upon activation, Ca²⁺ inhibits this lipid binding, thereby exposing phosphorylation sites of the protein, leading to an active TCR-CD3 complex. This feedback mechanism involving membrane lipids has been reported to amplify the signal of the TCR (Shi, Bi et al., 2013).

Another mechanism of action for the function of membrane lipids on TLR signaling could be the assembly of the receptor-signaling complex. It has been shown, for instance, that the ectodomain of TLR4 has a regulatory function by preventing spontaneous receptor dimerization and thus constitutive activation (Panter & Jerala, 2011). Receptor dimerization could also be induced or inhibited by altered lipid composition. TLR dimers are already formed in an unstimulated cell and traffic into lipid rafts upon stimulation. Upon ligand binding the TIR domains of both TLR molecules move closer and thus enable downstream signaling (Triantafilou et al., 2007). The membrane environment could be an important determinant to alter the conformation of the dimer and thus to facilitate the binding of interaction partners. Conversely, the TIR-containing interactors harbor different lipid modifications, which target them to lipid rafts such as the myristoylated TRAM (Nishiya, Kajita et al., 2007).

3.5.3 TLR DOWNSTREAM SIGNALING

Other regulatory mechanisms of membrane lipids in TLR signaling could be direct lipid-protein binding. This has already been described for the C16:0 ceramide species, mediating the activity of atypical protein kinase C ζ (PKC ζ), which is also an important downstream signaling protein of TLRs (Lim, Sutton et al., 2015, Wang, Krishnamurthy et al., 2009). Ceramides have further been described to bind to SET (phosphatase 2A inhibitor), inhibiting its binding to serine/threonine protein phosphatases (PPAs) and thereby activating their enzymatic function. Activation of PP2A, in turn, leads to the dephosphorylation of AKT, which regulates the signaling downstream of TLRs leading to the transcription of inflammatory cytokines (Canals, Roddy et al., 2012, Janssens & Beyaert, 2002). The kinase suppressor of Ras (KSR) is also a direct target of

ceramides and essential for the regulation of TNF α -induced ERK1/2 activation (Zhang, Yao et al., 1997).

As the best-studied lipid-protein interaction downstream of TLR signaling, S1P interacts with the RING domain of TRAF6 enhancing its autoubiquitination function. Interestingly, the kinases ERK1/2 downstream of TLR signaling mediate the phosphorylation of SPHKs, which is necessary for their translocation to the PM and their activation (Pitson, Moretti et al., 2003). This leads to increased intracellular levels of S1P upon stimulation, as has also been demonstrated in inflammatory *in vivo* models possibly forming a positive feedback loop (Snider, Kawamori et al., 2009). However, the exact role of S1P in inflammatory processes has not been identified yet. Some studies reported reduced inflammatory responses in *Sphk1* knockout mice (Baker, Barth et al., 2010) of which one was retracted (Puneet, Yap et al., 2013), which raises concerns and uncertainty about the role of SPHKs in inflammation. Another phosphorylated sphingolipid, Ceramide-1-phosphate (C1P), has been shown to bind specifically to TACE (TNF α converting enzyme) inhibiting its activity and thus the secretion of TNF α (Lamour, Wijesinghe et al., 2011). Exogenously added C1P could reduce the LPS-induced secretion of NF κ B-dependent cytokines by inhibiting the degradation of I κ B and the phosphorylation of the NF κ B subunit p65 in human PBMCs (Hankins, Fox et al., 2011).

Our data shows that perturbations in the sphingolipid metabolism lead to increased or decreased TLR-induced inflammatory responses. Interestingly, the transcriptional expression dynamics of the cytokine *Il6* do not change over time. This suggests that the downstream signaling in the genetically perturbed cell lines is modulated due to altered activity of TLR signaling amplifiers or silencers rather than temporal regulators.

3.5.4 CYTOKINE SECRETION

A recent study on PS and TLR signaling reported that the LPS-induced chemokine release of CXCL10 in THP-1 cells was greatly reduced in the presence of PS C38:4 while IL-1 β -induced cytokine release was not affected. This PS species also inhibited the response upon TLR2 and TLR7 signaling as well as the association of TLR4 with its cofactor CD14 or the microdomain marker GM1, as shown by fluorescence resonance energy transfer (FRET) (Parker et al., 2008). This finding suggests a specificity for PS C38:4 on TLR responses but not on IL-1 β receptor responses. In our work, PS C38:4 was identified to be negatively correlated with TLR-

induced IL-6 release highlighting its role as a negative regulator of TLR-mediated cytokine release.

The PC biosynthetic pathway is also connected to cytokine secretion as mice deficient for *CCT α* , the protein that is involved in the first step of PC synthesis, displayed impaired secretion of TNF α and IL-6 in response to LPS stimulation, as well as altered Golgi morphology. Intracellular staining of these cytokines revealed an accumulation inside the cell, most likely due to a secretory block (Tian, Pate et al., 2008). Interestingly, our work shows that all measured PC species are positively correlated with TLR-induced cytokine secretion suggesting them to be beneficial or even necessary for this process. Furthermore, we could identify the *Cers2* deficient cell line to have a strikingly similar phenotype, also accumulating intracellular IL-6 in the perinuclear region. However, this cell line does not show reduced PC levels but rather strongly reduced ceramide and mildly reduced PG levels, indicating that several lipid classes are important for the secretion of cytokines in response to TLR activation. A potential mechanism explaining these secretory blocks could involve the p110 δ PI3K isoform as it is induced by LPS or IFN γ in macrophages, it depends on a lipid substrate, and is important for membrane fission at the Golgi as loss-of-function cell lines and genetic inactivation in mice showed accumulating TNF α after stimulation (Low, Misaki et al., 2010).

Apart from the transport via the Golgi, vesicle fusion at the PM is also an important step in cytokine secretion that requires membrane lipid rearrangements. LPS stimulation has been shown to induce several components of the SNARE complex such as VAMP-3, which mediate the fusion of vesicles containing cytokines in stimulated cells (Stow, Manderson et al., 2006). TNF α and VAMP-3 have also been shown to colocalize in recycling endosomes and traffic to the PM together (Murray, Kay et al., 2005). And the insertion of endosomal membranes into the PM occurs at the phagocytic cup in a cholesterol-dependent manner (Kay, Murray et al., 2006). However, the secretion of the soluble cytokine IL-6 is independent of phagocytic cups (Manderson et al., 2007), indicating that there are several secretion mechanisms for different cytokines.

3.6 FUTURE PERSPECTIVES

3.6.1 *THE NEXT STEPS*

The work described here represents the first comprehensive characterization of lipid coregulation over a panel of lipid perturbations as well as the inference and validation of lipid function in inflammatory processes *in vitro* and *in vivo*. Further, we propose the circular network of lipid coregulation as a general, comprehensive visualization method to map lipid species and their function. Several avenues of research are now suggested, which build on the framework established here. (1) Extend the quantification to other lipid classes and metabolites. So far only a small part of the thousands of different lipids have been mapped onto the network due to limitations in the detection and quantification methods. As the technology of lipidomics advances we will be able to add more lipid classes and species to the network. Further quantification of other metabolites such as amino acids or sugars should also be included to advance our knowledge of the coregulation of all metabolites within the cell. (2) A time-resolved perturbation model using inducible genetic targeting coupled to lipidomics measurements could be used to elucidate the priority of changes in the lipid composition across the network. Also, drug treatment or serum deprivation over time could be used to interfere with the metabolic processes in the cell. This way the lipid flux across the network could be determined. (3) To further establish the connection of lipid metabolism and inflammation, time-resolved lipidomics over a variety of TLR stimulations and infection models could shed light on the inducible changes in the lipid composition in an inflamed cell. This way the spatio-temporal lipid changes as a response to inflammatory processes could be tracked and mapped onto the network. (4) By measuring other biological processes in the perturbed macrophages we could extend the predictive power of lipid function further, identifying lipids important for many different cellular processes.

3.6.2 *PREDICTION OF THE INFLAMMATORY PHENOTYPE*

Our work describes the powerful tool of predicting the inflammatory response solely based on changes in the lipid composition of cells. For future applications this finding could be pioneering early diagnosis of diseases and predispositions of patients. Of course, the toolset of lipidomics is still very limited due to the costly analysis and specialist training it requires,

however, for clinical purposes, lipidomics analysis and our framework could be an important innovation. In accordance to the genetic profile of a human, the lipid profile is based on the expression of proteins regulating lipid metabolism. Additionally, the lipid composition depends on environmental factors such as lipid uptake and turnover in the individual cell. This means, the lipid composition of a cell is the outcome of gene, protein, and environmental regulation, and thus provides a more downstream read-out of the actual state of the cell, which could be more accurate for the prediction of pathologies. Another important limitation for clinical use is the material needed for lipidomics analysis as, so far, large amounts are required to measure the abundance of lipid species (Chen, Hoene et al., 2013). The detection of biomarkers using lipidomics is currently already being applied in clinical approaches (Gorden, Myers et al., 2015). However, the advancement of single-cell lipidomics could be a groundbreaking method to analyze cells of different tissues and to be able to predict their individual responses.

3.6.3 OPPORTUNITIES FOR TARGETING LIPID METABOLISM IN THE CONTEXT OF INFLAMMATION

While the prediction of a diseased state is the first step in treatment, the second step could be the exploitation of targeting lipid metabolism to modulate the inflammatory response. Our work has shown that the individual lipid composition of a cell greatly impacts on its inflammatory response. Could we alter the lipid composition of a cell using small molecules to fine-tune its inflammatory response? As a prevalent inflammatory disease there is still no effective treatment for sepsis. One of the few available drugs is recombinant human activated protein C, which shows only a modest improvement and is used for a small subset of patients with a low risk for hemorrhage (Ulloa, Brunner et al., 2009). Our results show that changes in lipid composition alter the inflammatory response induced by several different TLRs, a circumstance that is beneficial for the treatment of severe sepsis. Other attractive lipid targets to prevent infections are the glycosphingolipids at the cell surface. These lipids are recognized by many pathogens and used as a signal to enter the cell (Hanada, 2005). The temporal downregulation of these lipids could reduce infections in an acute setting such as the confinement of an epidemic.

Our work further suggests that one mechanism of action of how lipids modulate the inflammatory response is the disruption or stabilization of TLR signaling complexes at the membrane or the assembly of adaptor proteins at the inner leaflet. Targeting these sites could

be an effective way to terminate or enhance inflammatory signaling specifically, without disrupting downstream signaling pathways important for other cellular functions or provoking side effects by targeting master transcription factors (Graversen, Svendsen et al., 2012). Eritoran, for instance, is an LPS mimetic that targets TLR4 antagonistically and prevents downstream signaling, at the same time reducing the side effects compared to other anti-inflammatories (Shirey, Lai et al., 2013). Other small molecule inhibitors were designed to disrupt the TIR-TIR interactions of TLRs and their adaptor proteins, thus acting anti-inflammatory and neuroprotective (Davis, Mann et al., 2006, Piao, Ru et al., 2013).

The unknown mechanism of action for drugs that are already used in the clinics to modulate the immune response could be changing of the lipid composition. The antimalarial drug chloroquine, for example, inhibits TLR9 signaling possibly by modulating the endosomal pH (Kuznik, Bencina et al., 2011). Lipid degradation in the endosome is also strongly pH dependent and could be the mechanism of action of how chloroquine directly reduces TLR function. A lipid mimetic drug already used successfully for therapeutic purposes is fingolimod (FTY720). It mimics sphingosine and can be phosphorylated by SPHK. Subsequently it binds to S1P receptors on immune cells and diminishes the inflammatory response and cell migration. This is especially important for the treatment of multiple sclerosis (Brinkmann, Billich et al., 2010). Even though the main mechanism of action is proposed to be blocking of the S1P receptors, it could be also acting intracellularly by inhibiting the specific interaction of S1P and proteins such as the TRAFs and thereby also downregulating the inflammatory response. Understanding the changes of lipid metabolism and the functional consequences in biological processes is, of course, also important in other disease settings. Lipid metabolism, inflammation, and cancer development are tightly linked, as obesity, for instance, is known to increase the risk of developing a tumor by at least 20% (Santos & Schulze, 2012).

3.7 CONCLUSIONS AND OUTLOOK

Taken together, we have identified the architecture of cellular lipid coregulation, which is conserved between mouse and human. This discovery also lets us propose a new framework for approaching, analyzing, and visualizing lipidomics data. Building on the success of the genomics and proteomics era, we hope to contribute to the advancement of lipidomics analysis and lipid biology. Our work shows that studying lipids and their functions in isolated systems or in ad hoc approaches will not lead to the major answers the field of lipidology is looking for. While the cell

invests energy in the synthesis of lipid species with various FA chains of different lengths, saturation, and hydroxylation it is still unclear how this variety translates into a functional role. To answer these questions and also to advance the knowledge on lipid function inside the cell, more global approaches have to be performed, such as the analysis of large sets of lipids in perturbed systems and their consequences on biological processes. In the future, we hope to be able to characterize a cell not only based on its genotype, proteotype, and phenotype, but also on its “lipotype”. Our work, described here, lays the foundation for deciphering the lipid code that is present in all living cells.

REFERENCES

- Akira S, Hemmi H (2003) Recognition of pathogen-associated molecular patterns by TLR family. *Immunol Lett* 85: 85-95
- Akira S, Takeda K (2004) Toll-like receptor signalling. *Nat Rev Immunol* 4: 499-511
- Aksoy E, Taboubi S, Torres D, Delbauve S, Hachani A, Whitehead MA, Pearce WP, Berenjeno-Martin I, Nock G, Filloux A, Beyaert R, Flamand V, Vanhaesebroeck B (2012) The p110 delta isoform of the kinase PI(3)K controls the subcellular compartmentalization of TLR4 signaling and protects from endotoxic shock. *Nat Immunol* 13: 1045-1054
- Alexander RT, Jaumouille V, Yeung T, Furuya W, Peltekova I, Boucher A, Zasloff M, Orlowski J, Grinstein S (2011) Membrane surface charge dictates the structure and function of the epithelial Na⁺/H⁺ exchanger. *Embo Journal* 30: 679-691
- Ali M, Fritsch J, Zigdon H, Pewzner-Jung Y, Schutze S, Futerman AH (2013) Altering the sphingolipid acyl chain composition prevents LPS/GLN-mediated hepatic failure in mice by disrupting TNFR1 internalization. *Cell Death Dis* 4
- Allen MJ, Myer BJ, Khokher AM, Rushton N, Cox TM (1997) Pro-inflammatory cytokines and the pathogenesis of Gaucher's disease: Increased release of interleukin-6 and interleukin-10. *Qjm-Mon J Assoc Phys* 90: 19-25
- Alley SH, Ces O, Templer RH, Barahona M (2008) Biophysical regulation of lipid biosynthesis in the plasma membrane. *Biophys J* 94: 2938-2954
- Arikketh D, Nelson R, Vance JE (2008) Defining the importance of phosphatidylserine synthase-1 (PSS1) - Unexpected viability of PSS1-deficient mice. *Journal of Biological Chemistry* 283: 12888-12897
- Aronova S, Wedaman K, Aronov PA, Fontes K, Ramos K, Hammock BD, Powers T (2008) Regulation of ceramide biosynthesis by TOR complex 2. *Cell Metab* 7: 148-158
- Ashe KM, Budman E, Bangari DS, Siegel CS, Nietupski JB, Wang B, Desnick RJ, Scheule RK, Leonard JP, Cheng SH, Marshall J (2015) Efficacy of Enzyme and Substrate Reduction Therapy with a Novel Antagonist of Glucosylceramide Synthase for Fabry Disease. *Mol Med* 21: 389-399
- Atilla-Gokcumen GE, Muro E, Relat-Goberna J, Sasse S, Bedigian A, Coughlin ML, Garcia-Manyes S, Eggert US (2014) Dividing Cells Regulate Their Lipid Composition and Localization. *Cell* 156: 428-439
- Avota E, Gulbins E, Schneider-Schaulies S (2011) DC-SIGN Mediated Sphingomyelinase-Activation and Ceramide Generation Is Essential for Enhancement of Viral Uptake in Dendritic Cells. *PLoS Pathog* 7
- Baker DA, Barth J, Chang R, Obeid LM, Gilkeson GS (2010) Genetic sphingosine kinase 1 deficiency significantly decreases synovial inflammation and joint erosions in murine TNF-alpha-induced arthritis. *J Immunol* 185: 2570-9
- Bar J, Linke T, Ferlinz K, Neumann U, Schuchman EH, Sandhoff K (2001) Molecular analysis of acid ceramidase deficiency in patients with Farber disease. *Hum Mutat* 17: 199-209
- Batra A, Pietsch J, Fedke I, Glauben R, Okur B, Stroh T, Zeitz M, Siegmund B (2007) Leptin-dependent toll-like receptor expression and responsiveness in preadipocytes and adipocytes. *Am J Pathol* 170: 1931-1941
- Bauer R, Voelzmann A, Breiden B, Schepers U, Farwanah H, Hahn I, Eckardt F, Sandhoff K, Hoch M (2009) Schlank, a member of the ceramide synthase family controls growth and body fat in *Drosophila*. *Embo J* 28: 3706-16
- Baumann CL, Aspalter IM, Sharif O, Pichlmair A, Bluml S, Grebien F, Bruckner M, Pasierbek P, Aumayr K, Planyavsky M, Bennett KL, Colinge J, Knapp S, Superti-Furga G (2010) CD14 is a coreceptor of Toll-like receptors 7 and 9. *J Exp Med* 207: 2689-2701

- Beard J, Attard GS, Cheetham MJ (2008) Integrative feedback and robustness in a lipid biosynthetic network. *J R Soc Interface* 5: 533-543
- Beeler T, Bacikova D, Gable K, Hopkins L, Johnson C, Slife H, Dunn T (1998) The *Saccharomyces cerevisiae* TSC10/YBR265w gene encoding 3-ketosphinganine reductase is identified in a screen for temperature-sensitive suppressors of the *Ca*²⁺-sensitive *csg2* Delta mutant. *Journal of Biological Chemistry* 273: 30688-30694
- Bevers EM, Comfurius P, Dekkers DWC, Zwaal RFA (1999) Lipid translocation across the plasma membrane of mammalian cells. *Bba-Mol Cell Biol L* 1439: 317-330
- Blott EJ, Griffiths GM (2002) Secretory lysosomes. *Nat Rev Mol Cell Bio* 3: 122-131
- Bohdanowicz M, Grinstein S (2013) Role of Phospholipids in Endocytosis, Phagocytosis, and Macropinocytosis. *Physiological reviews* 93: 69-106
- Bonham KS, Orzalli MH, Hayashi K, Wolf AI, Glanemann C, Weninger W, Iwasaki A, Knipe DM, Kagan JC (2014) A promiscuous lipid-binding protein diversifies the subcellular sites of toll-like receptor signal transduction. *Cell* 156: 705-16
- Botelho RJ, Teruel M, Dierckman R, Anderson R, Wells A, York JD, Meyer T, Grinstein S (2000) Localized biphasic changes in phosphatidylinositol-4,5-bisphosphate at sites of phagocytosis. *Journal of Cell Biology* 151: 1353-1367
- Botos I, Segal DM, Davies DR (2011) The Structural Biology of Toll-like Receptors. *Structure* 19: 447-459
- Boumann HA, Gubbens J, Koorengel MC, Oh CS, Martin CE, Heck AJR, Patton-Vogt J, Henry SA, de Kruijff B, de Kroon AIPM (2006) Depletion of phosphatidylcholine in yeast induces shortening and increased saturation of the lipid acyl chains: Evidence for regulation of intrinsic membrane curvature in a eukaryote. *Molecular biology of the cell* 17: 1006-1017
- Brash AR (2001) Arachidonic acid as a bioactive molecule. *J Clin Invest* 107: 1339-1345
- Breslow DK, Collins SR, Bodenmiller B, Aebersold R, Simons K, Shevchenko A, Ejsing CS, Weissman JS (2010) Orm family proteins mediate sphingolipid homeostasis. *Nature* 463: 1048-U65
- Breslow DK, Weissman JS (2010) Membranes in Balance: Mechanisms of Sphingolipid Homeostasis. *Molecular cell* 40: 267-279
- Bretscher MS, Munro S (1993) Cholesterol and the Golgi-Apparatus. *Science* 261: 1280-1281
- Brinkmann V, Billich A, Baumruker T, Heining P, Schmouder R, Francis G, Aradhye S, Burtin P (2010) Fingolimod (FTY720): discovery and development of an oral drug to treat multiple sclerosis (vol 9, pg 883, 2010). *Nat Rev Drug Discov* 9
- Brown MS, Goldstein JL (2009) Cholesterol feedback: from Schoenheimer's bottle to Scap's MELADL (vol 50, pg S15, 2009). *J Lipid Res* 50: 1255-1255
- Brügger B, Sandhoff R, Wegehingel S, Gorgas K, Malsam J, Helms JB, Lehmann WD, Nickel W, Wieland FT (2000) Evidence for segregation of sphingomyelin and cholesterol during formation of COPI-coated vesicles. *Journal of Cell Biology* 151: 507-517
- Bruni A, Bigon E, Battistella A, Boarato E, Mietto L, Toffano G (1984) Lysophosphatidylserine as Histamine Releaser in Mice and Rats. *Agents Actions* 14: 619-625
- Cai W, Du AL, Feng K, Zhao XN, Qian L, Ostrom RS, Xu CF (2013) Adenylyl Cyclase 6 Activation Negatively Regulates TLR4 Signaling through Lipid Raft-Mediated Endocytosis. *J Immunol* 191: 6093-6100
- Canals D, Roddy P, Hannun YA (2012) Protein Phosphatase 1 alpha Mediates Ceramide-induced ERM Protein Dephosphorylation A NOVEL MECHANISM INDEPENDENT OF PHOSPHATIDYLINOSITOL 4, 5-BIPHOSPHATE (PIP2) AND MYOSIN/ERM PHOSPHATASE. *Journal of Biological Chemistry* 287: 10145-10155
- Casal E, Federici L, Zhang W, Fernandez-Recio J, Priego EM, Miguel RN, DuHadaway JB, Prendergast GC, Luisi BF, Laue ED (2006) The crystal structure of the BAR domain from human Bin1/Amphiphysin II and its implications for molecular recognition. *Biochemistry-Us* 45: 12917-12928

- Causeret C, Geeraert L, Van der Hoeven G, Mannaerts GP, Van Veldhoven PP (2000) Further characterization of rat dihydroceramide desaturase: Tissue distribution, subcellular localization, and substrate specificity. *Lipids* 35: 1117-1125
- Chakraborty M, Lou CX, Huan CM, Kuo MS, Park TS, Cao GQ, Jiang XC (2013) Myeloid cell-specific serine palmitoyltransferase subunit 2 haploinsufficiency reduces murine atherosclerosis. *J Clin Invest* 123: 1784-1797
- Chang TY, Chang CCY, Ohgami N, Yamauchi Y (2006) Cholesterol sensing, trafficking, and esterification. *Annu Rev Cell Dev Bi* 22: 129-157
- Chang ZQ, Lee SY, Kim HJ, Kim JR, Kim SJ, Hong IK, Oh BC, Choi CS, Goldberg IJ, Park TS (2011) Endotoxin activates de novo sphingolipid biosynthesis via nuclear factor kappa B-mediated upregulation of Sptlc2. *Prostaglandins Other Lipid Mediat* 94: 44-52
- Chen SL, Hoene M, Li J, Li YJ, Zhao XJ, Haring HU, Schleicher ED, Weigert C, Xu GW, Lehmann R (2013) Simultaneous extraction of metabolome and lipidome with methyl tert-butyl ether from a single small tissue sample for ultra-high performance liquid chromatography/mass spectrometry. *J Chromatogr A* 1298: 9-16
- Chiba N, Masuda A, Yoshikai Y, Matsuguchi T (2007) Ceramide inhibits LPS-Induced production of IL-5,, IL-10,, and IL-13 from mast cells. *J Cell Physiol* 213: 126-136
- Choi JW, Lee CW, Chun J (2008) Biological roles of lysophospholipid receptors revealed by genetic null mice: An update. *Bba-Mol Cell Biol L* 1781: 531-539
- Ciesielski F, Griffin DC, Rittig M, Moriyon I, Bonev BB (2013) Interactions of lipopolysaccharide with lipid membranes, raft models - A solid state NMR study. *Bba-Biomembranes* 1828: 1731-1742
- Claus RA, Bunck AC, Bockmeyer CL, Brunkhorst FM, Losche W, Kinscherf R, Deigner HP (2005) Role of increased sphingomyelinase activity in apoptosis and organ failure of patients with severe sepsis. *Faseb Journal* 19: 1719-+
- Contreras FX, Ernst AM, Haberkant P, Bjorkholm P, Lindahl E, Gonen B, Tischler C, Elofsson A, von Heijne G, Thiele C, Pepperkok R, Wieland F, Brugger B (2012) Molecular recognition of a single sphingolipid species by a protein's transmembrane domain. *Nature* 481: 525-529
- Cornell RB, Goldfine H (1983) The coordination of sterol and phospholipid synthesis in cultured myogenic cells. Effect of cholesterol synthesis inhibition on the synthesis of phosphatidylcholine. *Biochim Biophys Acta* 750: 504-20
- Coskun U, Simons K (2011) Cell membranes: the lipid perspective. *Structure* 19: 1543-8
- D'Angelo G, Polishchuk E, Di Tullio G, Santoro M, Di Campli A, Godi A, West G, Bielawski J, Chuang CC, van der Spoel AC, Platt FM, Hannun YA, Polishchuk R, Mattjus P, De Matteis MA (2007) Glycosphingolipid synthesis requires FAPP2 transfer of glucosylceramide. *Nature* 449: 62-U43
- Davis CN, Mann E, Behrens MM, Gaidarova S, Rebek M, Rebek J, Bartfai T (2006) MyD88-dependent and -independent signaling by IL-1 in neurons probed by bifunctional toll/IL-1 receptor domain/BB-loop mimetics. *Proc Natl Acad Sci U S A* 103: 2953-2958
- De Francesco PN, Mucci JM, Ceci R, Fossati CA, Rozenfeld PA (2013) Fabry disease peripheral blood immune cells release inflammatory cytokines: Role of globotriaosylceramide. *Mol Genet Metab* 109: 93-99
- De Nardo D, Labzin LI, Kono H, Seki R, Schmidt SV, Beyer M, Xu DK, Zimmer S, Lahrmann C, Schildberg FA, Vogelhuber J, Kraut M, Ulas T, Kerkisiek A, Krebs W, Bode N, Grebe A, Fitzgerald ML, Hernandez NJ, Williams BRG et al. (2014) High-density lipoprotein mediates anti-inflammatory reprogramming of macrophages via the transcriptional regulator ATF3. *Nat Immunol* 15: 152-160
- Degroote S, Wolthoorn J, van Meer G (2004) The cell biology of glycosphingolipids. *Semin Cell Dev Biol* 15: 375-387
- Deguil J, Pineau L, Rowland Snyder EC, Dupont S, Beney L, Gil A, Frapper G, Ferreira T (2011) Modulation of lipid-induced ER stress by fatty acid shape. *Traffic* 12: 349-62

- Dennis EA (2006) The LIPID MAPS approach to eicosanoid lipidomics. *Prostaglandins Other Lipid Mediat* 79: 144-144
- Dennis EA, Deems RA, Harkewicz R, Quehenberger O, Brown HA, Milne SB, Myers DS, Glass CK, Hardiman G, Reichart D, Merrill AH, Sullards MC, Wang E, Murphy RC, Raetz CRH, Garrett TA, Guan ZQ, Ryan AC, Russell DW, McDonald JG et al. (2010) A Mouse Macrophage Lipidome. *Journal of Biological Chemistry* 285: 39976-39985
- Desfarges L, Durrens P, Juguelin H, Cassagne C, Bonneu M, Aigle M (1993) Yeast Mutants Affected in Viability Upon Starvation Have a Modified Phospholipid-Composition. *Yeast* 9: 267-277
- Devaux PF (1991) Static and Dynamic Lipid Asymmetry in Cell-Membranes. *Biochemistry-Us* 30: 1163-1173
- Di Paolo G, De Camilli P (2006) Phosphoinositides in cell regulation and membrane dynamics. *Nature* 443: 651-657
- Dickson RC, Lester RL, Nagiec MM (2000) Serine palmitoyltransferase. *Sphingolipid Metabolism and Cell Signaling, Pt A* 311: 3-9
- Dickson RC, Sumanasekera C, Lester RL (2006) Functions and metabolism of sphingolipids in *Saccharomyces cerevisiae*. *Prog Lipid Res* 45: 447-465
- dos Santos AXD, Riezman I, Aguilera-Romero MA, David F, Piccolis M, Loewith R, Schaad O, Riezman H (2014) Systematic lipidomic analysis of yeast protein kinase and phosphatase mutants reveals novel insights into regulation of lipid homeostasis. *Molecular biology of the cell* 25: 3234-3246
- Eder C (2009) Mechanisms of interleukin-1 beta release. *Immunobiology* 214: 543-553
- Ejsing CS, Sampaio JL, Surendranath V, Duchoslav E, Ekroos K, Klemm RW, Simons K, Shevchenko A (2009) Global analysis of the yeast lipidome by quantitative shotgun mass spectrometry. *Proc Natl Acad Sci U S A* 106: 2136-2141
- Endres NF, Das R, Smith AW, Arkhipov A, Kovacs E, Huang YJ, Pelton JG, Shan YB, Shaw DE, Wemmer DE, Groves JT, Kuriyan J (2013) Conformational Coupling across the Plasma Membrane in Activation of the EGF Receptor. *Cell* 152: 543-556
- Erridge C, Webb DJ, Spickett CM (2007) Toll-like receptor 4 signalling is neither sufficient nor required for oxidised phospholipid mediated induction of interleukin-8 expression. *Atherosclerosis* 193: 77-85
- Espenshade PJ, Hughes AL (2007) Regulation of sterol synthesis in eukaryotes. *Annu Rev Genet* 41: 401-427
- Fairn GD, Schieber NL, Ariotti N, Murphy S, Kuerschner L, Webb RI, Grinstein S, Parton RG (2011) High-resolution mapping reveals topologically distinct cellular pools of phosphatidylserine. *Journal of Cell Biology* 194: 257-275
- Famili I, Forster J, Nielson J, Palsson BO (2003) *Saccharomyces cerevisiae* phenotypes can be predicted by using constraint-based analysis of a genome-scale reconstructed metabolic network. *Proc Natl Acad Sci U S A* 100: 13134-13139
- Fantini J, Barrantes FJ (2009) Sphingolipid/cholesterol regulation of neurotransmitter receptor conformation and function. *Bba-Biomembranes* 1788: 2345-2361
- Feng B, Yao PM, Li Y, Devlin CM, Zhang D, Harding HP, Sweeney M, Rong JX, Kuriakose G, Fisher EA, Marks AR, Ron D, Tabas I (2003) The endoplasmic reticulum is the site of cholesterol-induced cytotoxicity in macrophages. *Nature cell biology* 5: 781-92
- Fensom AH, Neville BRG, Moser AE, Benson PF, Moser HW, Dulaney JT (1979) Prenatal Diagnosis of Farbers Disease. *Lancet* 2: 990-992
- Fessler MB, Parks JS (2011) Intracellular Lipid Flux and Membrane Microdomains as Organizing Principles in Inflammatory Cell Signaling. *J Immunol* 187: 1529-1535
- Flieger O, Engling A, Bucala R, Lue HQ, Nickel W, Bernhagen J (2003) Regulated secretion of macrophage migration inhibitory factor is mediated by a non-classical pathway involving an ABC transporter. *FEBS Lett* 551: 78-86

- Foster WJ, Janmey PA (2001) The distribution of polyphosphoinositides in lipid films. *Biophys Chem* 91: 211-218
- Friedrichson T, Kurzchalia TV (1998) Microdomains of GPI-anchored proteins in living cells revealed by crosslinking. *Nature* 394: 802-805
- Fritz JH, Ferrero RL, Philpott DJ, Girardin SE (2006) Nod-like proteins in immunity, inflammation and disease. *Nat Immunol* 7: 1250-1257
- Futerman AH, van Meer G (2004) The cell biology of lysosomal storage disorders. *Nat Rev Mol Cell Bio* 5: 554-565
- Gault CR, Obeid LM, Hannun YA (2010) An Overview of Sphingolipid Metabolism: From Synthesis to Breakdown. *Adv Exp Med Biol* 688: 1-23
- Gay NJ, Symmons MF, Gangloff M, Bryant CE (2014) Assembly and localization of Toll-like receptor signalling complexes. *Nature Reviews Immunology* 14: 546-558
- Gijon MA, Riekhof WR, Zarini S, Murphy RC, Voelker DR (2008) Lysophospholipid Acyltransferases and Arachidonate Recycling in Human Neutrophils. *Journal of Biological Chemistry* 283: 30235-30245
- Godi A, Di Campli A, Konstantakopoulos A, Di Tullio G, Alessi DR, Kular GS, Daniele T, Marra P, Lucocq JM, De Matteis MA (2004) FAPPs control Golgi-to-cell-surface membrane traffic by binding to ARF and PtdIns(4)P. *Nature cell biology* 6: 393-+
- Goldstein JL, Brown MS (1990) Regulation of the Mevalonate Pathway. *Nature* 343: 425-430
- Gombert AK, Moreira dos Santos M, Christensen B, Nielsen J (2001) Network identification and flux quantification in the central metabolism of *Saccharomyces cerevisiae* under different conditions of glucose repression. *J Bacteriol* 183: 1441-51
- Goodwin RG, Lupton S, Schmierer A, Hjerrild KJ, Jerzy R, Clevenger W, Gillis S, Cosman D, Namen AE (1989) Human Interleukin-7 - Molecular-Cloning and Growth-Factor Activity on Human and Murine B-Lineage Cells. *Proc Natl Acad Sci U S A* 86: 302-306
- Gorden DL, Myers DS, Ivanova PT, Fahy E, Maurya MR, Gupta S, Min J, Spann NJ, McDonald JG, Kelly SL, Duan JJ, Sullards MC, Leiker TJ, Barkley RM, Quehenberger O, Armando AM, Milne SB, Mathews TP, Armstrong MD, Li CJ et al. (2015) Biomarkers of NAFLD progression: a lipidomics approach to an epidemic. *J Lipid Res* 56: 722-736
- Gowda S, Yeang C, Wadgaonkar S, Anjum F, Grinkina N, Cutaia M, Jiang XC, Wadgaonkar R (2011) Sphingomyelin synthase 2 (SMS2) deficiency attenuates LPS-induced lung injury. *Am J Physiol-Lung C* 300: L430-L440
- Grabowski GA (2008) Lysosomal storage disease 1 - Phenotype, diagnosis, and treatment of Gaucher's disease. *Lancet* 372: 1263-1271
- Graversen JH, Svendsen P, Dagnaes-Hansen F, Dal J, Anton G, Etzerodt A, Petersen MD, Christensen PA, Moller HJ, Moestrup SK (2012) Targeting the Hemoglobin Scavenger receptor CD163 in Macrophages Highly Increases the Anti-inflammatory Potency of Dexamethasone. *Mol Ther* 20: 1550-1558
- Guan XL, Riezman I, Wenk MR, Riezman H (2010) Yeast Lipid Analysis and Quantification by Mass Spectrometry. *Method Enzymol* 470: 369-391
- Guan XL, Souza CM, Pichler H, Dewhurst G, Schaad O, Kajiwarra K, Wakabayashi H, Ivanova T, Castillon GA, Piccolis M, Abe F, Loewith R, Funato K, Wenk MR, Riezman H (2009) Functional Interactions between Sphingolipids and Sterols in Biological Membranes Regulating Cell Physiology. *Molecular biology of the cell* 20: 2083-2095
- Gulshan K, Brubaker G, Wang SH, Hazen SL, Smith JD (2013) Sphingomyelin Depletion Impairs Anionic Phospholipid Inward Translocation and Induces Cholesterol Efflux. *Journal of Biological Chemistry* 288: 37166-37179
- Hakomori S (2000) Traveling for the glycosphingolipid path. *Glycoconjugate J* 17: 627-647
- Han SM, Lone MA, Schreiner R, Chang A (2010) Orm1 and Orm2 are conserved endoplasmic reticulum membrane proteins regulating lipid homeostasis and protein quality control. *Proc Natl Acad Sci U S A* 107: 5851-5856

- Han XL, Gross RW (2005) Shotgun lipidomics: Electrospray ionization mass spectrometric analysis and quantitation of cellular lipidomes directly from crude extracts of biological samples. *Mass Spectrom Rev* 24: 367-412
- Hanada K (2005) Sphingolipids in infectious diseases. *Jpn J Infect Dis* 58: 131-148
- Hanada K (2014) Co-evolution of sphingomyelin and the ceramide transport protein CERT (vol 1841, pg 704, 2014). *Bba-Mol Cell Biol L* 1841: 1561-1562
- Hanada K, Kumagai K, Yasuda S, Miura Y, Kawano M, Fukasawa M, Nishijima M (2003) Molecular machinery for non-vesicular trafficking of ceramide. *Nature* 426: 803-809
- Hancock JF, Paterson H, Marshall CJ (1990) A Polybasic Domain or Palmitoylation Is Required in Addition to the Caax Motif to Localize P21ras to the Plasma-Membrane. *Cell* 63: 133-139
- Hankins HM, Baldrige RD, Xu P, Graham TR (2015) Role of Flippases, Scramblases and Transfer Proteins in Phosphatidylserine Subcellular Distribution. *Traffic* 16: 35-47
- Hankins JL, Fox TE, Barth BM, Unrath KA, Kester M (2011) Exogenous ceramide-1-phosphate reduces lipopolysaccharide (LPS)-mediated cytokine expression. *J Biol Chem* 286: 44357-66
- Hannun YA, Obeid LM (2008) Principles of bioactive lipid signalling: lessons from sphingolipids. *Nat Rev Mol Cell Bio* 9: 139-150
- Harder T, Rentero C, Zech T, Gaus K (2007) Plasma membrane segregation during T cell activation: probing the order of domains. *Curr Opin Immunol* 19: 470-475
- Harikumar KB, Yester JW, Surace MJ, Oyeniran C, Price MM, Huang WC, Hait NC, Allegood JC, Yamada A, Kong XQ, Lazear HM, Bhardwaj R, Takabe K, Diamond MS, Luo C, Milstien S, Spiegel S, Kordula T (2014) K63-linked polyubiquitination of transcription factor IRF1 is essential for IL-1-induced production of chemokines CXCL10 and CCL5. *Nat Immunol* 15: 231-238
- Heinz LX, Baumann CL, Köberlin MS, Snijder B, Gawish R, Shui GH, Sharif O, Aspalter IM, Muller AC, Kandasamy RK, Breitwieser FP, Pichlmair A, Bruckner M, Rebsamen M, Bluml S, Karonitsch T, Fauster A, Colinge J, Bennett KL, Knapp S et al. (2015) The Lipid-Modifying Enzyme SMPDL3B Negatively Regulates Innate Immunity. *Cell reports* 11: 1919-1928
- Henneberry AL, Wright MM, McMaster CR (2002) The major sites of cellular phospholipid synthesis and molecular determinants of fatty acid and lipid head group specificity. *Molecular biology of the cell* 13: 3148-3161
- Herrgard MJ, Lee BS, Portnoy V, Palsson BO (2006) Integrated analysis of regulatory and metabolic networks reveals novel regulatory mechanisms in *Saccharomyces cerevisiae*. *Genome Res* 16: 627-35
- Hla T, Lee MJ, Ancellin N, Paik JH, Kluk MJ (2001) Lysophospholipids - Receptor revelations. *Science* 294: 1875-1878
- Hojjati MR, Li ZQ, Jiang XC (2005) Serine palmitoyl-CoA transferase (SPT) deficiency and sphingolipid levels in mice. *Bba-Mol Cell Biol L* 1737: 44-51
- Hruska KS, LaMarca ME, Scott CR, Sidransky E (2008) Gaucher disease: Mutation and polymorphism spectrum in the glucocerebrosidase gene (GBA). *Hum Mutat* 29: 567-583
- Hui SW, Stewart TP, Yeagle PL, Albert AD (1981) Bilayer to Non-Bilayer Transition in Mixtures of Phosphatidylethanolamine and Phosphatidylcholine - Implications for Membrane-Properties. *Arch Biochem Biophys* 207: 227-240
- Huitema K, van den Dikkenberg J, Brouwers JF, Holthuis JC (2004) Identification of a family of animal sphingomyelin synthases. *Embo J* 23: 33-44
- Husebye H, Aune MH, Stenvik J, Samstad E, Skjeldal F, Halaas O, Nilsen NJ, Stenmark H, Latz E, Lien E, Mollnes TE, Bakke O, Espevik T (2010) The Rab11a GTPase Controls Toll-like Receptor 4-Induced Activation of Interferon Regulatory Factor-3 on Phagosomes. *Immunity* 33: 583-596
- Hynes RO (2002) Integrins: Bidirectional, allosteric signaling machines. *Cell* 110: 673-687
- Ichikawa S, Hirabayashi Y (1998) Glucosylceramide synthase and glycosphingolipid synthesis. *Trends Cell Biol* 8: 198-202

- Imai A, Gershengorn MC (1987) Regulation by Phosphatidylinositol of Rat Pituitary Plasma-Membrane and Endoplasmic-Reticulum Phosphatidylinositol Synthase Activities - a Mechanism for Activation of Phosphoinositide Resynthesis during Cell Stimulation. *Journal of Biological Chemistry* 262: 6457-6459
- Introne W, Boissy RE, Gahl WA (1999) Clinical, molecular, and cell biological aspects of Chediak-Higashi syndrome. *Mol Genet Metab* 68: 283-303
- Itoh T, De Camilli P (2006) BAR, F-BAR (EFC) and ENTH/ANTH domains in the regulation of membrane-cytosol interfaces and membrane curvature. *Bba-Mol Cell Biol L* 1761: 897-912
- James MJ, Gibson RA, Cleland LG (2000) Dietary polyunsaturated fatty acids and inflammatory mediator production. *Am J Clin Nutr* 71: 343s-348s
- Janeway CA, Medzhitov R (2002) Innate immune recognition. *Annu Rev Immunol* 20: 197-216
- Janssens S, Beyaert R (2002) A universal role for MyD88 in TLR/IL-1R-mediated signaling. *Trends Biochem Sci* 27: 474-482
- Jenkins RW, Clarke CJ, Canals D, Snider AJ, Gault CR, Heffernan-Stroud L, Wu BX, Simbari F, Roddy P, Kitatani K, Obeid LM, Hannun YA (2011) Regulation of CC Ligand 5/RANTES by Acid Sphingomyelinase and Acid Ceramidase. *Journal of Biological Chemistry* 286: 13292-13303
- Jo SH, Kim SD, Kim JM, Lee HY, Lee SY, Shim JW, Yun J, Im DS, Bae YS (2008) Lysophosphatidylglycerol stimulates chemotactic migration in human natural killer cells. *Biochem Biophys Res Commun* 372: 147-151
- Johnson KR, Johnson KY, Becker KP, Bielawski J, Mao CG, Obeid LM (2003) Role of human sphingosine-1-phosphate phosphatase 1 in the regulation of intra- and extracellular sphingosine-1-phosphate levels and cell viability. *Journal of Biological Chemistry* 278: 34541-34547
- Jülicher F, Lipowsky R (1993) Domain-Induced Budding of Vesicles. *Phys Rev Lett* 70: 2964-2967
- Kagan JC, Medzhitov R (2006) Phosphoinositide-mediated adaptor recruitment controls toll-like receptor signaling. *Cell* 125: 943-955
- Kawai T, Akira S (2010) The role of pattern-recognition receptors in innate immunity: update on Toll-like receptors. *Nat Immunol* 11: 373-384
- Kawasaki K, Kuge O, Yamakawa Y, Nishijima M (2001) Purification of phosphatidylglycerophosphate synthase from Chinese hamster ovary cells. *Biochemical Journal* 354: 9-15
- Kawasaki T, Kawai T (2014) Toll-like receptor signaling pathways. *Front Immunol* 5: 461
- Kay JG, Murray RZ, Pagan JK, Stow JL (2006) Cytokine secretion via cholesterol-rich lipid raft-associated SNAREs at the phagocytic cup. *Journal of Biological Chemistry* 281: 11949-11954
- Kell DB, Oliver SG (2004) Here is the evidence, now what is the hypothesis? The complementary roles of inductive and hypothesis-driven science in the post-genomic era. *Bioessays* 26: 99-105
- Kihara A (2014) Sphingosine 1-phosphate is a key metabolite linking sphingolipids to glycerophospholipids. *Biochim Biophys Acta* 1841: 766-72
- Kim YM, Brinkmann MM, Paquet ME, Ploegh HL (2008) UNC93B1 delivers nucleotide-sensing toll-like receptors to endolysosomes. *Nature* 452: 234-U80
- Kitatani K, Sheldon K, Anelli V, Jenkins RW, Sun Y, Grabowski GA, Obeid LM, Hannun YA (2009) Acid beta-Glucosidase 1 Counteracts p38 delta-dependent Induction of Interleukin-6 POSSIBLE ROLE FOR CERAMIDE AS AN ANTI-INFLAMMATORY LIPID. *Journal of Biological Chemistry* 284: 12979-12988
- Klemm RW, Ejning CS, Surma MA, Kaiser HJ, Gerl MJ, Sampaio JL, de Robillard Q, Ferguson C, Proszynski TJ, Shevchenko A, Simons K (2009) Segregation of sphingolipids and sterols during formation of secretory vesicles at the trans-Golgi network. *Journal of Cell Biology* 185: 601-612
- Köberlin MS, Snijder B, Heinz LX, Baumann CL, Fauster A, Vladimer GI, Gavin AC, Superti-Furga G (2015) A Conserved Circular Network of Coregulated Lipids Modulates Innate Immune Responses. *Cell* 162: 170-183
- Kolter T, Sandhoff K (2006) Sphingolipid metabolism diseases. *Bba-Biomembranes* 1758: 2057-2079

- Kondo Y, Ikeda K, Tokuda N, Nishitani C, Ohto U, Akashi-Takamura S, Ito Y, Uchikawa M, Kuroki Y, Taguchi R, Miyake K, Zhang Q, Furukawa K, Furukawa K (2013) TLR4-MD-2 complex is negatively regulated by an endogenous ligand, globotetraosylceramide. *Proc Natl Acad Sci U S A* 110: 4714-4719
- Koynova R, Caffrey M (1998) Phases and phase transitions of the phosphatidylcholines. *Bba-Rev Biomembranes* 1376: 91-145
- Kuge O, Saito K, Nishijima M (1999) Control of phosphatidylserine synthase II activity in Chinese hamster ovary cells. *Journal of Biological Chemistry* 274: 23844-23849
- Kuwata H, Matsumoto M, Atarashi K, Morishita H, Hirotani T, Koga R, Takeda K (2006) I kappa BNS inhibits induction of a subset of toll-like receptor-dependent genes and limits inflammation. *Immunity* 24: 41-51
- Kuznik A, Bencina M, Svajger U, Jeras M, Rozman B, Jerala R (2011) Mechanism of Endosomal TLR Inhibition by Antimalarial Drugs and Imidazoquinolines. *J Immunol* 186: 4794-4804
- Lacy P, Stow JL (2011) Cytokine release from innate immune cells: association with diverse membrane trafficking pathways. *Blood* 118: 9-18
- Lagarde M, Bernoud N, Thies F, Brossard N, Lemaitre-Delaunay D, Croset M, Lecerf J (2001) Lysophosphatidylcholine as a carrier of docosahexaenoic acid to target tissues. *World Rev Nutr Diet* 88: 173-177
- Lamond AI (2002) Molecular biology of the cell, 4th edition. *Nature* 417: 383-383
- Lamour NF, Wijesinghe DS, Mietla JA, Ward KE, Stahelin RV, Chalfant CE (2011) Ceramide kinase regulates the production of tumor necrosis factor alpha (TNFalpha) via inhibition of TNFalpha-converting enzyme. *J Biol Chem* 286: 42808-17
- Lee BL, Moon JE, Shu JH, Yuan L, Newman ZR, Schekman R, Barton GM (2013) UNC93B1 mediates differential trafficking of endosomal TLRs. *Elife* 2
- Lee SY, Lee HY, Kim SD, Shim JM, Bae YS (2007) Lysophosphatidylglycerol stimulates chemotactic migration and tube formation in human umbilical vein endothelial cells. *Biochem Biophys Res Commun* 363: 490-494
- Leon-Ponte M, Kirchhof MG, Sun T, Stephens T, Singh B, Sandhu S, Madrenas J (2005) Polycationic lipids inhibit the pro-inflammatory response to LPS. *Immunol Lett* 96: 73-83
- Leventis PA, Grinstein S (2010) The Distribution and Function of Phosphatidylserine in Cellular Membranes. *Annu Rev Biophys* 39: 407-427
- Levine T (2004) Short-range intracellular trafficking of small molecules across endoplasmic reticulum junctions. *Trends Cell Biol* 14: 483-490
- Levy M, Futerman AH (2010) Mammalian Ceramide Synthases. *lubmb Life* 62: 347-356
- Li CM, Park JH, Simonaro CM, He XX, Gordon RE, Friedman AH, Ehleiter D, Paris F, Manova K, Hepbaldikler S, Fuks Z, Sandhoff K, Kolesnick R, Schuchman EH (2002) Insertional mutagenesis of the mouse acid ceramidase gene leads to early embryonic lethality in homozygotes and progressive lipid storage disease in heterozygotes (vol 79, pg 218, 2002). *Genomics* 79: 890-890
- Li ZQ, Fan YF, Liu J, Li Y, Huan CM, Bui HH, Kuo MS, Park TS, Cao GQ, Jiang XC (2012) Impact of Sphingomyelin Synthase 1 Deficiency on Sphingolipid Metabolism and Atherosclerosis in Mice. *Arterioscl Throm Vas* 32: 1577-1584
- Liaunardy-Jopeace A, Bryant CE, Gay NJ (2014) The COP II adaptor protein TMED7 is required to initiate and mediate the delivery of TLR4 to the plasma membrane. *Sci Signal* 7
- Lim PS, Sutton CR, Rao S (2015) Protein kinase C in the immune system: from signalling to chromatin regulation. *Immunology*
- Lingwood D, Simons K (2010) Lipid Rafts As a Membrane-Organizing Principle. *Science* 327: 46-50
- Litman BJ, Mitchell DC (1996) A role for phospholipid polyunsaturation in modulating membrane protein function. *Lipids* 31: S193-S197
- Lonez C, Lensink MF, Ruysschaert JM, Vandenbranden M (2010) Fusogenic Activity of Cationic Lipids Correlates with Lipid Shape Distribution. *Biophys J* 98: 671a-671a

- Lopez-Montero I, Rodriguez N, Cribier S, Pohl A, Velez M, Devaux PF (2005) Rapid transbilayer movement of ceramides in phospholipid vesicles and in human erythrocytes. *Journal of Biological Chemistry* 280: 25811-25819
- Low PC, Misaki R, Schroder K, Stanley AC, Sweet MJ, Teasdale RD, Vanhaesebroeck B, Meunier FA, Taguchi T, Stow JL (2010) Phosphoinositide 3-kinase delta regulates membrane fission of Golgi carriers for selective cytokine secretion. *Journal of Cell Biology* 190: 1053-1065
- Lu DY, Chen HC, Yang MS, Hsu YM, Lin HJ, Tang CH, Lee CH, Lai CK, Lin CJ, Shyu WC, Lin FY, Lai CH (2012) Ceramide and Toll-Like Receptor 4 Are Mobilized into Membrane Rafts in Response to *Helicobacter pylori* Infection in Gastric Epithelial Cells. *Infect Immun* 80: 1823-1833
- Lykidis A, Baburina I, Jackowski S (1999) Distribution of CTP : phosphocholine cytidyltransferase (CCT) isoforms - Identification of a new CCT beta splice variant. *Journal of Biological Chemistry* 274: 26992-27001
- Maeda K, Anand K, Chiapparino A, Kumar A, Poletto M, Kaksonen M, Gavin AC (2013) Interactome map uncovers phosphatidylserine transport by oxysterol-binding proteins. *Nature* 501: 257-+
- Magalhaes MAO, Glogauer M (2010) Pivotal Advance: Phospholipids determine net membrane surface charge resulting in differential localization of active Rac1 and Rac2. *J Leukocyte Biol* 87: 545-555
- Makide K, Kitamura H, Sato Y, Okutani M, Aoki J (2009) Emerging lysophospholipid mediators, lysophosphatidylserine, lysophosphatidylthreonine, lysophosphatidylethanolamine and lysophosphatidylglycerol. *Prostaglandins Other Lipid Mediat* 89: 135-139
- Malatack JJ, Consolini DM, Bayever E (2003) The status of hematopoietic stem cell transplantation in lysosomal storage disease. *Pediatr Neurol* 29: 391-403
- Manderson AP, Kay JG, Hammond LA, Brown DL, Stow JL (2007) Subcompartments of the macrophage recycling endosome direct the differential secretion of IL-6 and TNF alpha. *Journal of Cell Biology* 178: 57-69
- Martin S, Pombo I, Poncet P, David B, Arock M, Blank U (2000) Immunologic stimulation of mast cells leads to the reversible exposure of phosphatidylserine in the absence of apoptosis. *Int Arch Allergy Imm* 123: 249-258
- Massey JB (2001) Interaction of ceramides with phosphatidylcholine, sphingomyelin and sphingomyelin/cholesterol bilayers. *Bba-Biomembranes* 1510: 167-184
- McGettrick AF, Brint EK, Paisson-McDermott EM, Rowe DC, Golenbock DT, Gay NJ, Fitzgerald KA, O'Neill LAJ (2006) Trif-related adapter molecule is phosphorylated by PKC epsilon during toll-like receptor 4 signaling. *Proc Natl Acad Sci U S A* 103: 9196-9201
- Mechtler TP, Stary S, Metz TF, De Jesus VR, Greber-Platzer S, Pollak A, Herkner KR, Streubel B, Kasper DC (2012) Neonatal screening for lysosomal storage disorders: feasibility and incidence from a nationwide study in Austria. *Lancet* 379: 335-341
- Mesmin B, Bigay J, von Filseck JM, Lacas-Gervais S, Drin G, Antonny B (2013) A Four-Step Cycle Driven by PI(4)P Hydrolysis Directs Sterol/PI(4)P Exchange by the ER-Golgi Tether OSBP. *Cell* 155: 830-843
- Meyer SGE, Karow W, de Groot H (2005) 2n-fatty from phosphatidylcholine label, sphingolipids - A novel role of phospholipase A(2)? *Bba-Mol Cell Biol L* 1735: 68-78
- Miguel RN, Wong J, Westoll JF, Brooks HJ, O'Neill LAJ, Gay NJ, Bryant CE, Monie TP (2007) A Dimer of the Toll-Like Receptor 4 Cytoplasmic Domain Provides a Specific Scaffold for the Recruitment of Signalling Adaptor Proteins. *PloS one* 2
- Milhas D, Clarke CJ, Hannun YA (2010) Sphingomyelin metabolism at the plasma membrane: Implications for bioactive sphingolipids. *FEBS Lett* 584: 1887-1894
- Miller WL (2007) Steroidogenic acute regulatory protein (StAR), a novel mitochondrial cholesterol transporter. *Bba-Mol Cell Biol L* 1771: 663-676
- Milo R (2013) What is the total number of protein molecules per cell volume? A call to rethink some published values. *Bioessays* 35: 1050-1055

- Moffatt MF, Kabesch M, Liang LM, Dixon AL, Strachan D, Heath S, Depner M, von Berg A, Bufer A, Rietschel E, Heinzmann A, Simma B, Frischer T, Willis-Owen SAG, Wong KCC, Illig T, Vogelberg C, Weiland SK, von Mutius E, Abecasis GR et al. (2007) Genetic variants regulating ORMDL3 expression contribute to the risk of childhood asthma. *Nature* 448: 470-475
- Mollinedo F, Calafat J, Janssen H, Martin-Martin B, Canchado J, Nabokina SM, Gajate C (2006) Combinatorial SNARE complexes modulate the secretion of cytoplasmic granules in human neutrophils. *J Immunol* 177: 2831-2841
- Mondal M, Mesmin B, Mukherjee S, Maxfield FR (2009) Sterols Are Mainly in the Cytoplasmic Leaflet of the Plasma Membrane and the Endocytic Recycling Compartment in CHO Cells. *Molecular biology of the cell* 20: 581-588
- Mullen TD, Hannun YA, Obeid LM (2012) Ceramide synthases at the centre of sphingolipid metabolism and biology. *Biochemical Journal* 441: 789-802
- Murakami Y, Tian L, Voss OH, Margulies DH, Krzewski K, Coligan JE (2014) CD300b regulates the phagocytosis of apoptotic cells via phosphatidylserine recognition. *Cell Death Differ* 21: 1746-1757
- Murray RZ, Kay JG, Sangermani DG, Stow JL (2005) A role for the phagosome in cytokine secretion. *Science* 310: 1492-1495
- Nagai Y, Akashi S, Nagafuku M, Ogata M, Iwakura Y, Akira S, Kitamura T, Kosugi A, Kimoto M, Miyake K (2002) Essential role of MD-2 in LPS responsiveness and TLR4 distribution. *Nat Immunol* 3: 667-672
- Nakahara K, Ohkuni A, Kitamura T, Abe K, Naganuma T, Ohno Y, Zoeller RA, Kihara A (2012) The Sjogren-Larsson Syndrome Gene Encodes a Hexadecenal Dehydrogenase of the Sphingosine 1-Phosphate Degradation Pathway. *Molecular cell* 46: 461-471
- Negishi H, Ohba Y, Yanai H, Takaoka A, Honma K, Yui K, Matsuyama T, Taniguchi T, Honda K (2005) Negative regulation of Toll-like-receptor signaling by IRF-4. *Proc Natl Acad Sci U S A* 102: 15989-15994
- Nielsen J (2009) Systems biology of lipid metabolism: From yeast to human. *FEBS Lett* 583: 3905-3913
- Nilsson A, Duan RD (2006) Absorption and lipoprotein transport of sphingomyelin. *J Lipid Res* 47: 154-71
- Nishiya T, Kajita E, Horinouchi T, Nishimoto A, Miwa S (2007) Distinct roles of TIR and non-TIR regions in the subcellular localization and signaling properties of MyD88. *FEBS Lett* 581: 3223-9
- Nishiya T, Kajita E, Miwa S (2006) Ligand-independent oligomerization of TLR4 regulated by a short hydrophobic region adjacent to the transmembrane domain. *Biochem Biophys Res Commun* 341: 1128-1134
- Ohtsuka T, Nishijima M, Akamatsu Y (1993) A Somatic-Cell Mutant Defective in Phosphatidylglycerophosphate Synthase, with Impaired Phosphatidylglycerol and Cardiolipin Biosynthesis. *Journal of Biological Chemistry* 268: 22908-22913
- Olkkonen VM, Li SQ (2013) Oxysterol-binding proteins: Sterol and phosphoinositide sensors coordinating transport, signaling and metabolism. *Prog Lipid Res* 52: 529-538
- Padgett GA, Reiquam CW, Gorham JR, Henson JB, Omary CC (1967) Comparative Studies of Chediak-Higashi Syndrome - Pathology. *Am J Pathol* 51: 553-&
- Palsson-McDermott EM, Doyle SL, McGettrick AF, Hardy M, Husebye H, Banahan K, Gong M, Golenbock D, Espevik T, O'Neill LAJ (2009) TAG, a splice variant of the adaptor TRAM, negatively regulates the adaptor MyD88-independent TLR4 pathway. *Nat Immunol* 10: 579-U30
- Panther G, Jerala R (2011) The Ectodomain of the Toll-like Receptor 4 Prevents Constitutive Receptor Activation. *Journal of Biological Chemistry* 286: 23334-23344
- Parenti G (2009) Treating lysosomal storage diseases with pharmacological chaperones: from concept to clinics. *Embo Mol Med* 1: 268-279
- Park SJ, Lee KP, Kang S, Chung HY, Bae YS, Okajima F, Im DS (2013) Lysophosphatidylethanolamine utilizes LPA(1) and CD97 in MDA-MB-231 breast cancer cells. *Cell Signal* 25: 2147-2154
- Parker LC, Prestwich EC, Ward JR, Smythe E, Berry A, Triantafilou M, Triantafilou K, Sabroe I (2008) A phosphatidylserine species inhibits a range of TLR- but not IL-1 beta-induced inflammatory responses by disruption of membrane microdomains. *J Immunol* 181: 5606-5617

- Patterson MC, Platt F (2004) Therapy of Niemann-Pick disease, type C. *Bba-Mol Cell Biol L* 1685: 77-82
- Peng X, Frohman MA (2012) Mammalian phospholipase D physiological and pathological roles. *Acta Physiol* 204: 219-226
- Perez C, Gerber S, Boilevin J, Bucher M, Darbre T, Aebi M, Reymond JL, Locher KP (2015) Structure and mechanism of an active lipid-linked oligosaccharide flippase. *Nature* 524: 433-8
- Perry DM, Newcomb B, Adada M, Wu BX, Roddy P, Kitatani K, Siskind L, Obeid LM, Hannun YA (2014) Defining a Role for Acid Sphingomyelinase in the p38/Interleukin-6 Pathway. *Journal of Biological Chemistry* 289: 22401-22412
- Perry RJ, Ridgway ND (2006) Oxysterol-binding protein and vesicle-associated membrane protein-associated protein are required for sterol-dependent activation of the ceramide transport protein. *Molecular biology of the cell* 17: 2604-2616
- Pettus BJ, Bielawska A, Subramanian P, Wijesinghe DS, Maceyka M, Leslie CC, Evans JH, Freiberg J, Roddy P, Hannun YA, Chalfant CE (2004) Ceramide 1-phosphate is a direct activator of cytosolic phospholipase A(2). *Journal of Biological Chemistry* 279: 11320-11326
- Pettus BJ, Chalfant CE, Hannun YA (2002) Ceramide in apoptosis: an overview and current perspectives. *Bba-Mol Cell Biol L* 1585: 114-125
- Pewzner-Jung Y, Ben-Dor S, Futerman AH (2006) When do lasses (longevity assurance genes) become CerS (ceramide synthases)? Insights into the regulation of ceramide synthesis. *Journal of Biological Chemistry* 281: 25001-25005
- Piao WJ, Ru LW, Piepenbrink KH, Sundberg EJ, Vogel SN, Toshchakov VY (2013) Recruitment of TLR adapter TRIF to TLR4 signaling complex is mediated by the second helical region of TRIF TIR domain. *Proc Natl Acad Sci U S A* 110: 19036-19041
- Pichlmair A, Schulz O, Tan CP, Naslund TI, Liljestrom P, Weber F, Sousa CRE (2006) RIG-I-mediated antiviral responses to single-stranded RNA bearing 5'-phosphates. *Science* 314: 997-1001
- Pitson SM, Moretti PAB, Zebol JR, Lynn HE, Xia P, Vadas MA, Wattenberg BW (2003) Activation of sphingosine kinase 1 by ERK1/2-mediated phosphorylation. *Embo Journal* 22: 5491-5500
- Platt FM, Jeyakumar M (2008) Substrate reduction therapy. *Acta Paediatr* 97: 88-93
- Plociennikowska A, Hromada-Judycka A, Borzecka K, Kwiatkowska K (2015) Co-operation of TLR4 and raft proteins in LPS-induced pro-inflammatory signaling. *Cell Mol Life Sci* 72: 557-581
- Pomorski T, Hrafnisdottir S, Devaux PF, van Meer G (2001) Lipid distribution and transport across cellular membranes. *Semin Cell Dev Biol* 12: 139-148
- Puneet P, Yap CT, Wong L, Yulin L, Koh DR, Moomchala S, Pfeilschifter J, Huwiler A (2013) Retraction. *Science* 341: 342
- Roelants FM, Baltz AG, Trott AE, Fereres S, Thorner J (2010) A protein kinase network regulates the function of aminophospholipid flippases. *Proc Natl Acad Sci U S A* 107: 34-39
- Rose IA, Hanson KR, Wilkinson KD, Wimmer MJ (1980) A Suggestion for Naming Faces of Ring Compounds. *P Natl Acad Sci-Biol* 77: 2439-2441
- Rowe DC, McGettrick AF, Latz E, Monks BG, Gay NJ, Yamamoto M, Akira S, O'Neill LA, Fitzgerald KA, Golenbock DT (2006) The myristoylation of TRIF-related adaptor molecule is essential for Toll-like receptor 4 signal transduction. *Proc Natl Acad Sci U S A* 103: 6299-6304
- Ruysschaert JM, Loney C (2015) Role of lipid microdomains in TLR-mediated signalling. *Bba-Biomembranes* 1848: 1860-1867
- Sakane F, Imai S, Kai M, Yasuda S, Kanoh H (2007) Diacylglycerol kinases: Why so many of them? *Bba-Mol Cell Biol L* 1771: 793-806
- Santos CR, Schulze A (2012) Lipid metabolism in cancer. *Febs J* 279: 2610-2623
- Sasai M, Linehan MM, Iwasaki A (2010) Bifurcation of Toll-Like Receptor 9 Signaling by Adaptor Protein 3. *Science* 329: 1530-1534

- Sato T, Aoki J, Nagai Y, Dohmae N, Takio K, Doi T, Arai H, Inoue K (1997) Serine phospholipid-specific phospholipase A that is secreted from activated platelets - A new member of the lipase family. *Journal of Biological Chemistry* 272: 2192-2198
- Schiffmann R (2015) The consequences of genetic and pharmacologic reduction in sphingolipid synthesis. *J Inher Metab Dis* 38: 77-84
- Schneider R, Brügger B, Sandhoff R, Zellnig G, Leber A, Lampl M, Athenstaedt K, Hrastnik C, Eder S, Daum G, Paltauf F, Wieland FT, Kohlwein SD (1999) Electrospray ionization tandem mass spectrometry (ESI-MS/MS) analysis of the lipid molecular species composition of yeast subcellular membranes reveals acyl chain-based sorting/remodeling of distinct molecular species en route to the plasma membrane. *The Journal of cell biology* 146: 741-54
- Schoenwaelder SM, Yuan YP, Josefsson EC, White MJ, Yao Y, Mason KD, O'Reilly LA, Henley KJ, Ono A, Hsiao S, Willcox A, Roberts AW, Huang DCS, Salem HH, Kile BT, Jackson SP (2009) Two distinct pathways regulate platelet phosphatidylserine exposure and procoagulant function. *Blood* 114: 663-666
- Schroder K, Muruve DA, Tschopp J (2009) Innate Immunity: Cytoplasmic DNA Sensing by the AIM2 Inflammasome. *Current Biology* 19: R262-R265
- Schuchman EH, Wasserstein MP (2015) Types A and B Niemann-Pick disease. *Best Pract Res Clin En* 29: 237-247
- Scott CC, Dobson W, Botelho RJ, Coady-Osberg N, Chavrier P, Knecht DA, Heath C, Stahl P, Grinstein S (2005) Phosphatidylinositol-4,5-bisphosphate hydrolysis directs actin remodeling during phagocytosis. *Journal of Cell Biology* 169: 139-149
- Semino C, Angelini G, Poggi A, Rubartelli A (2005) NK/iDC interaction results in IL-18 secretion by DCs at the synaptic cleft followed by NK cell activation and release of the DC maturation factor HMGB1. *Blood* 106: 609-616
- Sengupta P, Bosis E, Nachliel E, Gutman M, Smith SO, Mihalyne G, Zaitseva I, McLaughlin S (2009) EGFR Juxtamembrane Domain, Membranes, and Calmodulin: Kinetics of Their Interaction. *Biophys J* 96: 4887-4895
- Serhan CN, Savill J (2005) Resolution of inflammation: The beginning programs the end. *Nat Immunol* 6: 1191-1197
- Shakor ABA, Atia MM, Kwiatkowska K, Sobota A (2012) Cell surface ceramide controls translocation of transferrin receptor to clathrin-coated pits. *Cell Signal* 24: 677-684
- Sheedy FJ, O'Neill LAJ (2007) The troll in toll: Mal and TRAM as bridges for TLR2 and TLR4 signaling. *J Leukocyte Biol* 82: 196-203
- Shevchenko A, Simons K (2010) Lipidomics: coming to grips with lipid diversity. *Nat Rev Mol Cell Bio* 11: 593-598
- Shi XS, Bi YC, Yang W, Guo XD, Jiang Y, Wan CJ, Li LY, Bai YB, Guo J, Wang YJ, Chen XJ, Wu B, Sun HB, Liu WL, Wang JF, Xu CQ (2013) Ca²⁺ regulates T-cell receptor activation by modulating the charge property of lipids. *Nature* 493: 111-+
- Shimobayashi M, Oppliger W, Moes S, Jenö P, Hall MN (2013) TORC1-regulated protein kinase Npr1 phosphorylates Orm to stimulate complex sphingolipid synthesis. *Molecular biology of the cell* 24: 870-881
- Shiratori Y, Okwu AK, Tabas I (1994) Free cholesterol loading of macrophages stimulates phosphatidylcholine biosynthesis and up-regulation of CTP: phosphocholine cytidyltransferase. *J Biol Chem* 269: 11337-48
- Shirey KA, Lai WD, Scott AJ, Lipsky M, Mistry P, Pletneva LM, Karp CL, McAlees J, Gioannini TL, Weiss J, Chen WH, Ernst RK, Rossignol DP, Gusovsky F, Blanco JCG, Vogel SN (2013) The TLR4 antagonist Eritoran protects mice from lethal influenza infection. *Nature* 497: 498-+
- Sillence DJ, Platt FM (2003) Storage diseases: new insights into sphingolipid functions. *Trends Cell Biol* 13: 195-203

- Silvius JR, Leventis R (1993) Spontaneous Interbilayer Transfer of Phospholipids - Dependence on Acyl-Chain Composition. *Biochemistry-Us* 32: 13318-13326
- Simons K, Ikonen E (2000) Cell biology - How cells handle cholesterol. *Science* 290: 1721-1726
- Sims K, Haynes CA, Kelly S, Allegood JC, Wang E, Momin A, Leipelt M, Reichart D, Glass CK, Sullards MC, Merrill AH (2010) Kdo(2)-Lipid A, a TLR4-specific Agonist, Induces de Novo Sphingolipid Biosynthesis in RAW264.7 Macrophages, Which Is Essential for Induction of Autophagy. *Journal of Biological Chemistry* 285: 38568-38579
- Singh R, Kaushik S, Wang YJ, Xiang YQ, Novak I, Komatsu M, Tanaka K, Cuervo AM, Czaja MJ (2009) Autophagy regulates lipid metabolism. *Nature* 458: 1131-U64
- Siow DL, Wattenberg BW (2012) Mammalian ORMDL Proteins Mediate the Feedback Response in Ceramide Biosynthesis. *Journal of Biological Chemistry* 287: 40198-40204
- Slotte JP (2013) Biological functions of sphingomyelins. *Prog Lipid Res* 52: 424-437
- Snider AJ, Kawamori T, Bradshaw SG, Orr KA, Gilkeson GS, Hannun YA, Obeid LM (2009) A role for sphingosine kinase 1 in dextran sulfate sodium-induced colitis. *Faseb Journal* 23: 143-152
- Snijder B, Kandasamy RK, Superti-Furga G (2014) Toward effective sharing of high-dimensional immunology data. *Nat Biotechnol* 32: 755-9
- Sorre B, Callan-Jones A, Manneville JB, Nassoy P, Joanny JF, Prost J, Goud B, Bassereau P (2009) Curvature-driven lipid sorting needs proximity to a demixing point and is aided by proteins. *Proc Natl Acad Sci U S A* 106: 5622-5626
- Sprong H, van der Sluijs P, van Meer G (2001) How proteins move lipids and lipids move proteins. *Nat Rev Mol Cell Biol* 2: 504-13
- Steiner S, Smith S, Waechter CJ, Lester RL (1969) Isolation and Partial Characterization of a Major Inositol-Containing Lipid in Bakers Yeast, Mannosyl-Diinositol, Diphosphoryl-Ceramide. *Proc Natl Acad Sci U S A* 64: 1042-&
- Stewart CR, Stuart LM, Wilkinson K, van Gils JM, Deng JS, Halle A, Rayner KJ, Boyer L, Zhong RQ, Frazier WA, Lacy-Hulbert A, El Khoury J, Golenbock DT, Moore KJ (2010) CD36 ligands promote sterile inflammation through assembly of a Toll-like receptor 4 and 6 heterodimer. *Nat Immunol* 11: 155-U75
- Stow JL, Manderson AP, Murray RZ (2006) SNAREing immunity: the role of SNAREs in the immune system. *Nature Reviews Immunology* 6: 919-929
- Sun Y, Ishibashi M, Seimon T, Lee M, Sharma SM, Fitzgerald KA, Samokhin AO, Wang YB, Sayers S, Aikawa M, Jerome WG, Ostrowski MC, Bromme D, Libby P, Tabas IA, Welch CL, Tall AR (2009) Free Cholesterol Accumulation in Macrophage Membranes Activates Toll-Like Receptors and p38 Mitogen-Activated Protein Kinase and Induces Cathepsin K. *Circulation research* 104: 455-U75
- Sun YD, Drubin DG (2012) The functions of anionic phospholipids during clathrin-mediated endocytosis site initiation and vesicle formation. *J Cell Sci* 125: 6157-6165
- Sun YD, Miao YS, Yamane Y, Zhang C, Shokat KM, Takematsu H, Kozutsumi Y, Drubin DG (2012) Orm protein phosphoregulation mediates transient sphingolipid biosynthesis response to heat stress via the Pkh-Ypk and Cdc55-PP2A pathways. *Molecular biology of the cell* 23: 2388-2398
- Surma MA, Klose C, Klemm RW, Ejsing CS, Simons K (2011) Generic Sorting of Raft Lipids into Secretory Vesicles in Yeast. *Traffic* 12: 1139-1147
- Takahashi K, Shibata T, Akashi-Takamura S, Kiyokawa T, Wakabayashi Y, Tanimura N, Kobayashi T, Matsumoto F, Fukui R, Kouro T, Nagai Y, Takatsu K, Saitoh SI, Miyake K (2007) A protein associated with Toll-like receptor (TLR) 4 (PRAT4A) is required for TLR-dependent immune responses. *J Exp Med* 204: 2963-2976
- Takeda K, Akira S (2004) TLR signaling pathways. *Semin Immunol* 16: 3-9
- Takeda K, Akira S (2015) Toll-like receptors. *Curr Protoc Immunol* 109: 14.12.1-14.12.10
- Tamehiro N, Zhou S, Okuhira K, Benita Y, Brown CE, Zhuang DZ, Latz E, Hornemann T, von Eckardstein A, Xavier RJ, Freeman MW, Fitzgerald ML (2008) SPTLC1 binds ABCA1 to negatively regulate trafficking and cholesterol efflux activity of the transporter. *Biochemistry-Us* 47: 6138-6147

- Tani M, Kuge O (2010) Requirement of a specific group of sphingolipid-metabolizing enzyme for growth of yeast *Saccharomyces cerevisiae* under impaired metabolism of glycerophospholipids. *Mol Microbiol* 78: 395-413
- Tatematsu M, Ishii A, Oshiumi H, Horiuchi M, Inagaki F, Seya T, Matsumoto M (2010) A Molecular Mechanism for Toll-IL-1 Receptor Domain-containing Adaptor Molecule-1-mediated IRF-3 Activation. *Journal of Biological Chemistry* 285: 20128-20136
- Tatsuta T, Scharwey M, Langer T (2014) Mitochondrial lipid trafficking. *Trends Cell Biol* 24: 44-52
- Testerink N, van der Sanden MHM, Houweling M, Helms JB, Vaandrager AB (2009) Depletion of phosphatidylcholine affects endoplasmic reticulum morphology and protein traffic at the Golgi complex. *J Lipid Res* 50: 2182-2192
- Tian Y, Pate C, Andreolotti A, Wang LM, Tuomanen E, Boyd K, Claro E, Jackowski S (2008) Cytokine secretion requires phosphatidylcholine synthesis. *Journal of Cell Biology* 181: 945-957
- Triantafyllou K, Triantafyllou M, Gamper F, Haston R, Mouratis M, Morath S (2007) Membrane sorting of toll-like receptor (TLR)-2/6 and TLR2/1 heterodimers at the cell surface determines heterotypic associations with CD36 and intracellular targeting. *Inflamm Res* 56: S122-S122
- Ulloa L, Brunner M, Ramos L, Deitch EA (2009) Scientific and Clinical Challenges in Sepsis. *Curr Pharm Design* 15: 1918-1935
- Van Helvoort A, Vant Hof W, Ritsema T, Sandra A, Van Meer G (1994) Conversion of Diacylglycerol to Phosphatidylcholine on the Basolateral Surface of Epithelial (Madin-Darby Canine Kidney) Cells - Evidence for the Reverse Action of a Sphingomyelin Synthase. *Journal of Biological Chemistry* 269: 1763-1769
- van Meer G (2005) Cellular lipidomics. *Embo Journal* 24: 3159-3165
- van Meer G (2011) Dynamic Transbilayer Lipid Asymmetry. *Csh Perspect Biol* 3
- van Meer G, Halter D, Sprong H, Somerharju P, Egmond MR (2006) ABC lipid transporters: Extruders, flippases, or flopless activators? *FEBS Lett* 580: 1171-1177
- van Meer G, Hoetzel S (2010) Sphingolipid topology and the dynamic organization and function of membrane proteins. *FEBS Lett* 584: 1800-1805
- van Meer G, Voelker DR, Feigenson GW (2008) Membrane lipids: where they are and how they behave. *Nat Rev Mol Cell Biol* 9: 112-24
- Vance DE, Vance JE (2009) Physiological consequences of disruption of mammalian phospholipid biosynthetic genes. *J Lipid Res* 50: S132-S137
- Vance JE (2008) Thematic review series: Glycerolipids. Phosphatidylserine and phosphatidylethanolamine in mammalian cells: two metabolically related aminophospholipids. *J Lipid Res* 49: 1377-1387
- Vance JE, Tasseva G (2013) Formation and function of phosphatidylserine and phosphatidylethanolamine in mammalian cells. *Bba-Mol Cell Biol L* 1831: 543-554
- Vionnet C, Roubaty C, Ejsing CS, Knudsen J, Conzelmann A (2011) Yeast Cells Lacking All Known Ceramide Synthases Continue to Make Complex Sphingolipids and to Incorporate Ceramides into Glycosylphosphatidylinositol (GPI) Anchors. *Journal of Biological Chemistry* 286: 6769-6779
- Vitner EB, Farfel-Becker T, Eilam R, Biton I, Futerman AH (2012) Contribution of brain inflammation to neuronal cell death in neuronopathic forms of Gaucher's disease. *Brain* 135: 1724-1735
- Walker AK, Jacobs RL, Watts JL, Rottiers V, Jiang K, Finnegan DM, Shioda T, Hansen M, Yang F, Niebergall LJ, Vance DE, Tzoneva M, Hart AC, Naar AM (2011) A conserved SREBP-1/phosphatidylcholine feedback circuit regulates lipogenesis in metazoans. *Cell* 147: 840-52
- Walton KA, Gugiu BG, Thomas M, Basseri RJ, Eliav DR, Salomon RG, Berliner JA (2006) A role for neutral sphingomyelinase activation in the inhibition of LPS action by phospholipid oxidation products. *J Lipid Res* 47: 1967-1974

- Wang D, Lou J, Ouyang CA, Chen WL, Liu YQ, Liu XY, Cao XT, Wang JL, Lu LR (2010) Ras-related protein Rab10 facilitates TLR4 signaling by promoting replenishment of TLR4 onto the plasma membrane. *Proc Natl Acad Sci U S A* 107: 13806-13811
- Wang G, Krishnamurthy K, Umapathy NS, Verin AD, Bieberich E (2009) The carboxyl-terminal domain of atypical protein kinase Czeta binds to ceramide and regulates junction formation in epithelial cells. *J Biol Chem* 284: 14469-75
- Wang S, Robinet P, Smith JD, Gulshan K (2015) ORMDL orosomucoid-like proteins are degraded by free-cholesterol-loading-induced autophagy. *Proc Natl Acad Sci U S A* 112: 3728-33
- Ward DM, Griffiths GM, Stinchcombe JC, Kaplan J (2000) Analysis of the lysosomal storage disease Chediak-Higashi syndrome. *Traffic* 1: 816-822
- Wenger DA, Rafi MA, Luzi P (1997) Molecular genetics of Krabbe disease (globoid cell leukodystrophy): Diagnostic and clinical implications. *Hum Mutat* 10: 268-279
- Wenk MR (2005) The emerging field of lipidomics. *Nat Rev Drug Discov* 4: 594-610
- Wenk MR (2010) Lipidomics: New Tools and Applications. *Cell* 143: 888-895
- Whitmore MM, Iparraguirre A, Kubelka L, Weninger W, Hai T, Williams BRG (2007) Negative regulation of TLR-Signaling pathways by activating transcription factor-3. *J Immunol* 179: 3622-3630
- Worgall TS (2008) Regulation of lipid metabolism by sphingolipids. *Subcell Biochem* 49: 371-85
- Xia P, Gamble JR, Rye KA, Wang LJ, Hii CST, Cockerill P, Khew-Goodall Y, Bert AG, Barter PJ, Vadas MA (1998) Tumor necrosis factor-alpha induces adhesion molecule expression through the sphingosine kinase pathway. *Proc Natl Acad Sci U S A* 95: 14196-14201
- Xia P, Wang LJ, Moretti PAB, Albanese N, Chai FG, Pitson SM, D'Andrea RJ, Gamble JR, Vadas MA (2002) Sphingosine kinase interacts with TRAF2 and dissects tumor necrosis factor-alpha signaling. *Journal of Biological Chemistry* 277: 7996-8003
- Yamaji T, Kumagai K, Tomishige N, Hanada K (2008) Two sphingolipid transfer proteins, CERT and FAPP2: Their roles in sphingolipid metabolism. *lubmb Life* 60: 511-518
- Yamashita T, Wada R, Sasaki T, Deng CX, Bierfreund U, Sandhoff K, Proia RL (1999) A vital role for glycosphingolipid synthesis during development and differentiation. *Proc Natl Acad Sci U S A* 96: 9142-9147
- Yamauchi Y, Hayashi M, Abe-Dohmae S, Yokoyama S (2003) Apolipoprotein A-I activates protein kinase C alpha signaling to phosphorylate and stabilize ATP binding cassette transporter A1 for the high density lipoprotein assembly. *Journal of Biological Chemistry* 278: 47890-47897
- Yang Y, Liu B, Dai J, Srivastava PK, Zammit DJ, Lefrançois L, Li ZH (2007) Heat shock protein gp96 is a master chaperone for toll-like receptors and is important in the innate function of macrophages. *Immunity* 26: 215-226
- Yang YC, Ciarletta AB, Temple PA, Chung MP, Kovacic S, Witekgiannotti JS, Leary AC, Kriz R, Donahue RE, Wong GG, Clark SC (1986) Human IL-3 (Multi-Csf) - Identification by Expression Cloning of a Novel Hematopoietic Growth-Factor Related to Murine IL-3. *Cell* 47: 3-10
- Yeung T, Grinstein S (2007) Lipid signaling and the modulation of surface charge during phagocytosis. *Immunol Rev* 219: 17-36
- Yoshimura A, Naka T, Kubo M (2007) SOCS proteins, cytokine signalling and immune regulation. *Nature Reviews Immunology* 7: 454-465
- Yvan-Charvet L, Welch C, Pagler TA, Ranalletta M, Lamkanfi M, Han S, Ishibashi M, Li R, Wang N, Tall AR (2008) Increased Inflammatory Gene Expression in ABC Transporter-Deficient Macrophages Free Cholesterol Accumulation, Increased Signaling via Toll-Like Receptors, and Neutrophil Infiltration of Atherosclerotic Lesions. *Circulation* 118: 1837-1847
- Zanghellini J, Natter K, Jungreuthmayer C, Thalhammer A, Kurat CF, Gogg-Fassolter G, Kohlwein SD, von Grunberg HH (2008) Quantitative modeling of triacylglycerol homeostasis in yeast - metabolic requirement for lipolysis to promote membrane lipid synthesis and cellular growth. *Febs J* 275: 5552-5563

-
- Zanoni I, Ostuni R, Marek LR, Barresi S, Barbalat R, Barton GM, Granucci F, Kagan JC (2011) CD14 Controls the LPS-Induced Endocytosis of Toll-like Receptor 4. *Cell* 147: 868-880
- Zarewych DM, Kindzelskii AL, Todd RF, Petty HR (1996) LPS induces CD14 association with complement receptor type 3, which is reversed by neutrophil adhesion. *J Immunol* 156: 430-433
- Zhang YH, Yao B, Delikat S, Bayoumy S, Lin XH, Basu S, McGinley M, ChanHui PY, Lichenstein H, Kolesnick R (1997) Kinase suppressor of Ras is ceramide-activated protein kinase. *Cell* 89: 63-72
- Zhu X, Owen JS, Wilson MD, Li H, Griffiths GL, Thomas MJ, Hiltbold EM, Fessler MB, Parks JS (2010a) Macrophage ABCA1 reduces MyD88-dependent Toll-like receptor trafficking to lipid rafts by reduction of lipid raft cholesterol. *J Lipid Res* 51: 3196-206
- Zhu XW, Owen JS, Wilson MD, Li HT, Griffiths GL, Thomas MJ, Hiltbold EM, Fessler MB, Parks JS (2010b) Macrophage ABCA1 reduces MyD88-dependent Toll-like receptor trafficking to lipid rafts by reduction of lipid raft cholesterol. *J Lipid Res* 51: 3196-3206

Curriculum Vitae

Name: Marielle Susan Köberlin (born: Klein)
Position: PhD student
Current address: CeMM: Research Center for Molecular Medicine
of the Austrian Academy of Sciences
Lazarettgasse 14, AKH BT 25.3
1090 Vienna, Austria
Contact details: +43 1 40160 70 045 | +43 699 19908115 | mkoeberlin@cemm.oeaw.ac.at

EDUCATION:

Current: ***PhD candidate***, Molecular Signal Transduction PhD Program of the Medical University of Vienna, Austria
2011: ***Master of Science*** (Diplom-Biologist univ.), Faculty of Biology (specialized in molecular biochemistry, neurobiology and pharmacology), Ludwig Maximilian University of Munich, Germany

RESEARCH EXPERIENCE:

2011 – Current: ***PhD student***: Investigating the Role of Sphingolipids in Innate Immunity
Laboratory of Prof. Giulio Superti-Furga
Thesis Committee Members:
Dr. Anne-Claude Gavin and Prof. Christoph Binder

Scientific techniques:

- Generation of 124 stable shRNA cell lines targeting 24 different genes (lentiviral transduction)
- Screening of 87 stable shRNA cell lines stimulated with different TLR ligands (cytokine expression measured by ELISA and qRT PCR, receptor surface expression and internalization measured by FACS)
- Lipid extraction of different cell lines for lipidomics analysis
- Cell culture supplementation of individual lipid species
- Cell culture techniques for various cell lines and primary human fibroblasts
- Transient and stable transfection of cells with DNA
- Cloning

2010: *Undergraduate Research Student:*

Institute of Clinical Molecular Biology, Helmholtz Center, German Research Center for Environmental Health, Munich, Germany

Supervisor: Dr. Berit Jungnickel

Topic: Protein stability of activation-induced cytidine deaminase (AID) depends on its cellular localization

Using different small molecules and cell stressors, I could monitor the localization of fluorescently labeled proteins by confocal microscopy and FACS-based analysis. As a negative control I genetically perturbed AID using siRNA.

2009: *Undergraduate Research Student:*

AG Chemical Genomics, Max-Planck-Institute of Psychiatry, Munich, Germany

Supervisor: Dr. Felix Hausch

Topic: Design and implementation of an enzymatic inhibition assay for Cyclosporin A

I established the assay by first cloning, expressing and purifying different proteins of the cyclophilin family before measuring the level of enzymatic inhibition with a fluorescently labeled Cyclosporin A.

2006 – 2010: *Student Research Assistant:*

Max-Planck-Institute of Neurobiology, Martinsried, Germany

Supervisor: Dr. Sonia Paixao

My responsibilities included managing a mouse colony by separating and tagging the offspring and determining their genotypes using PCR. Further, I prepared whole animal or brain histology sections and performed staining, microscopy and quantitation using MetaMorph software.

TEACHING:

2009: *Teaching Assistant:*

Introduction to molecular genetics, Faculty of Biology, Genetics Department, Ludwig Maximilian University of Munich, Germany.

Advisor: Dr. Andreas Brachmann

LEADERSHIP:

2012 – 2013: *PhD student representative:*

CeMM, Research Center for Molecular Medicine of the Austrian Academy of Sciences, Vienna, Austria

During my time as a PhD student representative at CeMM I tutored new PhD students, organized social platforms for scientific discussions with other representatives, hosted international seminar speakers and interviewed applicants for a pre- and postdoctoral program manager position.

PUBLICATIONS:

2015: “A Conserved Circular Network of Coregulated Lipids Modulates Innate Immune Responses”, **Marielle S. Köberlin***, Berend Snijder*, Leonhard X. Heinz, Christoph L. Baumann, Astrid Fauster, Gregory I. Vladimer, Anne-Claude Gavin, and Giulio Superti-Furga, in press at **Cell** (2015), <http://dx.doi.org/10.1016/j.cell.2015.05.051>

2015: “The lipid-modifying enzyme SMPDL3B negatively regulates innate immunity”, Leonhard X. Heinz*, Christoph L. Baumann*, **Marielle S. Köberlin**, Berend Snijder, Riem Gawish, Guanghou Shui, Omar Sharif, Irene M. Aspalter, André C. Müller, Richard K. Kandasamy, Florian P. Breitwieser, Andreas Pichlmair, Manuela Bruckner, Manuele Rebsamen, Stephan Blüml, Thomas Karonitsch, Astrid Fauster, Jacques Colinge, Keiryn L. Bennett, Sylvia Knapp, Markus R. Wenk and Giulio Superti-Furga, in press at **Cell Reports** (2015), <http://dx.doi.org/10.1016/j.celrep.2015.05.006>

2010: “Facile synthesis of a fluorescent Cyclosporin A analogue to study Cyclophilin 40 and Cyclophilin 19 Ligands”, Steffen Gaali, Christian Kozany, Bastiaan Hoogeland, **Marielle Klein**, and Felix Hausch, **ACS Medicinal Chemistry Letters** 2010 1 (9), 536-539

INVITED ORAL PRESENTATIONS:

- 2015:** “Functional mapping of the lipid landscape in innate immunity”; Keystone Symposium: Systems Biology of Lipid Metabolism. Selected short talk; session: Lipids in Immune System Regulation. Breckenridge, Colorado, USA.
- 2013:** “The ceramidome and Toll-like receptor signaling”; Symposium: Molecular Mechanisms of Cell Signaling: Cells don’t play dice. Session 1: Signaling in the immune system, student talk. Vienna, Austria.
- 2012:** “The ceramidome and Toll-like receptor signaling”; FEBS Workshop Lipids: from Lipidomics to Disease and Green Energy. Spetses, Greece.

POSTER PRESENTATIONS:

- 2013:** “The ceramidome and Toll-like receptor signaling”. Marielle Klein, Leonhard Heinz, Berend Snijder, Christoph L. Baumann, Manuela Bruckner, Kumaran Kandasamy, Astrid Fauster, Jacques Colinge, Keiryn L. Bennett, Guanghou Shui, Markus R. Wenk, Giulio Superti-Furga. Gordon Research Conference: Lipids, Molecular & Cellular Biology of, Waterville Valley, NH, USA.
- 2012:** “The ceramidome and Toll-like receptor signaling”. Marielle Klein, Leonhard Heinz, Christoph L. Baumann, Manuela Bruckner, Kumaran Kandasamy, Jacques Colinge, Keiryn L. Bennett, Astrid Fauster, Nurhuda Abdul Aziz, Markus R. Wenk, Giulio Superti-Furga. Gordon Research Conference: Glycolipid & Sphingolipid Biology, Lucca, Italy.
- 2012:** “The ceramidome and Toll-like receptor signaling”. Marielle Klein, Leonhard Heinz, Christoph L. Baumann, Manuela Bruckner, Kumaran Kandasamy, Jacques Colinge, Keiryn L. Bennett, Astrid Fauster, Nurhuda Abdul Aziz, Markus R. Wenk, Giulio Superti-Furga. 4th International Singapore Lipid Symposium, National University of Singapore.
- 2011:** “Investigating interacting proteins of endosomal Toll-like receptors”. Marielle Klein, Astrid Fauster, Christoph Baumann, Manuela Bruckner, Giulio Superti-Furga. TOLL 2011: Decoding Innate Immunity, Riva Del Garda, Italy.